Deeply virtual Compton scattering in a relativistic quark model

Dissertation
zur Erlangung des Grades
"Doktor der Naturwissenschaften"

am Fachbereich Physik, Mathematik und Informatik
der Johannes-Gutenberg-Universität
in Mainz

Thomas Spitzenberg
aus Hannover

Mainz, September 2007

Tief virtuelle Comptonstreuung im relativistischen Quarkmodell

Abstract

This thesis is mainly concerned with a model calculation for generalized parton distributions (GPDs). We calculate vectorial- and axial GPDs for the $N \to N$ and $N \to \Delta$ transition in the framework of a light front quark model. This requires the elaboration of a connection between transition amplitudes and GPDs. We provide the first quark model calculations for $N \to \Delta$ GPDs. The examination of transition amplitudes leads to various model independent consistency relations. These relations are not exactly obeyed by our model calculation since the use of the impulse approximation in the light front quark model leads to a violation of Poincare covariance. We explore the impact of this covariance breaking on the GPDs and form factors which we determine in our model calculation and find large effects. The reference frame dependence of our results which originates from the breaking of Poincare covariance can be eliminated by introducing spurious covariants. We extend this formalism in order to obtain frame independent results from our transition amplitudes.

Zusammenfassung

Das Thema dieser Arbeit ist eine Modellrechnung für verallgemeinerte Partonverteilungen (GPDs). Es werden vektorielle- und axiale GPDs für die $N \to N$ und $N \to \Delta$ Übergänge im Rahmen eines Quarkmodells im Lichtkegelformalismus berechnet. Hierzu muß zunächst ein Zusammenhang zwischen Übergangsamplituden und den GPDs hergestellt werden. Die Untersuchung der Übergangsamplituden führt zu einer Vielzahl modellunabhängiger Konsistenzrelationen. Diese Relationen werden von den im Modell berechneten Übergangsamplituden nicht exakt erfüllt, da die Verwendung der Impulsnäherung im Quarkmodell auf dem Lichtkegel zu einer Verletzung der Poincare Kovarianz führt. Der Einfluß dieser Brechung der Kovarianz auf die Berechnung von GPDs und Formfaktoren wird untersucht. Es ergeben sich große Effekte, unter anderem die Abhängigkeit der Ergebnisse von der Wahl des Bezugssystems. Letztere kann durch die Einführung zusätzlicher unphysikalischer Kovarianten eliminiert werden. In dieser Arbeit wird der entsprechende Formalismus erweitert um für alle hier betrachteten Observablen Ergebnisse aus den Übergangsamplituden zu erhalten welche unabhängig von der Wahl des Bezugssystems sind.

Contents

Chapter 1

Introduction

After the first measurement of the proton form factor by Hofstadter in 1955 [1] it was obvious that hadrons exhibit a substructure. Since then not only a large variety of hadrons has been discovered but patterns allowing to classify them have arisen. The idea of $SU_F(3)$ multiplets in 1961 [2] lead to the remarkable prediction of the Ω^- resonance which was discovered in 1964. The ostensible discrepancy between this idea and the Pauli principle was resolved soon after [3][4] by the postulation of color. With the realization that quarks not only represented a successful mathematical construct but could be understood as real partons which make up the hadrons the time was ripe for QCD. In 1971 t'Hooft proved the renormalizability [5] of Yang Mills theories [6] and two years later asymptotic freedom of the latter was announced [7] [8]. In the same year this theory was applied to describe the interactions between quarks [9] [10] and has subsequently been referred to as quantum chromo dynamics (**QCD**).

Since then QCD has experienced several experimental confirmations and is widely accepted as theory for describing the strong interaction. Three decades have passed with hadronic physics still being an active research area which provides many open questions and challenges to both theory and experiment.

QCD is a non abelian gauge theory with quarks which are nearly massless (for u, d and s quarks) and massless gluons as gauge bosons. In this respect it very much resembles QED and in fact the bare lagrangian

$$\mathcal{L} = \sum_f \bar{\psi}_f \left(i \not{D} - m_f \right) \psi_f - \frac{1}{4} tr_c \, F^{\mu\nu} F_{\mu\nu}$$

is identical to the QED lagrangian with the only exception of a different Lie algebra leading to the appearance of the $SU(3)$ structure constants f^{abc} in the definition of the field strength tensor:

$$\begin{aligned} F^a_{\mu\nu} &= \partial_\mu A^a_\nu - \partial_\nu A^a_\mu + g f^{abc} A^b_\mu A^c_\nu \\ D_\mu \psi_f &= \partial_\mu \psi_f - i g \frac{\lambda^a}{2} A^a_\mu \psi_f \quad . \end{aligned}$$

This additional term gives rise to gluon self interactions. These lead to a running coupling resulting in asymptotic freedom. On the other hand this implies large values for the strong

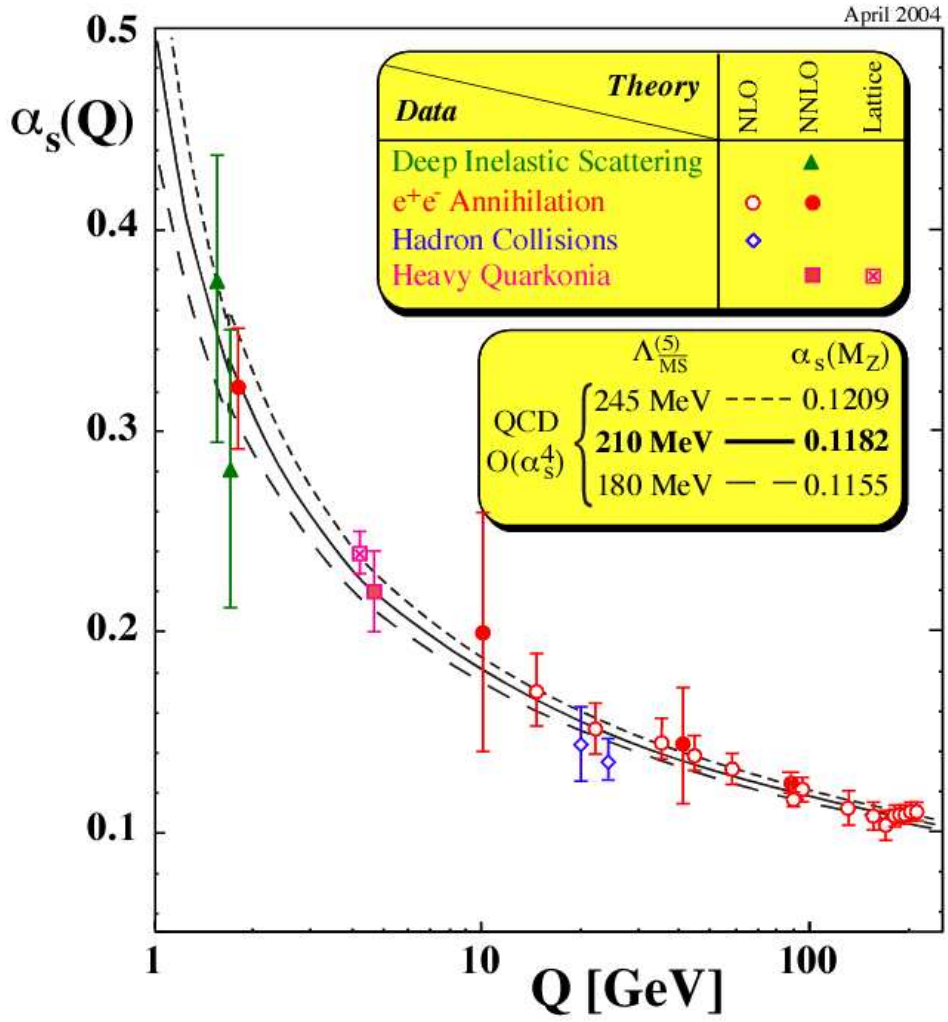

Figure 1.1: *The QCD running coupling α_S taken from [11]*

coupling constant at lower energy scales. Hence the scope of perturbative techniques for QCD is limited to the small coupling region which can be explored in high energy scattering experiments. However the large and important low energy sector is not covered by pQCD.

The world of the strong interactions consists of hadrons. Their fermionic constituents, the quarks as described by QCD are never observed alone[1]. The QCD constituents always form color neutral objects, moreover so far only three quark and quark- antiquark states have been confirmed experimentally[2]. The strong binding effect which forbids free quarks or gluons is called confinement. Mechanisms for confinement have been suggested [14] and experience support from lattice QCD; see e.g. [15]. However a rigorous explanation from first principles has not been found so far.

[1]For signatures from free quarks see articles on the quark gluon plasma e.g. [12]
[2]The recent search for exotic baryons (pentaquarks) seems to be futile [13] as many searches before.

At large distances/ low energies (which is also called the infrared domain) another field theoretical approach is possible. With the observation that chiral symmetry dominates the low energy dynamics the small pion mass can be used as an expansion parameter and an effective field theory can be constructed which posseses all symmetries of QCD [16]. This most prominent example for a successful effective field theory is called chiral perturbation theory χPT [17] and has become an active field of research, particularly since baryons could be included in the formalism [18]. However effective field theories are never renormalizable and hence require more and more low energy constants with every order. The latter are free parameters which have to be determined from experiment.

Hence only for very small momenta precise predictions for hadronic physics observables can be obtained using χPT while it breaks down completely close to its convergence radius of roughly 1 GeV. Lattice QCD is the only field theoretical access to the intermediate range between the realms of χPT and pQCD. Despite the progress during the last decade lattice QCD still experiences manyfold difficulties. For instance the implementation of dynamical fermions with small masses requires a huge numerical effort. Even though computers become faster every year lattice calculations are still far away from a successful implementation of the physical masses for the light quarks. Thus one relies on (chiral) extrapolation towards the physical quark masses. A second problem is connected to the use of euclidean time which complicates the exploration of dynamical properties. For example one cannot calculate DIS structure functions directly but has only access to a couple of moments. Consequently some observables are easy to obtain, while others are practically unreachable. Finally a general drawback of lattice QCD is the lack of physical intuition concerning the question which physical mechanisms contribute to a result which has been "measured" on the lattice. It is of course often possible to define adequate observables to confirm or reject physical pictures which one has already developed.

Therefore in the interesting intermediate energy regime model calculations are often necessary to obtain an estimate for physical observables or in order to understand the physical picture behind an effect that has been measured.

One set of models which are frequently applied in hadronic physics are quark models. These models start from the success of the quark hypothesis to explain the baryon- and meson multiplets and proceed towards a description of hadronic physics with (constituent) quarks being the only degrees of freedom. Their interaction potential is based on phenomenology and sometimes is "QCD inspired". The quark model wave function compiles all dynamical model input. It is obtained from a variational ansatz such that important baryonic properties (i.e. the mass spectrum) are reproduced. In the seventies the quark model was successfully applied to describe the baryon spectrum and magnetic moments of the baryons. However it soon became clear that the momenta of the constituent quarks called for a relativistic description.

In 1949 Dirac has given a classification [19] of forms of relativistic dynamics which combine the restricted principle of relativity with the Hamiltonian formulation of dynamics. He distinguished three genuinely different forms of hamiltonian dynamics. They differ in the choice of the kinematical subgroup (stability group) which leaves a hyperplane on which physical initial conditions are specified invariant. This choice determines which operators are kinematical, i.e. interaction independent. The other generators of the Poincare group are called dynamical

operators.

Dirac discussed 3 different forms. The instant form being most familiar has the 0 component of the total momentum P^0 and the Lorentz boosts $\vec{K}$ as dynamical operators. The point form is determined by the total momentum four vector P^μ being dynamical. The light front form possesses the largest kinematical subgroup and therefore has only three dynamical generators. They are a combination of four momentum components, $P^- = P^0 - P^3$ and combinations of boosts K and rotations J, $F^1 = k^1 - J^2$ and $F^2 = K^2 + J^1$.

All these descriptions have been applied to quark models. The earliest description of a **LF** quark model was provided in 1976 [20]. The **LF** form possessing the largest possible kinematical subgroup has proven particularly useful for a relativistic description of quark models since in a **LF** formulation the relativistic covariance of the wave functions comes for free. A drawback of the application of the commonly used impulse approximation in the description of e.g. elastic scattering within models is the breaking of Poincare covariance. The impulse approximation neglects many body contributions to the current and is difficult to avoid.

In [21] a fresh look on elastic scattering using the light front form was provided by allowing the null plane direction to change while spurious effects are absorbed into non physical form factors. This idea could be applied to restore reference frame independence in a **LF** model description of vectorial nucleon form factors despite the use of the impulse approximation [22].

Having provided a short and selective review about theoretical tools which are applied in hadronic physics we will next focus our attention on different processes in hadronic physics which give insight into the structure of hadrons. The strong binding due to the large QCD coupling constant is a major challenge in the description of hadronic physics. A baryon for example cannot simply be considered as a three quark system which is confined due to the exchange of gluons. The situation differs entirely from the atom whose mass can be understood from the mass of its constituents with a small correction due to the photonic interaction. Instead the nucleon dynamics determines the nucleon mass entirely. Thus the hadron should rather be regarded as a dynamic system consisting of valence quarks, and a cloud of fluctuating quark- antiquark pairs and gluons.

If one wants to learn anything about the hadron structure it is not very useful to study pure hadronic processes to learn about the properties of hadrons. In this context hadron physicists sometimes use the metaphor of learning about the structure of swiss clocks by scattering them against each other, observing their traces and thus learn about their structure. Instead a well understood probe is called for to research hadronic properties. This probe is the electromagnetic interaction which is well understood and can be successfully described by QED. In an ideal situation one can also disentangle the hard (perturbative) part of the examined reaction from the soft (non perturbative) part. In the language of theoretical physics such a separation is called factorization theorem. Deeply inclusive scattering is an example of such a process. In a certain kinematical regime (Bjorken limit) factorization can be proven. Then the leptonic side can be described by QED while the hadronic side factorizes into a hard and a soft part with the latter being parameterized by universal hadronic observables. In this case these observables are parton distributions. DIS is an inclusive process where the total cross section is measured and the final states are not specified.

On the other hand exclusive processes like elastic scattering single out a specific final state. Elastic scattering on nucleons can be parameterized by form factors. They provide complimentary information about the hadrons. One can think of them as a Fourier transform of e.g. the electric charge distribution within the nucleon (in a certain reference system, the Breit frame).

With the advent of high luminosity accelerators and powerful detectors another class of exclusive processes became experimentally accessible. In deeply virtual Compton scattering (DVCS) a virtual photon hits a nucleon target which then emits a real photon. This process can be understood as Compton scattering on a quark which is then embedded in the nucleon. It is parameterized by generalized parton distributions [23][24]. These observables are kinematically rich and contain both form factors and parton distributions as special limits. Since factorization of DVCS can be proven [25] GPDs are universal observables which provide new insight into the structure of hadrons. These GPDs appear in the parametrization of other processes as well (deeply virtual meson production, doubly virtual Compton scattering, two photon exchange,...).

Besides the nucleon itself one can study its excitations. The best explored nucleon resonance is the $\Delta(1232)$. This resonance is the first excited state of the nucleon. The Δ resonance possesses the quantum numbers $J^P = \frac{3}{2}^+$. The isospin quadruplet consists of Δ^{++}, Δ^+, Δ^0 and Δ^-. It has a mass of 1232 MeV and a decay width of roughly 180 MeV. Its main decay mode (nearly 100%) is $\Delta \to N\pi$. While it is of course impossible to perform experiments with a Δ target one can study the properties of the $N \to \Delta$ transition. In fact transition form factors and even transition GPDs can be studied in a way similar to the $N \to N$ transition.

This thesis is organized as follows: In chapter 2 we will introduce DVCS and GPDs and emphasize particularly the $N \to \Delta$ transition DVCS process.

In chapter 3 the quark model which we use to access these GPDs is introduced. The **LF** formalism and the overlap representation for DVCS transition amplitudes from which the GPDs can be obtained will be presented.

The model independent relations between DVCS transition amplitudes and GPDs will be provided in chapter 4. Particular emphasis will be put on the derivation of relations among the DVCS transition amplitudes which follow from Poincare covariance.

In chapter 5 we discuss a possibility to overcome covariance breaking effects of the impulse approximation by providing spurious covariants for the processes of our interest.

Finally we will discuss our results in chapter 6 and provide an outlook.

Chapter 2

Deeply Virtual Compton Scattering

2.1 $N \to N$ DVCS

Virtual Compton Scattering is the (exclusive) process with a virtual photon probing a target and a real photon being emitted. Since this process (with a hadron as target) is a semileptonic process and the leptonic part of it is well understood it can serve as a probe for the less well known hadron structure. The graph which describes VCS is displayed in fig. 2.1. At leading

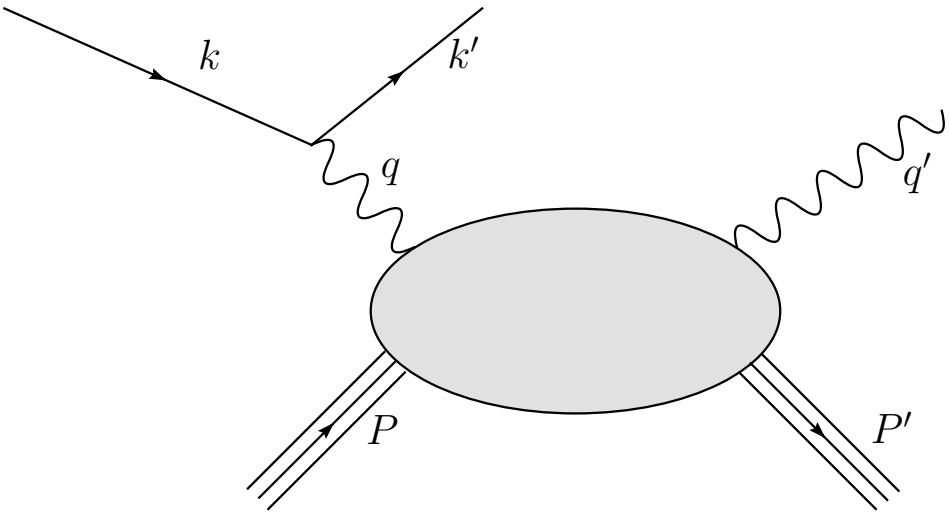

Figure 2.1: *This graph describes VCS.*

order in QED this process is described by the virtual photon exchange between the electron and the nucleon.

Following Ji [26] we define the kinematics in a symmetric way. We choose q^μ and $\bar{P}^\mu$ collinear in z direction. We introduce two light-like vectors $\tilde{p}^\mu = \frac{\bar{P}^+}{2}(1,0,0,1)$ and $n^\mu = \frac{1}{\bar{P}^+}(1,0,0,-1)$, so that $\tilde{p}^2 = n^2 = 0$ and $\tilde{p} \cdot n = 1$. Before we can express all momenta in terms of $\tilde{p}^\mu$, n^μ and $\vec{\Delta}^\mu_\perp$ we introduce the skewedness variable ξ as momentum fraction of the momentum transfer

variable $\Delta = q - q'$ along the $\tilde{p}^\mu$ direction:

$$\Delta^+ = -2\xi \bar{P}^+ \quad . \tag{2.1}$$

Then we find

$$\begin{aligned}
\bar{P}^\mu =& \tilde{p}^\mu + \frac{\bar{m}^2}{2} n^\mu \\
\Delta^\mu =& -2\xi \tilde{p}^\mu + \Delta_\perp^\mu + \xi \bar{m}^2 n^\mu \\
P^\mu =& \bar{P}^\mu - \frac{\Delta^\mu}{2} = (1+\xi)\tilde{p}^\mu - \frac{\Delta_\perp^\mu}{2} + \frac{1-\xi}{2}\bar{m}^2 n^\mu \\
P'^\mu =& \bar{P}^\mu + \frac{\Delta^\mu}{2} = (1-\xi)\tilde{p}^\mu + \frac{\Delta_\perp^\mu}{2} + \frac{1+\xi}{2}\bar{m}^2 n^\mu \\
q^\mu =& -2\xi' \tilde{p}^\mu + \frac{Q^2}{4\xi'} n^\mu \\
q'^\mu =& q^\mu - \Delta^\mu = -2(\xi' - \xi)\tilde{p}^\mu - \Delta_\perp^\mu + \Big(\frac{Q^2}{4\xi'} - \xi \bar{m}^2\Big) n^\mu
\end{aligned}$$

with

$$\begin{aligned}
\bar{m}^2 =& M_N^2 - \frac{\Delta^2}{4} \\
\xi' =& \frac{\bar{P}\cdot q}{\bar{m}^2}\Big(-1 + \sqrt{1 + \frac{Q^2 \bar{m}^2}{(\bar{P}\cdot q)^2}}\Big) \\
\xi =& \xi' \frac{Q^2 - \Delta^2}{Q^2 + 4\xi'^2 \bar{m}^2} \quad .
\end{aligned}$$

Here ξ and ξ' are fixed by the conditions $q^2 = -Q^2$ and $q'^2 = 0$.

Analogously to DIS one can consider the limit of high photon virtualities, i.e. the Bjorken limit $Q^2 = -q^2 \to \infty$, $P \cdot q \to \infty$ and $Q^2/P \cdot q$ finite. In this limit the hadronic tensor is dominated by the so called handbag diagrams:

Then in the Bjorken limit one has

$$\xi' = \xi = \frac{x_B/2}{1 - x_B/2} \quad .$$

As the longitudinal momentum fractions of the nucleons cannot be negative ξ is bounded by

$$0 < \xi < \frac{\sqrt{-t}}{\sqrt{4\bar{m}^2}} < 1 \quad .$$

It is useful to express $\vec{\Delta}_\perp$ in terms of ξ and t. One obtains

$$\vec{\Delta}_\perp^2 = -(1-\xi^2)t - 4\xi^2 M_N^2 \quad .$$

The DVCS amplitude can be evaluated by contracting the photon polarization vectors with the hadronic tensor $H^{\mu\nu}$

$$T = \epsilon_\mu(q)\epsilon_\nu^\star(q') H^{\mu\nu}$$

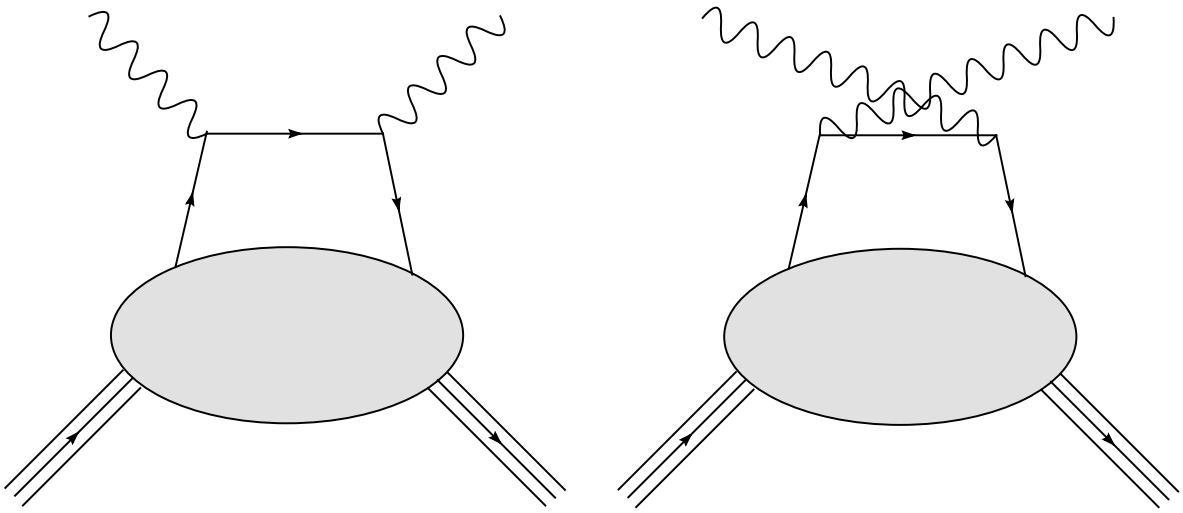

Figure 2.2: *The dominant DVCS contributions, the handbag diagrams.*

with

$$H^{\mu\nu} = -i \int d^4y e^{-i(q\cdot y)} \langle P' \mid T\big[J^\mu(y), J^\nu(0)\big] \mid P\rangle \quad .$$

Since the DVCS process takes place at zero transverse separation ($\vec{y}_\perp = 0$) and equal **LF** time ($y^+ = 0$) it is convenient to introduce the notation $y^\mu = \lambda n^\mu$ to simplify the evaluation of the hadronic tensor. In the Bjorken regime the evaluation of the handbag diagrams yields

$$\begin{aligned} H^{\mu\nu} = &-\frac{1}{4\pi}\int_{-1}^{1} dx \Bigg[(\tilde{p}^\mu n^\nu + \tilde{p}^\nu n^\mu - g^{\mu\nu}) \cdot \Big(\frac{1}{x-\xi+i\epsilon} + \frac{1}{x+\xi-i\epsilon}\Big) \\ &\cdot \int d\lambda e^{i\lambda x} \langle P' \mid \bar{\psi}(-\frac{\lambda n}{2}) \not{n} \tau_3 \psi(\frac{\lambda n}{2}) \mid P\rangle_{y^+=0,\vec{y}_\perp=\vec{0}} - i\epsilon^{\mu\nu\alpha\beta}\tilde{p}_\alpha n_\beta \\ &\Big(\frac{1}{x-\xi+i\epsilon} - \frac{1}{x+\xi-i\epsilon}\Big) \cdot \int d\lambda e^{i\lambda x} \langle P' \mid \bar{\psi}(-\frac{\lambda n}{2}) \not{n} \tau_3 \gamma_5 \psi(\frac{\lambda n}{2}) \mid P\rangle_{y^+=0,\vec{y}_\perp=\vec{0}} \Bigg] \quad . \end{aligned} \tag{2.2}$$

We call the objects

$$G^{+(N\to N)}_{V,\lambda'\lambda} = \int \frac{d\lambda}{4\pi} e^{i\lambda x} \langle P', \lambda' \mid \bar{\psi}_q(-\frac{\lambda n}{2}) \not{n} \tau_3 \psi_q(\frac{\lambda n}{2}) \mid P, \lambda\rangle_{y^+=0,\vec{y}_\perp=\vec{0}} \tag{2.3}$$

and

$$G^{+(N\to N)}_{A,\lambda'\lambda} = \int \frac{d\lambda}{4\pi} e^{i\lambda x} \langle P', \lambda' \mid \bar{\psi}_q(-\frac{\lambda n}{2}) \not{n} \tau_3 \gamma_5 \psi_q(\frac{\lambda n}{2}) \mid P, \lambda\rangle_{y^+=0,\vec{y}_\perp=\vec{0}}$$

vectorial and axial (soft) transition amplitudes respectively. Since the quark fields in the bilocal operator have a non zero light like separation one should introduce a gauge link

$$P\, e^{ig\int dx^\mu A_\mu}$$

here to ensure color gauge invariance of the expressions. However one can choose the light cone gauge $A^+ = 0$ in which this gauge link becomes unity. Therefore it will be suppressed in

all further expressions. Using all possible covariants one parameterizes these amplitudes by

$$G^{+(N\to N)}_{V,\lambda'\lambda} = \frac{1}{2\bar{P}^+}\bar{u}(P',\lambda')\left(\not{n}H^q(x,\xi,t) + \frac{i\sigma^{\mu\nu}n_\mu}{2M_N}\Delta_\nu E^q(x,\xi,t)\right)u(P,\lambda)$$

and

$$G^{+(N\to N)}_{A,\lambda'\lambda} = \frac{1}{2\bar{P}^+}\bar{u}(P',\lambda')\left(\not{n}\gamma_5\tilde{H}^q(x,\xi,t) + \frac{\Delta\cdot n}{2M_N}\gamma_5\tilde{E}^q(x,\xi,t)\right)u(P,\lambda) \quad .$$

The objects which appear in this parametrization are called generalized parton distributions (GPDs). They can depend on the kinematical variables ξ and t. Additionally they depend on the average quark momentum fraction x and a renormalization scale μ which we will suppress in the following. Here we have defined the momentum transfer variable

$$t = \Delta^2 \quad .$$

The average quark light front momentum fraction x is defined as $\bar{k}^+ = \frac{1}{2}(k^+ + k'^+) = x\bar{P}^+$ with k and k' being the momenta of the initial and the final quark momenta in the handbag diagrams. Thus the support in x of the GPDs is $[-1,1]$ with a negative momentum fraction corresponding to the antiquark contribution.

These GPDs parameterize the soft, i.e. the non perturbative part

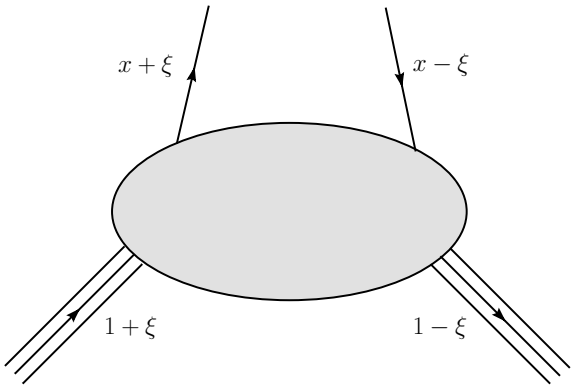

Figure 2.3: *The soft amplitude which is parameterized by GPDs.*

of the hadronic tensor. Since GPDs are kinematically richer than the parton distributions which parameterize DIS one can gain more physical insight into the nucleon structure from them. In fact in the limit $\Delta^\mu \to 0$ they reduce to the ordinary parton distributions

$$H^q(x,0,0) = \begin{cases} q(x), & x>0 \\ -\bar{q}(-x), & x<0 \end{cases}$$
$$\tilde{H}^q(x,0,0) = \begin{cases} \Delta q(x), & x>0 \\ \Delta\bar{q}(-x), & x<0 \end{cases} \quad .$$

The GPDs $E(x,\xi,t)$ and $\tilde{E}(x,\xi,t)$ have no analogous limit since the associated tensors in DIS vanish in the forward limit $\Delta^\mu \to 0$. Hence $E(x,\xi,t)$ and $\tilde{E}(x,\xi,t)$ are new leading twist objects which can only be accessed in hard exclusive electroproduction processes.

The first moment of the GPDs establishes another link to known observables. By integrating over x one obtains the relations

$$\begin{aligned}
\int_{-1}^{1} dx\, H^q(x,\xi,t) =& F_1^q(t) \\
\int_{-1}^{1} dx\, E^q(x,\xi,t) =& F_2^q(t) \\
\int_{-1}^{1} dx\, \tilde{H}^q(x,\xi,t) =& G_A^q(t) \\
\int_{-1}^{1} dx\, \tilde{E}^q(x,\xi,t) =& G_P^q(t) \quad .
\end{aligned}$$

Here e.g $F_1^q(t)$ represents the elastic Dirac form factor for the quark flavor q in the nucleon. Using isospin symmetry and neglecting the contributions from the strange quark sea one can express the usual form factors by

$$\begin{aligned}
F_1^p(t) =& \frac{2}{3}F_1^u(t) - \frac{1}{3}F_1^d(t) \\
F_1^n(t) =& \frac{2}{3}F_1^d(t) - \frac{1}{3}F_1^u(t) \\
F_2^p(t) =& \frac{2}{3}F_2^u(t) - \frac{1}{3}F_2^d(t) \\
F_2^n(t) =& \frac{2}{3}F_2^d(t) - \frac{1}{3}F_2^u(t) \\
G_A(t) =& G_A^u(t) - G_A^d(t) \\
\overset{0}{G}_A(t) =& G_A^u(t) + G_A^d(t) \\
G_P(t) =& G_P^u(t) - G_P^d(t) \\
\overset{0}{G}_P(t) =& G_P^u(t) + G_P^d(t)
\end{aligned}$$

where $G_A(t)$ ($\overset{0}{G}_A(t)$) are the isovector (isoscalar) axial form factors of the nucleon and similarly $G_P(t)$ ($\overset{0}{G}_P(t)$) are the isovector (isoscalar) pseudo axial form factors of the nucleon.

From equation 2.2 one can see that the GPDs cannot be accessed directly in DVCS. Instead one measures a convolution with x.

An interesting sum rule can be obtained by considering the form factors of the energy momentum tensor

For the convenient expression of the symmetric energy momentum tensor we introduce the notation

$$a^{(\mu}b^{\nu)} = \frac{1}{2}(a^\mu b^\nu + a^\nu b^\mu) \quad .$$

Then the transition amplitude for the energy momentum tensor can be expressed in terms of

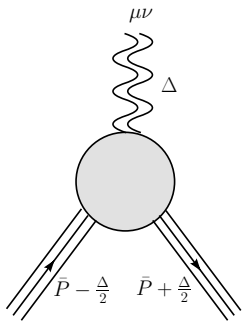

Figure 2.4: *The graviton form factor.*

graviton form factors:

$$\begin{aligned}\langle \bar{P}+\frac{\Delta}{2} \mid T^{\mu\nu}(0) \mid \bar{P}-\frac{\Delta}{2}\rangle =&\frac{1}{2\bar{P}^+}\bar{u}(\bar{P}+\frac{\Delta}{2})\bigg(A(t)\gamma^{(\mu}\bar{P}^{\nu)}+B(t)\bar{P}^{(\mu}i\sigma^{\nu)\alpha}\frac{\Delta_\alpha}{2M_N}\\ &+C(t)\frac{1}{M_N}(\Delta^\mu\Delta^\nu-tg^{\mu\nu})+\bar{C}(t)M_N g^{\mu\nu}\bigg)u(\bar{P}-\frac{\Delta}{2})\\ =&\frac{1}{2\bar{P}^+}\bar{u}(\bar{P}+\frac{\Delta}{2})\bigg(A(t)\frac{\bar{P}^\mu\bar{P}^\nu}{M_N}+(A(t)+B(t))\bar{P}^{(\mu}i\sigma^{\nu)\alpha}\frac{\Delta_\alpha}{2M_N}\\ &+C(t)\frac{1}{M_N}(\Delta^\mu\Delta^\nu-tg^{\mu\nu})+\bar{C}(t)M_N g^{\mu\nu}\bigg)u(\bar{P}-\frac{\Delta}{2}) \quad .\end{aligned}$$

In the last line the Gordon identity has been used. Now one can consider the angular momentum operator

$$\begin{aligned}J\langle \bar{P},\uparrow\mid \bar{P},\uparrow\rangle =&\langle \bar{P},\uparrow\mid \widehat{J}^{12}\mid \bar{P},\uparrow\rangle\\ =&\epsilon_{ij3}\langle \bar{P},\uparrow\mid \int d^3\vec{x}\,x^i T^{0j}(x)\mid \bar{P},\uparrow\rangle\\ =&\epsilon_{ij3}\lim_{\Delta\to 0}\int d^3\vec{x}\langle \bar{P}+\frac{\Delta}{2},\uparrow\mid x^i e^{-i\vec{x}\cdot\vec{\Delta}}T^{0j}(0)\mid \bar{P}-\frac{\Delta}{2},\uparrow\rangle\\ =&\epsilon_{ij3}\lim_{\Delta\to 0}\bigg(\Big[-i\frac{\partial}{\partial\Delta^i}(2\pi)^3\delta^{(3)}(\vec{\Delta})\Big]\Big[A(t)+B(t)\Big]\\ &\cdot\frac{1}{2\bar{P}^+}\bar{u}(\bar{P}+\frac{\Delta}{2})\bar{P}^{(0}i\sigma^{j)\alpha}\frac{\Delta_\alpha}{2M_N}u(\bar{P}-\frac{\Delta}{2})\bigg)\\ =&-\epsilon_{ij3}(2\pi)^3\delta^{(3)}(0)\Big[A(0)+B(0)\Big]\frac{1}{2M_N}\frac{1}{2\bar{P}^+}\bar{u}(\bar{P})\cdot\frac{1}{2}\Big[\bar{P}^0\sigma^{ji}+\bar{P}^j\sigma^{0i}\Big]u(\bar{P}) \quad .\end{aligned}$$

Without loss of generality we consider the rest frame $\bar{P}^\mu=(M_N,0,0,0)$. Then one finds

$$\begin{aligned}\langle \bar{P},\uparrow\mid \widehat{J}^{12}\mid \bar{P},\uparrow\rangle =&2\pi^3\delta^{(3)}(0)\Big[A(0)+B(0)\Big]\frac{1}{2}\frac{1}{2\bar{P}^+}\bar{u}(\bar{P})\sigma^{12}u(\bar{P})\\ =&\frac{1}{2}\Big[A(0)+B(0)\Big]\langle \bar{P},\uparrow\mid \bar{P},\uparrow\rangle \quad .\end{aligned}$$

So one can conclude that the quark angular momentum can be expressed in terms of the graviton form factors $A(t)$ and $B(t)$ at $t = 0$.

$$J = \frac{1}{2}\Big[A(0) + B(0)\Big] \quad .$$

Physically one can interpret J as total spin of the nucleon which can be decomposed into a quark and a gluonic contribution $J^q + J^g = \frac{1}{2}$:

$$J^{q,g} = \frac{1}{2}\Big(A^{q,g}(0) + B^{q,g}(0)\Big) \quad .$$

We can establish a connection between the tensorial form factors and the GPDs by contracting the tensorial transition amplitude with $n_\mu n_\nu$. The quark contribution to the energy momentum tensor reads

$$\begin{aligned} T_q^{\mu\nu} =& \frac{1}{2}\Big(\bar\psi_q \gamma^{(\mu} i\vec{D}^{\nu)}\psi_q + \bar\psi_q \gamma^{(\mu} i\overleftarrow{D}^{\nu)}\psi_q\Big) \\ =& : \bar\psi_q \gamma^{(\mu} i\overleftrightarrow{D}^{\nu)}\psi_q \quad . \end{aligned}$$

Then one finds

$$\begin{aligned} &\langle \bar P + \frac{\Delta}{2} \mid T_q^{\mu\nu}(0) \mid \bar P - \frac{\Delta}{2}\rangle n_\mu n_\nu \\ =&\langle \bar P + \frac{\Delta}{2} \mid \bar\psi_q(0) i\gamma^{(\mu} \overleftrightarrow{D}^{\nu)}\psi_q(0) \mid \bar P - \frac{\Delta}{2}\rangle n_\mu n_\nu \\ =&\frac{1}{2\bar P^+}\bar u(\bar P + \frac{\Delta}{2})\left(\frac{1}{M_N}\Big[A(t) + 4\xi^2 C(t)\Big] + \Big[A(t) + B(t)\Big] i\sigma^{\nu\alpha}\frac{\Delta_\alpha}{2M_N} n_\nu\right) u(\bar P - \frac{\Delta}{2}) \quad . \end{aligned}$$

On the other hand side one has

$$\begin{aligned} &\int_{-1}^{1} dx\, \frac{\bar P^+}{2\pi}\int dy^- e^{ix\bar P^+ y^-}\langle \bar P + \frac{\Delta}{2} \mid \bar\psi_q(-\frac{y}{2}) i\not{n}(n\cdot\overleftrightarrow{D})\psi_q(\frac{y}{2}) \mid \bar P - \frac{\Delta}{2}\rangle_{y^+=0,\vec y_\perp=0} \\ =&\int_{-1}^{1} dx\, x\, \frac{\bar P^+}{2\pi}\int dy^- e^{ix\bar P^+ y^-}\langle \bar P + \frac{\Delta}{2} \mid \bar\psi_q(-\frac{y}{2})\not{n}\psi_q(\frac{y}{2}) \mid \bar P - \frac{\Delta}{2}\rangle_{y^+=0,\vec y_\perp=0} \\ =&\int_{-1}^{1} dx\, \frac{1}{2\bar P^+}\bar u(\bar P + \frac{\Delta}{2})\left(\frac{1}{M_N} x\, H(x,\xi,t) + x\Big[H(x,\xi,t) + E(x,\xi,t)\Big] i\sigma^{\nu\alpha}\frac{\Delta_\alpha}{2M_N}\right) u(\bar P - \frac{\Delta}{2}) \quad . \end{aligned}$$

And finally one has

$$\begin{aligned} &\int_{-1}^{1} dx\, x\, G^{+(N\to N)}_{V,\lambda'\lambda} \\ =&\int_{-1}^{1} dx\, x \frac{\bar P^+}{2\pi}\int dy^-\, e^{ix\bar P^+ y^-}\langle \bar P + \frac{\Delta}{2} \mid \bar\psi_q(-\frac{y}{2})\not{n}\psi_q(\frac{y}{2}) \mid \bar P - \frac{\Delta}{2}\rangle_{y^+=0,\vec y_\perp=\vec 0} \\ =&\int dy^- \frac{\bar P^+}{2\pi}\int_{-1}^{1} dx\, e^{ix\bar P^+ y^-}\langle \bar P + \frac{\Delta}{2} \mid \bar\psi_q(-\frac{y}{2}) i\not{n}\overleftrightarrow{D}^{\nu} n_\nu \psi_q(\frac{y}{2}) \mid \bar P - \frac{\Delta}{2}\rangle_{y^+=0,\vec y_\perp=\vec 0} \\ =&\int dy^- \delta(y^-)\langle \bar P + \frac{\Delta}{2} \mid \bar\psi_q(-\frac{y}{2}) i\not{n}\overleftrightarrow{D}^{\nu} n_\nu \psi_q(\frac{y}{2}) \mid \bar P - \frac{\Delta}{2}\rangle_{y^+=0,\vec y_\perp=\vec 0} \\ =&\langle \bar P + \frac{\Delta}{2} \mid \bar\psi_q(0) i\not{n}\overleftrightarrow{D}^{\nu} n_\nu \psi_q(0) \mid \bar P - \frac{\Delta}{2}\rangle \\ =&\langle \bar P + \frac{\Delta}{2} \mid T_q^{\mu\nu}(0) \mid \bar P - \frac{\Delta}{2}\rangle n_\mu n_\nu \quad . \end{aligned}$$

Comparing the expressions one can read off

$$\int_{-1}^{1} dx\, x\Big[H^q(x,\xi,t) + E^q(x,\xi,t)\Big] = A^q(t) + B^q(t)$$

and hence arrive at Ji's sum rule [27]

$$J^q = \frac{1}{2}\int_{-1}^{1} dx\, x\Big[H^q(x,\xi,0) + E^q(x,\xi,0)\Big] \quad .$$

Physically J^q is the fraction of the nucleon angular momentum that is carried by a quark of the flavor q. The quark angular momentum can be decomposed into a sum of intrinsic quark spin and the orbital contribution.

$$J^q = \frac{1}{2}\Delta\Sigma + L^q \quad .$$

In 1971 Ellis and Jaffe proposed a sum rule [28] based on the assumption that the nucleon spin is mainly given by the valence quark contributions. However the EMC collaboration [29] found a significant deviation of the Ellis Jaffe sum rule which revealed that this could not be correct. Now Ji's sum rule provides an additional tool to address the spin structure of the nucleon experimentally. In fact most of the nucleon spin is carried by the quark angular momentum [30] in contradiction to the oversimplified picture of the nucleon.

By considering higher spin twist 2 local operators one can derive an other interesting property of the nucleon GPDs, the so called polynomiality property. Using Lorentz invariance one can show that the N'th Mellin moment of the GPDs are polynomials of the maximal order $N+1$ [24].

$$\begin{aligned}\int_{-1}^{1} dx\, x^N\, H^q(x,\xi) =& h_0^{q(N)} + h_2^{q(N)}\xi^2 + ... + h_{N+1}^{q(N)}\xi^{N+1} \\ \int_{-1}^{1} dx\, x^N\, E^q(x,\xi) =& e_0^{q(N)} + e_2^{q(N)}\xi^2 + ... + e_{N+1}^{q(N)}\xi^{N+1} \quad .\end{aligned}$$

Time reversal invariance dictates that the polynomials only contain even powers of the skewedness parameter ξ. This implies that the highest power of ξ is $N+1$ for odd N and N for even N. Additionally the highest power of ξ for H^q and E^q are related for odd N:

$$e_{N+1}^{q(N)} = -h_{N+1}^{q(N)} \quad .$$

One can check whether the polynomiality condition is satisfied by evaluating the integral constraints

$$\int_{-1}^{1} \frac{dx}{x}\Big(H^q(x,\xi+xz) - H^q(x,\xi)\Big) = -\int_{-1}^{1} \frac{dx}{x}\Big(E^q(x,\xi+xz) - E^q(x,\xi)\Big) = z\sum_{n=0}^{\infty} h_{N+1}^{q(N)} z^N \quad .$$

A way to model GPDs such that the polynomiality condition is automatically satisfied by introducing so called double distributions has been proposed [31].

Besides the soft transition amplitudes which we have discussed in eqs. 2.3 and 2.4 one can construct four additional twist 2 soft transition amplitudes in QCD [33] and [34], namely

$$\begin{aligned}
&\int \frac{d\lambda}{4\pi} e^{i\lambda x} \langle P', \lambda' \mid \bar{\psi}_q(-\frac{\lambda n}{2}) i\sigma^{\mu i} n_\mu \psi_q(\frac{\lambda n}{2}) \mid P, \lambda \rangle \\
=&\frac{1}{2\bar{P}^+} \bar{u}(P', \lambda') \Bigg(H_T^q(x,\xi,t) i\sigma^{\mu i} n_\mu + \tilde{H}_T^q(x,\xi,t) \frac{(\bar{P}\cdot n)\Delta^i - (\Delta \cdot n)\bar{P}^i}{M_N^2} \\
&+ E_T^q(x,\xi,t) \frac{\left(\not{n} \Delta^i - \gamma^i (\Delta \cdot n) \right)}{2M_N} + \tilde{E}_T^q(x,\xi,t) \frac{\not{n} \bar{P}^i - (\bar{P}\cdot n)\gamma^i}{M_N} \Bigg) u(P,\lambda)
\end{aligned}$$

$$\begin{aligned}
&\int \frac{d\lambda}{4\pi} e^{i\lambda x} \langle P', \lambda' \mid F^{\nu i}(-\frac{\lambda n}{2}) n_\nu F^{\mu i}(\frac{\lambda n}{2}) n_\mu \mid P, \lambda \rangle_{y^+=0, \vec{y}_\perp = \vec{0}} \\
=&\frac{1}{2\bar{P}^+} \bar{u}(P', \lambda') \Bigg(H^g(x,\xi,t) \not{n} + E^g(x,\xi,t) \frac{i\sigma^{\mu\alpha} n_\mu \Delta_\alpha}{2M_N} \Bigg) u(P,\lambda)
\end{aligned}$$

$$\begin{aligned}
&- i \int \frac{d\lambda}{4\pi} e^{i\lambda x} \langle P', \lambda' \mid F^{\nu i}(-\frac{\lambda n}{2}) n_\nu \tilde{F}^{\mu i}(\frac{\lambda n}{2}) n_\mu \mid P, \lambda \rangle_{y^+=0, \vec{y}_\perp = \vec{0}} \\
=&\frac{1}{2\bar{P}^+} \bar{u}(P', \lambda') \Bigg(\tilde{H}^g(x,\xi,t) \not{n} \gamma_5 + \tilde{E}^g(x,\xi,t) \frac{(\Delta \cdot n)\gamma_5}{2M_N} \Bigg) u(P,\lambda)
\end{aligned}$$

$$\begin{aligned}
&- \int \frac{d\lambda}{4\pi} e^{i\lambda x} \langle P', \lambda' \mid \mathbf{S} F^{\mu i}(-\frac{\lambda n}{2}) n_\mu F^{\nu j}(\frac{\lambda n}{2}) n_\nu \mid P, \lambda \rangle_{y^+=0, \vec{y}_\perp = \vec{0}} \\
=&\mathbf{S} \frac{(\bar{P}\cdot n)\Delta^j - (\Delta \cdot n)\bar{P}^j}{2M_N \bar{P}^+} \frac{1}{2\bar{P}^+} \bar{u}(P', \lambda') \Bigg(H_T^g(x,\xi,t) i\sigma^{\mu i} n_\mu + \tilde{H}_T^g(x,\xi,t) \frac{(\bar{P}\cdot n)\Delta^i - (\Delta \cdot n)\bar{P}^i}{M_N^2} \\
&+ E_T^g(x,\xi,t) \frac{\not{n} \Delta^i - (\Delta \cdot n)\gamma^i}{2M_N} + \tilde{E}_T^g \frac{\not{n} \bar{P}^i - (\bar{P}\cdot n)\gamma^i}{M_N} \Bigg) u(P,\lambda) \quad .
\end{aligned}$$

Here i and j have to be chosen as transverse indices in order to guarantee non vanishing transition amplitudes. $\mathbf{S}$ denotes symmetrization of the indices i and j and subtraction of the trace. The dual tensor $\tilde{F}^{\mu\nu}$ is defined by $\tilde{F}^{\mu\nu} = \frac{1}{2}\epsilon^{\mu\nu\rho\lambda} F_{\rho\lambda}$. Again we have suppressed the gauge link appearing in the bilocal operators by assuming light cone gauge. The corresponding GPDs allow for additional insights into the quark and gluon structure of the nucleon.

While $H^q(x,\xi,t)$, $E^q(x,\xi,t)$, $\tilde{H}^q(x,\xi,t)$ and $\tilde{E}^q(x,\xi,t)$ conserve quark helicity the chiral odd GPDs $H_T^q(x,\xi,t)$, $E_T^q(x,\xi,t)$, $\tilde{H}_T^q(x,\xi,t)$ and $\tilde{E}_T^q(x,\xi,t)$ flip the quark helicity of the struck quark. While the chiral even GPDs can be accessed experimentally in various hard exclusive processes the situation is more difficult for the chiral odd GPDs. While at least one process has been proposed to study the chiral odd GPDs experimentally [32] the prospects are less promising for these GPDs. Similarly for the gluons there exist four chiral even (gluon helicity conserving) and four chiral odd GPDs.

Although $H_T^q(x,\xi,t)$, $E_T^q(x,\xi,t)$, $\tilde{H}_T^q(x,\xi,t)$ and $\tilde{E}_T^q(x,\xi,t)$ are accessible in the framework of

quark models [35] we will restrict further investigation to the GPDs defined in eqs. 2.3 and 2.4 in the following chapters.

In order to extract GPDs from experimental data it is important to ensure that power corrections to the leading twist parametrization of the soft amplitude are small. In [25] factorization to all orders at leading twist has been proven for DVCS. This proof involved the operator product expansion in which the bilocal operator $\bar{\psi}(-\frac{\lambda n}{2})\mathcal{O}\psi(\frac{\lambda n}{2})$ is expressed in an infinite series of higher spin local operators. Thus the DVCS amplitude factorizes into a hard and a soft part with the latter containing the nonperturbative physics which is parameterized by the GPDs.

DVCS can be considered beyond leading twist. For example in [36] it has been considered to twist 3 accuracy. The authors give a parametrization for the soft amplitudes including twist 3 GPDs. They find

$$\begin{aligned} G^{\mu(N\to N)}_{V,\lambda'\lambda} &= \int \frac{d\lambda}{4\pi} e^{i\lambda x} \langle P',\lambda' \mid \bar{\psi}_q(-\frac{\lambda n}{2}) \not{n} \tau_3 \psi_q(\frac{\lambda n}{2}) \mid P,\lambda\rangle_{y^+=0,\vec{y}_\perp=\vec{0}} \\ &= \frac{1}{2\bar{P}^+}\bar{u}(P',\lambda')\Bigg(\gamma^\mu H(x,\xi,t) + \frac{i\sigma^{\mu\nu}}{2M_N}E(x,\xi,t) \\ &\quad + \frac{\Delta^\mu_\perp}{M_N}\Big[G_1(x,\xi,t) + M_N \not{n} G_2(x,\xi,t)\Big] + \gamma^\mu_\perp G_3(x,\xi,t)\Bigg) u(P,\lambda) \end{aligned}$$

and

$$\begin{aligned} G^{\mu(N\to N)}_{A,\lambda'\lambda} &= \int \frac{d\lambda}{4\pi} e^{i\lambda x} \langle P',\lambda' \mid \bar{\psi}_q(-\frac{\lambda n}{2}) \not{n} \tau_3 \gamma_5 \psi_q(\frac{\lambda n}{2}) \mid P,\lambda\rangle_{y^+=0,\vec{y}_\perp=\vec{0}} \\ &= \frac{1}{2\bar{P}^+}u(P',\lambda')\Bigg(\gamma^\mu\gamma_5 \tilde{H}(x,\xi,t) + \frac{\Delta^\mu}{2M_N}\gamma_5 \tilde{E}(x,\xi,t) \\ &\quad + \frac{\Delta^\mu_\perp}{M_N}\gamma_5 \tilde{G}_1(x,\xi,t) + \gamma^\mu_\perp \gamma_5 \tilde{G}_2(x,\xi,t) + \Delta^\mu_\perp \not{n}\gamma_5 \tilde{G}_3(x,\xi,t)\Bigg) u(P,\lambda) \quad . \end{aligned}$$

Actually we claim that only two of the three twist 3 GPDs which they introduce are independent. In chapter 4 we provide a counting argument for the soft amplitudes which shows that there can only be two vectorial and axial twist 3 GPDs each.

We will end the theoretical survey of DVCS by mentioning an intuitive physical interpretation of the GPDs. While form factors can be understood (in the Breit frame) as Fourier transform of the electric charge distribution and magnetization density and the forward parton distributions can be pictured as parton densities in the longitudinal momentum x (in the infinite momentum frame) it took some time after the GPDs had been introduced to develop a similarly intuitive physical picture for the GPDs. In 2002 Burkardt [37] gave an interpretation for GPDs with $\xi = 0$ in impact parameter space. The impact parameter space GPDs are defined by

$$q(x,\vec{b}_\perp) = \int \frac{d^2\vec{\Delta}_\perp}{2\pi^2} H^q(x,-\vec{\Delta}^2_\perp) e^{-i\vec{b}_\perp\cdot\vec{\Delta}_\perp}$$

and analogously for the other GPDs. He showed that these GPDs could be interpreted as parton distributions in the transverse plane for given values of x. This picture was extended

in [38] to finite values of skewedness. In this work quantum phase space Wigner distributions were applied which provide a three dimensional picture of the hadron. A drawback of the use of the Wigner distributions is that a probabilistic interpretation had to be abandoned. In the following two figures we give the results from the latter interpretation.

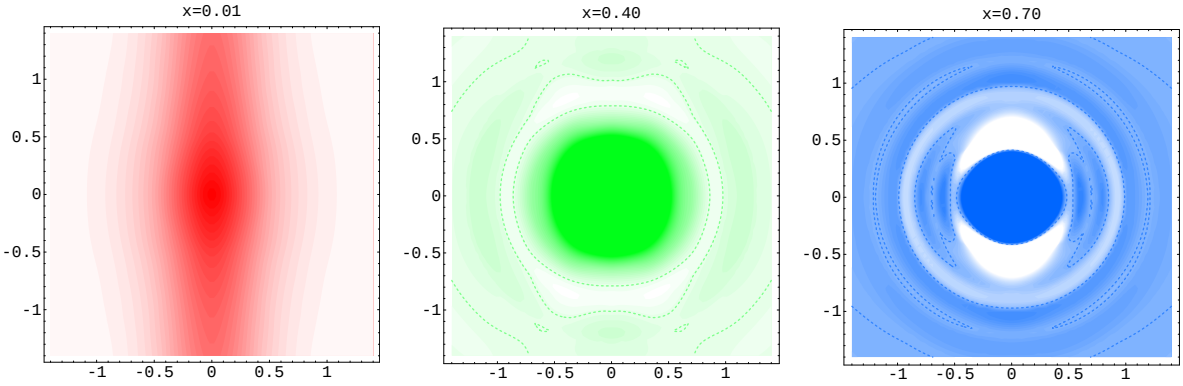

Figure 2.5: *The u-quark phase-space charge distribution at different values of x. The vertical and horizontal axis corresponds to z and $\mid \vec{r}_\perp \mid$ respectively, measured in fm. This figure has been taken from [38]. The GPDs are obtained in a model calculation as specified in the reference.*

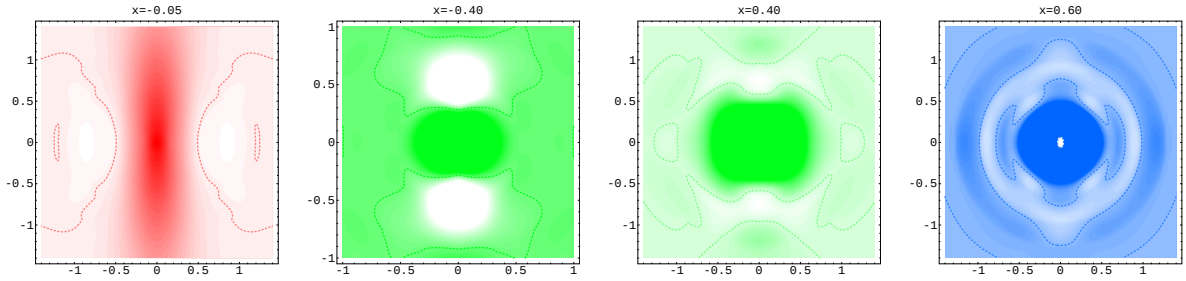

Figure 2.6: *The u-quark phase-space charge distribution at different negative values of x (left panels) and d-quark phase space charge distribution at different values of x. This figure has been taken from [38].*

Next we turn our attention to experimental aspects of DVCS. This process is measured in lepton production of real photons, i.e.

$$e + p \to ep\gamma$$
$$\mu + p \to \mu p\gamma \quad .$$

In the deeply virtual regime the lepton masses become irrelevant for the analysis. One main difficulty in the extraction of GPDs is that apart from Compton scattering the Bethe-Heitler process contributes to the same final state.

Therefore one measures an interference between the Bethe-Heitler amplitude and the Compton amplitude. Defining the inelasticity parameter

$$y = \frac{k \cdot P}{q \cdot P}$$

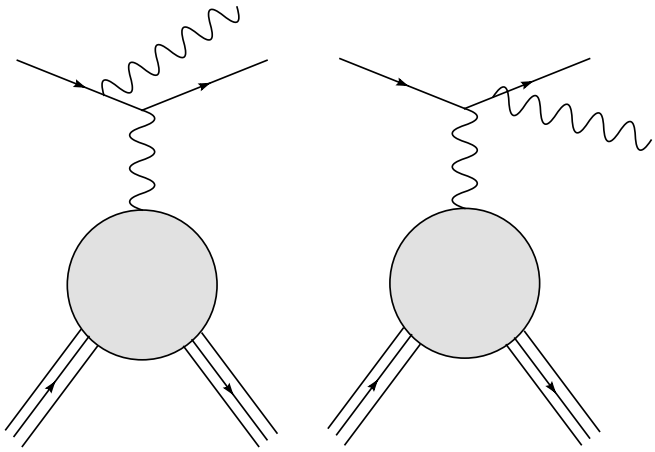

Figure 2.7: *The Bethe-Heitler processes contribute to the amplitude of $ep \to ep\gamma$ scattering.*

and the azimuthal angle between the hadronic and the leptonic plane ϕ as in figure 2.8 the

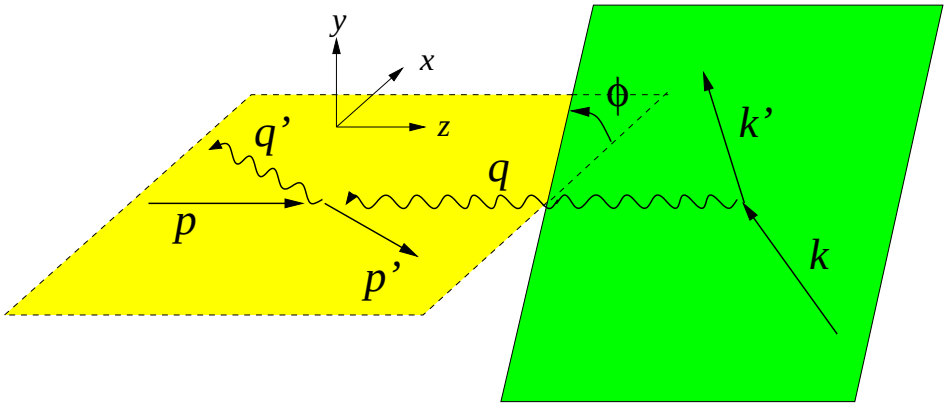

Figure 2.8: *The kinematics of $ep \to ep\gamma$ in the center of mass frame of the final state proton and photon. This figure has been taken from [39].*

differential electroproduction cross section on an unpolarized target reads

$$\frac{d\sigma(ep \to ep\gamma)}{d\phi\, dt\, dQ^2\, dx_B} = \frac{\alpha_{EM}^3}{8\pi} \frac{x_B y^2}{Q^4} \frac{1}{\sqrt{1 + 4x_B^2 \frac{M_N^2}{Q^2}}} \frac{1}{e^6} \sum_{\text{spins}}{}' \mid \mathcal{T}_{VCS} + \mathcal{T}_{BH} \mid^2$$

where $\sum'_{\text{spins}}$ denotes the sum over the spins of the final state proton and photon and the averaging over the initial proton polarization. The condition $Q^2 \gg -t$ in DVCS favors the Bethe-Heitler contribution over the DVCS contribution. This can be counteracted by choosing a small value for y.

The purpose of the first measurements were to test in a model independent way whether the Q^2 behavior followed the factorization theorem prediction, i.e. whether the deeply virtual limit is reached in the accessible kinematical regime. This could be verified by considering

the beam spin asymmetry

$$A(\phi) = \frac{d\sigma(e^{\uparrow}p) - d\sigma(e^{\downarrow}p)}{d\sigma(e^{\uparrow}p) + d\sigma(e^{\downarrow}p)}$$

for which the twist expansion predicts

$$A(\phi) = \alpha sin(\phi) + \beta sin(2\phi) \tag{2.4}$$

with α corresponding to twist 2 contributions and β corresponding to twist 3 contributions. These measurements were performed at HERMES [40] at a lepton beam energy of $E = 27.6$ GeV and at CLAS a similar experiment was performed [41] with $E = 4.25$ GeV, $Q^2 = 1.25$ GeV^2, $x_B = 0.19$, $t = -0.19$ GeV^2. Both results supported the expectation that for the given kinematics one has indeed reached the deeply virtual regime. In fact in each experiment the parameter β was found to be compatible with zero. The results for the beam spin asymmetries is displayed in fig. 2.9.

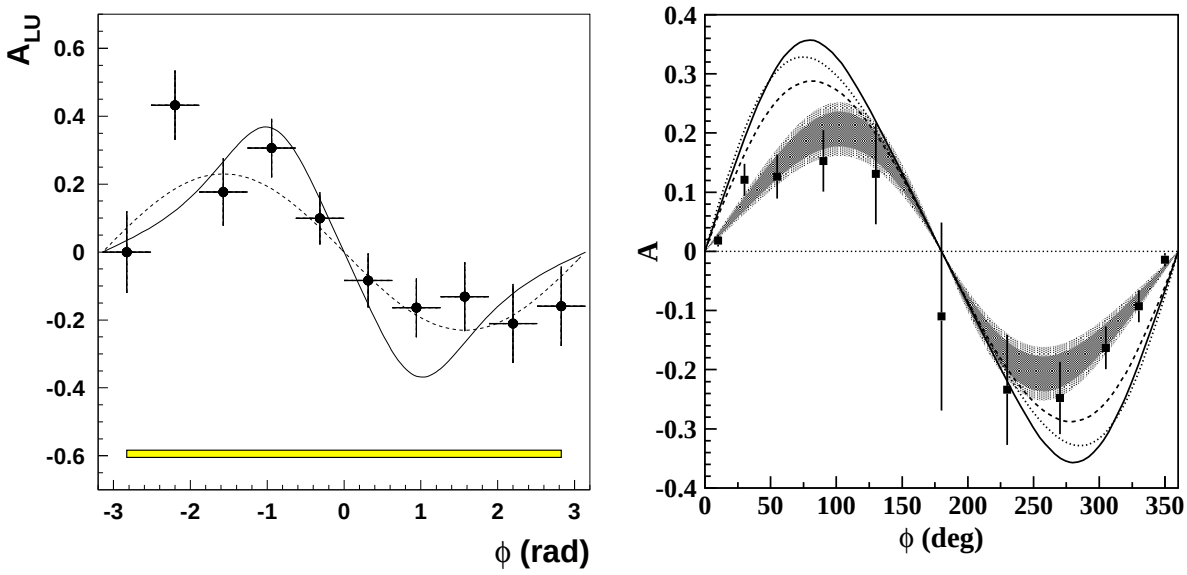

Figure 2.9: *The ϕ dependence of the beam spin asymmetry. The left panel displays the HERMES result. Here the data correspond to the missing mass region between -1.5 and $+1.7$ GeV. The dashed curve represents a $sin(\phi)$ dependence with an amplitude of 0.23, while the solid curve represents the result of a model calculation [42]. The horizontal error bars represent the bin width, and the error band below represents the systematic uncertainty.*
The right panel shows the CLAS result. The dark shaded region is the range of the fitted function $A(\phi)$ from eq. 2.4 defined by the statistical errors of the parameters α and β The light shaded region includes systematic uncertainties added linearly to the statistical uncertainties. The fitted parameters are $\alpha = 0.202 \pm 0.028^{stat} \pm 0.013^{sys}$ and $\beta = -0.024 \pm 0.021^{stat} \pm 0.009^{sys}$. The curves represent three different model calculations.

In both experiments another difficulty in measuring DVCS arose, namely to ensure that one measure exclusively. At HERMES the scattered proton was not detected. Hence one had to deal with background contributions from $ep \to ep\pi^0$. At CLAS the final state photon was not detected. Thus one had to cope with photon dissociation as background process.

The results from the first dedicated DVCS measurements from JLAB/Hall A have been published [43] in 2006. In fig. 2.10 the differential cross sections for DVCS to order twist-3 are displayed. Here $d\Sigma$ denotes the helicity dependent cross section and $d\sigma$ the helicity independent cross section. From these cross sections the angular harmonics $\mathcal{C}^{\mathcal{I}}$ and $\Delta\mathcal{C}^{\mathcal{I}}$ can

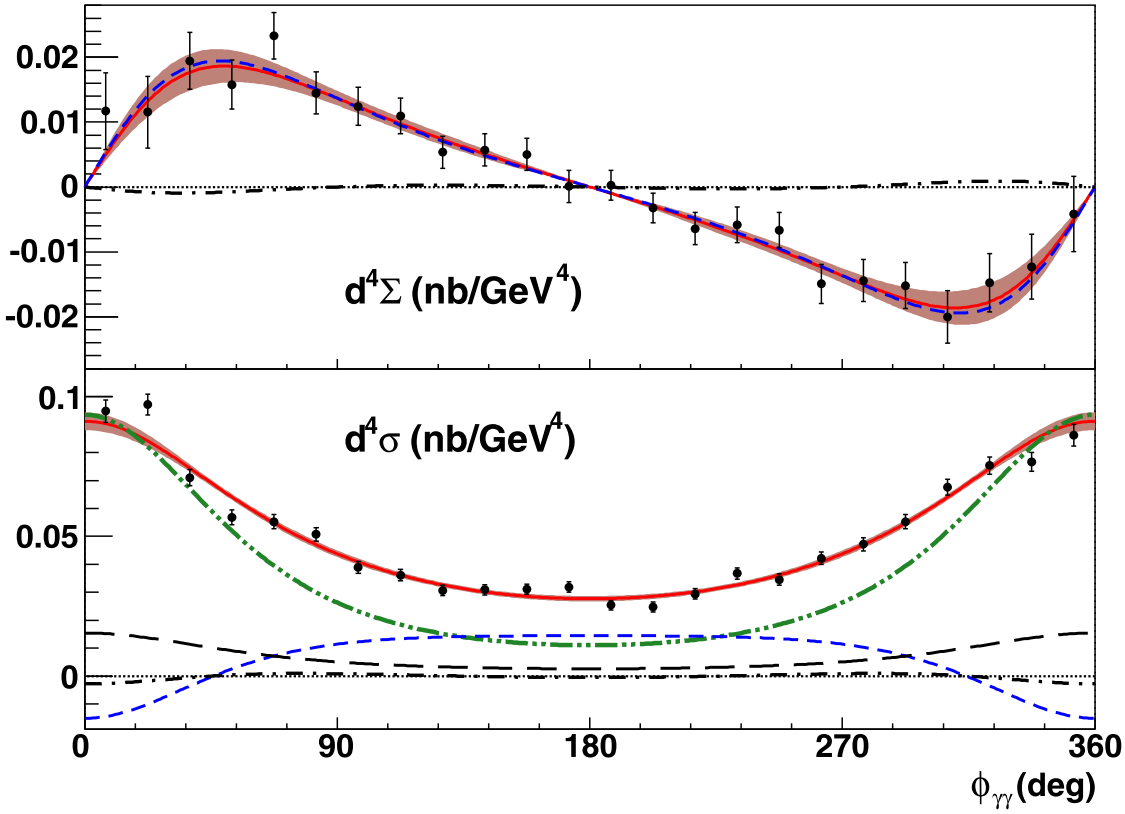

Figure 2.10: *Data and fit to $d^4\Sigma/[dQ^2 dx_{Bj} dt d\phi_{\gamma\gamma}]$ and $d^4\sigma/[dQ^2 dx_{Bj} dt d\phi_{\gamma\gamma}]$ as a function of $\phi_{\gamma\gamma}$. Both are in the bin $\langle Q^2,\, t\rangle = (2.3, -0.28)\ GeV^2$ at $\langle x_{Bj}\rangle = 0.36$. Error bars show statistical uncertainties. Solid lines show total fits with one-σ statistical error bands. For discussion of systematic uncertainties we refer to [43]. The dot-dot-dashed line is the $|$ Bethe-Heitler $|^2$ contribution to $d^4\sigma$. The short dashed lines in $d^4\Sigma$ and $d^4\sigma$ are the fitted Im and Re parts of $\mathcal{C}^{\mathcal{I}}(\mathcal{F})$, respectively. The long-dashed line is the fitted $Re[\mathcal{C}^{\mathcal{I}} + \Delta\mathcal{C}^{\mathcal{I}}](\mathcal{F})$ term. The dot-dashed curves are the fitted Im and Re parts of $\mathcal{C}^{\mathcal{I}}(\mathcal{F}^{eff})$.*

be extracted. They depend on the interference of the Bethe-Heitler amplitude with the set $\mathcal{F} = \{\mathcal{H}, \mathcal{E}, \tilde{\mathcal{H}}, \tilde{\mathcal{E}}\}$ of twist 2 Compton form factors or the related set $\mathcal{F}^{\rm eff}$ of effective twist-3 Compton form factors, namely

$$\begin{aligned}
\mathcal{C}^{\mathcal{I}}(\mathcal{F}) =& F_1\mathcal{H} + \xi G_M \tilde{\mathcal{H}} - \frac{t}{4M_N^2} F_2 \mathcal{E} \\
\mathcal{C}^{\mathcal{I}}(\mathcal{F}^{\rm eff}) =& F_1\mathcal{H}^{\rm eff} + \xi G_M \tilde{\mathcal{H}}^{\rm eff} - \frac{t}{4M_N^2} F_2 \mathcal{E}^{\rm eff} \\
[\mathcal{C}^{\mathcal{I}} + \Delta\mathcal{C}^{\mathcal{I}}](\mathcal{F}) =& F_1\mathcal{H} - \frac{t}{4M_N^2} F_2 \mathcal{E} - \xi^2 G_M (\mathcal{H} + \mathcal{E}) \quad .
\end{aligned}$$

Here the elastic form factors $F_1(t)$, $F_2(t)$ and $G_M(t) = F_1(t) + F_2(t)$ appear. The Compton form factors are defined in terms of the GPDs H^q, E^q, $\tilde{H}^q$ and $\tilde{E}^q$, e.g.

$$\mathcal{H}(x,\xi,t) = \sum_q \left[\frac{e_q}{e}\right]^2 \left\{ i\pi \left[H^q(\xi,\xi,t) - H^q(-\xi,\xi,t)\right] + \mathcal{P}\int_{-1}^{1} dx \frac{2x}{\xi^2 - x^2} H^q(x,\xi,t) \right\} \quad .$$

In fig. 2.11 the angular harmonics are displayed. The left panel demonstrates the absence of a Q^2 dependence of $\mathrm{Im}[\mathcal{C}^{\mathcal{I}}(\mathcal{F})]$ which supports the dominance of twist-2 in the DVCS amplitude. The right panel shows the t dependence of real and imaginary parts of the twist-2 angular harmonics. They are compared with a Regge model calculation which is in qualitative agreement with the experimental findings.

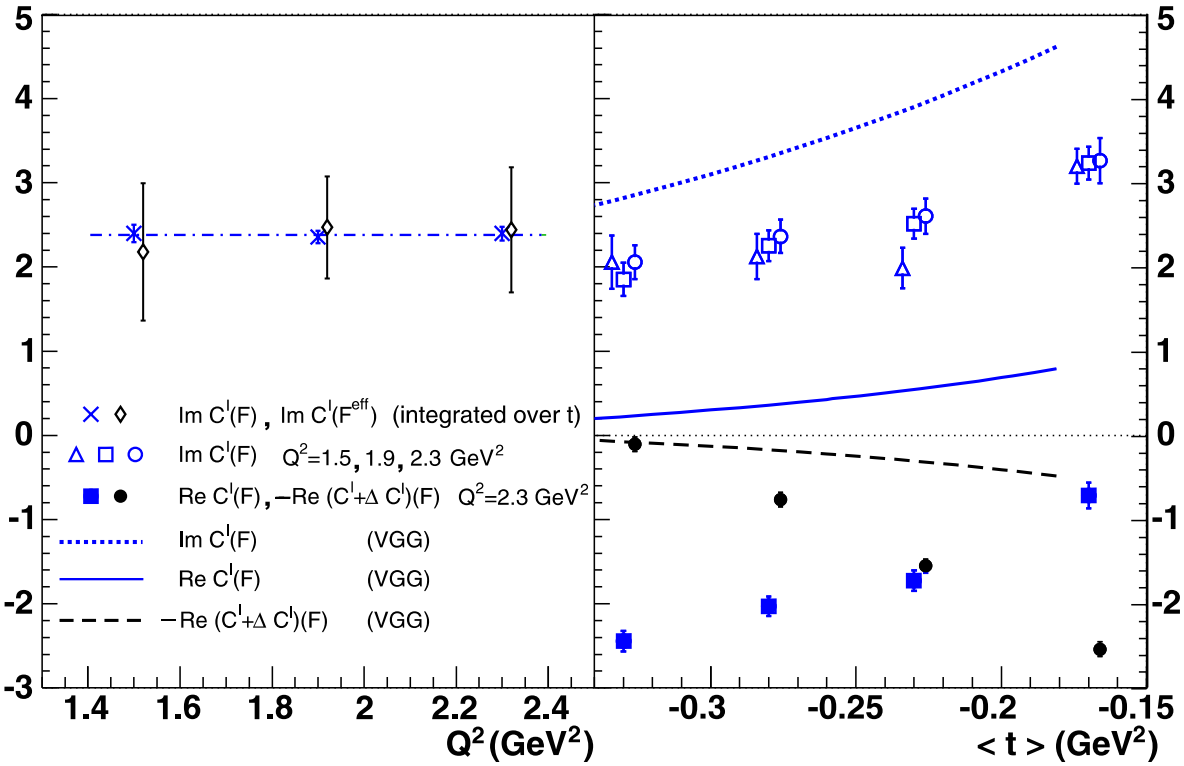

Figure 2.11: *Left: Q^2 dependence of Im parts of (twist-2) $\mathcal{C}^{\mathcal{I}}(\mathcal{F})$ and (twist-3) $\mathcal{C}^{\mathcal{I}}(\mathcal{F}^{eff})$ angular harmonics, averaged over t. The horizontal line is the fitted average of $Im[\mathcal{C}^{\mathcal{I}}(\mathcal{F})]$. Right: Extracted Re and Im parts of the twist-2 angular harmonics as functions of t. The Regge model (VGG [44]) curves are described extensively in [43]. Superposed points in both panels are offset for visual clarity. The error bars show statistical uncertainties.*

In summary one can state that the existing facilities are able to address the measurement of DVCS and therefore GPDs can be regarded not only as a theoretical playground but can be accessed in experiments.

2.2 $N \to \Delta$ DVCS

The study of deeply virtual Compton scattering can be extended towards considering resonant final states. The most prominent example for this is $N \to \Delta$ DVCS. The soft amplitude for this process can be parameterized in terms of $N \to \Delta$ transition GPDs. There exist three independent leading twist GPDs each. We choose the parametrization for the $p \to \Delta^+$ transition

$$\begin{aligned} G_{V,\lambda'\lambda}^{+,(p\to\Delta^+)} =& \int \frac{d\lambda}{4\pi} e^{i\lambda x} \langle \Delta; P', \lambda' \mid \bar{\psi}(-\frac{\lambda n}{2}) \not{n} \tau_3 \psi(\frac{\lambda n}{2}) \mid p; N, \lambda \rangle_{y^+=0, \vec{y}_\perp = \vec{0}} \\ =& \sqrt{\frac{1}{6}} \frac{1}{2\bar{P}^+} \bar{u}_\nu(P', \lambda') \Big[\kappa_M^{+\nu} H_M^\star(x,\xi,t) + \kappa_E^{+\nu} H_E^\star(x,\xi,t) + \kappa_C^{+\nu} H_C^\star(x,\xi,t) \Big] u(P,\lambda) \end{aligned}$$

$$\begin{aligned} G_{A,\lambda'\lambda}^{+,(p\to\Delta^+)} =& \int \frac{d\lambda}{4\pi} e^{i\lambda x} \langle \Delta; P', \lambda' \mid \bar{\psi}(-\frac{\lambda n}{2}) \not{n} \tau_3 \gamma_5 \psi(\frac{\lambda n}{2}) \mid p; N, \lambda \rangle_{y^+=0, \vec{y}_\perp = \vec{0}} \\ =& \frac{1}{2} \frac{1}{2\bar{P}^+} \bar{u}_\nu(P', \lambda') \Big[\tilde{\kappa}_1^{+\nu} C_1(x,\xi,t) + \tilde{\kappa}_2^{+\nu} C_2(x,\xi,t) + \tilde{\kappa}_3^{+\nu} C_3(x,\xi,t) \\ & + \tilde{\kappa}_4^{+\nu} C_4(x,\xi,t) \Big] u(P,\lambda) \end{aligned}$$

which was given in [45] and [46]. The covariants which appear in these expressions read

$$\begin{aligned} \kappa_M^{\mu\nu} =& i \frac{3(M_\Delta + M_N)}{2M_N \big[(M_\Delta + M_N)^2 - t\big]} \epsilon^{\mu\nu\rho\lambda} \bar{P}_\rho \Delta_\lambda \\ \kappa_E^{\mu\nu} =& -\kappa_M^{\mu\nu} - \frac{6(M_\Delta + M_N)}{M_N \big[(M_\Delta - M_N)^2 - t\big] \big[(M_\Delta + M_N)^2 - t\big]} \epsilon^{\mu\kappa\alpha\beta} \bar{P}_\alpha \Delta_\beta \, \epsilon_\kappa^{\ \nu\alpha'\beta'} \bar{P}_{\alpha'} \Delta_{\beta'} \gamma_5 \\ \kappa_C^{\mu\nu} =& \frac{3(M_\Delta + M_N)}{M_N \big[(M_\Delta - M_N)^2 - t\big] \big[(M_\Delta + M_N)^2 - t\big]} \Big[(\bar{P} \cdot \Delta) \, \Delta^\mu \Delta^\nu - t \bar{P}^\mu \Delta^\nu \Big] \gamma_5 \end{aligned}$$

and

$$\begin{aligned} \tilde{\kappa}_1^{\mu\nu} =& g^{\mu\nu} \\ \tilde{\kappa}_2^{\mu\nu} =& \frac{\Delta^\mu \Delta^\nu}{M_N^2} \\ \tilde{\kappa}_3^{\mu\nu} =& \frac{g^{\mu\nu} \not{\Delta} - \gamma^\mu \Delta^\nu}{M_N} \\ \tilde{\kappa}_4^{\mu\nu} =& \frac{2((\bar{P} \cdot \Delta) g^{\mu\nu} - \bar{P}^\mu \Delta^\nu)}{M_N^2} \quad . \end{aligned}$$

In the parametrization the Delta is described by the Rarita Schwinger spinor $u^\nu(P', \lambda')$ which is constructed in the appendix. The isospin convention differs by a factor 2 from the definition used for the respective form factors, hence the sum rules acquire a factor 2. Sum rules and other properties of these $N \to \Delta$ GPDs will be discussed extensively in chapter 4. Actually the axial soft transition amplitude given above is overparameterized with four covariants. In chapter 4 we will only use κ_1, κ_3 and κ_4 to parameterize this amplitude.

The kinematics has to be adapted for the $N \to \Delta$ transition. One has

$$\begin{aligned}
\bar{P}^\mu =& \tilde{p}^\mu + \frac{\bar{M}^2}{2} n^\mu \\
\Delta^\mu =& -2\xi\tilde{p}^\mu + \Delta_\perp^\mu + \frac{\Big[(1+\xi)M_\Delta^2 - (1-\xi)M_N^2\Big] - \frac{\xi t}{2}}{2} n^\mu \\
P^\mu =& \bar{P}^\mu - \frac{\Delta^\mu}{2} = (1+\xi)\tilde{p}^\mu - \frac{\Delta_\perp^\mu}{2} + \frac{-\frac{\xi}{2}M_\Delta^2 + (1-\frac{\xi}{2})M_N^2 - \frac{(1-\xi)t}{4}}{2} n^\mu \\
P'^\mu =& \bar{P}^\mu + \frac{\Delta^\mu}{2} = (1-\xi)\tilde{p}^\mu + \frac{\Delta_\perp^\mu}{2} + \frac{(1+\frac{\xi}{2})M_\Delta^2 + \frac{\xi}{2}M_N^2 - \frac{(1+\xi)t}{4}}{2} n^\mu \\
q^\mu =& -2\xi'\tilde{p}^\mu + \frac{Q^2}{4\xi'} n^\mu \\
q'^\mu =& q^\mu - \Delta^\mu = -2(\xi'-\xi)\tilde{p}^\mu - \Delta_\perp^\mu + \Big(\frac{Q^2}{4\xi'} - \frac{(1+\xi)M_\Delta^2 - (1-\xi)M_N^2 - \frac{\xi t}{2}}{2}\Big) n^\mu
\end{aligned} \tag{2.5}$$

with

$$\begin{aligned}
\bar{M}^2 =& \frac{1}{2}(M_\Delta^2 + M_N^2) - \frac{\Delta^2}{4} \\
\xi' =& \frac{\bar{P}\cdot q}{\bar{M}^2}\Big(-1 + \sqrt{1 + \frac{Q^2\bar{M}^2}{(\bar{P}\cdot q)^2}}\Big) \\
\xi =& \frac{\xi'\Big[Q^2 - \Delta^2 - 2(M_\Delta^2 - M_N^2)\xi'\Big]}{Q^2 - 4\xi'^2\bar{M}^2} \quad .
\end{aligned}$$

In the Bjorken limit we again find

$$\xi = \xi' = \frac{x_B/2}{1 - x_B/2} \quad .$$

The boundary for the skewedness parameter ξ due to the requirement that the longitudinal momentum fractions must be positive reads

$$0 < \xi < \frac{-M_\Delta^2 + M_N^2 + \sqrt{t^2 - 2(M_\Delta^2 + M_N^2)t + (M_\Delta^2 - M_N^2)^2}}{2(M_\Delta^2 + M_N^2) - t} < 1 \quad .$$

Finally we have the useful relation

$$\vec{\Delta}_\perp^2 = -(1-\xi^2)t - 2\xi\Big[(1+\xi)M_\Delta^2 - (1-\xi)M_N^2\Big] \quad .$$

Contrary to the $N \to N$ transition the $N \to \Delta$ transition is not so well explored. Among the known theoretical input for the $N \to \Delta$ GPDs are large N_C relations which relate them to the nucleon GPDs. The leading large N_C relations were given in [45] and read

$$\begin{aligned}
H_M^\star(x,\xi,t) =& \frac{2}{\sqrt{3}}\Big[E^u(x,\xi,t) - E^d(x,\xi,t)\Big] \\
C_1(x,\xi,t) =& \sqrt{3}\Big[\tilde{H}^u(x,\xi,t) - \tilde{H}^d(x,\xi,t)\Big] \\
C_2(x,\xi,t) =& \frac{\sqrt{3}}{4}\Big[\tilde{E}^u(x,\xi,t) - \tilde{E}^d(x,\xi,t)\Big] \quad .
\end{aligned} \tag{2.6}$$

Recently additional large N_C inspired relations were given [47]:

$$H^\star_E(x,\xi,t) = \frac{1}{3\sqrt{2}} \frac{M_\Delta^2 - M_N^2}{Q^2} \left[2H^d(x,\xi,t) - H^u(x,\xi,t) - \frac{Q^2}{4M_N^2} \Big(2E^d(x,\xi,t) - E^u(x,\xi,t) \Big) \right]$$
$$H^\star_C(x,\xi,t) = \frac{4M_\Delta^2}{M_\Delta^2 - M_N^2} H^E(x,\xi,t) \quad . \tag{2.7}$$

The experimental situation for the $N \to \Delta$ transition naturally is less explored than the $N \to N$ transition. The magnetic $N \to \Delta$ transition form factor is quite well measured. It is displayed in the figure below.

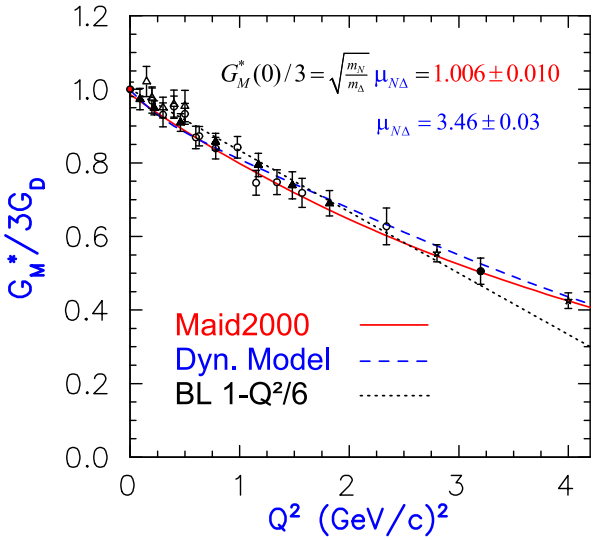

Figure 2.12: *The dominant vector form factor for the $N \to \Delta$ transition. This figure is taken from [48].*

For the electric and Coulomb form factors less is known. It is custom to give the ratios

$$E/M = -\frac{G^\star_E(Q^2)}{G^\star_M(Q^2)}$$
$$S/M \propto -\frac{G^\star_C(Q^2)}{G^\star_M(Q^2)} \quad .$$

From perturbative QCD the limit of these ratios is known [49] [50] for large values of Q^2.

$$E/M = 1 \quad .$$
$$S/M \propto \sqrt{\left(\frac{M_\Delta^2 + M_N^2 + Q^2}{2M_\Delta} \right)^2 - M_N^2} \, \frac{log(Q^2/\Lambda^2)}{Q^2} \quad .$$

For low values of Q^2 a good description of experimental data for the ratios E/M and S/M has been obtained using chiral perturbation theory [51].

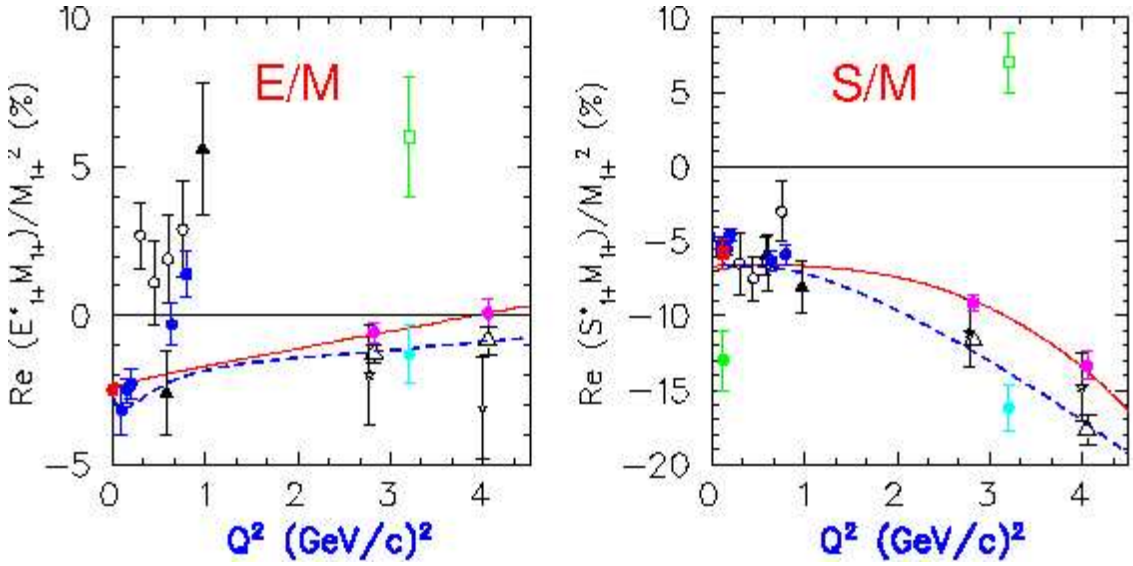

Figure 2.13: *The E/M and S/M ratios for the $N \to \Delta$ transition. This figure is taken from [48].*

After this short survey of $N \to \Delta$ transition form factors which are connected to the GPDs via sum rules we discuss the experimental aspects of $N \to \Delta$ DVCS.

As already mentioned in the last section it is often difficult to measure $N \to N$ DVCS exclusively. For example at HERMES the final state proton could not be detected. Thus the processes shown in fig. 2.14 can not be distinguished.

For the non resonant contributions estimates have been given [52] by parameterizing the associated DVCS processes. Model calculations for $N \to \Delta$ transition GPDs like we provide them in this thesis can be used to implement a Monte Carlo simulation for the resonant contribution and thus giving an estimate for this background process.

Luckily it is possible to perform dedicated experiments to measure $N \to \Delta$ DVCS exclusively thus allowing to access $N \to \Delta$ GPDs experimentally. At CLAS@JLAB such a measurement was performed [53]. The CLAS detector provides sufficient energy and angular resolution to identify the final states in the reaction $ep \to e'n'\pi^+$. The kinematics is sketched in the figure below.

Like for $N \to N$ DVCS one has to deal with the concurring Bethe-Heitler process.

The invariant mass spectrum of the $(n\pi^+)$ final state in the process $ep \to e\gamma(\pi^+ n)$ clearly demonstrates that in this experiment it is possible to distinguish $\Delta(1232)$, $N^\star(1520)$ and $N^\star(1680)$ in the final states.

In conclusion we can state that $N \to \Delta$ GPDs not only help in identifying background contributions to $N \to N$ DVCS measurements but provide an interesting experimental issue in itself.

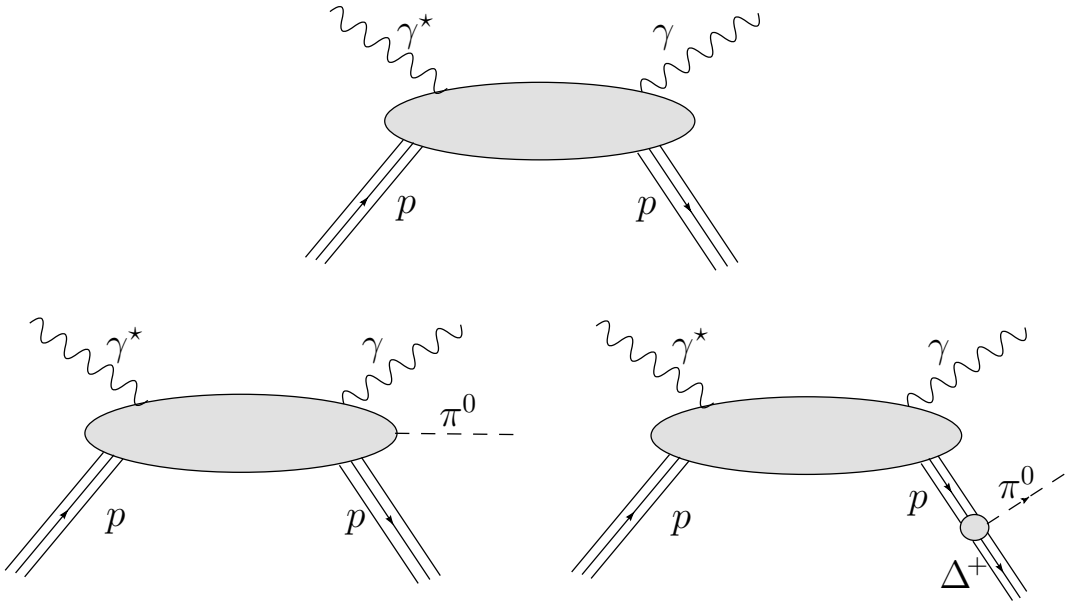

Figure 2.14: *Three contributions which cannot be distinguished by the detector at HERMES. The upper figure is $N \to N$ DVCS. The lower left contribution is the non resonant contribution to the process $ep \to e'\gamma\pi^0 p'$. The lower right figure gives the resonant contribution to $ep \to e'\gamma\pi^0 p'$.*

2.3 Other related processes

In this section we will provide a short overview for physical processes associated with GPDs. As one learns from the factorization theorem GPDs are universal quantities. Hence it is no wonder that they turn up again in the parametrization of similar processes.

One example is hard electroproduction of mesons, $eN \to e'N'M$. Analogously to DVCS factorization could be shown for this process if the incoming virtual photon is longitudinally polarized [54]. The diagram for the factorized meson electroproduction amplitude is given in fig. 2.17.

The amplitudes for electroproduction of longitudinally polarized vector mesons read

$$M^L_{V_L} = -ie\frac{4}{9}\frac{1}{Q}\Big[\int_0^1 dz \frac{\Phi_{V_L}(z)}{z}\Big]\frac{1}{2}(4\pi\alpha_S) \cdot \left(A_{V_L\,N}\bar{u}(P')\not{n}u(P) + B_{V_L\,N}\bar{u}(P')i\sigma^{\kappa\lambda}\frac{n_\kappa \Delta_\lambda}{2M_N}u(P)\right)$$

where $\Phi_{V_L}(z)$ is the distribution amplitude for a longitudinally polarized vector meson. The GPDs enter in the amplitudes A and B. For the different vector mesons they read [55]

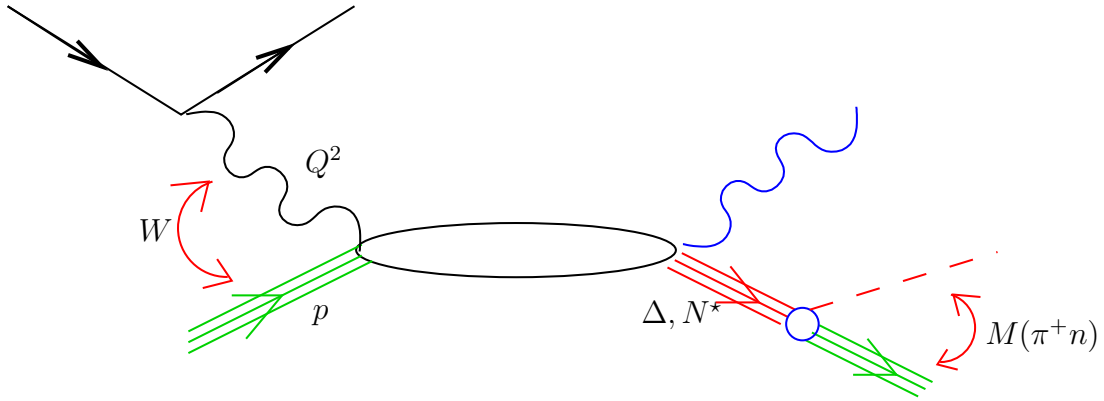

Figure 2.15: *The kinematics for the process $ep \to e'p\pi^+$ measured at CLAS@JLAB.*

$$
\begin{aligned}
A_{\rho_L^0 p} &= \int_{-1}^{1} dx \frac{1}{\sqrt{2}} (e_u H^u - e_d H^d) \Big(\frac{1}{x-\xi+i\epsilon} + \frac{1}{x+\xi-i\epsilon} \Big) \\
B_{\rho_L^0 p} &= \int_{-1}^{1} dx \frac{1}{\sqrt{2}} (e_u E^u - e_d E^d) \Big(\frac{1}{x-\xi+i\epsilon} + \frac{1}{x+\xi-i\epsilon} \Big) \\
A_{\rho_L^+ n} &= - \int_{-1}^{1} dx (H^u - H^d) \Big(\frac{e_u}{x-\xi+i\epsilon} + \frac{e_d}{x+\xi-i\epsilon} \Big) \\
B_{\rho_L^+ n} &= - \int_{-1}^{1} dx (E^u - E^d) \Big(\frac{e_u}{x-\xi+i\epsilon} + \frac{e_d}{x+\xi-i\epsilon} \Big) \\
A_{\omega_L p} &= \int_{-1}^{1} dx \frac{1}{\sqrt{2}} (e_u H^u + e_d H^d) \Big(\frac{1}{x-\xi+i\epsilon} + \frac{1}{x+\xi-i\epsilon} \Big) \\
B_{\omega_L p} &= \int_{-1}^{1} dx \frac{1}{\sqrt{2}} (e_u E^u + e_d E^d) \Big(\frac{1}{x-\xi+i\epsilon} + \frac{1}{x+\xi-i\epsilon} \Big) \quad .
\end{aligned}
$$

While in DVCS one always gets a convolution of GPDs one obtained them directly if doubly virtual Compton scattering (VVCS) could be accessed experimentally.

A process where VVCS is involved is the long studied elastic scattering process. In 2003 Guichon and Vanderhaeghen remarked [56] that for high virtualities the leading one photon exchange process is insufficient to describe the experimental results for elastic scattering. Thus they considered the two photon exchange process.

In a partonic picture the leading contributions to this two photon exchange process stem from the box diagrams [57]

Recognizing the soft amplitudes in the box diagrams it comes as no surprise that GPDs appear in the parametrization of two photon exchange processes.

Finally just like we presented in the last section for $N \to \Delta$ transition, DVCS can be extended towards other resonance transitions. The results from CLAS have already proven that it is possible to discriminate at least three different resonance regions. Therefore the study of

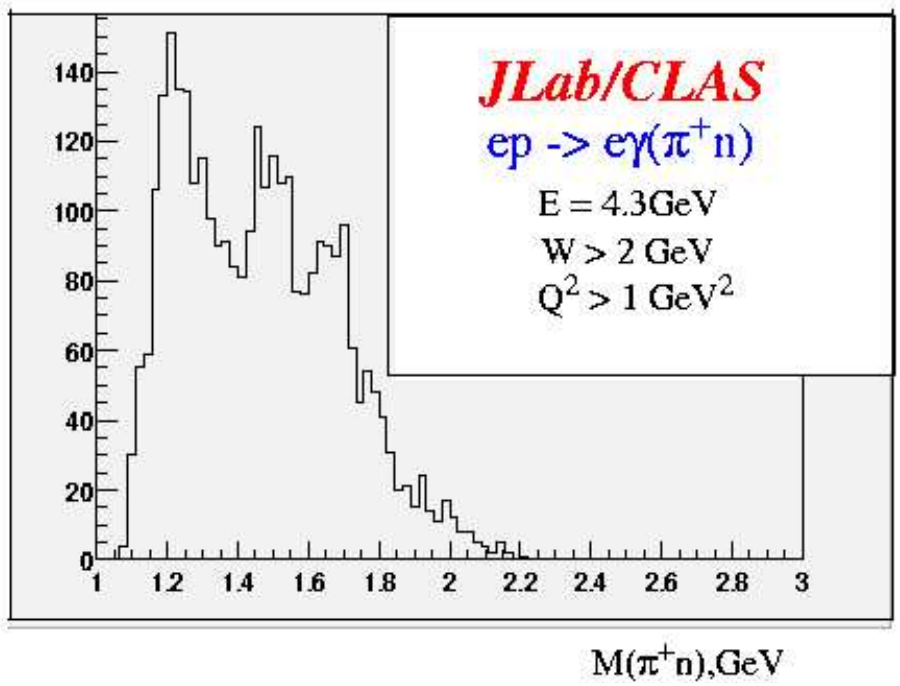

Figure 2.16: *The invariant mass spectrum of the $(n\pi^+)$ final state in the process $ep \to e\gamma(\pi^+ n)$.*

other resonance transition processes seems worthwhile.

The framework of quark models provides a possible tool to access such $N \to$ resonance transition GPDs. Like for $N \to N$ GPDs the first steps that have to be performed are to write down the parametrization for the soft amplitudes.

As an example we consider the $N \to S_{11}$ transition. Applying kinematic constraints and the equation of motion one finds the minimal set of independent Lorentz covariants: γ^μ, $\bar{P}^\mu$, Δ^μ and $\gamma^\mu\gamma_5$, $\bar{P}^\mu\gamma_5$, $\Delta^\mu\gamma_5$. Since $N \to S_{11}$ is a parity odd transition ($J^\pi = \frac{1}{2}^+ \to J^\pi = \frac{1}{2}^-$) the soft amplitudes can be parameterized as following

$$
\begin{aligned}
G^{+,(p\to S_{11})}_{V,\lambda'\lambda} &= \int \frac{d\lambda}{4\pi} e^{i\lambda x} \langle S_{11}; P', \lambda' \mid \bar{\psi}(-\frac{\lambda n}{2}) \not{n} \tau_3 \psi(\frac{\lambda n}{2}) \mid p; N, \lambda \rangle_{y^+=0, \vec{y}_\perp = \vec{0}} \\
&= \frac{1}{2\bar{P}^+} \bar{u}(P', \lambda') \Big[B_1(x,\xi,t) \not{n}\gamma_5 + B_2(x,\xi,t)(\bar{P}\cdot n)\gamma_5 + B_3(x,\xi,t)(\Delta \cdot n)\gamma_5 \Big] u(P,\lambda) \\
G^{+,(p\to S_{11})}_{A,\lambda'\lambda} &= \int \frac{d\lambda}{4\pi} e^{i\lambda x} \langle S_{11}; P', \lambda' \mid \bar{\psi}(-\frac{\lambda n}{2}) \not{n} \tau_3 \gamma_5 \psi(\frac{\lambda n}{2}) \mid p; N, \lambda \rangle_{y^+=0, \vec{y}_\perp = \vec{0}} \\
&= \frac{1}{2\bar{P}^+} \bar{u}(P', \lambda') \Big[\tilde{B}_1(x,\xi,t) \not{n} + \tilde{B}_2(x,\xi,t)(\bar{P}\cdot n) + \tilde{B}_3(x,\xi,t)(\Delta \cdot n) \Big] u(P,\lambda) \quad .
\end{aligned}
$$

The kinematics and sum rules can be discussed along the lines of arguments in the last section.

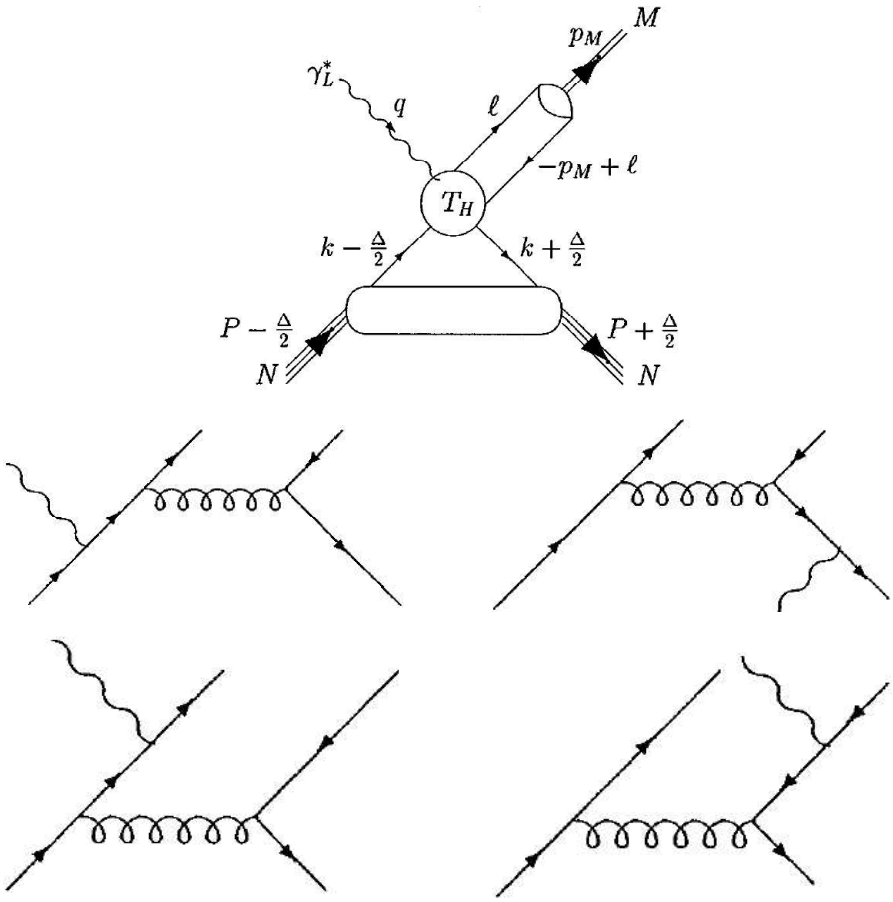

Figure 2.17: *The factorized meson electroproduction amplitude. The lower 4 panels constitute the leading order diagrams for the hard scattering part T_H of the meson electroproduction amplitude. These figures have been taken from [55].*

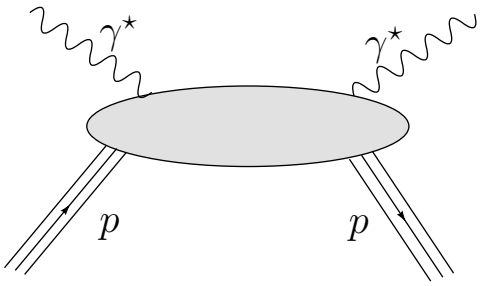

Figure 2.18: *In VVCS both the initial and the final photon are off-shell.*

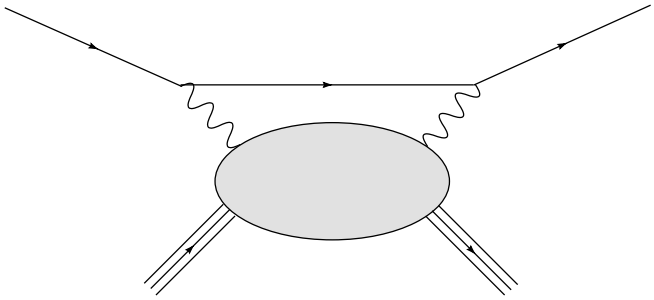

Figure 2.19: *Two photon exchange processes have to be considered to describe elastic scattering at high virtualities.*

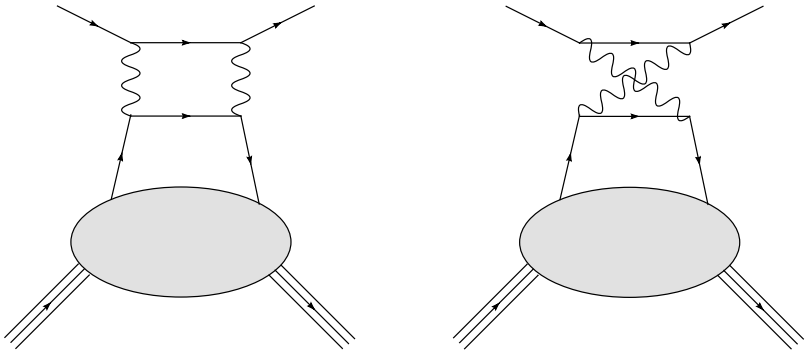

Figure 2.20: *The box diagrams which are the leading contributions to two photon exchange.*

Chapter 3

Quark models on the light front

3.1 Introduction

Quark models have been studied already before the advent of QCD when it became clear that the partons inside the baryons obeyed flavor symmetry. Although it was very early obvious that the constituent quarks with a high mass about a third of the nucleon mass are different from the current quarks (which can be probed in DIS) (see e.g. [58]) quark models achieved to explain many of the observed properties of the baryons, like masses, magnetic moments, existence of excited states in a qualitative way[1].

The idea of quark models can be shortly summarized as following: Three constituent quarks form a baryon in such a way that they obey flavor, color and spin symmetry. Many predictions (like magnetic moments) can be obtained from the SU(6) symmetry alone. The baryon spectrum was first calculated using non relativistic interactions [59]. The remarkable success of this description however also displays the arbitrariness of quark models as the many discrepancies can be absorbed into more and more parameters of the model.

Since the 1960's quark models have been refined more and more. Various ideas to include relativistic kinematics have been developed. They include relativistic versions of quark models (for an overview see [60]), additional interactions like pion dynamics [61] and allowing for constituent quark substructure (see e.g. [62]).

In this thesis we employ a relativistic quark model using the light front form. In 1941 Dirac discovered that there exist three forms of relativistic dynamics [19]. The light front has the largest possible kinematical subgroup and allows for an easy implementation of a fully relativistic wave function. This dynamical form has firstly been introduced to the idea of quark models by Terent'ev and Berestetsky [63]. Reducing the Fock space to three quark states and identifying them with constituent quarks allows for an access of not only form factors but even of generalized parton distributions. This overlap representation has been worked out by Diehl et al. [64] and has been applied to calculate nucleon GPDs in a quark model [65].

[1] Roughly speaking the predictions of quark model calculations describe the properties of baryons to an accuracy of 30% (which includes the prediction of number of baryon states)

Even if the quark model which we use is relativistic in itself the calculation of observables requires an approximation which destroys relativistic covariance. We will discuss this drawback at the end of this chapter.

3.2 From SU(6) to quark model wave functions

The observation behind the quark model idea is the observation of the approximate symmetry of SU(6). To be more precise the observation of the remarkable pattern in the masses and hypercharges of the observed baryon spectrum. The ground state hadrons can be ordered in the following patterns:

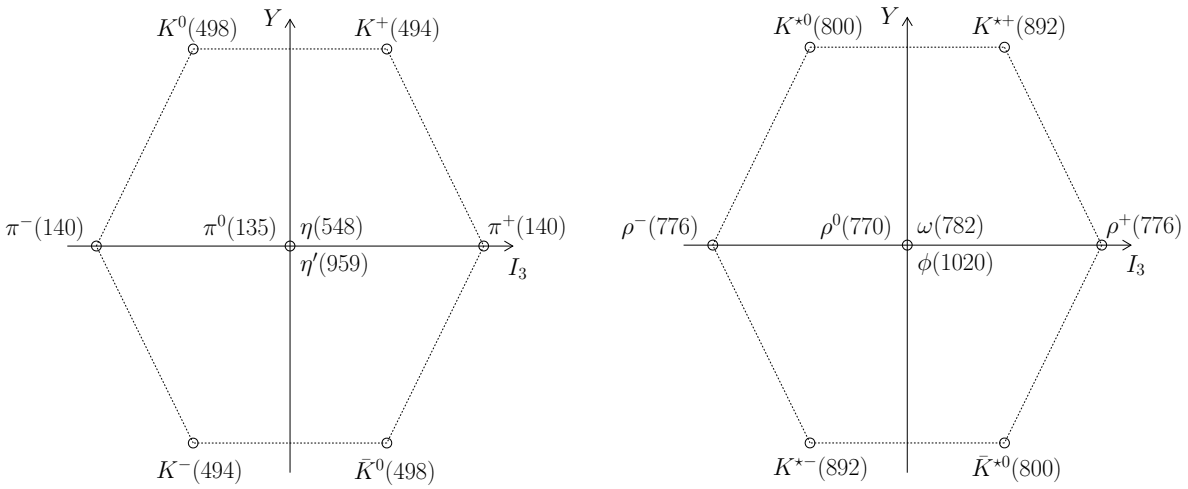

Figure 3.1: *Pseudo scalar (left figure) and vector (right figure) meson nonets. The numbers in brackets are the meson masses in MeV.*

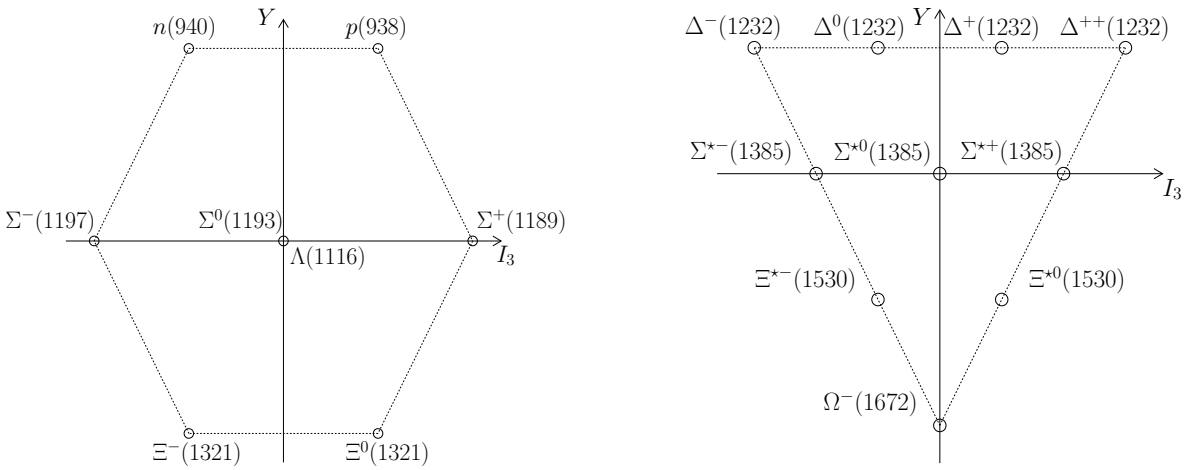

Figure 3.2: *Baryon octet (left figure) and baryon decuplet (right figure). The numbers in brackets are the baryon masses in MeV.*

Here the hyper charge is defined as the sum of baryon number and strangeness

$$Y = B + S$$

and the isospin projection I_3 can be expressed via the Gell-Mann - Nishijima relation

$$Q = I_3 + \frac{Y}{2} \quad .$$

More often than not it is a symmetry which results in such a pattern. In this case the symmetry behind this pattern is flavor $SU(3)$. In fact a fundamental triplet consisting of three quarks exists of which these patterns emerge naturally.

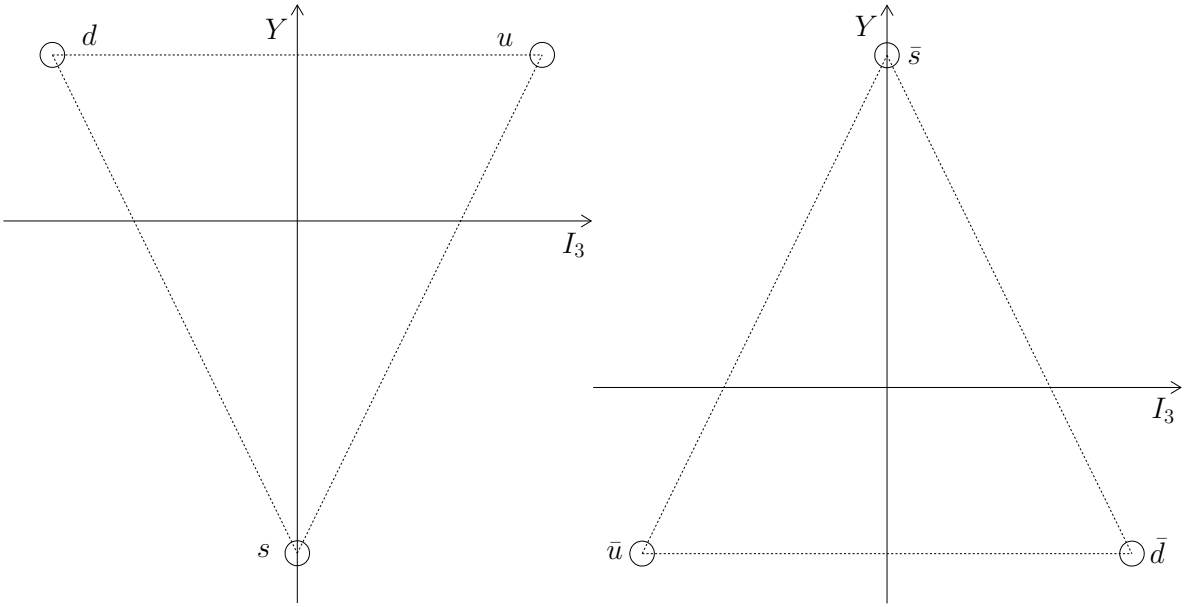

Figure 3.3: *The fundamental quark triplet and antitriplet.*

The properties of the quarks which appear in this fundamental triplet are summarized in the following table:

flavor	Q	I_3	S	B	Y
up	$\frac{2}{3}$	$\frac{1}{2}$	0	$\frac{1}{3}$	$\frac{1}{3}$
down	$-\frac{1}{3}$	$-\frac{1}{2}$	0	$\frac{1}{3}$	$\frac{1}{3}$
strange	$-\frac{1}{3}$	0	-1	$\frac{1}{3}$	$-\frac{2}{3}$

Table 3.1: *Properties of the light quarks.*

Then the meson nonet can be expressed as quark antiquark states

$$\bar{q}q \equiv 3 \otimes \bar{3} = 1 \oplus 8 \quad .$$

In fact the pseudoscalar meson nonet can be understood as a meson octet (K^0, K^+, K^- $\bar{K}^0$, $\pi^{\pm 0}, \eta_8$) and a meson singlet η_1. The physical mesons η, η' are then mixtures of the states η_1 and η_8 which is possible since they possess the same quantum numbers $J^P = 0^-$.

The same argument applies to the vector meson nonet ($J^P = 1^-$). A singlet ω_1 and an octet state ω_8 mix (in a nearly ideal way[2]) to produce the physical vector mesons ω and ϕ.

In order to understand the baryon octet and decuplet one has to consider a three quark state

$$qqq \equiv 3 \otimes 3 \otimes 3 = 1 \oplus 8 \oplus 8 \oplus 10 \quad .$$

It can be decomposed into an antisymmetric singlet, a mixed symmetric and a mixed antisymmetric octet and a symmetric decuplet. However this only solves the problem partly. While we can identify the decuplet and one octet there is obviously one octet missing. Further more possible candidates for the baryon singlet like $\Lambda(1405)$ have quantum numbers J^P which differ from those of the octet (unlike for the meson nonet).

The question whether all representations can be realized in the ground state is answered by the Pauli principle. Firstly the existence of the Δ^{++} requires an additional quantum number, color. A totally antisymmetric color wave function reconciles the existence of $\Delta^{++} \equiv u^\uparrow u^\uparrow u^\uparrow$ with the Pauli principle. The latter then obviously requires a symmetric wave function $\Psi_{space,\,spin,\,flavor}$. The spatial wave function for the ground state is symmetric. Since spin $SU(2)$ provides no antisymmetric state the singlet baryon is forbidden in the ground state. In the same spirit one can show that there can only be one ground state octet. The physical multiplets can in fact be obtained from symmetry arguments alone. One has to consider the (broken) $SU(6)$ symmetry which is provided by spin and flavor: $SU(2) \times SU(3)$. Then one can decompose

$$6 \otimes 6 \otimes 6 = 56 \oplus 70 \oplus 70 \oplus 20$$

where the 56 plet contains symmetric spin flavor states and includes the decuplet $(10, 4)$ and the octet $(8, 2)$. There are 70 plets with mixed (anti)symmetric spin flavor states (M_S, M_A) each and a 20 plet with antisymmetric spin flavor states.

From the Pauli principle it follows that the spatial wave functions must be symmetric for the 56 plet, mixed (anti)symmetric for the 70 plets and antisymmetric for the 20 plet. Consequently the lowest lying 56 plet has the spatial wave function $(1s)^3$, for the lowest lying 70 plet one has $(1s)^2(1p)$ and for the lowest lying 20 plet $(1s)(1p)^2$. This implies a mass ordering for these multiplets resulting in the 56 plet lying below the 70 plet and the latter lying below the 20 plet. This explains the different behavior of the baryon octet in contrast to the meson nonet.

The baryon mass spectrum gives rise to the idea of constituent quark masses in the order of a third of the nucleon mass. This symmetry reasoning allowed the prediction of the Ω^- baryon in the decuplet before it was observed.

The quark model consists basically of the explicit construction of wave functions which obey the above symmetry arguments and identifying the quarks in the fundamental triplet with constituent quarks of roughly a third of the nucleon mass.

[2]The ideal mixing angle between the states is such that for the flavor contents one obtains $\phi = \bar{s}s$ and $\omega = \frac{1}{\sqrt{2}}(u\bar{u} + d\bar{d})$.

In the following we will restrict ourselves to the construction of baryon wave functions. These wave functions can be written as product of color-, spatial-, flavor- and spin wave function.

$$\Psi(\vec{p}_i, \tau_i, \lambda_i, c_i) = \theta(c_i) \cdot \psi(p_i) \cdot \phi(\tau_i) \cdot \chi(\lambda_i) \quad .$$

Concerning the color wave function $\theta(c_i)$ we only need to know that it is antisymmetric. This can be realized using the Slater determinant. In the following we will omit it.

In $SU(2)$ spin one can construct symmetric, mixed symmetric and mixed antisymmetric states:

$$\chi_S^{\frac{3}{2}} = \uparrow\uparrow\uparrow \qquad \chi_S^{\frac{1}{2}} = \frac{1}{\sqrt{3}}\Big(\uparrow\uparrow\downarrow + \uparrow\downarrow\uparrow + \downarrow\uparrow\uparrow\Big)$$

$$\chi_S^{-\frac{1}{2}} = \frac{1}{\sqrt{3}}\Big(\uparrow\downarrow\downarrow + \downarrow\uparrow\downarrow + \downarrow\downarrow\uparrow\Big) \qquad \chi_S^{-\frac{3}{2}} = \downarrow\downarrow\downarrow$$

$$\chi_{M,S}^{\uparrow} = \frac{1}{\sqrt{6}}\Big(2\uparrow\uparrow\downarrow - (\uparrow\downarrow + \downarrow\uparrow)\uparrow\Big) \qquad \chi_{M,S}^{\downarrow} = \frac{1}{\sqrt{6}}\Big((\uparrow\downarrow + \downarrow\uparrow)\downarrow - 2\downarrow\downarrow\uparrow\Big)$$

$$\chi_{M,A}^{\uparrow} = \frac{1}{\sqrt{2}}(\uparrow\downarrow - \downarrow\uparrow)\uparrow \qquad \chi_{M,A}^{\downarrow} = \frac{1}{\sqrt{2}}(\uparrow\downarrow - \downarrow\uparrow)\downarrow \quad . \tag{3.1}$$

In flavor $SU(3)$ symmetric, mixed symmetric, mixed antisymmetric and antisymmetric states are possible. Since the quantum numbers of the quarks have to match the quantum numbers of the desired baryon the wave function can be obtained by a Clebsch-Gordon construction. Identification with the observed baryons explains the labeling of the possible flavor states given below:

$$\phi_S^{\Delta^{++}} = uuu \qquad \phi_S^{\Delta^{+}} = \frac{1}{\sqrt{3}}\Big(uud + udu + duu\Big)$$

$$\phi_S^{\Delta^{0}} = \frac{1}{\sqrt{3}}\Big(udd + dud + ddu\Big) \qquad \phi_S^{\Delta^{-}} = ddd$$

$$\phi_S^{\Sigma^{\star+}} = \frac{1}{\sqrt{3}}\Big(uus + usu + suu\Big) \qquad \phi_S^{\Sigma^{\star0}} = \frac{1}{\sqrt{6}}\Big(uds + usd + dus + dsu + sud + sdu\Big)$$

$$\phi_S^{\Sigma^{\star-}} = \frac{1}{\sqrt{3}}\Big(dds + dsd + sdd\Big) \qquad \phi_S^{\Xi^{\star0}} = \frac{1}{\sqrt{3}}\Big(uss + sus + ssu\Big)$$

$$\phi_S^{\Xi^{\star-}} = \frac{1}{\sqrt{3}}\Big(dss + sds + ssd\Big) \qquad \phi_S^{\Omega^{-}} = sss$$

$$\phi_{M,S}^{p} = \frac{1}{\sqrt{6}}\Big(2uud - (ud + du)u\Big) \qquad \phi_{M,S}^{n} = \frac{1}{\sqrt{6}}\Big((ud + du)d - 2ddu\Big)$$

$$\phi_{M,S}^{\Sigma^{+}} = \frac{1}{\sqrt{6}}\Big(2uus - (us + su)u\Big) \qquad \phi_{M,S}^{\Sigma^{0}} = \frac{1}{\sqrt{12}}\Big(sdu + sud + dsu + usd - 2(du + ud)s\Big)$$

$$\phi_{M,S}^{\Lambda} = \frac{1}{2}\Big(dsu - usd + sdu - sud\Big) \qquad \phi_{M,S}^{\Sigma^{-}} = \frac{1}{\sqrt{6}}\Big(2dds - (ds + sd)d\Big)$$

$$\phi_{M,S}^{\Xi^{0}} = \frac{1}{\sqrt{6}}\Big((us + su)s - 2ssu\Big) \qquad \phi_{M,S}^{\Xi^{-}} = \frac{1}{\sqrt{6}}\Big((ds + sd)s - 2ssd\Big)$$

$$\phi^{p}_{M,A} = \frac{1}{\sqrt{2}}(ud-du)u \qquad \phi^{n}_{M,A} = \frac{1}{\sqrt{2}}(ud-du)d$$
$$\phi^{\Sigma^+}_{M,A} = \frac{1}{\sqrt{2}}(us-su)u \qquad \phi^{\Sigma^0}_{M,A} = \frac{1}{2}(dsu+usd-sud-sdu)$$
$$\phi^{\Lambda}_{M,A} = \frac{1}{\sqrt{12}}\Big(sdu-sud+usd-dsu-2(du-ud)s\Big) \qquad \phi^{\Sigma^-}_{M,A} = \frac{1}{\sqrt{2}}(ds-sd)d$$
$$\phi^{\Xi^0}_{M,A} = \frac{1}{\sqrt{2}}(us-su)s \qquad \phi^{\Xi^-}_{M,A} = \frac{1}{\sqrt{2}}(ds-sd)s$$

$$\phi^{\Lambda}_{A} = \frac{1}{\sqrt{6}}\Big(s(du-ud)+usd-dsu+(du-ud)s\Big) \tag{3.2}$$

Then combining spin and flavor in $SU(2)_{\text{spin}} \times SU(3)_{\text{flavor}}$ one finds the spin flavor wave functions for the multiplets. We give them in the following table:

multiplet	symmetry	wave function	degeneracy
56	S	$\phi_S\chi_S$	(10,4)
		$\frac{1}{\sqrt{2}}(\phi_{M,S}\chi_{M,S}+\phi_{M,A}\chi_{M,A})$	(8,2)
70	M,S	$\phi_S\chi_{M,S}$	(10,2)
		$\phi_{M,S}\chi_S$	(8,4)
		$\frac{1}{\sqrt{2}}(\phi_{M,A}\chi_{M,A}-\phi_{M,S}\chi_{M,S})$	(8,2)
		$\phi_A\chi_{M,A}$	(1,2)
70	M,A	$\phi_S\chi_{M,A}$	(10,2)
		$\phi_{M,A}\chi_S$	(8,4)
		$\frac{1}{\sqrt{2}}(\phi_{M,S}\chi_{M,A}+\phi_{M,A}\chi_{M,S})$	(8,2)
		$\phi_A\chi_{M,S}$	(1,2)
20	A	$\phi_A\chi_S$	(1,4)
		$\frac{1}{\sqrt{2}}(\phi_{M,S}\chi_{M,A}-\phi_{M,A}\chi_{M,S})$	(8,2)

Table 3.2: *The spin flavor wave functions for the baryon multiplets.*

Before proceeding with the discussion of spatial wave functions let us apply these $SU(6)$ wave functions to calculate the magnetic moments μ_p, μ_n and $\mu^{\star}_{p\Delta^+}$. The required baryon spin flavor states can be read off from the tables above:

$$\begin{aligned} \mid p,\lambda\rangle &= \frac{1}{\sqrt{2}}\Big(\phi^{p}_{M,S}\chi^{\lambda}_{M,S}+\phi^{p}_{M,A}\chi^{\lambda}_{M,A}\Big) \\ \mid n,\lambda\rangle &= \frac{1}{\sqrt{2}}\Big(\phi^{n}_{M,S}\chi^{\lambda}_{M,S}+\phi^{n}_{M,A}\chi^{\lambda}_{M,A}\Big) \\ \mid \Delta^+,\lambda\rangle &= \phi^{\Delta^+}_{S}\chi^{\lambda}_{S} \quad . \end{aligned} \tag{3.3}$$

We consider the magnetic moment operator

$$M = \mu\Big(\frac{2}{3}\sigma_u - \frac{1}{3}\sigma_d - \frac{1}{3}\sigma_s\Big) \quad .$$

Exploiting the wave function symmetry one then can write

$$\sum_{i=1}^{3}\langle p,\uparrow|\ M_z^i\ |\ p,\uparrow\rangle = 3\mu\langle p,\uparrow|\ e^{(3)}\sigma_z^{(3)}\ |\ p,\uparrow\rangle \quad .$$

The matrix elements can now be calculated using the spin flavor wave functions above. One finds

$$\begin{aligned}
&\langle\phi^p_{M,A}\mid e^{(3)}\mid\phi^p_{M,A}\rangle = \frac{2}{3} && \langle\phi^n_{M,A}\mid e^{(3)}\mid\phi^n_{M,A}\rangle = -\frac{1}{3}\\
&\langle\phi^p_{M,S}\mid e^{(3)}\mid\phi^p_{M,S}\rangle = 0 && \langle\phi^n_{M,S}\mid e^{(3)}\mid\phi^n_{M,S}\rangle = \frac{1}{3}\\
&\langle\phi^{\Delta^+}_{S}\mid e^{(3)}\mid\phi^p_{M,A}\rangle = 0 && \langle\phi^{\Delta^+}_{S}\mid e^{(3)}\mid\phi^p_{M,S}\rangle = \frac{\sqrt{2}}{3}\\
&\langle\chi^{\uparrow}_{M,A}\mid\sigma_z^{(3)}\mid\chi^{\uparrow}_{M,A}\rangle = 1 && \langle\chi^{\uparrow}_{M,S}\mid\sigma_z^{(3)}\mid\chi^{\uparrow}_{M,S}\rangle = -\frac{1}{3}\\
&\langle\chi^{\uparrow}_{S}\mid\sigma_z^{(3)}\mid\chi^{\uparrow}_{M,A}\rangle = 0 && \langle\chi^{\uparrow}_{S}\mid\sigma_z^{(3)}\mid\chi^{\uparrow}_{M,S}\rangle = \frac{2\sqrt{2}}{3} \quad .
\end{aligned}$$

Combining the above results one obtains

$$\mu_p = \mu \qquad\qquad \mu_n = -\frac{2}{3}\mu\mu^{\star}_{p\Delta^+} = \frac{2\sqrt{2}}{3}\mu \quad .$$

The experimental value for the ratio of proton and neutron magnetic moment

$$\frac{\mu_p}{\mu_n} = -1.46$$

is remarkably well described. Concerning the magnetic transition moment $\mu^{\star}_{p\Delta^+}$ one has to emphasize that this pure $SU(6)$ calculation still presumes that the baryon 56 plet is degenerate.

Therefore the description of the baryon spectrum requires knowledge about the spatial wave function. Thus we have to extend our symmetry consideration to the group $SU(6)\times O(3)$. It is custom to develop the spatial wave function in terms of harmonic oscillator wave functions. For the positive parity baryons (which include the Δ and the nucleon) the resulting supermultiplets up to $N=2$ can be classified by

N	multiplet	spin flavor symmetry	spatial symmetry
0	$(56,0^+_0)$	S	S
2	$(56,0^+_2)$	S	S
	$(70,0^+_2)$	M	M
	$(56,2^+_2)$	S	S
	$(70,2^+_2)$	M	M
	$(20,1^+_2)$	A	A

Table 3.3: *The lowest lying multiplets of $SU(6)\times O(6)$.*

All the above super multiplets contain the octet $(8,2)$ and except for $(20,1_2^+)$ also contain the decuplet[3] $(10,4)$. Thus the spatial wave functions 0_{S_S}, 2_{S_S}, 2_{S_M}, 2_{D_S}, 2_{D_M} and 2_{P_A} have to be combined with the respective spin flavor wave functions to produce the $\frac{1}{2}^+$ octet and the $\frac{3}{2}^+$ decuplet. Obviously different excited states of the harmonic oscillator can contribute to these J^P states. Whether only the ground state contributes to the lowest lying physical positive baryons depends on the interaction which breaks the $SU(6)$ symmetry.

We will shortly review a prominent example of an early quark model, the Isgur-Karl model [59][66]. They combine a harmonic oscillator with an anharmonic perturbation U and a hyperfine interaction V^{hyp}.

$$H = \sum_{i=1}^{3}\Big(m_i + \frac{\vec{p}_i^{\,2}}{2m_i}\Big) + \frac{K}{2}\sum_{i<j}\vec{r}_{ij}^{\,2} + \sum_{i<j}\Big(U(\vec{r}_{ij}) + V_{ij}^{\text{hyp}}\Big) \quad .$$

Their hyperfine interaction only contains spin-spin and tensor contributions:

$$V_{ij}^{\text{hyp}} = \frac{2\alpha_S}{3m_i m_j}\Big(\frac{8\pi}{3}\delta^{(3)}(\vec{r}_{ij})\vec{s}_i\cdot\vec{s}_j + \frac{3(\vec{s}_i\cdot\hat{r}_{ij})(\vec{s}_j\cdot\hat{r}_{ij}) - \vec{s}_i\cdot\vec{s}_j}{r_{ij}^3}\Big) \quad .$$

While the notation α_S still suggests that the meaning of the hyperfine interaction is described by one gluon exchange the omission of spin-orbit terms reveals that this interaction is rather phenomenologically motivated and α_S bears no special meaning in the Isgur-Karl model. The anharmonic perturbation which removes the degeneracy of the $N=2$ harmonic oscillator energies is not specified in the IK model. Instead five parameters are introduced to distinguish these states.

In order to obtain the spatial wave functions with the respective symmetry N_{L_π} one firstly must eliminate the spurious center of mass coordinate. In the simple case of equal quark masses this is done by introducing the coordinates

$$\begin{aligned}\rho &= \frac{1}{\sqrt{2}}(\vec{r}_1 - \vec{r}_2)\\ \lambda &= \frac{1}{\sqrt{6}}(\vec{r}_1 + \vec{r}_2 - 2\vec{r}_3)\\ \Rightarrow H_0 &= \frac{p_\lambda^2}{2m} + \frac{p_\rho^2}{2m} + \frac{3K}{2}(\rho^2+\lambda^2) \quad .\end{aligned}$$

Then one can identify the harmonic oscillator wave functions with a given symmetry and combine them with the spin-flavor wave functions with corresponding symmetry.

The tensor force term triggers admixtures between the super multiplets given in tab. 3.3. As an example we quote the physical state for the nucleon

$$|\,N\rangle \approx 0.9\,|\,N,0_{S_S}\rangle - 0.34\,|\,N,2_{S_S}\rangle - 0.27\,|\,N,2_{S_M}\rangle - 0.06\,|\,N,2_{D_M}\rangle \quad .$$

A similar admixture of d-waves in the Δ allows for a finite electric $N \to \Delta$ transition amplitude, which was forbidden in pure $SU(6)$ by the Moorhouse selection rule [67].

[3]The angular momentum involved in the d wave allows for the existence of the decuplet $(10,4)$ even if the latter does not appear in the 70 plet given in tab. 3.2.

Once the physical baryon states are constructed one can calculate the matrix elements (using the interaction hamiltonian and thus obtain the baryon spectrum. To avoid misunderstandings, the free parameters of the model $m_{u/d}$, m_s, α_S, K and the above mentioned five parameters for the anharmonic distortion are fitted to the baryon spectrum. Nevertheless the predictive power of this model is quite high concerning the number of baryon states which are described by it.

Let us conclude this review of the IK model with the presentation of its predictions for the baryon spectrum. The ground state baryons are described very successfully and even for the excited baryon states one finds good agreement with the data.

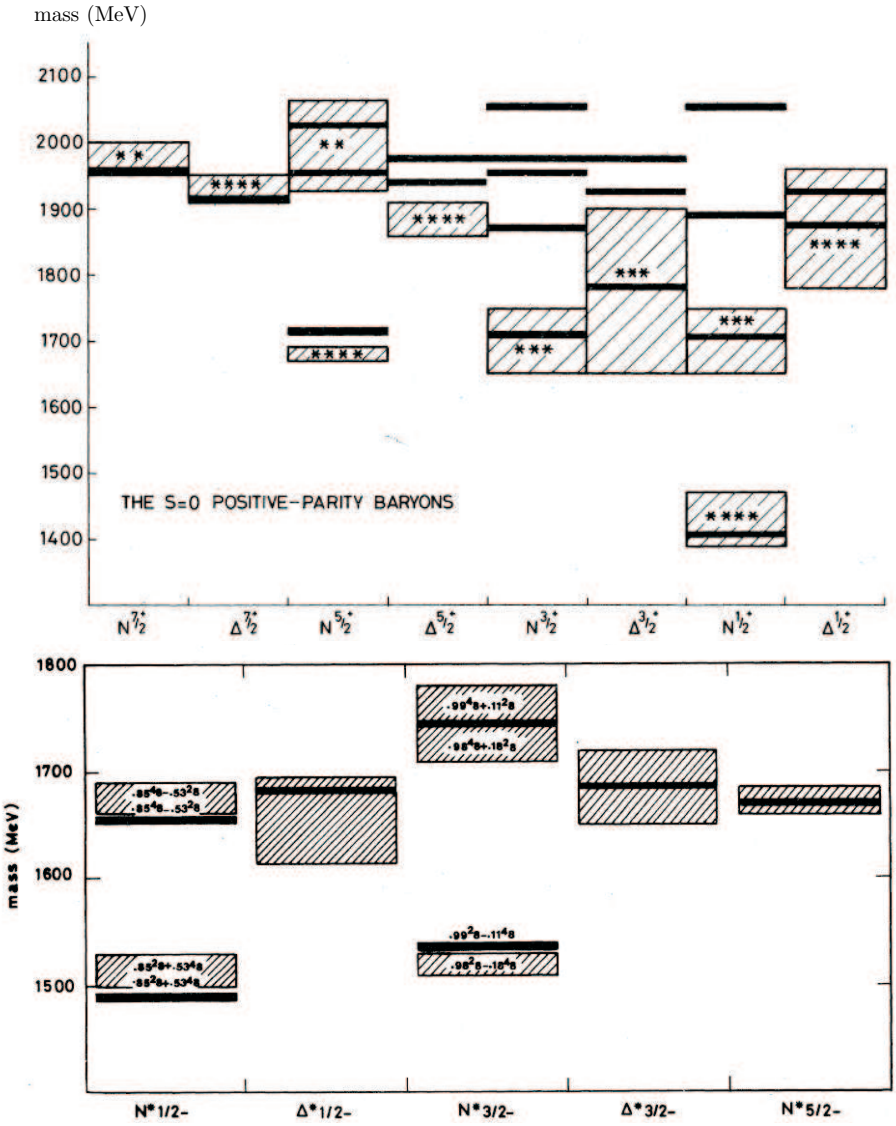

Figure 3.4: *The positive (upper figure) and negative (lower figure) parity baryons with S=0 as predicted by the IK model (solid bar) and seen in experiment (shaded region). These figures have been taken from [59] and [66].*

The quark model which we will employ throughout this thesis is in a sense much simpler than the Isgur Karl model. We follow the idea of Schlumpf [68] and choose the simplest possible ansatz for the spatial wave function, i.e. a gaussian. As we are not interested in calculating the baryon spectrum we do not have to bother with specifying the interaction that describes the quark model, either. Instead the only two free parameters, the quark mass and the slope of the gaussian are adjusted such that the form factor $G_M^p(Q^2)$ is well described. Obviously this ansatz implies less predictive power than e.g. the IK model, but it has the merit of phenomenological simplicity. In another way this model is more elaborate as it treats the quark model relativistically. We will discuss this in more detail in the next section.

3.3 Quark models on the light front

In a relativistic model treatment Poincare invariance has to be respected. This means that the generators of the Poincare group (space time translations P^μ and pure Lorentz transformations $M^{\mu\nu}$) have to satisfy the commutation relations

$$\begin{aligned}
[P^\mu, P^\nu] &= 0 \\
[M^{\mu\nu}, P^\sigma] &= i(P^\mu g^{\nu\sigma} - P^\nu g^{\mu\sigma}) \\
[M^{\mu\nu}, M^{\rho\sigma}] &= i(g^{\nu\rho} M^{\mu\sigma} - g^{\mu\rho} M^{\nu\sigma} + g^{\mu\sigma} M^{\nu\rho} - g^{\nu\sigma} M^{\mu\rho}) \quad .
\end{aligned}$$

The physical interpretation of the Lorentz transformations is apparent if one rewrites them such that they become the generators of angular momentum and Lorentz boosts

$$\begin{aligned}
J^i &= \frac{1}{2}\epsilon_{ijk} M^{jk} \\
K^i &= M^{0i}
\end{aligned}$$

In 1949 Dirac has given a classification [19] of forms of relativistic dynamics which combine the restricted principle of relativity with the Hamiltonian formulation of dynamics. He distinguished three genuinely different forms of hamiltonian dynamics. They differ in the choice of the kinematical subgroup (stability group) which leaves a hyperplane on which physical initial conditions are specified (i.e. quantization is done with respect to the coordinate which spans the hyperplane) invariant. The other generators of the Poincare group are called dynamical operators (Dirac called them Hamiltonians).

Firstly there is the familiar instant form (IF) where the three vector of total momentum $\vec{P}$ and $\vec{J}$ are kinematical, while the 0 component of total momentum P^0 and the Lorentz boosts $\vec{K}$ are dynamical operators. In the instant form the invariant hyperplane of the kinematical subgroup is given by $t = t_0$.

Secondly the point (PF) form which has $M^{\mu\nu}$ as kinematical subgroup while the components of the total momentum four vector P^μ are the dynamical operators. The quantization surface for the point form is given by $x_\mu x^\mu = a^2 > 0$ with $x^0 > 0$.

Finally there is the (light) front form (LF) which we will use to formulate the quark model

which we use in this thesis. With the generators

$$\begin{aligned} P^+ &= P^0 + P^3 \\ \vec{P}^\perp & \\ E^1 &= M^{+1} = K^1 + J^2 \\ E^2 &= M^{+2} = K^2 - J^1 \\ J_z &= M^{12} \\ K_z &= M^{-+} \end{aligned}$$

the front form has the largest possible kinematical subgroup. The dynamical generators are

$$\begin{aligned} P^- & \\ F^1 &= M^{-1} = K^1 - J^2 \\ F^2 &= M^{-2} = K^2 + J^1 \quad . \end{aligned}$$

The kinematical operators leave the hyperplane $t + z = 0$ invariant.

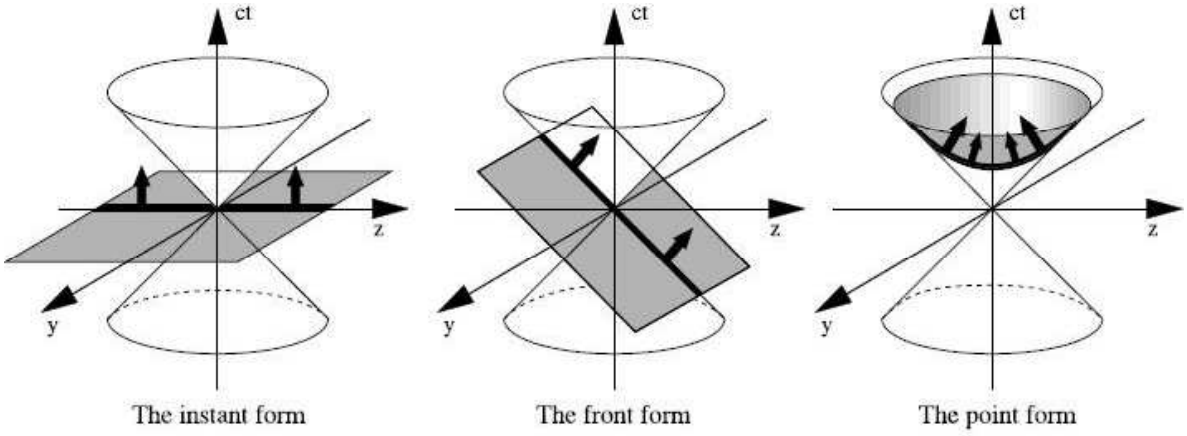

Figure 3.5: *Illustration of the forms of relativistic dynamics.*

For the light front coordinates we choose the convention

$$\begin{aligned} A^\pm &= A^0 \pm A^3 \\ \vec{A}^\perp &= (A^1, A^2) \quad . \end{aligned}$$

The light front Hamiltonian

$$P^- = \frac{M^2 + \vec{P}^\perp 2}{P^+} > 0 \quad .$$

is bounded hence its sign depends on P^+ alone. This property is an advantage of the **LF** form which becomes transparent if one considers specific processes. For example if one considers electromagnetic form factors of the nucleon the fact that P^+ is always non negative forbids contributions from diagrams which change the number of partons in the nucleon. One can

choose the Drell-Yan frame where q^+, the + component of the photon is zero. Then it follows from the positivity constraint on P^+ that diagrams like in fig. 3.6 that would contribute to off-diagonal Fock amplitudes are forbidden.

In the instant form on the contrary one would have to consider amplitudes with different Fock states, for instance $\langle qqqq\bar{q} \mid J^\mu \mid qqq\rangle$. In constituent quark models (**CQM**) one misses all contributions of amplitudes that contain higher Fock states. But at least it is assuring that in the **LF** form the form factors can be evaluated consistently in the sense, that the model assumption of the **CQM** concerning the number of partons in the nucleon is compatible with the evaluation of the electromagnetic form factors. The same holds for DVCS in the kinematical regime $\xi \leq x \leq 1$.

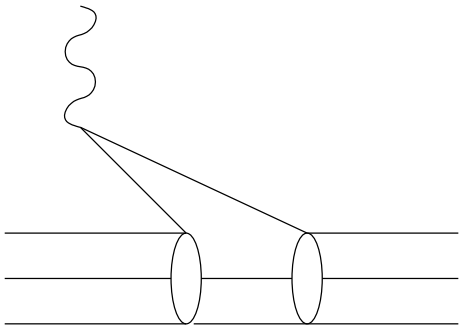

Figure 3.6: *This graph is forbidden in the Drell-Yan frame*

In the following we will present a convenient derivation of LF boosts and spinors by identifying the LF form with the infinite momentum frame (IMF). This idea goes back to Susskind [69].

Consider two reference frames. In the reference frame A (**A**) a baryon is at rest, in the reference frame B (**B**), it has the four momentum

$$P^\mu = \begin{pmatrix} E \\ 0 \\ 0 \\ P \end{pmatrix} \quad .$$

The Lorentz boost [4] $L_c(\omega_P)$ which maps **A** to **B** is thus expressed using the baryon momentum. Next consider a particle (e.g. a quark) with the momentum k^μ in **A**. If we denote its momentum in **B** by p^μ the Lorentz boost $L_c(\omega_P)$ acts like

$$p^\mu = L_c(\omega_P)\, k^\mu = \begin{pmatrix} k_0\, cosh(\omega) + k_3\, sinh(\omega) \\ k_1 \\ k_2 \\ k_0\, sinh(\omega) + k_z\, cosh(\omega) \end{pmatrix} \quad ,$$

where

$$cosh(\omega_P) = \frac{E}{M} \quad \text{and} \quad sinh(\omega_P) = \frac{P}{M} \quad .$$

[4] During the identification of IMF and LF we will denote instant form boosts with L_c and light front boosts with L_f.

The **IMF** is now obtained from **B** by sending the baryon momentum in z–direction to infinity. In this limit the z–component of the quark momentum p_z does not stay finite either. Instead one considers the finite fraction

$$\eta := \frac{p_z}{P} \quad .$$

With help of this momentum fraction one can expand p_0 and E:

$$\begin{aligned} p_0 &= \sqrt{m^2 + p_z^2 + p_\perp^2} = \sqrt{\eta^2 P^2 + p_\perp^2 + m^2} = \eta\, P + \frac{p_\perp^2 + m^2}{2\eta\, P} + O(P^{-2}) \\ E &= \sqrt{P^2 + M^2} = P + \frac{M^2}{2P} + O(P^{-2}) \quad . \end{aligned}$$

Here M denotes the mass of the baryon and m the mass of the (free) quark. Using

$$k^\mu = L_c^{-1}(\omega_P) p^\mu$$

one obtains

$$\begin{aligned} k_0 &= \left[\left(\eta\, P + \frac{p_\perp^2 + m^2}{2\eta P} + O(P^{-2}) \right) \frac{1}{M} \left(P + \frac{M^2}{2P} + O(P^{-2}) \right) - \eta\, P \frac{P}{M} \right] \\ &= \frac{1}{2} \left(M\, \eta + \frac{p_\perp^2 + m^2}{\eta\, M} \right) + O(P^{-1}) \qquad \text{and} \\ k_3 &= \left[- \left(\eta\, P + \frac{p_\perp^2 + m^2}{2\eta P} + O(P^{-2}) \right) \frac{P}{M} + \eta\, P \frac{1}{M} \left(P + \frac{M^2}{2P} + O(P^{-2}) \right) \right] \\ &= \frac{1}{2} \left(M\, \eta - \frac{p_\perp^2 + m^2}{\eta\, M} \right) + O(P^{-1}) \quad . \end{aligned}$$

In the infinite momentum limit one can then define

$$\begin{aligned} k^+ &:= k_0 + k_3 = \eta\, M \\ k^- &:= k_0 - k_3 = \frac{p_\perp^2 + m^2}{\eta\, M} \quad , \end{aligned}$$

which agrees with our notation for light front coordinates. Note that the quark momentum fraction is identical with the + component of the light front momentum fraction:

$$x := \frac{p^+}{P^+} = \frac{p^0 + p^3}{E + P} = \frac{\left(\frac{P}{M} k^0 + \frac{E}{M} k^3\right) + \left(\frac{E}{M} k^0 + \frac{P}{M} k^3\right)}{E + P} = \frac{k^+}{M} = \eta \quad .$$

In the following, **LF** momenta shall be denoted with $\tilde{k} = (k^+, k^\perp, k^-)$. Formally the **IMF** and **LF** form can be identified in the following way:

$$\tilde{k} = \lim_{P \to \infty} \left[L_c^{-1}(\omega_P) L_c(\omega_p) \right] \begin{pmatrix} m \\ 0 \\ 0 \\ 0 \end{pmatrix} =: L_f(\omega_k) \begin{pmatrix} m \\ 0 \\ 0 \\ 0 \end{pmatrix} \quad .$$

In order to establish an identification of all **LF** generators of the Poincare group consider a Lorentz frame **C**, where the quark has the momentum k'^μ and which is connected to **B** via a (canonical) boost in z-direction:

$$k'^\mu = L_c(\omega_z) p^\mu$$

The **LF** boost in z-direction can then be identified with the **IMF** boost in z-direction, via

$$\begin{aligned}
\tilde{k}' &= \lim_{P\to\infty} \left[L_c(\omega_z)L_c(\omega_p)\right] \begin{pmatrix} m \\ 0 \\ 0 \\ 0 \end{pmatrix} \\
&= \lim_{P\to\infty} \left[L_c(\omega_z)L_c(\omega_P)\right] \lim_{P\to\infty} \left[L_c^{-1}(\omega_P)L_c(\omega_p)\right] \begin{pmatrix} m \\ 0 \\ 0 \\ 0 \end{pmatrix} \\
&= \lim_{P\to\infty} \left[L_c(\omega_z)L_c(\omega_P)\right] \tilde{k} \quad \text{. Thus} \\
L_f(\omega_z) &:= \lim_{P\to\infty} \left[L_c(\omega_z)L_c(\omega_P)\right] \quad .
\end{aligned}$$

obviously then the **LF**–boost in z-direction acts on **LF** momenta like

$$\begin{aligned}
k'^{+} &= L_f(\omega_z)k^{+} = exp(\omega_z)k^{+} \\
k'^{\perp} &= L_f(\omega_z)k^{\perp} = k^{\perp} \\
k'^{-} &= L_f(\omega_z)k^{-} = exp(-\omega_z)k^{-} \quad .
\end{aligned}$$

This boost is generated by one of the Poincare group generators, namely K_z.

Next we want to identify the **LF** boosts in perpendicular direction. Let **D** be the Lorentz frame which is obtained from **B** by a rotation around the x-axis with the angle[5] $\epsilon_x =: \omega_y \cdot \frac{M}{P}$. For the quark momentum in **D** one finds

$$\begin{aligned}
k'_y &= cos(\epsilon_x)p_y + sin(\epsilon_x)p_z \qquad \text{and} \\
k'_z &= cos(\epsilon_x)p_z - sin(\epsilon_x)p_y \quad .
\end{aligned}$$

After taking the limit $P \to \infty$ one can identify this (infinitesimal) **IMF** rotation around the x-axis with the so called **LF** boosts in y-direction by defining

$$L_f(\omega_y) := \lim_{P\to\infty} \left[R(\epsilon_x)L_c(\omega_P)\right] \quad .$$

One finds:

$$\begin{aligned}
k'^{+} &= L_f(\omega_y)k^{+} = k^{+} \\
k'_x &= L_f(\omega_y)k_x = k_x \\
k'_y &= L_f(\omega_y)k_y = k_y + \omega_y k^{+} \quad .
\end{aligned}$$

With the particle being on shell it follows

$$k'^{-} = L_f(\omega_y)k^{-} = k^{-} + \omega_y \left(2k_y + \omega_y\, k^{+}\right) \quad .$$

From these transformation laws one can read off, that this Lorentz transformation is generated by the sum of the generators for a boost in x-direction and a rotation around the y-axis

$$E^1 = k^1 + J^2 \quad .$$

[5]The labeling of ω_y is no misprint but reveals the fact that the **LF** boost in y-direction relates to an infinitesimal rotation around the x-axis in the **IMF**

The same can be done for a rotation around the y-axis in the **IMF**. Here one finds

$$k'^{-} = L_f(\omega_x)k^{-} = k^{-} + \omega_x \left(2k_x + \omega_x\, k^{+}\right)$$

which is generated by

$$E^2 = k^1 - J^2 \quad .$$

The invariance of the hypersphere perpendicular to the **LF** time $t+z$ under the above defined **LF** boosts can be seen from the fact, that the + component is only multiplied with a factor under these transformations. (Additionally one can see easily that the **LF** boosts form a group). The other 4 Poincare transformations which belong to the **LF** kinematical subgroup are the rotation around the z-axis (only the perpendicular components change, the IMF limit does not matter), translations in x- and y-direction (with the same argument) and the translation in - direction (generated by P^+). The three remaining Poincare transformations (translation in **LF** time generated by the **LF** Hamiltonian P^-, F^1 and F^2 form the dynamical subgroup.

A key issue for the convenient use of the **LF** form for composite particles is the possibility to separate the internal momenta of the composite system from the external ones such, that the internal momenta are invariant under the kinematical subgroup.

Consider for example a baryon consisting of three quarks. Denote the baryon momentum by $\tilde{P} = (P^+, \vec{P}_\perp)$ and the quark momenta by $\tilde{p}_i = (p_i^+, \vec{p}_{i\perp})$. Then one can choose e.g. the internal coordinates

$$\begin{aligned} x_i &:= \frac{p_i^+}{P^+} \\ k_{\perp i} &= p_{i\perp} - x_i P_\perp \end{aligned} \tag{3.4}$$

such that

$$\begin{aligned} \sum_i x_i &= 1 \\ \sum_i k_{i\perp} &= 0 \quad . \end{aligned}$$

From the explicit transformation rules for the kinematical subgroup one can verify the invariance of the above chosen internal momenta. As examples we verify their invariance under **LF** boosts.

For a **LF** boost in z-direction one finds:

$$\begin{aligned} x_i \to x_i' = \frac{p_i'^+}{P'^+} = \frac{exp(\omega_z)p_i^+}{\exp(\omega_z)P^+} = \frac{p_i'^+}{P'^+} = x_i \quad \text{and} \\ \vec{k}_{i\perp} \to \vec{k}'_{i\perp} = \vec{p}'_{i\perp} - x_i'\vec{P}'_\perp = \vec{p}_{i\perp} - x_i\vec{P}_\perp = \vec{k}_{i\perp} \quad . \end{aligned}$$

Under a **LF** boost in perpendicular direction one verifies:

$$\begin{aligned} x_i \to x_i' = \frac{p_i'^+}{P'^+} = \frac{p_i^+}{P^+} = x_i \quad \text{and} \\ \vec{k}_{i\perp} \to \vec{k}'_{i\perp} = \vec{p}'_{i\perp} - x_i'\vec{P}'_\perp = \vec{p}_{i\perp} + \vec{\omega}_\perp p_i^+ - x_i\left(\vec{P}_\perp + \vec{\omega}_\perp P^+\right) \\ = \left(\vec{p}_{i\perp} - x_i\vec{P}_\perp\right) + \vec{\omega}_\perp\left(p_i^+ - x_i P^+\right) = \vec{k}_{i\perp} \quad . \end{aligned}$$

Invariance under the other 4 transformations of the kinematical subgroup can be verified analogously. This property is one key issue which features the LF form as it guarantees that wave functions which are expressed in terms of internal coordinates are invariant under Lorentz boosts.

Next we have to construct LF spinors. The transformation of instant form spinors into LF spinors is known as Melosh rotation [70]. From the requirement of Lorentz invariance of the Lagrangian for a free spin 1/2 particle one knows how the representations of the Lorentz–boost for four vectors and spinors are connected. Infinitesimally this connection can be written as

$$\begin{aligned} x^\mu \to x'^\mu = \Lambda^{\mu\nu} x_\nu &= (g^{\mu\nu} + \epsilon^{\mu\nu})\, x_\nu \\ \psi(x^\mu) \to \psi'(x'^\mu) = S(\Lambda)\psi(x^\mu) &= \left(1 - \frac{i}{4}\epsilon^{\mu\nu}\sigma_{\mu\nu}\right)\psi(x^\mu) \quad . \end{aligned}$$

For the boost in z–direction (needed for $L_c(\omega_P)$) one has

$$\Lambda^\mu_{\ \nu} = \begin{pmatrix} cosh(\omega) & 0 & 0 & -sinh(\omega) \\ 0 & 1 & 0 & 0 \\ 0 & 0 & 1 & 0 \\ -sinh(\omega) & 0 & 0 & cosh(\omega) \end{pmatrix} \to \epsilon_{\mu\nu} = \begin{pmatrix} 0 & 0 & 0 & -\omega \\ 0 & 0 & 0 & 0 \\ 0 & 0 & 0 & 0 \\ \omega & 0 & 0 & 0 \end{pmatrix} \quad .$$

Together with

$$\frac{i}{4}\sigma^{30} = -\frac{i}{4}\sigma^{03} = \frac{1}{8}\left(\gamma^0\gamma^3 - \gamma^3\gamma^0\right) = \frac{1}{4}\begin{pmatrix} 0 & 0 & + & 0 \\ 0 & 0 & 0 & - \\ + & 0 & 0 & 0 \\ 0 & - & 0 & 0 \end{pmatrix}$$

one finds

$$\begin{aligned} S(L_c(\omega_P)) = exp\left(-\frac{i}{4}\epsilon^{\mu\nu}\sigma_{\mu\nu}\right) &= exp\begin{pmatrix} 0 & 0 & \frac{\omega}{2} & 0 \\ 0 & 0 & 0 & -\frac{\omega}{2} \\ \frac{\omega}{2} & 0 & 0 & 0 \\ 0 & -\frac{\omega}{2} & 0 & 0 \end{pmatrix} \\ &= \begin{pmatrix} cosh(\frac{\omega}{2}) & 0 & sinh(\frac{\omega}{2}) & 0 \\ 0 & cosh(\frac{\omega}{2}) & 0 & -sinh(\frac{\omega}{2}) \\ sinh(\frac{\omega}{2}) & 0 & cosh(\frac{\omega}{2}) & 0 \\ 0 & -sinh(\frac{\omega}{2}) & 0 & cosh(\frac{\omega}{2}) \end{pmatrix} \quad . \end{aligned}$$

With the expressions for the **IF** spinors (see appendix A) one finds for the **LF** spinors

$$\begin{aligned} u_{LF}(\tilde{k}, s) &= \lim_{P\to\infty}\left[S(L_c^{-1}(\omega_P))S(L_c(\omega_p))u(0,s)\right] \\ &= \lim_{P\to\infty}\left[S(L_c^{-1}(\omega_P))u(\vec{p},s)\right] \\ &= \lim_{P\to\infty}\sqrt{p_0+m}\begin{pmatrix} \left[cosh(\frac{\omega}{2}) - \frac{\sigma_3\vec{\sigma}\cdot\vec{p}}{p_0+m}\,sinh(\frac{\omega}{2})\right]\chi(s) \\ \left[-\sigma_3 sinh(\frac{\omega}{2}) + \frac{\vec{\sigma}\cdot\vec{p}}{p_0+m}\,cosh(\frac{\omega}{2})\right]\chi(s) \end{pmatrix} \quad . \end{aligned}$$

To evaluate the infinite momentum limit an expansion of this expression in powers of P^{-1} is required. With

$$cosh(\frac{\omega}{2}) = \sqrt{\frac{E+M}{2M}} \qquad \text{and}$$
$$sinh(\frac{\omega}{2}) = \sqrt{\frac{E-M}{2M}} = \sqrt{\frac{E+M}{2M}}\frac{P}{E+M} = \sqrt{\frac{E+M}{2M}}\left(1 - \frac{M}{P} + O(P^{-2})\right)$$

one yields

$$u_{LF}(\tilde{k}, s) = \frac{1}{\sqrt{2k^+}} \begin{pmatrix} \left[m + k^+ + \vec{\sigma}_\perp \vec{k}_\perp \sigma_3\right] \chi(s) \\ \left[-\sigma_3 \left(m - k^+\right) + \vec{\sigma}_\perp \vec{k}_\perp\right] \chi(s) \end{pmatrix} \quad . \tag{3.5}$$

introducing $k_L = k_1 - ik_2$ and $k_R = k_1 + ik_2$ one finds the light front spinors

$$u^\uparrow_{LF} = \frac{1}{\sqrt{2k^+}} \begin{pmatrix} m + k^+ \\ k_R \\ k^+ - m \\ k_R \end{pmatrix} \quad ; \qquad u^\downarrow_{LF} = \frac{1}{\sqrt{2k^+}} \begin{pmatrix} -k_L \\ k^+ + m \\ k_L \\ -k^+ + m \end{pmatrix} \quad .$$

For later convenience we give here the representation for the Melosh rotation in a two component Pauli spinor basis. It can be read off from eq. 3.5 and the normalization condition for the Pauli spinors in **IF** and **LF**:

$$\chi^{\uparrow,\downarrow}_{LF}(\tilde{k}) = R_{cf}(\tilde{k})\chi^{\uparrow,\downarrow}(k^\mu) \qquad \text{with} \qquad R_{cf}(\tilde{k}) = \frac{(m + k^+) + \vec{\sigma}_\perp \vec{k}_\perp \sigma_3}{\sqrt{(m + k^+)^2 + \vec{k}^2_\perp}} \quad . \tag{3.6}$$

We should emphasize that the meaning of **LF** spin is different from the canonical spin (as one sees already from the fact that the Melosh rotation mixes the "spin states"):

$$\bar{u}(k, \lambda')u_{LF}(\tilde{k}, \lambda) \neq 0 \quad \text{for } \lambda \neq \lambda' \quad .$$

In the instant form it denotes the spin projection in z-direction whereas in **LF** form it is an eigenvalue of the helicity operator, although only in the $\vec{k}_\perp = 0$ frame it is the projection of spin along the direction of motion.

Until now we have shown how the Melosh rotation looks for a free spin 1/2 particle state and thus how it acts on a spinor. Next we have to consider a composite particle. Let us construct a hadron state. Again we use a different notation for **IF** and **LF** momenta:

$$\tilde{k} = (k^+, \vec{k}_\perp) \qquad \textbf{LF}$$
$$\vec{k} = (k_x, k_y, k_z) \qquad \textbf{IF} \quad .$$

Furthermore states will be denoted with [f] (light front) and [c] (canonical=instant) respectively. The meaning of the respective spin variable then follows from the context. The Melosh transformation does not affect the isospin so in the following we will not display this degree of freedom explicitly. We will denote the momentum of the composite particle with $\tilde{P}$, the momenta of the constituents with $\tilde{p}_i$ and the internal coordinates of the constituents (eq. 3.4) with $(x_i, \vec{p}_{i\perp})$.

First the light front hadron states can be expressed in terms of single particle states:

$$\mid \tilde{P},\lambda\rangle_{[f]} = \sum_{\beta}\int [\frac{dx}{\sqrt{x}}][d^2\vec{p}_\perp]\psi_\beta^{\lambda[f]}(\tilde{p}_1,\tilde{p}_2,\tilde{p}_3) \mid \beta,\tilde{p}_1,\tilde{p}_2,\tilde{p}_3\rangle \tag{3.7}$$

where β is an index for color, helicity and flavor (implying the CG construction for the respective hadron) and

$$[\frac{dx}{\sqrt{x}}] = \delta(1-\sum_{j=1}^{3}x_j)\prod_{i=1}^{3}\frac{dx_i}{\sqrt{x_i}}$$

$$[d^2\vec{p}_\perp] = 16\pi^3\delta^{(2)}(\vec{P}_\perp - \sum_{j=1}^{3}\vec{p}_{j\perp})\prod_{i=1}^{3}\frac{d^2\vec{p}_{i\perp}}{16\pi^3} \quad .$$

These states are normalized according to

$${}_{[f]}\langle\tilde{P}',\lambda' \mid P,\lambda\rangle_{[f]} = 16\pi^3P^+\delta(P^+-P'^+)\delta^{(2)}(\vec{P}'_\perp-\vec{P}_\perp)\delta_{\lambda'\lambda} \quad .$$

The normalization of the wave function reads

$$\sum_{\beta}\int [dx][d\vec{p}_\perp] \mid \psi_\beta^{\lambda[f]}(\tilde{p}_1,\tilde{p}_2,\tilde{p}_3) \mid^2 = 1 \quad .$$

Bearing in mind that **LF** spin has a different meaning than the canonical spin the main difficulty in working with the **LF** form lies in the construction of the wave function $\psi_\beta^{\lambda[f]}(\tilde{p}_1,\tilde{p}_2,\tilde{p}_3)$. In order to apply the $SU(6)$ construction of the hadron wave functions it is necessary to establish a connection between the **IF** wave function and the **LF** wave function.

In the instant form one can write the hadron state as

$$\mid \vec{P},\lambda\rangle_{[c]} = \sum_{\beta}\int\prod_{i=1}^{3}\Big(d\vec{p}_i\Big)\psi_\beta^{\lambda[c]}(\vec{p}_1,\vec{p}_2,\vec{p}_3) \mid \beta,\vec{p}_1,\vec{p}_2,\vec{p}_3\rangle \quad . \tag{3.8}$$

The **IF** hadron states are normalized according to

$${}_{[c]}\langle\vec{P}',\lambda' \mid \vec{P},\lambda\rangle_{[c]} = \delta^{(3)}(\vec{P}'-\vec{P})\delta_{\beta'\beta} \quad .$$

The wave function normalization reads

$$\sum_{\beta}\int\prod_{i=1}^{3}\Big(\vec{p}_i\Big) \mid \psi_\beta^{\lambda[c]}(\vec{p}_1,\vec{p}_2,\vec{p}_3) \mid^2 = 1 \quad . \tag{3.9}$$

Following eq. 3.6 the single quark state transforms according to

$$\mid \tilde{p},\lambda,\rangle_{[f]} = \sqrt{2p_0(2\pi)^3}\sum_{\lambda'}D^{\frac{1}{2}}_{\lambda'\lambda}\left(R_{cf}(\tilde{p})\right) \mid \vec{p},\lambda',\rangle_{[c]} \quad . \tag{3.10}$$

The factor $\sqrt{16\pi^3p_0}$ stems from the different normalization of the states in **LF** and **IF** and from the Jacobi determinant $\mid \frac{\partial\tilde{p}}{\partial\vec{p}} \mid$. The connection between instant and light front form

can be established easiest in the rest frame of the composite state. We denote the free mass operator of the non interacting three body system by M_0. It can be written as

$$M_0 = \sum_i \sqrt{\vec{p}_i^{\,2} + m^2} \quad .$$

Then the Fock states are related according to (eq. 3.10)

$$\mid \tilde{0}, \lambda\rangle_{[f]} = \sqrt{2M_0(2\pi)^3} \mid \vec{0}, \lambda\rangle_{[c]} \quad . \tag{3.11}$$

Now one can evaluate the Jacobi determinant (note, that $P^+ = M_0$) in order to find

$$\begin{aligned}
[dx][d\vec{p}_\perp] &= 16\pi^3\delta(1 - \sum_{i=1}^{3} x_i)\delta^{(2)}(\vec{p}_{i\perp}) \prod_{i=1}^{3} \frac{1}{16\pi^3} dx_i \, d\vec{p}_{i\perp} \\
&= 16\pi^3\delta(1 - \sum_{i=1}^{3} \frac{p_i^0 + p_i^3}{M_0})\delta^{(2)}(\vec{p}_{i\perp}) d^3\vec{p} \prod_{i=1}^{3} \left(\frac{1}{16\pi^3} \frac{dx_i}{dp^3} \right) \\
&= 16\pi^3 M_0 \delta^{(3)}(\sum_{i=1}^{3} \vec{p}_i) d^3\vec{p} \prod_{i=1}^{3} \frac{1}{16\pi^3} \frac{dp^3 + dp^0}{M_0 \, dp^3} \\
&= 16\pi^3 M_0 \delta^{(3)}(\sum_{i=1}^{3} \vec{p}_i) d^3\vec{p} \prod_{i=1}^{3} \left(\frac{1}{16\pi^3} \frac{x_i}{p_i^0} \right) \quad .
\end{aligned}$$

Using the Melosh rotation eq. 3.10, eq. 3.7 and eq. 3.11 in the rest frame one then obtains

$$\begin{aligned}
\mid \vec{0}, \lambda\rangle_{[c]} =& \sqrt{\frac{1}{16\pi^3 M_0}} 16\pi^3 M_0 \sum_{\lambda_i} \int d^3\vec{p} \left[\prod_{i=1}^{3} \frac{1}{16\pi^3\sqrt{x_i}} \frac{x_i}{p_i^0} \right] \delta^{(3)}(\sum \vec{p}_i) \\
& \cdot \psi_\lambda^{[f]}(x_i, \vec{p}_{i\perp}, \lambda_i) \prod_{i=1}^{3} \left[\sqrt{16\pi^3 p_i^0} \sum_{\lambda_i'} D^{\frac{1}{2}}_{\lambda_i'\lambda_i}(R_{cf}(\tilde{p}_i)) \mid \vec{p}_i, \lambda_i'\rangle_{[c]} \right] \\
=& \sqrt{16\pi^3 M_0} \sum_{\lambda_i} \delta^{(3)}(\sum \vec{p}_i) \psi_\lambda^{[f]}(x_i, \vec{p}_{i\perp}, \lambda_i) \int d^3\vec{p} \\
& \cdot \prod_{i=1}^{3} \sqrt{\frac{x_i}{16\pi^3 p_i^0}} D^{\frac{1}{2}}_{\lambda_i'\lambda_i}(R_{cf}(\tilde{p}_i)) \mid \vec{p}_i, \lambda_i'\rangle_{[c]} \quad .
\end{aligned} \tag{3.12}$$

On the other hand the canonical Fock state in the rest frame is given by eq. 3.9:

$$\mid \vec{0}, \lambda\rangle_{[c]} = \sum_{\lambda_i} \int d^3p \, \delta^{(3)}(\sum \vec{p}_i) \psi_\lambda^{[c]}(\vec{p}_i, \lambda_i) \left(\prod_{i=1}^{3} \mid \vec{p}_i, \lambda_i\rangle_{[c]} \right) \quad .$$

Using the canonical normalization for the single quark state ${}_{[c]}\langle \vec{p}_i', \lambda_i' \mid \vec{p}_i, \lambda_i\rangle_{[c]} = \delta(\vec{p}_i - \vec{p}_i')\delta_{\lambda_i\lambda_i'}$ one obtains the canonical wave function

$$\psi_\lambda^{[c]}(\vec{p}_i, \lambda_i) =_{[c]} \langle \vec{p}_1, \lambda_1 \mid \langle \vec{p}_2, \lambda_2 \mid \langle \vec{p}_3, \lambda_3 \mid \vec{0}, \lambda\rangle_{[c]} \quad .$$

With (eq. 3.12) one finds

$$\psi^{[c]}_{\lambda}(\vec{p}_1,\vec{p}_2,\vec{p}_3,\lambda_1,\lambda_2,\lambda_3) = \frac{1}{16\pi^3}\sqrt{\frac{M_0 x_1 x_2 x_3}{p_1^0 p_2^0 p_3^0}} \sum_{\lambda_1',\lambda_2',\lambda_3'} D^{\frac{1}{2}}_{\lambda_1'\lambda_1}\left(R_{cf}(\tilde{p}_1)\right)$$
$$D^{\frac{1}{2}}_{\lambda_2'\lambda_2}\left(R_{cf}(\tilde{p}_2)\right) D^{\frac{1}{2}}_{\lambda_3'\lambda_3}\left(R_{cf}(\tilde{p}_3)\right) \psi^{[f]}_{\lambda}(x_1,x_2,x_3,\vec{p}_{1\perp},\vec{p}_{2\perp},\vec{p}_{3\perp},\lambda_1',\lambda_2',\lambda_3') \quad .$$

This relation can of course be inverted in order to gain the **LF** wave function from the instant form wave function

$$\psi^{[f]}_{\lambda}(\tilde{p}_1,\tilde{p}_2,\tilde{p}_3,\lambda_1,\lambda_2,\lambda_3) = 16\pi^3\sqrt{\frac{p_1^0 p_2^0 p_3^0}{M_0 x_1 x_2 x_3}} \sum_{\lambda_1',\lambda_2',\lambda_3'} D^{\frac{1}{2}\star}_{\lambda_1'\lambda_1}\left(R_{cf}(\tilde{p}_1)\right)$$
$$D^{\frac{1}{2}\star}_{\lambda_2'\lambda_2}\left(R_{cf}(\tilde{p}_2)\right) D^{\frac{1}{2}\star}_{\lambda_3'\lambda_3}\left(R_{cf}(\tilde{p}_3)\right) \psi^{[c]}_{\lambda}(\vec{p}_1,\vec{p}_2,\vec{p}_3,\lambda_1',\lambda_2',\lambda_3') \quad . \tag{3.13}$$

As we have already mentioned the **LF** wave function is invariant under light front boosts. In another language this is due to the fact that the Wigner rotation for LF boosts is unity.

Before we are ready to evaluate transition amplitudes we need to specify the spatial part of the wave function. Following [68] we use

$$\begin{aligned}\psi(\vec{p}_1,\vec{p}_2,\vec{p}_3) =& \exp\left(-\frac{M_0^2}{2\alpha}\right)\\ \alpha =& 0.56\,GeV^2\\ m =& 0.267\,GeV^2 \quad .\end{aligned} \tag{3.14}$$

Here m is the constituent quark mass and α a free parameter in the gaussian. α and m are chosen such that the magnetic proton form factor is well described up to $Q^2 = 1$ GeV^2. In order to reproduce the dipole behavior for high values of Q^2 a spatial wave function of the type $\psi(\vec{p}_1,\vec{p}_2,\vec{p}_3) = \frac{N}{(M_0^2+\alpha^2)^n}$ is better suited [71].

We are nearly ready to evaluate the transition amplitudes $G^{\mu}_{\lambda'\lambda}$. However we have to introduce an approximation at this point, the so called spectator quark (or impulse) approximation. In the impulse approximation we assume that the scattering occurs over such a short time that the binding forces during the interaction can be neglected. In a partonic interpretation this implies that the quark which is struck by a photon does not interact with the other partons in the hadron which therefore remain spectators in the process. In the next section we will discuss consequences of this approximation.

The calculations which we present in the following were partly done before. Some of the following results can be found (often in a different notation or with different conventions) in one of the following papers: [64], [65], [72], [73] and [74].

A heuristic approach to obtain the expressions for $G^{\mu}_{\lambda',\lambda}$ starts with the observation (see

e.g [68]) that $G^+_{\lambda',\lambda}$ can be expressed by

$$G^+_{\lambda',\lambda} \propto \int [d\tilde{k}]\psi^\star(1',2',3')\cdot\psi(1,2,3)\sum_{\text{spins}} CG(\text{spins})\,\langle 1' \mid M^\dagger(1')\mathbf{1}M(1)\mid 1\rangle$$
$$\cdot\,\langle 2' \mid M^\dagger(2')\mathbf{1}M(2)\mid 2\rangle\cdot\langle 3' \mid M^\dagger(3')\Big(\frac{1}{2\sqrt{k'^+k^+}}\bar{u}^{LF}(k'_3,\lambda'_3)\gamma^+u^{LF}(k_3,\lambda)\Big)M(3)\mid 3\rangle \quad .$$

Here $CG(spins)$ stands for some Clebsch Gordon coefficients which have to appear in the construction of the nucleons involved. The $[\tilde{dk}]$ sketches the 6 dimensional integral for form factors (5 dimensional for GPDs). The $M(i)$ denote the Melosh rotations for the single quarks. The label LF in the spinors emphasizes that light front Dirac spinors are meant here. In fact the clumsy expression $\frac{1}{2\sqrt{k'^+k^+}}\bar{u}^{LF}(k'_3,\lambda'_3)\gamma^+u^{LF}(k_3,\lambda)$ turns out to be 1. From this expression one can argue handwavingly that the non plus transition amplitudes can be obtained in a similar way by substituting e.g.

$$\bar{u}^{LF}(k'_3,\lambda'_3)\gamma^+u^{LF}(k_3,\lambda)\to\bar{u}^{LF}(k'_3,\lambda'_3)\gamma^\perp u^{LF}(k_3,\lambda) \quad .$$

It will turn out that the result of this description agrees with the findings of a rigorous derivation using LF quantization.

With the **LF** spinors

$$u^{LF}(p,\uparrow)=\frac{1}{\sqrt{2p^+}}\begin{pmatrix}p^++m\\ p^R\\ p^+-m\\ p^R\end{pmatrix}\quad,\qquad u^{LF}(p,\downarrow)=\frac{1}{\sqrt{2p^+}}\begin{pmatrix}-p^L\\ p^++m\\ p^L\\ m-p^+\end{pmatrix}$$
$$\bar{u}^{LF}(p',\uparrow)=\frac{1}{\sqrt{2p'^+}}\Big(p'^++m,\ \ p'^L,\ \ m-p'^+,\ \ -p'^L\Big)$$
$$\bar{u}^{LF}(p',\downarrow)=\frac{1}{\sqrt{2p'^+}}\Big(-p'^R,\ \ p'^++m,\ \ -p'^R,\ \ p'^+-m\Big)$$

and the shorthand notation

$$O_{\lambda',\lambda}=\frac{1}{2\sqrt{p'^+p^+}}\bar{u}^{LF}(p',\lambda')\,O\,u^{LF}(p,\lambda)$$

one can work out the table

O	1	γ^+	γ^x
$O_{\uparrow,\uparrow}$	$\frac{m}{2}\left(\frac{1}{p'^+}+\frac{1}{p^+}\right)$	1	$\frac{1}{2}\left(\frac{p'^x}{p'^+}+\frac{p^x}{p^+}\right)-\frac{i}{2}\left(\frac{p'^y}{p'^+}-\frac{p^y}{p^+}\right)$
$O_{\downarrow,\uparrow}$	$\frac{1}{2}\left(\frac{p^x}{p^+}-\frac{p'^x}{p'^+}\right)+\frac{i}{2}\left(\frac{p^y}{p^+}-\frac{p'^y}{p'^+}\right)$	0	$\frac{m}{2}\left(\frac{1}{p'^+}-\frac{1}{p^+}\right)$
$O_{\uparrow,\downarrow}$	$\frac{1}{2}\left(\frac{p'^x}{p'^+}-\frac{p^x}{p^+}\right)+\frac{i}{2}\left(\frac{p^y}{p^+}-\frac{p'^y}{p'^+}\right)$	0	$-\frac{m}{2}\left(\frac{1}{p'^+}-\frac{1}{p^+}\right)$
$O_{\downarrow,\downarrow}$	$\frac{m}{2}\left(\frac{1}{p'^+}+\frac{1}{p^+}\right)$	1	$\frac{1}{2}\left(\frac{p'^x}{p'^+}+\frac{p^x}{p^+}\right)+\frac{i}{2}\left(\frac{p'^y}{p'^+}-\frac{p^y}{p^+}\right)$

O	γ^y	γ^-
$O_{\uparrow,\uparrow}$	$\frac{1}{2}\left(\frac{p'^y}{p'^+}+\frac{p^y}{p^+}\right)+\frac{i}{2}\left(\frac{p'^x}{p'^+}-\frac{p^x}{p^+}\right)$	$\frac{m^2+p^xp'^x+p^yp'^y+i(p^yp'^x-p'^yp^x)}{p^+p'^+}$
$O_{\downarrow,\uparrow}$	$\frac{im}{2}\left(\frac{1}{p'^+}-\frac{1}{p^+}\right)$	$\frac{m\left[(p^x-p'^x)+i(p^y-p'^y)\right]}{p'^+p^+}$
$O_{\uparrow,\downarrow}$	$\frac{im}{2}\left(\frac{1}{p'^+}-\frac{1}{p^+}\right)$	$\frac{m\left[(p'^x-p^x)+i(p^y-p'^y)\right]}{p'^+p^+}$
$O_{\downarrow,\downarrow}$	$\frac{1}{2}\left(\frac{p'^y}{p'^+}+\frac{p^y}{p^+}\right)-\frac{i}{2}\left(\frac{p'^x}{p'^+}-\frac{p^x}{p^+}\right)$	$\frac{m^2+p^xp'^x+p^yp'^y-i(p^yp'^x-p'^yp^x)}{p^+p'^+}$

O	γ_5	$\gamma^+\gamma_5$	$\gamma^x\gamma_5$
$O_{\uparrow,\uparrow}$	$\frac{m}{2}\left(\frac{1}{p'^+}-\frac{1}{p^+}\right)$	1	$\frac{1}{2}\left(\frac{p'^x}{p'^+}+\frac{p^x}{p^+}\right)-\frac{i}{2}\left(\frac{p'^y}{p'^+}-\frac{p^y}{p^+}\right)$
$O_{\downarrow,\uparrow}$	$\frac{1}{2}\left(\frac{p^x}{p^+}-\frac{p'^x}{p'^+}\right)+\frac{i}{2}\left(\frac{p^y}{p^+}-\frac{p'^y}{p'^+}\right)$	0	$\frac{m}{2}\left(\frac{1}{p'^+}+\frac{1}{p^+}\right)$
$O_{\uparrow,\downarrow}$	$\frac{1}{2}\left(\frac{p^x}{p^+}-\frac{p'^x}{p'^+}\right)-\frac{i}{2}\left(\frac{p^y}{p^+}-\frac{p'^y}{p'^+}\right)$	0	$\frac{m}{2}\left(\frac{1}{p'^+}+\frac{1}{p^+}\right)$
$O_{\downarrow,\downarrow}$	$\frac{m}{2}\left(\frac{1}{p^+}-\frac{1}{p'^+}\right)$	-1	$-\frac{1}{2}\left(\frac{p^x}{p^+}+\frac{p'^x}{p'^+}\right)+\frac{i}{2}\left(\frac{p^y}{p^+}-\frac{p'^y}{p'^+}\right)$

O	$\gamma^y\gamma_5$	$\gamma^-\gamma_5$
$O_{\uparrow,\uparrow}$	$\frac{1}{2}\left(\frac{p'^y}{p'^+}+\frac{p^y}{p^+}\right)+\frac{i}{2}\left(\frac{p'^x}{p'^+}-\frac{p^x}{p^+}\right)$	$\frac{-m^2+p^xp'^x+p^yp'^y+i(p^yp'^x-p'^yp^x)}{p^+p'^+}$
$O_{\downarrow,\uparrow}$	$\frac{im}{2}\left(\frac{1}{p'^+}+\frac{1}{p^+}\right)$	$\frac{m\left[(p^x+p'^x)+i(p^y+p'^y)\right]}{p'^+p^+}$
$O_{\uparrow,\downarrow}$	$-\frac{im}{2}\left(\frac{1}{p'^+}+\frac{1}{p^+}\right)$	$\frac{m\left[(p^x+p'^x)-i(p^y+p'^y)\right]}{p'^+p^+}$
$O_{\downarrow,\downarrow}$	$-\frac{1}{2}\left(\frac{p'^y}{p'^+}+\frac{p^y}{p^+}\right)+\frac{i}{2}\left(\frac{p'^x}{p'^+}-\frac{p^x}{p^+}\right)$	$\frac{m^2-p^xp'^x-p^yp'^y+i(p^yp'^x-p'^yp^x)}{p^+p'^+}$

(3.15)

Using this table one can represent the one body current operators J^μ and J^μ_5 in terms of pauli matrices. For example one can read off from the table

$$\langle p',\lambda' \mid J^+_5 \mid p,\lambda\rangle = \frac{1}{2\sqrt{p'^+p^+}}\bar{u}^{LF}(p',\lambda')\gamma^+\gamma_5 u^{LF}(p,\lambda) = \chi^\dagger_{\lambda'}\sigma_z\chi_\lambda \qquad \longrightarrow \qquad J^+_5 \to \sigma_z \quad .$$

To complete this representation one finds

$$
\begin{aligned}
J^+ &\to \mathbf{1} \\
J^x &\to \frac{1}{2}\Big(\frac{p'^x}{p'^+}+\frac{p^x}{p^+}\Big)\mathbf{1}+\frac{m}{2}\Big(\frac{1}{p^+}-\frac{1}{p'^+}\Big)\mathbf{i\sigma_x}+\frac{1}{2}\Big(\frac{p^y}{p^+}-\frac{p'^y}{p'^+}\Big)\mathbf{i\sigma_z} \\
J^y &\to \frac{1}{2}\Big(\frac{p'^y}{p'^+}+\frac{p^y}{p^+}\Big)\mathbf{1}+\frac{m}{2}\Big(\frac{1}{p'^+}-\frac{1}{p^+}\Big)\mathbf{i\sigma_x}+\frac{1}{2}\Big(\frac{p'^x}{p'^+}-\frac{p^x}{p^+}\Big)\mathbf{i\sigma_z} \\
J^- &\to \frac{m^2+p'^xp^x+p'^yp^y}{p^+p'^+}\mathbf{1}+\frac{m(p^y-p'^y)}{p^+p\prime+}\mathbf{i\sigma_x}+\frac{m(p'^x-p^x)}{p^+p\prime+}\mathbf{i\sigma_y}+\frac{p^yp'^x-p'^yp^x}{p^+p'^+}\mathbf{i\sigma_z} \\
\\
J_5^+ &\to \sigma_\mathbf{z} \\
J_5^x &\to \frac{1}{2}\Big(\frac{p^y}{p^+}-\frac{p'^y}{p'^+}\Big)\mathbf{i1}+\frac{m}{2}\Big(\frac{1}{p^+}+\frac{1}{p'^+}\Big)\sigma_\mathbf{x}+\frac{1}{2}\Big(\frac{p^x}{p^+}+\frac{p'^x}{p'^+}\Big)\sigma_\mathbf{z} \\
J_5^y &\to \frac{1}{2}\Big(\frac{p'^x}{p'^+}-\frac{p^x}{p^+}\Big)\mathbf{i1}+\frac{m}{2}\Big(\frac{1}{p'^+}+\frac{1}{p^+}\Big)\sigma_\mathbf{y}+\frac{1}{2}\Big(\frac{p'^y}{p'^+}+\frac{p^y}{p^+}\Big)\sigma_\mathbf{z} \\
J_5^- &\to \frac{p^yp'^x-p'^yp^x}{p^+p'^+}\mathbf{i1}+\frac{m(p^x+p'^x)}{p^+p'^+}\sigma_\mathbf{x}+\frac{m(p'^y+p^y)}{p^+p'^+}\sigma_\mathbf{y}+\frac{p'^xp^x+p'^yp^y-m^2}{p^+p'^+}\sigma_\mathbf{z} \quad . \qquad (3.16)
\end{aligned}
$$

Finally the Melosh rotation for these operators have to be applied. In a Pauli spinor basis one needs (eq. 3.6)

$$
\begin{aligned}
R_{cf}(p') &= \frac{m+xM_0'-i\vec{\sigma}(\hat{n}\times\vec{p}'_\perp)}{\sqrt{(m+xM_0')^2+\vec{p}'^2_\perp}} \\
R^\star_{cf}(p) &= \frac{m+xM_0+i\vec{\sigma}(\hat{n}\times\vec{p}_\perp)}{\sqrt{(m+xM_0)^2+\vec{p}^2_\perp}} \quad . \qquad (3.17)
\end{aligned}
$$

Using $\sigma_i\sigma_j=\delta_{ij}+i\epsilon_{ijk}\sigma_k$ and introducing the notation $M:=m+xM_0$ and $M':=m+xM_0'$ while dropping the common denominator one finds

$$
\begin{aligned}
M(p') &\to M'+ip'^y\sigma_x-ip'^x\sigma_y \\
M^\star(p) &\to M-ip^y\sigma_x+ip^x\sigma_y \quad .
\end{aligned}
$$

Now one can evaluate how the Melosh rotation acts on the pauli matrices which appear in the one body currents. Starting with the unit matrix which appears already in J^+ one computes

$$
\begin{aligned}
M(p')\mathbf{1}M^\star(p) =&(M'+ip'^y\sigma_x-ip'^x\sigma_y)\mathbf{1}(M-ip^y\sigma_x+ip^x\sigma_y) \\
=&(MM'+p^xp'^x+p^yp'^y)+i(Mp'^y-M'p^y)\sigma_x+i(M'p^x-Mp'^x)\sigma_y \\
&+i(p'^xp^y-p^xp'^y)\sigma_z \\
=&: A+i\vec{B}\cdot\vec{\sigma} \quad .
\end{aligned}
$$

Hence one has

$$M(p')\mathbf{1}M^\star(p) = \chi^\dagger(A + i\vec{B}\cdot\vec{\sigma})\chi = \begin{pmatrix} A + iB_z & B_y + iB_x \\ -B_y + iB_x & A - iB_z \end{pmatrix}$$

$$M(p')\mathbf{i1}M^\star(p) = \chi^\dagger(iA - \vec{B}\cdot\vec{\sigma})\chi = \begin{pmatrix} -B_z + iA & -B_x + iB_y \\ -B_x - iB_y & B_z + iA \end{pmatrix}$$

with

$$A = M'M + p'^y p^y + p'^x p^x \qquad \text{and} \qquad \vec{B} = \begin{pmatrix} Mp'^y - M'p^y \\ M'p^x - Mp'^x \\ p'^x p^y - p^x p'^y \end{pmatrix} \quad . \tag{3.18}$$

Similarly we have

$$\begin{aligned} M(p')\sigma_\mathbf{z}M^\star(p) =& (M' + ip'^y\sigma_x - ip'^x\sigma_y)\sigma_\mathbf{z}(M - ip^y\sigma_x + ip^x\sigma_y) \\ =& i(p^x p'^y - p'^x p^y) + (Mp'^x + M'p^x)\sigma_x + (M'p^y + Mp'^y)\sigma_y \\ &+ (MM' - p^x p'^x - p^y p'^y)\sigma_z \\ =& : iA + \vec{B}\cdot\vec{\sigma} \quad . \end{aligned}$$

Therefore one can express

$$M(p')\sigma_\mathbf{z}M^\star(p) = \chi^\dagger(iA + \vec{B}\cdot\vec{\sigma})\chi = \begin{pmatrix} B_z + iA & B_x - iB_y \\ B_x + iB_y & -B_z + iA \end{pmatrix}$$

$$M(p')\mathbf{i}\sigma_\mathbf{z}M^\star(p) = \chi^\dagger(-A + i\vec{B}\cdot\vec{\sigma})\chi = \begin{pmatrix} -A + iB_z & B_y + iB_x \\ -B_y + iB_x & -A - iB_z \end{pmatrix}$$

with

$$A = p^x p'^y - p'^x p^y \qquad \text{and} \qquad \vec{B} = \begin{pmatrix} Mp'^x + M'p^x \\ M'p^y + Mp'^y \\ MM' - p'^x p^x - p'^y p^y \end{pmatrix} \quad . \tag{3.19}$$

Note that this notation is different from [72]. The expressions can be related via

$$\tilde{A} = B_z, \qquad \tilde{B}_x = B_y, \qquad \tilde{B}_y = B_x, \qquad \tilde{B}_z = -A \quad .$$

Finally we have

$$M(p')\sigma_\mathbf{x}M^\star(p) = : iA + \vec{B}\cdot\vec{\sigma}$$

with

$$A = Mp'^y - M'p^y \qquad \text{and} \qquad \vec{B} = \begin{pmatrix} MM' + p'^y p^y - p'^x p^x \\ -(p^x p'^y + p'^x p^y) \\ -(Mp'^x + M'p^x) \end{pmatrix} \quad . \tag{3.20}$$

Likewise

$$M(p')\sigma_{\mathbf{y}}M^{\star}(p) =: iA + \vec{B}\cdot\vec{\sigma}$$

with

$$A = M'p^x - Mp'^x \qquad \text{and} \qquad \vec{B} = \begin{pmatrix} -(p'^y p^x + p'^x p^y) \\ M'M + p'^x p^x - p'^y p^y \\ -(Mp'^y + M'p^y) \end{pmatrix} \quad . \tag{3.21}$$

Of course the results given above can be obtained in a more rigorous way by using LF quantization. This is what will be presented in the following.

In **LF** theory it is convenient to introduce so called "good" and "bad" components of the fermion field. The reason is that in field theory one can use one of them, the "good" component ϕ as independent field which gets quantized and then express the "bad" component χ in terms of the independent field ϕ using the equation of motion, i.e. the Dirac equation.

The "good" and "bad" components ϕ and χ are obtained from the 4 component fermion field ψ using projectors:

$$\begin{aligned} \Lambda^{\pm} =& \frac{1}{4}\gamma^{\mp}\gamma^{\pm} = \frac{1}{2}(1 \pm \gamma^0\gamma^3) = \frac{1}{2}\gamma^0\gamma^{\pm} \\ \phi =& \Lambda^{+}\psi \qquad \chi = \Lambda^{-}\psi \quad . \end{aligned}$$

Projector properties for $\Lambda^{\pm}$ can readily be verified:

$$\Lambda^{\pm}\Lambda^{\mp} = 0 \qquad \Lambda^{\pm}\Lambda^{\pm} = \Lambda^{\pm} \qquad \Lambda^{+} + \Lambda^{-} = 1 \quad .$$

To simplify the following expressions we define

$$\vec{\alpha}^{\perp} = \gamma^0\gamma^{\perp} \quad .$$

and provide some useful algebraic relations which will be frequently used in the following:

$$\begin{array}{llll} \Lambda^{+} = \frac{1}{2}\gamma_0\gamma^{+} & \alpha_{\perp} = \gamma_0\gamma_{\perp} & \gamma_{\perp}\Lambda^{\pm} = \Lambda^{\pm}\gamma_{\perp} & \{\gamma^{\mu},\gamma_5\} = 0 \\ \gamma_0\Lambda^{\pm} = \Lambda^{\mp}\gamma_0 & \alpha_{\perp}\Lambda^{\pm} = \Lambda^{\mp}\alpha_{\perp} & \gamma_3\Lambda^{\pm} = \Lambda^{\mp}\gamma_3 & \\ \gamma_5\Lambda^{\pm} = \Lambda^{\pm}\gamma_5 & (\Lambda^{\pm})^{\dagger} = \Lambda^{\pm} & \Lambda^{\mp} = 2\Lambda^{\pm}\gamma^0 & \end{array} \quad . \tag{3.22}$$

Next the one body currents can be expressed in terms of "good" and "bad" LF field compo-

nents. One finds

$$\begin{aligned}
j^+ &= \bar{\psi}\gamma^+\psi \\
&= \bar{\psi}(2\Lambda^-\gamma^0)\psi \\
&= \bar{\psi}(2\gamma^0\Lambda^+)\psi \\
&= \bar{\psi}(2\gamma^0\Lambda^+\Lambda^+)\psi \\
&= \bar{\psi}\left(2\gamma^0(\Lambda^+)^\dagger\Lambda^+\right)\psi \\
&= 2\psi^\dagger(\Lambda^+)^\dagger\phi \\
&= 2(\Lambda^+\psi)^\dagger\phi \\
&= 2\phi^\dagger\phi
\end{aligned}$$

$$\begin{aligned}
j^\perp &= \bar{\psi}\gamma^\perp\psi \\
&= \psi^\dagger\vec{\alpha}^\perp\psi \\
&= \psi^\dagger\vec{\alpha}^\perp(\Lambda^+ + \Lambda^-)\psi \\
&= \psi^\dagger\vec{\alpha}^\perp\Lambda^+\Lambda^+\psi + \psi^\dagger\vec{\alpha}^\perp\Lambda^-\Lambda^-\psi \\
&= \psi^\dagger\Lambda^-\vec{\alpha}^\perp\Lambda^+\psi + \psi^\dagger\Lambda^+\vec{\alpha}^\perp\Lambda^-\psi \\
&= \chi^\dagger\alpha^\perp\phi + \phi^\dagger\alpha^\perp\chi
\end{aligned}$$

$$\begin{aligned}
j^- &= \bar{\psi}\gamma^-\psi \\
&= \bar{\psi}(2\Lambda^+\gamma^0)\psi \\
&= \bar{\psi}(2\gamma^0\Lambda^-)\psi \\
&= \bar{\psi}(2\gamma^0\Lambda^-\Lambda^-)\psi \\
&= \bar{\psi}\left(2\gamma^0(\Lambda^-)^\dagger\Lambda^-\right)\psi \\
&= 2\psi^\dagger(\Lambda^-)^\dagger\chi \\
&= 2(\Lambda^-\psi)^\dagger\chi \\
&= 2\chi^\dagger\chi \quad .
\end{aligned} \tag{3.23}$$

Similarly one finds

$$\begin{aligned}
j_5^+ &= \bar{\psi}\gamma^+\gamma_5\psi = 2\phi^\dagger\gamma_5\phi \\
j_5^\perp &= \bar{\psi}\gamma^\perp\gamma_5\psi = \chi^\dagger\alpha^\perp\gamma_5\phi + \phi^\dagger\alpha^\perp\gamma_5\chi \\
j_5^- &= \bar{\psi}\gamma^-\gamma_5\psi = 2\chi^\dagger\gamma_5\chi \quad .
\end{aligned}$$

The next task is the afore mentioned quantization of the "good" component ϕ and the substitution of the dynamically dependent bad LF component χ.

The equation of motion is the Dirac equation

$$(i\not{D} - m)\,\psi = 0$$
$$\left[i\left(\frac{1}{2}\gamma^+ D^- + \frac{1}{2}\gamma^- D^+\right) - i\vec{\gamma}^\perp \vec{D}^\perp - m\right]\psi = 0 \quad .$$

Now we multiply this equation from left with $\Lambda^-\gamma^0$

$$\left[i\left(\frac{1}{2}\Lambda^-\gamma^0\gamma^+ D^- + \frac{1}{2}\Lambda^-\gamma^0\gamma^- D^+\right) - i\Lambda^-\vec{\alpha}^\perp \vec{D}^\perp - m\Lambda^-\gamma^0\right]\psi = 0$$
$$\left[i\left(\Lambda^-\Lambda^+ D^- + \Lambda^-\Lambda^- D^+\right) - i\vec{\alpha}^\perp\Lambda^+\vec{D}^\perp - m\gamma^0\Lambda^+\right]\psi = 0$$
$$iD^+\chi - i\vec{\alpha}^\perp\vec{D}^\perp\phi - m\gamma^0\phi = 0 \quad .$$

In QCD the covariant derivative reads $D = \partial - igA$ and using LF gauge one ends up with

$$\chi = \frac{1}{\partial^+}\left[\vec{\alpha}^\perp(\vec{\partial}^\perp - igA^\perp)\phi - im\gamma^0\phi\right] \quad . \tag{3.24}$$

and thus one has expressed the bad LF component through the only independent fields ϕ and $\vec{A}^\perp$.

Certainly the constituent quark model is not QCD. It is not even a field theory. The philosophy behind calling the prescription to obtain the transition amplitudes spectator quark approximation is to understand the constituent quarks as dressed fermions of some underlying field theory (maybe QCD) where the derivation for the transition amplitudes holds. Then restricting oneself to the leading Fock component (quark model) is a restriction of the Fock space of the underlying field theory. We will postpone the discussion of this approximation and the partonic picture behind it to the next section. The above equations simplify in the case of the truncated Fock state, the Gluon fields can simply be neglected.

The hadron - hadron transition amplitudes which can be related to GPDs read

$$G^{q,O}_{\lambda'\lambda} = \sum_c \int \frac{dz^-}{4\pi} e^{ix\bar{P}^+z^-}\langle \tilde{P}', \lambda' \mid \bar{\psi}^c_q(-\frac{\tilde{z}}{2})O\psi^c_q(\frac{\tilde{z}}{2}) \mid \tilde{P}, \lambda\rangle \quad .$$

This expression can be evaluated step by step. One uses the hadron state and integral measure of eq. 3.7. Next the one particle states which appear here can be expressed using creation operators:

$$\mid \beta, \tilde{p}_1, \tilde{p}_2, \tilde{p}_3\rangle = \prod_{i=1}^{3} b^\dagger(\omega_i) \mid 0\rangle \quad .$$

The ω_i are collective coordinates for momentum, helicity, flavor and color of the i-th quark.

The current operators have been expressed in terms of ϕ and χ so far. These fields have to be quantized next:

$$\phi_q(\tilde{z}) = \int \frac{dk^+\, d^2\vec{k}_\perp}{16\pi^3 k^+}\theta(k^+)\sum_\mu \Big(b_q(\tilde{k},\mu)u_+(\tilde{k},\mu)e^{-ikz} + d^\dagger_q(\tilde{k},\mu)v_+(\tilde{k},\mu)e^{ikz}\Big)$$

where $u_+ = \Lambda^+ u$, $v_+ = \Lambda^+ v$, q stands for the quark flavor (color index is suppressed), $\tilde{k} = (k^+, \vec{k}_\perp)$ and the commutation relation for creation/annihilation operators read

$$\Big\{ b_{q'}(\tilde{k}', \mu'), b_q^\dagger(\tilde{k}, \mu) \Big\} = \Big\{ d_{q'}(\tilde{k}', \mu'), d_q^\dagger(\tilde{k}, \mu) \Big\} = 16\pi^3 k^+ \delta(k'^+ - k^+) \delta^{(2)}(\vec{k}'_\perp - \vec{k}_\perp) \delta_{\mu'\mu} \delta_{q'q} \quad .$$

This implies the normalization

$$\langle \tilde{k}', \omega' \mid \tilde{k}, \omega \rangle = 16\pi^3 k^+ \delta^{(2)}(\vec{k}'_\perp - \vec{k}_\perp) \delta(k'^+ - k^+) \delta_{\omega,\omega'} \quad . \tag{3.25}$$

Using the Dirac equation one obtains a representation for the dynamical dependent field χ:

$$\begin{aligned}
\chi_q(\tilde{z}) &= \frac{1}{\partial^+} \Big[\vec{\alpha}_\perp \cdot \partial_\perp - im\gamma^0 \Big] \phi_q(\tilde{z}) \\
&= \frac{1}{\partial^+} \Big[\vec{\alpha}_\perp \cdot \partial_\perp - im\gamma^0 \Big] \int \frac{dk^+ \, d^2\vec{k}_\perp}{16\pi^3 k^+} \theta(k^+) \sum_\mu \Big(b_q(\tilde{k}, \mu) u_+(\tilde{k}, \mu) e^{-ikz} + d_q^\dagger(\tilde{k}, \mu) v_+(\tilde{k}, \mu) e^{ikz} \Big) \\
&= \int \frac{dk^+ \, d^2\vec{k}_\perp}{16\pi^3 k^+} \theta(k^+) \sum_\mu \Bigg[\Big(\frac{\vec{\alpha}_\perp \cdot \vec{k}_\perp}{k^+} + \frac{m}{k^+} \gamma^0 \Big) b_q(\tilde{k}, \mu) u_+(\tilde{k}, \mu) e^{-ikz} \\
&\qquad + \Big(\frac{\vec{\alpha}_\perp \cdot \vec{k}_\perp}{k^+} - \frac{m}{k^+} \gamma^0 \Big) d_q^\dagger(\tilde{k}, \mu) v_+(\tilde{k}, \mu) e^{ikz} \Bigg] \quad .
\end{aligned}$$

Before the length of the formula diverges let us perform the integral $\int \frac{dz^-}{4\pi} e^{ix\bar{P}^+ z^-} \phi_q^\dagger(-\frac{z^-}{2}) O \phi_q(\frac{z^-}{2})$ after which some of the terms above will disappear:

$$\begin{aligned}
&\int \frac{dz^-}{4\pi} e^{ix\bar{P}^+ z^-} \bar{\phi}_q(-\frac{z^-}{2}) O \phi_q(\frac{z^-}{2}) \\
&= \int \frac{dz^-}{4\pi} e^{ix\bar{P}^+ z^-} \int \frac{dk^+ d\vec{k}_\perp}{16\pi^3 k^+} \frac{dk'^+ d\vec{k}'_\perp}{16\pi^3 k'^+} \theta(k^+) \theta(k'^+) \sum_{\mu,\mu'} \\
&\quad \Big(b_q^\dagger(k', \mu') u_+^\dagger(k', \mu') e^{ik'^+(-\frac{z^-}{2})} + d_q(k', \mu') v_+(k', \mu') e^{-ik'^+(-\frac{z^-}{2})} \Big) \\
&\quad O \Big(b_q(k, \mu) u_+(k, \mu) e^{-ik^+(\frac{z^-}{2})} + d_q^\dagger(k, \mu) v_+^\dagger(k, \mu) e^{ik^+(\frac{z^-}{2})} \Big) \\
&= \int \frac{dk^+ d\vec{k}_\perp}{16\pi^3 k^+} \frac{dk'^+ d\vec{k}'_\perp}{16\pi^3 k'^+} \theta(k^+) \theta(k'^+) \sum_{\mu,\mu'} \\
&\quad \Big(\delta(2x\bar{P}^+ - k^+ + k'^+) d_q(k', \mu') b_q(k, \mu) v_+(k', \mu') \, O \, u_+(k, \mu) \\
&\quad + \delta(2x\bar{P}^+ - k'^+ - k^+) b_q^\dagger(k', \mu') b_q(k, \mu) u_+^\dagger(k', \mu') \, O \, u_+(k, \mu) \\
&\quad + \delta(2x\bar{P}^+ + k'^+ - k^+) d_q(k', \mu') b_q(k, \mu) v_+(k', \mu') \, O \, u_+(k, \mu) \\
&\quad + \delta(2x\bar{P}^+ + k'^+ + k^+) d_q(k', \mu') d_q^\dagger(k, \mu) v_+(k', \mu') \, O \, v_+^\dagger(k, \mu) \Big) \quad .
\end{aligned} \tag{3.26}$$

For transition elements which are diagonal in the Fock space only two of the expressions in the operator sum can contribute. We only have to consider these contributions in our calculation since the quark model restricts the Fock space to three quark states only. Restricting oneself to the kinematic region $x > 0$ (no information loss due to symmetry) the theta functions $\theta(k^+)$ and $\theta(k'^+)$ leave the term with $b^\dagger b$ as only contribution.

Taking only these contributions into account the operators O which appear in the equation above can be evaluated as follows:

$$\chi^\dagger\alpha^i_\perp\phi + \phi^\dagger\alpha^i_\perp\chi = \phi^\dagger\left[\Big(\frac{\vec{\alpha}_\perp\cdot\vec{k}'_\perp}{k'^+} + \frac{m}{k'^+}\gamma^0\Big)\alpha^i_\perp + \alpha^i_\perp\Big(\frac{\vec{\alpha}_\perp\cdot\vec{k}_\perp}{k^+} + \frac{m}{k^+}\gamma^0\Big)\right]\phi \quad .$$

Using

$$\Big(\vec{A}\cdot\vec{\alpha}_\perp\Big)\alpha_x = A_x - iA_y\gamma^0\gamma^3\gamma_5$$
$$\Big(\vec{A}\cdot\vec{\alpha}_\perp\Big)\alpha_y = A_y + iA_x\gamma^0\gamma^3\gamma_5$$

one finds

$$O^x = 1\Big(\frac{k'^x}{k^x} + \frac{k^x}{k^+}\Big) + \gamma^x\Big(\frac{m}{k'^+} - \frac{m}{k^+}\Big) + i\gamma_0\gamma_3\gamma_5\Big(\frac{k^y}{k^+} - \frac{k'^y}{k'^+}\Big) \quad .$$

Similarly one has

$$O^y = 1\Big(\frac{k'^y}{k'^+} + \frac{k^y}{k^+}\Big) + \gamma^y\Big(\frac{m}{k'^+} - \frac{m}{k^+}\Big) + i\gamma_0\gamma_3\gamma_5\Big(\frac{k'^x}{k'^+} - \frac{k^x}{k^+}\Big) \quad .$$

Then using

$$(\vec{A}_\perp\cdot\vec{\alpha}_\perp)(\vec{B}_\perp\cdot\vec{\alpha}_\perp) = (A_xB_x + A_yB_y) + (A_xB_y - A_yB_x)i\gamma^0\gamma^3\gamma_5$$
$$(\vec{A}_\perp\cdot\vec{\alpha}_\perp)\gamma^0 = -A_\perp\cdot\gamma^\perp$$
$$(\gamma^0\vec{A}_\perp\cdot\vec{\alpha}_\perp) = A_\perp\cdot\gamma^\perp$$

one finds

$$O^- = \frac{2}{k^+k'^+}\left[(m^2 + k'^xk^x + k'^yk^y) + i(k'^xk^y - k^xk'^y)\gamma^0\gamma^3\gamma_5 + m(k^x - k'^x)\gamma^x + m(k^y - k'^y)\gamma^y\right] \quad .$$

Applying the algebraic relations given in eq. 3.22 one similarly finds

$$O^x_5 = \gamma_5\Big(\frac{k'^x}{k^x} + \frac{k^x}{k^+}\Big) + \gamma^x\gamma_5\Big(\frac{m}{k^+} + \frac{m}{k'^+}\Big) + i\gamma_0\gamma_3\Big(\frac{k^y}{k^+} - \frac{k'^y}{k'^+}\Big)$$
$$O^y_5 = \gamma_5\Big(\frac{k'^y}{k'^+} + \frac{k^y}{k^+}\Big) + \gamma^y\gamma_5\Big(\frac{m}{k^+} + \frac{m}{k'^+}\Big) + i\gamma_0\gamma_3\Big(\frac{k'^x}{k'^+} - \frac{k^x}{k^+}\Big)$$
$$O^-_5 = \frac{2}{k^+k'^+}\Big[\Big(k'^xk^x + k'^yk^y - m^2\Big)\gamma_5 + i\Big(k'^xk^y - k^xk'^y\Big)\gamma_0\gamma_3 + m\Big(k^x + k'^x\Big)\gamma^x\gamma_5$$
$$+ m\Big(k^y + k'^y\Big)\gamma^y\gamma_5\Big] \quad .$$

As next step the matrix element $\langle\tilde{P}',\lambda' \mid \phi^{c\dagger}_q(\tilde{k}')\phi^c_q(\tilde{k}) \mid \tilde{P},\lambda\rangle$ has to be evaluated. For the moment this discussion shall be restricted to the structure of creation and annihilation

operators. Applying commutator relations iteratively one finds

$$\begin{aligned}
&\sum_c \sum_{\mu,\mu'} \sum_{j_1,j_2,j_3} \sum_{i_1,i_2,i_3} \langle 0 \mid b^{c_{j_1}}_{q_{j_1}}(\tilde{p}'_{j_1},\lambda'_{j_1}) b^{c_{j_2}}_{q_{j_2}}(\tilde{p}'_{j_2},\lambda'_{j_2}) b^{c_{j_3}}_{q_{j_3}}(\tilde{p}'_{j_3},\lambda'_{j_3}) \\
&\qquad b^{c\dagger}_q(\tilde{k}',\mu') b^c_q(\tilde{k},\mu)\ b^{c_{i_1}\dagger}_{q_{i_1}}(\tilde{p}_{i_1},\lambda_{i_1}) b^{c_{i_2}\dagger}_{q_{i_2}}(\tilde{p}_{i_2},\lambda_{i_2}) b^{c_{i_3}\dagger}_{q_{i_3}}(\tilde{p}_{i_3},\lambda_{i_3}) \mid 0\rangle \\
=&\sum_c \sum_{\mu,\mu'} \sum_{j_1,j_2,j_3} \sum_{i_1,i_2,i_3} \epsilon_{i_1,i_2,i_3}\epsilon_{j_1,j_2,j_3}\ \langle \tilde{p}'_{j_1},\lambda'_{j_1},q_{j_1},c_{j_1} \mid \tilde{p}_{i_1},\lambda_{i_1},q_{i_1},c_{i_1}\rangle \\
&\cdot \langle \tilde{p}'_{j_2},\lambda'_{j_2},q_{j_2},c_{j_2} \mid \tilde{p}_{i_2},\lambda_{i_2},q_{i_2},c_{i_2}\rangle \cdot \langle \tilde{p}'_{j_3},\lambda'_{j_3},q_{j_3},c_{j_3} \mid b^{c\dagger}_q(\tilde{k}',\mu') b^c_q(\tilde{k},\mu) \mid \tilde{p}_{i_3},\lambda_{i_3},q_{i_3},c_{i_3}\rangle \quad .
\end{aligned}$$

When the color sum is performed including the wave functions only diagonal terms can survive ($i_k = j_k$) since the three quark wave function is antisymmetric in color space while the operator $\sum_c b^{c\dagger} b^c$ is color neutral. In this case the operator structure above collapses towards

$$\sum_{\mu'\mu} \sum_{i=1}^{3} \left[\Big(\prod_{j=1, j\neq i}^{3} \langle \tilde{p}'_j,\lambda'_j,q_j \mid \tilde{p}_j,\lambda_j,q_j\rangle \Big) \langle \tilde{p}'_i,\lambda'_i,q_i \mid \tilde{k}',\mu',q\rangle \langle \tilde{k},\mu,q \mid \tilde{p}_i,\lambda_i,q_i\rangle \right] \quad .$$

Exploiting flavor symmetry for the quarks, choosing the third quark as active quark and using the one particle state normalization one arrives at

$$\begin{aligned}
&3\Big(16\pi^3\Big)^2 k^+ k'^+ \sum_{\mu'\mu} \delta^{(2)}(\vec{p}'_{3\perp} - \vec{k}'_\perp)\delta(p'^+_3 - k'^+)\delta_{q'_3 q}\delta_{\lambda'_3\mu'}\delta^{(2)}(\vec{p}_{3\perp} - \vec{k}_\perp)\delta(p^+_3 - k^+)\delta_{q_3,q}\delta_{\lambda_3\mu} \\
&\quad \cdot \left[\Big(\prod_{j=1}^{2} \langle \tilde{p}'_j,\lambda'_j,q_j \mid \tilde{p}_j,\lambda_j,q_j\rangle \Big) \right] \quad .
\end{aligned}$$

This derivation holds analogously with an arbitrary operator O sandwiched between $b^{c\dagger}_q(\tilde{k}',\mu')$ and $b^c_q(\tilde{k},\mu)$ as long as it is color blind. Using these simplifications one can evaluate the matrix element $\langle \tilde{P}',\lambda' \mid \phi^\dagger_q\, O\, \phi_q \mid \tilde{P},\lambda\rangle$ further:

$$\begin{aligned}
\langle \tilde{P}',\lambda' \mid b^\dagger_q(\tilde{k}',\mu')\, O\, b_q(\tilde{k},\mu) \mid \tilde{P},\lambda\rangle = 3k^+k'^+p_1^+p_2^+ &\sum_{\mu'\mu} \sum_{\lambda'_1,\lambda'_2,\lambda'_3} \sum_{\lambda_1,\lambda_2,\lambda_3} \sum_{q'_1,q'_2,q'_3} \sum_{q_1,q_2,q_3} \\
&\Big(\prod_{i=1}^{3} \int \frac{dx'_i}{\sqrt{x'_i}} d^2\vec{p}'_{i\perp} \Big) \delta(1 - \sum_j x_j)\delta^{(2)}(\vec{P}'_\perp - \sum_j p'_{j\perp}) \\
&\Big(\prod_{i=1}^{3} \int \frac{dx_i}{\sqrt{x_i}} d^2\vec{p}_{i\perp} \Big) \delta(1 - \sum_j x_j)\delta^{(2)}(\vec{P}_\perp - \sum_j p_{j\perp}) \Big) \\
&\delta_{q'_3 q}\delta_{q_3 q}\delta_{\lambda'_3\mu'}\delta_{\lambda_3\mu}\delta(p'^+_3 - k'^+)\delta^{(2)}(\vec{p}'_{3\perp} - \vec{k}'_\perp) \\
&\delta(p^+_3 - k^+)\delta^{(2)}(p_{3\perp} - k_\perp)\delta(p'^+_1 - p^+_1)\delta^{(2)}(\vec{p}'_{1\perp} - \vec{p}_{1\perp}) \\
&\delta(p'^+_2 - p^+_2)\delta^{(2)}(\vec{p}'_{2\perp} - \vec{p}_{2\perp})\psi^{\lambda'\star}_q(\tilde{p}'_1,\tilde{p}'_2,\tilde{p}'_3,\lambda'_1,\lambda'_2,\lambda'_3,q'_1,q'_2,q'_3) \\
&O\,\psi^\lambda_q(\tilde{p}_1,\tilde{p}_2,\tilde{p}_3,\lambda_1,\lambda_2,\lambda_3,q_1,q_2,q_3)
\end{aligned}$$

$$
\begin{aligned}
&= 3\sum_{\mu'\mu}\sum_{\lambda_1\lambda_2}\sum_{q_1q_2}\Big(\prod_{i=1}^{3}\int dx_i d^2\vec{p}_{i\perp}\Big)\sqrt{\tilde{x}'\tilde{x}}\delta(1-x_1-x_2-\tilde{x})\\
&\quad \delta^{(2)}(\vec{P}_\perp-\vec{p}_{1\perp}-\vec{p}_{2\perp}-\vec{k}_\perp)\delta^{(2)}(\vec{P}'_\perp-\vec{p}_{1\perp}-\vec{p}_{2\perp}-\vec{k}'_\perp)\\
&\quad \delta(1-x_1-x_2-\tilde{x}')\psi_q^{\lambda'\star}(\tilde{p}_1,\tilde{p}_2,\tilde{k}',\lambda_1,\lambda_2,\mu',q_1,q_2,q)\\
&\quad O\psi_q^{\lambda}(\tilde{p}_1,\tilde{p}_2,\tilde{k},\lambda_1,\lambda_2,\mu,q_1,q_2,q) \quad .
\end{aligned}
$$

Finally the results so far can be summarized in order to obtain an expression for the transition amplitude $G^{q,O}_{\lambda'\lambda}$:

$$
\begin{aligned}
G^{q,O}_{\lambda'\lambda} &= 3\sum_{\mu'\mu}\int\frac{dk^+d^2\vec{k}_\perp}{8\pi^3\sqrt{2k^+}}\int\frac{dk'^+d^2\vec{k}'_\perp}{8\pi^3\sqrt{2k'^+}}\theta(k^+)\theta(k'^+)\delta(2x\bar{P}^+-k^+-k'^+)\\
&\quad\cdot\langle P',\lambda'\mid\phi_q(-\frac{z^-}{2})\,O\,\phi_q(\frac{z^-}{2})\mid P,\lambda\rangle\\
&= \frac{6}{(16\pi^3)^2\bar{P}^+}\sum_{\mu'\mu}\sum_{\lambda_1\lambda_2}\sum_{q_1q_2}\int dk^+d^2\vec{k}_\perp dk'^+d^2\vec{k}'_\perp dx_1d^2\vec{p}_{1\perp}dx_2d^2\vec{p}_{2\perp}\theta(k^+)\theta(k'^+)\\
&\quad \delta(2xP^+-k^+-k'^+)\delta(1-x_1-x_2-\tilde{x})\delta(1-x_1-x_2-\tilde{x}')\delta^{(2)}(\vec{P}_\perp-\vec{p}_{1\perp}-\vec{p}_{2\perp}-\vec{k}_\perp)\\
&\quad \delta^{(2)}(\vec{P}'_\perp-\vec{p}_{1\perp}-\vec{p}_{2\perp}-\vec{k}'_\perp)\psi_q^{\lambda'\star}(\tilde{p}_1,\tilde{p}_2,\tilde{k}',\lambda_1,\lambda_2,\mu',q_1,q_2,q)\\
&\quad O\psi_q^{\lambda}(\tilde{p}_1,\tilde{p}_2,\tilde{k},\lambda_1,\lambda_2,\mu,q_1,q_2,q)\\
&= \frac{3}{(16\pi^3)^2}\sum_{\mu'\mu}\sum_{\lambda_1\lambda_2}\sum_{q_1q_2}\Big(\prod_{i=1}^{2}\int dx_id^2\vec{p}_{i\perp}\Big)\theta(1-x_1-x_2)\\
&\quad \psi_q^{\lambda'\star}(x_1,x_2,1-x_1-x_2,\vec{p}_{1\perp},\vec{p}_{2\perp},\vec{P}'_\perp-\vec{p}_{1\perp}-\vec{p}_{2\perp},\lambda_1,\lambda_2,\mu',q_1,q_2,q)\\
&\quad O\psi_q^{\lambda}(x_1,x_2,1-x_1-x_2,\vec{p}_{1\perp},\vec{p}_{2\perp},\vec{P}_\perp-\vec{p}_{1\perp}-\vec{p}_{2\perp},\lambda_1,\lambda_2,\mu,q_1,q_2,q) \quad .
\end{aligned}
$$

The evaluation of the transition amplitudes is now nearly finished. We write the integral appearing here in a more symmetric way by defining averaged quark momenta

$$
\begin{aligned}
\bar{p}_{i\perp} &= \frac{1}{2}\Big(\vec{p}_{i\perp}+\vec{p}'_{i\perp}\Big)\\
\bar{x}_i &= \frac{1}{2}\Big(x_i+x'_i\Big) \quad .
\end{aligned}
$$

The invariance of the LF wave function under LF boosts bears a simplification as the wave function only depends on the inner coordinates $y_i, \tilde{\kappa}_{i\perp}$. For the struck quark they read

$$
\begin{aligned}
y'_j &= \frac{\bar{p}^\perp_j+\frac{1}{2}\Delta^+}{\bar{P}^+-\frac{1}{2}\Delta^+} = \frac{\bar{x}_j-\xi}{1-\xi} \qquad & \vec{\kappa}'_{\perp j} &= \vec{p}_{\perp j}+\frac{1}{2}\frac{1-\bar{x}_j}{1-\xi}\vec{\Delta}_\perp\\
y_j &= \frac{\bar{p}^\perp_j-\frac{1}{2}\Delta^+}{\bar{P}^+-\frac{1}{2}\Delta^+} = \frac{\bar{x}_j+\xi}{1+\xi} \qquad & \vec{\kappa}_{\perp j} &= \vec{p}_{\perp j}-\frac{1}{2}\frac{1-\bar{x}_j}{1+\xi}\vec{\Delta}_\perp \quad .
\end{aligned}
$$

For the spectator quarks we have

$$
\begin{aligned}
y'_i &= \frac{\bar{x}_i}{1-\xi} \qquad & \vec{\kappa}'_{\perp i} &= \vec{p}_{\perp i}-\frac{1}{2}\frac{\bar{x}_i}{1-\xi}\vec{\Delta}_\perp\\
y_i &= \frac{\bar{x}_i}{1+\xi} \qquad & \vec{\kappa}'_{\perp i} &= \vec{p}_{\perp i}+\frac{1}{2}\frac{\bar{x}_i}{1+\xi}\vec{\Delta}_\perp \quad .
\end{aligned}
$$

Consequently we can rewrite the transition amplitudes as

$$G^{q,O}_{\lambda'\lambda} = \frac{3}{\sqrt{1-\xi^2}} \sum_{\lambda_i \tau_i} \int [d\bar{x}][d\bar{p}_\perp] \delta(\bar{x} - \bar{x}_3)\theta(\bar{x}_3) \psi^{\lambda'\star}_q(\vec{\kappa}'_{i\perp}, y'_i, \lambda_i, \tau_i) O \psi^{\lambda}_q(\vec{\kappa}_{i\perp}, y_i, \lambda_i, \tau_i) \quad (3.27)$$

Here we have returned to the usual notation to denote the quark flavors by τ_i. It is important to emphasize that these inner coordinates only appear in the wave function but not in the kinematical factors obtained from the evaluation of the operators. The determination of the latter factors will conclude this calculation.

Generally one can sandwich the operators $O^+, O^+_5, O^\perp, O^\perp_5, O^-, O^-_5$ between the projectors in order to obtain the equivalent operators $\tilde{O}$ so that

$$u^\dagger_+ O u_+ = u^\dagger \Lambda_+ O \Lambda_+ u = \bar{u}\gamma_0 \Lambda_+ O \Lambda_+ u =: \bar{u}\tilde{O}u \quad .$$

In doing so we obtain

$$\begin{aligned}
&O^+ = 2 \to \tilde{O}^+ = \gamma_0 \Lambda^+ 2 \Lambda^+ = \gamma^+ \\
&O^+_5 = 2\gamma_5 \to \tilde{O}^+_5 = \gamma_0 \Lambda^+ 2 \gamma_5 \Lambda^+ = \gamma^+ \gamma_5 \\
&O^x = 1\Big(\frac{p'^x}{p^x} + \frac{p^x}{p^+}\Big) + \gamma^x \Big(\frac{m}{p'^+} - \frac{m}{p^+}\Big) + i\gamma_0\gamma_3\gamma_5 \Big(\frac{p^y}{p^+} - \frac{p'^y}{p'^+}\Big) \\
&\to \tilde{O}^x = \frac{1}{2}\left[\Big(\frac{p'^x}{p^x} + \frac{p^x}{p^+}\Big)\gamma^+ + \Big(\frac{m}{p^+} - \frac{m}{p'^+}\Big)\gamma^x\gamma^+ + i\Big(\frac{p^y}{p^+} - \frac{p'^y}{p'^+}\Big)\gamma^+\gamma_5\right] \\
&O^y = 1\Big(\frac{p'^y}{p'^+} + \frac{p^y}{p^+}\Big) + \gamma^y \Big(\frac{m}{p'^+} - \frac{m}{p^+}\Big) + i\gamma_0\gamma_3\gamma_5 \Big(\frac{p'^x}{p'^+} - \frac{p^x}{p^+}\Big) \\
&\to \tilde{O}^y = \frac{1}{2}\left[\Big(\frac{p'^y}{p'^+} + \frac{p^y}{p^+}\Big)\gamma^+ + \Big(\frac{m}{p^+} - \frac{m}{p'^+}\Big)\gamma^y\gamma^+ + i\Big(\frac{p'^x}{p'^+} - \frac{p^x}{p^+}\Big)\gamma^+\gamma_5\right] \quad .
\end{aligned}$$

Applying the algebraic relations given in eq. 3.22 one can evaluate

$$\begin{aligned}
&O^x_5 = \gamma_5\Big(\frac{p'^x}{p^x} + \frac{p^x}{p^+}\Big) + \gamma^x\gamma_5\Big(\frac{m}{p^+} + \frac{m}{p'^+}\Big) + i\gamma_0\gamma_3\Big(\frac{p^y}{p^+} - \frac{p'^y}{p'^+}\Big) \\
&\to \tilde{O}^x_5 = \frac{1}{2}\left[\Big(\frac{p'^x}{p'^+} + \frac{p^x}{p^+}\Big)\gamma^+\gamma_5 + \Big(\frac{m}{p'^+} + \frac{m}{p^+}\Big)\gamma^x\gamma_5\gamma^+ + i\Big(\frac{p^y}{p^+} - \frac{p'^y}{p'^+}\Big)\gamma^+\right] \\
&O^y_5 = \gamma_5\Big(\frac{p'^y}{p'^+} + \frac{p^y}{p^+}\Big) + \gamma^y\gamma_5\Big(\frac{m}{p^+} + \frac{m}{p'^+}\Big) + i\gamma_0\gamma_3\Big(\frac{p'^x}{p'^+} - \frac{p^x}{p^+}\Big) \\
&\to \tilde{O}^y_5 = \frac{1}{2}\left[\Big(\frac{p'^y}{p'^+} + \frac{p^y}{p^+}\Big)\gamma^+\gamma_5 + \Big(\frac{m}{p^+} + \frac{m}{p'^+}\Big)\gamma^y\gamma_5\gamma^+ + i\Big(\frac{p'^x}{p'^+} - \frac{p^x}{p^+}\Big)\gamma^+\right] \quad .
\end{aligned}$$

Next one finds

$$O^- = \frac{2}{p^+ p'^+}\left[(m^2 + p'^x p^x + p'^y p^y) + i(p'^x p^y - p^x p'^y)\gamma^0\gamma^3\gamma_5 + m(p^x - p'^x)\gamma^x + m(p^y - p'^y)\gamma^y\right] \quad .$$

Using

$$\begin{aligned}\gamma^0\Lambda^+\Lambda^+ &= \frac{1}{2}\gamma^+ \\ \gamma^0\Lambda^+\gamma^0\gamma^3\gamma_5\Lambda^+ &= \frac{1}{2}\gamma^+\gamma^0\gamma^3\gamma_5 = \frac{1}{2}(\gamma^3\gamma_5+\gamma^0\gamma_5) = \frac{1}{2}\gamma^+\gamma^5 \\ \gamma^0\Lambda^+\gamma^\perp\Lambda^+ &= \frac{1}{2}\gamma^+\gamma^\perp = -\frac{1}{2}\gamma^\perp\gamma^+ \quad .\end{aligned}$$

we conclude

$$\begin{aligned}\tilde{O}^- = \frac{1}{p^+p'^+}\Bigg[&\Big(m^2+p'^xp^x+p'^yp^y\Big)\gamma^+ + i\Big(p'^xp^y-p^xp'^y\Big)\gamma^+\gamma_5 + m\Big(p'^x-p^x\Big)\gamma^x\gamma^+ \\ &+ m\Big(p'^y-p^y\Big)\gamma^y\gamma^+\Bigg] \quad .\end{aligned}$$

Applying eq. 3.22 provides

$$\begin{aligned}O_5^- = \frac{2}{p^+p'^+}\Bigg[&\Big(p'^xp^x+p'^yp^y-m^2\Big)\gamma_5 + i\Big(p'^xp^y-p^xp'^y\Big)\gamma_0\gamma_3 + m\Big(p^x+p'^x\Big)\gamma^x\gamma_5 \\ &+ m\Big(p^y+p'^y\Big)\gamma^y\gamma_5\Bigg] \\ \rightarrow \tilde{O}_5^- = \frac{1}{p^+p'^+}\Bigg[&\Big(p'^xp^x+p'^yp^y-m^2\Big)\gamma^+\gamma_5 + i\Big(p'^xp^y-p^xp'^y\Big)\gamma^+ \\ &+ m\Big(p'^x+p^x\Big)\gamma^x\gamma_5\gamma^+ + m\Big(p'^y+p^y\Big)\gamma^y\gamma_5\gamma^+\Bigg] \quad .\end{aligned}$$

For the sake of comparison with the results from the earlier ad hoc calculation one has to translate the operators $\tilde{O}$ into the language of pauli matrices. In order to do so one can use table 3.15 and add

O	$\gamma^x\gamma^+$	$\gamma^y\gamma^+$	$\gamma^x\gamma_5\gamma^+$	$\gamma^y\gamma_5\gamma^+$
$O_{\uparrow,\uparrow}$	0	0	0	0
$O_{\downarrow,\uparrow}$	-1	$-i$	1	i
$O_{\uparrow,\downarrow}$	1	$-i$	1	$-i$
$O_{\downarrow,\downarrow}$	0	0	0	0

.

With these tables at hand one can express the currents in term of pauli matrices. One finds back the results from the heuristic derivation which were given in eq. 3.16. Additionally however we have obtained the correct factors for the integrand and reference system to which the kinematic variables refer.

Having all pieces together we can perform the calculation for the transition amplitudes. The

transition amplitudes related to the form factors ($F^{q,O}_{\lambda'\lambda}$) simply bears an additional integration over $\bar{x}$. For the spin flavor wave function we have to combine the formulae given in eqs. 3.1, 3.2 and 3.3. The expressions for the different operators are given in eq. 3.16. Actually we rather calculate the transition amplitudes $\tilde{G}^{q,O}_{\lambda'\lambda}$ which we define as

$$\begin{aligned}\tilde{G}^{q,O^+}_{\lambda'\lambda} &= G^{q,O^+}_{\lambda'\lambda} \\ \tilde{G}^{q,O^\perp}_{\lambda'\lambda} &= 2\bar{P}^+ G^{q,O^\perp}_{\lambda'\lambda} \\ \tilde{G}^{q,O^-}_{\lambda'\lambda} &= (2\bar{P}^+)^2 G^{q,O^-}_{\lambda'\lambda} \quad .\end{aligned}$$

$\bar{P}^+$ is no intrinsic scale in the model calculation therefore we absorb it in the definition of the transition amplitudes. In the next chapter it will become clear that redefinition is not problematic. The expressions from the operators have to be combined with the results from the Melosh rotation as given in eqs. 3.18, 3.19, 3.20 and 3.21 where now the denominators of eq. 3.17 have to be taken into account as well. Then we can evaluate eq. 3.27 numerically. We have written a C^{++} program to perform this calculation which uses the Monte Carlo algorithm VEGAS [75] to perform the 5 dimensional (GPDs) or 6 dimensional (form factors) integral numerically.

3.4 Covariance breaking effects and applicability of LF quark models

A hamiltonian description of quantum mechanics, like we apply it in a **LF** description is not manifestly covariant. Covariance is achieved by summing up the contributions from all possible Fock state transitions. Thus an expression like in eq. 3.26 satisfies covariance as long as all Fock states are taken into account.

In order to calculate observables within our LF quark model we identify the quark model wave function with the leading Fock space light front wave function. This is a questionable assumption in itself. Usually the quarks which are described in a quark model are thought of as dressed quarks, i.e. their interaction mimics the gluon dynamics which would describe hadronic processes in a field theory. If we want to maintain a partonic interpretation in which the model quarks are identified with the quarks that appear in a field theory we have to conclude that the kinematical regime which can be successfully described by the model is restricted to the valence quark domain, i.e

$$|x| \gg 0 \quad . \tag{3.28}$$

For small values of x the results can hardly be expected to describe the physics correctly.

The next consequence of our model calculation follows from the truncation of the Fock space to three quark states only. An immediate consequence is the impulse approximation. Many body interactions among the quarks like those in fig. 3.7 are not treated in the restricted Fock space.

Hence from our introductory remark it is immediately obvious that the impulse approximation violates relativistic covariance. Not only does the truncation of the Fock space lead to the impulse approximation, it also neglects the contributions of fig. 3.8.

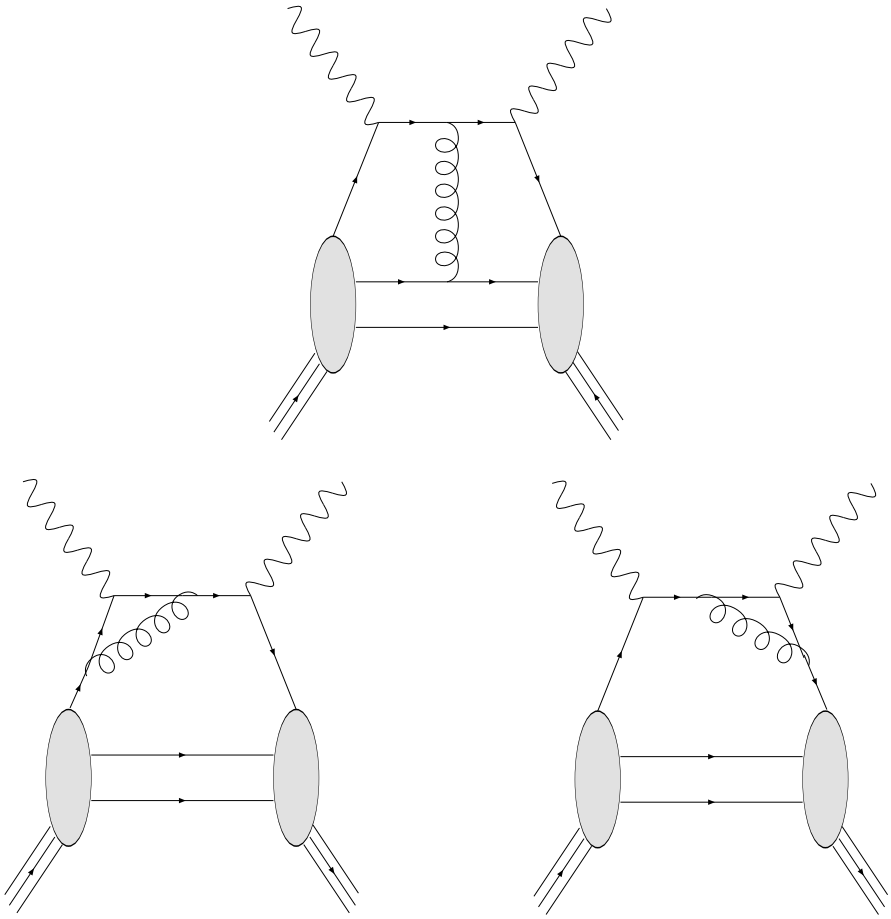

Figure 3.7: *Many body contributions which are not included due to the restricted Fock space of our model. The vertex corrections (lower panels) could in principle be included.*

Since the Fock state composition of a hadron changes if one applies a dynamical Lorentz transformation to the system it is clear that this neglect also triggers covariance breaking effects.

These covariance breaking becomes manifest in the following observations:

- The sum rules $\int dx\, G^{O^\mu}_{\lambda'\lambda}(x,\xi,t) = F^{O^\mu}_{\lambda'\lambda}(t)$ are not satisfied for $\xi \neq 0$. This can be explained from the fact that a change in the skewedness variable ξ can be understood as a boost of the reference system. Then if covariance is not satisfied the results for different values of ξ can differ. Qualitatively one can state that the model calculation can only be trusted for small values of ξ since the larger the skewedness variable becomes the more important the neglected off diagonal Fock transition elements become. In the limit $\xi = 0$ (Drell-Yan frame) off diagonal Fock transitions cannot occur.
- Consistency relations among the transition amplitudes like the angular condition in the case of the $N \to \Delta$ transition are not satisfied. As we will show in the next chapter these consistency relations can be derived assuming relativistic covariance alone. Since the latter is violated it is clear that the consistency relations do not hold.

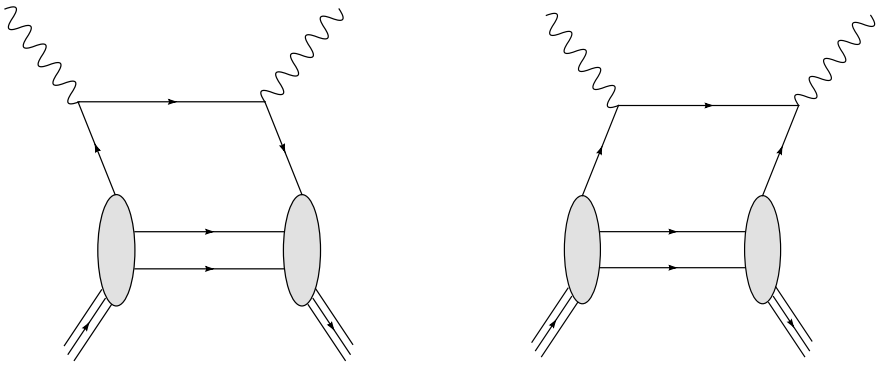

Figure 3.8: *These graphs imply a Fock state transition $qqq\bar{q}q \to qqq$ (left) or $qqq \to qqq\bar{q}q$ (right) and are therefore not included in our model calculation.*

- Gauge invariance is broken. This becomes particularly obvious in the case of the $N \to \Delta$ transition where due to the kinematics ($\Delta^- \neq 0$ for $\xi = 0$) a non trivial gauge condition can be given which connects $F^+_{\lambda'\lambda}$ and $F^x_{\lambda'\lambda}$.

For form factors it has been tried to fix the breaking of covariance by introducing many body currents [76]. While this ad hoc correction is successful for the description of form factors a similar description for GPDs is at least questionable as it is not in the spirit of a partonic picture on which the description to obtain the DVCS transition amplitudes relies.

Another consequence of the Fock space truncation is that the kinematical regime which can be accessed by a model calculation is restricted to

$$|x| \geq \xi \quad . \tag{3.29}$$

since in this (DGLAP) region only diagonal Fock state transitions can contribute.

Next we would like to turn our attention to the severe consequences which the truncated Fock space has for the bad **LF** transition amplitudes $G^{\perp}_{\lambda'\lambda}$ and $G^-_{\lambda'\lambda}$. They suffer exceedingly from the restriction of the Fock space. This can be understood from the expressions for the one body currents in terms of LF components (eq. 3.23). If we express the bad LF component χ in terms of the good LF component (eq. 3.24) it is clear that the omission of gluon contributions affects the results for the transition amplitudes differently. The effects are strongest for $G^-_{\lambda'\lambda}$ while for the good transition amplitude $G^+_{\lambda'\lambda}$ no direct consequence from this term follows. A possible way to overcome this kind of covariance breaking effects would be to include many body current contributions and to introduce an effective potential in the equation of motion which relates the good and bad **LF** components and thus to mimic the gluon contribution. However we think that this ansatz is incompatible with the partonic picture of the overlap representation. The philosophy which we prefer is to realize covariance using the spurious covariants formalism (see chapter 5) and maybe to extend the model towards higher Fock states as it was done in [35].

Finally we address the question how severe the covariance breaking effects are. In the kinematical domain in which the valence quark picture is a reasonable assumption (eqs. 3.28 and

3.29) we would expect a typical quark model uncertainty, i.e. 30% accuracy for the amplitude relations (involving only good bf LF component transition amplitudes). The severity of this model error depends on the interplay of these transition amplitudes with respect to the extraction of the GPDs and form factors. This will be discussed in the next chapter. For the sum rule predictions we expect small deviations in the order of ξ. For the bad **LF** component transition amplitudes we expect a significant inconsistency.

Chapter 4

Transition amplitudes

4.1 Introduction

In this thesis we want to obtain GPDs from a quark model calculation. As we have seen in the last chapter however the objects which we obtain from the model are transition amplitudes between different initial and final hadron states. Therefore we need to establish a connection between these amplitudes and the GPDs.

This is done by evaluating the representation which parameterizes the transition amplitude directly in terms of hadronic degrees of freedom, e.g.

$$G^{+\,(N\to N)}_{V,\,\lambda'\lambda} = \frac{1}{2\bar{P}^+}\bar{u}(P',\lambda')\Big[\gamma^+ H(x,\xi,t) + \frac{i\sigma^{+\nu}\Delta_\nu}{2M_N}E(x,\xi,t)\Big]u(P,\lambda) \quad . \tag{4.1}$$

By evaluating the r.h.s. of eq. 4.1 for different helicities of in- and outgoing hadron in a given reference frame we obtain an expression for the transition amplitudes in terms of GPDs. The inversion of such relations provides the desired result, GPDs expressed in terms of transition amplitudes. The number of independent transition amplitudes should equal the number of GPDs. Therefore the question of counting the independent transition amplitudes arises immediately. For the example of the $N \to N$ transition in eq. 4.1 we find 2 (twist 2) GPDs while we can write down 4 amplitudes for vectorial and axial $N \to N$ transitions each: $G^+_{\uparrow\uparrow}$, $G^+_{\downarrow\downarrow}$, $G^+_{\downarrow\uparrow}$ and $G^+_{\uparrow\downarrow}$. These amplitudes are connected via parity which leads to the trivial relations

$$\begin{aligned} G^+_{V,\uparrow\uparrow} &= \Big(G^+_{V,\downarrow\downarrow}\Big)^\star & \qquad G^+_{V,\uparrow\downarrow} &= -\Big(G^+_{V,\downarrow\uparrow}\Big)^\star \\ G^+_{A,\uparrow\uparrow} &= -\Big(G^+_{A,\downarrow\downarrow}\Big)^\star & \qquad G^+_{A,\uparrow\downarrow} &= \Big(G^+_{A,\downarrow\uparrow}\Big)^\star \quad . \end{aligned}$$

Reduction of the number of independent amplitudes is not always as simple as in the example above. In this chapter we will provide a general way to derive non trivial amplitude relations, like e.g. the angular condition for the $N \to \Delta$ transition.

When we compare the calculation of GPDs and form factors we can remark many similarities. Just as GPDs are obtained from transition amplitudes, form factors are obtained

from similar transition amplitudes. We can stress this analogy by introducing the notation

$$F^{\mu}_{\lambda'\lambda}(t) = \int_{-1}^{1} dx \, \frac{1}{\sqrt{1-\xi^2}} \, G^{\mu}_{\lambda'\lambda}(x,\xi,t) \quad . \tag{4.2}$$

Moreover since the same covariants turn up in the parametrization of the transition amplitudes $F_{\lambda'\lambda}(t)$ as in the parametrization of the transition amplitudes $G_{\lambda'\lambda}(x,\xi,t)$, e.g.

$$F^{\mu\,(N\to N)}_{V,\,\lambda'\lambda} = \frac{1}{2\sqrt{P'^{+}P^{+}}} \bar{u}(P',\lambda') \Big[\gamma^{\mu} F_1(t) + \frac{i\sigma^{\mu\nu}\Delta_{\nu}}{2M_N} F_2(t) \Big] u(P,\lambda)$$

it is clear where sum rules like

$$F_1(t) = \int_{-1}^{1} dx \, H(x,\xi,t)$$

arise from. For this reason we will refer to eq. 4.2 as generic sum rule. In the following we will drop the indices q, V/A and $(N \to N)$ or $(N \to \Delta)$ whenever the context ensures unambiguity.

At this point we want to emphasize differences between form factors and GPDs which lead to important consequences: GPDs of a given twist are defined through the parametrization of transition amplitudes $G^{\mu}_{\lambda'\lambda}$ with a given Lorentz index. For example twist 2 GPDs are connected to the $G^{+}_{\lambda'\lambda}$ only. On the other hand form factors contain contributions of different twists. They can be obtained from any (linearly independent) combination of transition amplitudes $F^{\mu}_{\lambda'\lambda}$. In the framework of a LF model calculation it is common to derive form factors from the amplitudes $F^{+}_{\lambda'\lambda}$ only[1] but in principle any combination of independent amplitudes $F^{\mu}_{\lambda'\lambda}$ has to lead to the same results.

This difference between form factors and GPDs has interesting consequences:

- For some processes more form factors than GPDs of a given twist exist. This leads to non trivial sum rules which differ from the form
  $FF(t) = \int dx \, GPD(x,\xi,t)$
- Relativistic covariance requires additional amplitude relations between the $F^{\mu}_{\lambda'\lambda}$ with different Lorentz indices

We would like to emphasize that such relations depend on the reference frame only. They are entirely independent of the model which is being used as input for the transition amplitudes.

Amplitude relations between transition amplitudes $G^{\mu}_{\lambda'\lambda}$ with different Lorentz indices μ do not exist[2]. Instead the amplitudes $G^{\perp}_{\lambda'\lambda}$ are related to twist 3 GPDs and the amplitudes $G^{-}_{\lambda'\lambda}$ determine GPDs of twist 4 [77].

If one assumes however, that genuine higher twist effects are small enough compared to leading twist contributions one can treat the leading twist GPDs $H, E, \tilde{H}$ and $\tilde{E}$ like the

[1] For model calculations which suffer from consequences of approximations there exist strong arguments to prefer these so called good light front components, i.e. "$\mu = +$".

[2] Relations between G^{x} and G^{y} which determine GPDs of the same twist are an exception.

form factors in the sense that they can be extracted from any combination of independent transition amplitudes $G^{\mu}_{\lambda'\lambda}$. This way one obtains amplitude relations among transition amplitudes $G^{\mu}_{\lambda'\lambda}$ with different Lorentz indices μ which hold approximately[3] for large values of Q^2. There are two reasons why we derive such relations. Firstly one obtains an estimate of the size of higher twist contributions in the framework of the considered model calculation. Secondly the reference to transition amplitudes with $\mu \neq +$ allows to extend the "spurious covariants" formalism towards DVCS. The latter is a useful tool for overcoming bad effects from covariance violating approximations in model calculations and will be introduced in the next chapter.

4.2 Leading twist GPDs from good LF transition amplitudes

As easiest example let us calculate the expressions for the nucleon GPDs. These results can already be found in [65, 72].

With our conventions for DVCS kinematics and spinor normalization (c.f. appendix) we can evaluate eq. 4.1 in order to obtain

$$\begin{aligned} G_{V,\uparrow\uparrow}^{q,+(N\to N)} &= \frac{1}{2\bar{P}^+}\bar{u}(P',\uparrow)\Big[\gamma^+ H^q(x,\xi,t) + \frac{i\sigma^{+\nu}\Delta_\nu}{2M_N}E^q(x,\xi,t)\Big]u(P,\uparrow) \\ &= \sqrt{1-\xi^2}H^q(x,\xi,t) - \frac{\xi^2}{\sqrt{1-\xi^2}}E^q(x,\xi,t) \end{aligned}$$

$$\begin{aligned} G_{V,\downarrow\uparrow}^{q,+(N\to N)} &= \frac{1}{2\bar{P}^+}\bar{u}(P',\downarrow)\Big[\gamma^+ H^q(x,\xi,t) + \frac{i\sigma^{+\nu}\Delta_\nu}{2M_N}E^q(x,\xi,t)\Big]u(P,\uparrow) \\ &= \frac{\Delta_x}{2\sqrt{(1-\xi^2)}M_N}E^q(x,\xi,t) \quad . \end{aligned}$$

These relations can easily be inverted and yield

$$\begin{aligned} H^q(x,\xi,t) &= \frac{1}{\sqrt{1-\xi^2}}G_{V,\uparrow\uparrow}^{q,+(N\to N)} + \frac{2M_N\xi^2}{\sqrt{1-\xi^2}\Delta_x}G_{V,\downarrow\uparrow}^{q,+(N\to N)} \\ E^q(x,\xi,t) &= \frac{2M_N\sqrt{1-\xi^2}}{\Delta_x}G_{V,\downarrow\uparrow}^{q,+(N\to N)} \quad . \end{aligned} \tag{4.3}$$

For the axial $N \to N$ transition one finds

$$\begin{aligned} G_{A,\uparrow\uparrow}^{q,+(N\to N)} &= \frac{1}{2\bar{P}^+}\bar{u}(P',\uparrow)\Big[\gamma^+\gamma_5\tilde{H}^q(x,\xi,t) + \frac{\Delta^+\gamma_5}{2M_N}\tilde{E}^q(x,\xi,t)\Big]u(P,\uparrow) \\ &= \sqrt{1-\xi^2}\tilde{H}^q(x,\xi,t) - \frac{\xi^2}{\sqrt{1-\xi^2}}\tilde{E}^q(x,\xi,t) \\ G_{A,\downarrow\uparrow}^{q,+(N\to N)} &= \frac{1}{2\bar{P}^+}\bar{u}(P',\downarrow)\Big[\gamma^+\gamma_5\tilde{H}^q(x,\xi,t) + \frac{\Delta^+\gamma_5}{2M_N}\tilde{E}^q(x,\xi,t)\Big]u(P,\uparrow) \\ &= \frac{\xi\Delta_x}{2\sqrt{1-\xi^2}M_N}\tilde{E}^q(x,\xi,t) \quad . \end{aligned}$$

[3] Since contributions of twist d scale like Q^{-d}.

The inversion of these relations yields

$$\tilde{H}^q(x,\xi,t) = \frac{1}{\sqrt{1-\xi^2}} G_{A,\uparrow\uparrow}^{q,+(N\to N)} + \frac{2\xi M_N}{\sqrt{1-\xi^2}\Delta_x} G_{A,\downarrow\uparrow}^{q,+(N\to N)}$$
$$\tilde{E}^q(x,\xi,t) = \frac{2\sqrt{1-\xi^2}M_N}{\xi\Delta_x} G_{A,\downarrow\uparrow}^{q,+(N\to N)} \quad . \tag{4.4}$$

It is natural to use the same set of covariants as for elastic $N \to N$ scattering in order to parameterize the leading twist DVCS hadronic tensor. In doing so one establishes connections between $H(x,\xi,t)$ and $F_1(t)$, $E(x,\xi,t)$ and $F_2(t)$ and between $\tilde{H}(x,\xi,t)$ and $G_A(t)$, which allow the development of physically intuitive pictures for these GPDs.

There is however a drawback of this choice of covariants which we do not find expressed anywhere in the literature. Our criticism concerns the use of the covariant $\frac{\Delta^\mu}{2M_N}\gamma_5$, which generates $\tilde{E}(x,\xi,t)$. As it can be seen from eq. 4.4 $\tilde{E}(x,\xi,t)$ is ill defined for $\xi = 0$. We should remark at this point that

- this is no artefact of the choice of the reference frame
- this problem does not arise for the corresponding form factor $G_P(t)$ since the latter can be obtained from another combination of $F^\mu_{A,\lambda'\lambda}$, while twist two GPDs are unambiguously connected to the good LF components

If one would use the covariant $\frac{i\sigma^{\mu\nu}}{2M_N}\gamma_5$ which is traditionally connected with the second class axial tensor form factor $G_T(t)$ such a problem was avoided (at the expense of a less intuitive meaning of the resulting GPD):

$$G_{A,\lambda'\lambda}^{q,+(N\to N)} = \frac{1}{2\bar{P}^+}\bar{u}(P',\lambda')\Big[\gamma^+\gamma_5\tilde{H}^q(x,\xi,t) + \frac{i\sigma^{+\nu}\Delta_\nu\gamma_5}{2M_N}\tilde{X}^q(x,\xi,t)\Big]u(P,\lambda)$$
$$\longrightarrow$$
$$\tilde{X}^q(x,\xi,t) = \frac{2\sqrt{1-\xi^2}M_N}{\Delta_x} G_{A,\downarrow\uparrow}^{q,+(N\to N)} \quad . \tag{4.5}$$

Of course the problem with $\tilde{E}(x,\xi,t)$ mentioned above can easily be circumvented by explaining

$$\tilde{E}^q(x,0,t) = \lim_{\xi\to 0}\frac{2\sqrt{1-\xi^2}M_N}{\xi\Delta_x} G_{A,\downarrow\uparrow}^{q,+(N\to N)} \quad , \tag{4.6}$$

which is a well defined limit. The reason for our comment concerns the calculation of $\tilde{E}(x,\xi,t)$ in [72]. In a model calculation which applies the impulse approximation the error in the transition amplitudes due to breaking of Lorentz symmetry is of the order ξ. Therefore the predictions which are obtained in [72] for $\tilde{H}(x,\xi,t)$ suffer from a small error (proportional to ξ) due to the use of the impulse approximation, which is tolerable as long as small values of skewedness ξ are concerned. From relation eq. 4.4 however it is obvious that the results for $\tilde{E}$ obtained in this model calculation have less predictive power.

Next we turn to the $N \to \Delta$ transition. Using the parametrization for the $p \to \Delta^+$ DVCS

hadronic tensor in terms of nucleon and Δ degrees of freedom the vectorial transition amplitudes can be written

$$G_{V,\,\lambda'\lambda}^{+\,(p\to\Delta^+)} = \frac{1}{2\sqrt{6}\bar{P}^+}\bar{u}_\nu(P',\lambda')\Big[\kappa_1^{+\nu}H_1(x,\xi,t) + \kappa_2^{+\nu}H_2(x,\xi,t) + \kappa_3^{+\nu}H_3(x,\xi,t)\Big]u(P,\lambda) \quad .$$

with a convenient set of covariants

$$\begin{aligned}
\kappa_1^{\mu\nu} &= (\gamma^\mu\Delta^\nu - \not{\Delta}g^{\mu\nu})\gamma_5 \\
\kappa_2^{\mu\nu} &= (P'^\mu\Delta^\nu - (P'\cdot\Delta)g^{\mu\nu})\gamma_5 \\
\kappa_3^{\mu\nu} &= (\Delta^\mu\Delta^\nu - \Delta^2 g^{\mu\nu})\gamma_5 \quad .
\end{aligned} \tag{4.7}$$

At this point we should comment on the isospin convention. The GPDs are defined with a different isospin factor compared to the form factors. The convention we introduce here refers to the $p \to \Delta^+$ transition. The other transitions can simply be related [46] to the above transitions by:

$$\begin{aligned}
G_{V,\,\lambda'\lambda}^{+\,(p\to\Delta^{++})} &= \sqrt{\frac{3}{2}}G_{V,\,\lambda'\lambda}^{+\,(p\to\Delta^+)} \\
G_{V,\,\lambda'\lambda}^{+\,(p\to\Delta^{0})} &= \sqrt{\frac{1}{2}}G_{V,\,\lambda'\lambda}^{+\,(p\to\Delta^+)} \quad .
\end{aligned}$$

When we evaluate the vectorial $N \to \Delta$ transition amplitudes we have to recall that the kinematics for this transition differs from the kinematics for the $N \to N$ transition. Particularly the variable Δ_x bears the different meaning

$$\Delta_x = \sqrt{-(1-\xi^2)t - 2\xi\Big[(1+\xi)M_\Delta^2 - (1-\xi)M_N^2\Big]}$$

now. For kinematical details and the construction of the Rarita- Schwinger spinor $u^\mu(P,\lambda)$ which describes the Delta resonance we refer to the appendix. We find the following expressions for the vectorial $N \to \Delta$ transition amplitudes:

$$\begin{aligned}
G_{V,\,\frac{3}{2}\uparrow}^{+\,(p\to\Delta^+)} =& \frac{\sqrt{1+\xi}\Delta_x}{2\sqrt{3(1-\xi)}}H_1(x,\xi,t) + \frac{\Delta_x\, A}{4\sqrt{3(1-\xi^2)}}H_2(x,\xi,t) \\
&- \frac{\xi\Delta_x\, A}{2\sqrt{3(1-\xi^2)}(1-\xi)}H_3(x,\xi,t) \\
G_{V,\,\frac{1}{2}\uparrow}^{+\,(p\to\Delta^+)} =& \frac{2\xi M_\Delta A - \Delta_x^2}{6\sqrt{1-\xi^2}M_\Delta}H_1(x,\xi,t) + \frac{4\xi M_\Delta A - \Delta_x^2}{12\sqrt{1-\xi^2}}H_2(x,\xi,t) \\
&+ \left(\frac{\Big[(1+\xi)^2 M_\Delta - (1-\xi)M_N\Big]\Delta_x^2}{6(1-\xi^2)^{\frac{3}{2}}M_\Delta}\right. \\
&\left. + \frac{\xi\Big[(1-3\xi)(1+\xi)M_\Delta^2 - (1-\xi)^2 M_N^2\Big]A}{6(1-\xi^2)^{\frac{3}{2}}M_\Delta}\right)H_3(x,\xi,t)
\end{aligned}$$

$$
\begin{aligned}
G_{V,\,\frac{1}{2}\downarrow}^{+\,(p\to\Delta^+)} =& \frac{\Big[(1-\xi)M_N - 2\xi M_\Delta\Big]\Delta_x}{6\sqrt{1-\xi^2}M_\Delta} H_1(x,\xi,t) \\
&- \frac{\Big[(1+5\xi)M_\Delta - (1-\xi)M_N\Big]\Delta_x}{12\sqrt{1-\xi^2}} H_2(x,\xi,t) \\
&- \frac{\left(\Delta_x^2 - \xi\Big[(1-\xi)^2 M_N^2 - (1-\xi^2)M_N M_\Delta + 4\xi(1+\xi)M_\Delta^2\Big]\right)\Delta_x}{6(1-\xi^2)^{\frac{3}{2}}M_\Delta} H_3(x,\xi,t) \\
G_{V,\,\frac{3}{2}\downarrow}^{+\,(p\to\Delta^+)} =& -\frac{\Delta_x^2}{4\sqrt{3(1-\xi^2)}} H_2(x,\xi,t) + \frac{\xi\Delta_x^2}{2\sqrt{3(1-\xi^2)}(1-\xi)} H_3(x,\xi,t) \quad . \qquad (4.8)
\end{aligned}
$$

Here we have introduced the shortcut notation

$$
A = (1+\xi)M_\Delta - (1-\xi)M_N \quad . \qquad (4.9)
$$

There are infinitely many possibilities to obtain the three GPDs $H_1(x,\xi,t)$, $H_2(x,\xi,t)$ and $H_3(x,\xi,t)$ from these four transition amplitudes. Meaningful extractions avoid kinematical singularities. In a fully covariant calculation of the transition amplitudes all prescriptions have to lead to the same results for the GPDs. However we break relativistic covariance in our model calculation. Therefore we require two different prescriptions in order to check the consequences of these covariance breaking effects. Two different prescriptions which fulfill this requirement are:

- Prescription I: Ignore $G_{V,\,\frac{3}{2}\downarrow}^{+\,(p\to\Delta^+)}$ and determine the three GPDs from the other three transition amplitudes
- Prescription II: Same principle, this time ignoring $G_{V,\,\frac{1}{2}\downarrow}^{+\,(p\to\Delta^+)}$

The formulae resulting from these inversions are obtained using Mathematica and will not be given explicitly here for lack of space. We only provide one example here:

$$
H_1(x,\xi,t) = \frac{2\sqrt{3(1-\xi)}}{\sqrt{1+\xi}\Delta_x}\Big(G_{V,\,\frac{3}{2}\uparrow}^{+\,(p\to\Delta^+)} + \frac{(1+\xi)M_\Delta - (1-\xi)M_N}{\Delta_x} G_{V,\,\frac{3}{2}\downarrow}^{+\,(p\to\Delta^+)}\Big) \quad . \qquad (4.10)
$$

The linear dependence among the 4 transition amplitudes reveals a non trivial relation between $G_{\frac{3}{2}\uparrow}^{+}$, $G_{\frac{1}{2}\uparrow}^{+}$, $G_{\frac{1}{2}\downarrow}^{+}$ and $G_{\frac{3}{2}\downarrow}^{+}$. This amplitude relation which stems from relativistic covariance is known as the angular condition [78]. It will be discussed in a broader context in section 4.4.

The GPDs $H_1(x,\xi,t)$, $H_2(x,\xi,t)$ and $H_3(x,\xi,t)$ can be related to the physically more meaningful GPDs $H_M^\star(x,\xi,t)$, $H_E^\star(x,\xi,t)$ and $H_C^\star(x,\xi,t)$ by relating the two respective sets of covariants:

$$
(\kappa_1,\ \kappa_2,\ \kappa_3) = M\,(\kappa_M,\ \kappa_E,\ \kappa_C) \quad .
$$

Consequently one finds

$$
\begin{pmatrix} H_M^\star(x,\xi,t) \\ H_E^\star(x,\xi,t) \\ H_C^\star(x,\xi,t) \end{pmatrix} = M \begin{pmatrix} H_1(x,\xi,t) \\ H_2(x,\xi,t) \\ H_3(x,\xi,t) \end{pmatrix} \quad . \qquad (4.11)
$$

The matrix M has firstly been given in [79] and for our slightly different choice of covariants can be found in [80]. These relations between sets of covariants can be derived using the Clifford algebra and the equations of motion for the nucleon and the Δ resonance. This construction will be performed in appendix C.

$$M = \frac{M_N}{3(M_\Delta + M_N)} \begin{pmatrix} \frac{\sigma+2q^+}{M_\Delta} & \sigma & 2t \\ \frac{\sigma}{M_\Delta} & \sigma & 2t \\ 4M_\Delta & 4M_\Delta^2 & 2\sigma \end{pmatrix} \quad , \tag{4.12}$$

where $\sigma = M_\Delta^2 - M_N^2 + t$ and $q^+ = (M_\Delta + M_N)^2 - t$.

Finally we explore the axial $N \to \Delta$ transition amplitudes. They can be parameterized by

$$G^{+\,(p\to\Delta^+)}_{A,\,\lambda'\lambda} = \frac{1}{4\bar{P}^+}\bar{u}_\nu(P',\lambda')\Big[\tilde{\kappa}_1^{+\nu}C_1(x,\xi,t) + \tilde{\kappa}_3^{+\nu}C_3(x,\xi,t) + \tilde{\kappa}_4^{+\nu}C_4(x,\xi,t)\Big]u(P,\lambda) \tag{4.13}$$

with the covariants reading

$$\begin{aligned} \tilde{\kappa}_1^{\mu\nu} &= g^{\mu\nu} \\ \tilde{\kappa}_3^{\mu\nu} &= \frac{g^{\mu\nu}\not{\Delta} - \gamma^\mu\Delta^\nu}{M_N} \quad . \\ \tilde{\kappa}_4^{\mu\nu} &= \frac{2\Big[(\bar{P}\cdot\Delta)g^{\mu\nu} - \bar{P}^\mu\Delta^\nu\Big]}{M_N^2} \end{aligned}$$

Since there exist 4 axial $N \to \Delta$ form factors, the so called Adler form factors [81] the reader may wonder why the remaining covariant

$$\tilde{\kappa}_2^{\mu\nu} = \frac{\Delta^\mu\Delta^\nu}{M_N^2}$$

does not have to be considered as well. However at leading twist (i.e. the GPDs are determined by the good LF components $G^+_{\lambda'\lambda}$ only) the fourth covariant is not independent:

$$\begin{aligned} \tilde{\kappa}_2^{+\nu} =& \frac{\Delta^+\Delta^\nu}{M_N^2} \\ =& \xi\left(\frac{2\Big[\frac{M_\Delta^2-M_N^2}{2}g^{+\nu} + \frac{\Delta^+}{2\xi}\Delta^\nu\Big] - (M_\Delta^2 - M_N^2)g^{+\nu}}{M_N^2}\right) \\ =& \xi\left(\frac{2\Big[(\bar{P}\cdot\Delta)g^{+\nu} - \bar{P}^+\Delta^\nu\Big]}{M_N^2} - \frac{(M_\Delta^2 - M_N^2)g^{+\nu}}{M_N^2}\right) \\ =& \xi\Big[\tilde{\kappa}_4^{+\nu} - \frac{M_\Delta^2 - M_N^2}{M_N^2}\tilde{\kappa}_1^{+\nu}\Big] \end{aligned} \tag{4.14}$$

The reason for preferring the covariant $\tilde{\kappa}_4^{+\nu}$ over $\tilde{\kappa}_2^{+\nu}$ is the singularity for $\xi = 0$ in the GPD $C_2(x,\xi,t)$ if one chose C_1, C_2 and C_3 to parameterize $G^{+\,(p\to\Delta^+)}_{A,\,\lambda'\lambda}$. Unlike in the case of

$\tilde{E}(x,\xi,t)$ where the apparent singularity at $\xi = 0$ turned out to be a well defined limit (eq. 4.6) this is not true here. One finds

$$C_2(x,\xi,t) = -\frac{2\sqrt{2(1-\xi^2)}(1-\xi)M_N^2}{\xi\Delta_x^2} G^{+\,(p\to\Delta^+)}_{A,\,\frac{3}{2}\downarrow}$$

and at least in our model calculation we find a finite result for $G^{+\,(p\to\Delta^+)}_{A,\,\frac{3}{2}\downarrow}$ at $\xi = 0$. Another reason why $\tilde{\kappa}_2^{\mu\nu}$ is an inconvenient choice will be transparent in the following section: The corresponding form factor $C_6(t)$ requires at least one bad transition amplitude to be evaluated.

By the way a similar argument applies for the use of a possible fourth vectorial $N \to \Delta$ GPD. Of course gauge invariance is no longer a constraint which could forbid a covariant like $g^{\mu\nu}\gamma_5$. But again at leading twist it is not independent of the other three covariants:

$$\begin{aligned} g^{+\nu}\gamma_5 &= \frac{\Big[2\xi(P'\cdot\Delta) + (1-\xi)t\Big] g^{+\nu}\gamma_5}{2\xi(P'\cdot\Delta) + (1-\xi)t} \\ &= -\frac{2\xi\Big[P'^{+}\Delta^{\nu} - (P'\cdot\Delta)g^{+\nu}\Big]\gamma_5 + (1-\xi)\Big[\Delta^{+}\Delta^{\nu} - t g^{+\nu}\Big]\gamma_5}{2\xi(P'\cdot\Delta) + (1-\xi)t} \\ &= -\frac{2\xi\kappa_2^{+\nu} + (1-\xi)\kappa_3^{+\nu}}{t + \xi(M_\Delta^2 - M_N^2)} \quad . \end{aligned}$$

After these remarks we are ready to proceed and evaluate the axial transition amplitudes in order to find

$$\begin{aligned} G^{+\,(p\to\Delta^+)}_{A,\,\frac{3}{2}\uparrow} =& -\frac{\sqrt{1+\xi}\Delta_x}{2\sqrt{2(1-\xi)}M_N} C_3(x,\xi,t) - \frac{\Delta_x\, B}{2\sqrt{2(1-\xi^2)}(1-\xi)M_N^2} C_4(x,\xi,t) \\ G^{+\,(p\to\Delta^+)}_{A,\,\frac{1}{2}\uparrow} =& \frac{\sqrt{1-\xi}B}{2\sqrt{6(1+\xi)}M_\Delta} C_1(x,\xi,t) + \frac{\Delta_x^2 - 2\xi M_\Delta\, B}{2\sqrt{6}(1-\xi^2)^{\frac{3}{2}}M_\Delta M_N} C_3(x,\xi,t) \\ &+ \frac{\Delta_x^2\Big[2(1+\xi)M_\Delta + (1-\xi)\Big] - \xi\Big[(3-\xi)(1+\xi)M_\Delta^2 + (1-\xi)^2 M_N^2 B\Big]}{2\sqrt{6}(1-\xi^2)^{\frac{3}{2}}M_\Delta M_N^2} C_4(x,\xi,t) \\ G^{+\,(p\to\Delta^+)}_{A,\,\frac{1}{2}\downarrow} =& \frac{\sqrt{1-\xi}\Delta_x}{2\sqrt{6(1+\xi)}M_\Delta} C_1(x,\xi,t) - \frac{\Big[(1-\xi)M_N + 2\xi M_\Delta\Big]\Delta_x}{2\sqrt{6(1-\xi^2)}M_N M_\Delta} C_3(x,\xi,t) \\ &+ \frac{\Delta_x\Big[\Delta_x^2 - \xi(1-\xi)^2 M_N^2 - (\xi + 5\xi^2 + 3\xi^3 - \xi^4)M_\Delta^2 - (1-\xi^2)M_N M_\Delta\Big]}{2\sqrt{6}(1-\xi^2)^{\frac{3}{2}}M_\Delta M_N^2} C_4(x,\xi,t) \\ G^{+\,(p\to\Delta^+)}_{A,\,\frac{3}{2}\downarrow} =& -\frac{\Delta_x^2}{2\sqrt{2(1-\xi^2)}(1-\xi)M_N^2} C_4(x,\xi,t) \quad . \end{aligned}$$

Here we have introduced the shortcut notation

$$B = (1+\xi)M_\Delta + (1-\xi)M_N \quad . \tag{4.15}$$

In order to obtain the axial GPDs $C_1(x,\xi,t)$, $C_2(x,\xi,t)$ and $C_3(x,\xi,t)$ from the axial transition amplitudes the same remark as for the vectorial GPDs holds. In fact the above mentioned

prescriptions I and II both avoid kinematical singularities also for the axial transition. As example we provide the expression for $C_4(x,\xi,t)$ resulting from prescription II:

$$C_4(x,\xi,t) = -\frac{2\sqrt{2}(1-\xi)(1-\xi^2)^{\frac{3}{2}}M_N^2}{\Delta_x^2} G^{+\,(p\to\Delta^+)}_{A,\,\frac{3}{2}\downarrow} \quad .$$

4.3 Form factors and sum rules

As mentioned in the introduction the way how we obtain form factors from the transition amplitudes $F^{\mu}_{\lambda'\lambda}$ is identical to the way how we get GPDs from the respective transition amplitudes $G^{+}_{\lambda'\lambda}$. We will give the relations here as well as the resulting sum rules.

For the vectorial $N \to N$ transition we have

$$\begin{aligned} F^{q,\,+\,(N\to N)}_{V,\,\uparrow\uparrow} &= \frac{1}{2\sqrt{P'^{+}P^{+}}}\bar{u}(P',\uparrow)\Big[\gamma^{+}F_1(t) + \frac{i\sigma^{+\nu}\Delta_\nu}{2M_N}F_2(t)\Big]u(P,\uparrow) = F_1(t) \\ F^{q,\,+\,(N\to N)}_{V,\,\downarrow\uparrow} &= \frac{1}{2\sqrt{P'^{+}P^{+}}}\bar{u}(P',\downarrow)\Big[\gamma^{+}F_1(t) + \frac{i\sigma^{+\nu}\Delta_\nu}{2M_N}F_2(t)\Big]u(P,\uparrow) = \frac{\Delta_x}{2M_N}F_2(t) \quad . \end{aligned} \tag{4.16}$$

Since we have the same number of twist 2 GPDs and form factors for this transition the generic sum rule (eq. 4.2) leads to

$$\begin{aligned} F_1(t) &= \int_{-1}^{1} dx\, H(x,\xi,t) \\ F_2(t) &= \int_{-1}^{1} dx\, E(x,\xi,t) \quad . \end{aligned}$$

The situation is different for the axial transition form factors. Here we can also include the second class term $\frac{i\sigma^{\mu\nu}}{2M_N}\gamma_5$. The latter changes its sign under charge conjugation and since the $SU(2)$ flavor symmetry is almost an exact symmetry the resulting axial tensor form factor $G_T(t)$ is very small and can be neglected. For the moment we will discuss it however since it provides a fresh perspective on sum rules for axial GPDs. We have

$$F^{q,\,\mu\,(N\to N)}_{A,\,\lambda'\lambda} = \frac{1}{2\sqrt{P'^{+}P^{+}}}\bar{u}(P',\lambda')\Big[\gamma^{\mu}\gamma_5 G_A(t) + \frac{\Delta^{\mu}\gamma_5}{2M_N}G_P(t) + \frac{i\sigma^{\mu\nu}\Delta_\nu\gamma_5}{2M_N}G_T(t)\Big]u(P,\lambda)$$

leading to

$$\begin{aligned} G_A(t) &= F^{+}_{\uparrow\uparrow} \\ G_P(t) &= \frac{2M_N\Big[2M_N F^{+}_{\uparrow\uparrow} - F^{x}_{\downarrow\uparrow}\Big]}{\Delta_x^2} \\ G_T(t) &= \frac{2M_N}{\Delta_x}F^{+}_{\downarrow\uparrow} \quad . \end{aligned} \tag{4.17}$$

The generic sum rule (eq. 4.2) can now be evaluated for its plus components which correspond to the twist 2 GPDs. Using the equation of motion and the Clifford algebra the covariants

can now be reexpressed in terms of the convenient set of covariants $\gamma^\mu\gamma_5$, $\Delta^\mu\gamma_5$ and $\bar{P}^\mu\gamma_5$:

$$\begin{aligned}\bar{u}(P')\frac{i\sigma^{\mu\nu}\Delta_\nu}{2M_N}\gamma_5 u(P) &= \bar{u}(P')\left(-\frac{P'^\nu}{4M_N}\Big[\gamma^\mu,\gamma^\nu\Big]\gamma_5 + \frac{P^\nu}{4M_N}\Big[\gamma^\mu,\gamma^\nu\Big]\gamma_5\right)u(P)\\ &= \frac{1}{2M_N}\bar{u}(P')\left(\not{P}'\gamma^\mu\gamma_5 + \gamma_5\gamma^\mu\not{P} - 2\bar{P}^\mu\gamma_5\right)u(P)\\ &= -\bar{u}(P')\frac{\bar{P}^\mu}{M_N}\gamma_5 u(P) \quad .\end{aligned}$$

At leading twist we can use $\Delta^+ = -2\xi\bar{P}^+$ which then leads to

$$F^+_{\lambda'\lambda} = \frac{1}{2\sqrt{P'^+P^+}}\bar{u}(P',\lambda')\left(\gamma^+\gamma_5 G_A(t) - \frac{\bar{P}^+}{M_N}\Big[G_T(t) + \xi G_P(t)\Big]\gamma_5\right)u(P,\lambda)$$

and

$$G^+_{\lambda'\lambda} = \frac{1}{2\bar{P}^+}u(P',\lambda')\left(\gamma^+\gamma_5\tilde{H}(x,\xi,t) - \frac{2\xi\bar{P}^+}{2M_N}\tilde{E}(x,\xi,t)\gamma_5\right)u(P,\lambda) \quad .$$

With both $F^+_{\uparrow\uparrow}$ and $F^+_{\downarrow\uparrow}$ being non zero[4] we evaluate eq. 4.2 for the flip and non flip transitions and thus find

$$\begin{aligned}\int_{-1}^{1} dx\,\tilde{E}(x,\xi,t) &= G_P(t) + \frac{1}{\xi}G_T(t)\\ \int_{-1}^{1} dx\,\tilde{H}(x,\xi,t) &= G_A(t) \quad .\end{aligned} \tag{4.18}$$

The sum rule result certainly violates the polynomiality condition [26]. This is not problematic, since this condition requires time reversal invariance, which is broken due to $G_T(t) \neq 0$.

This result looks only slightly different from the sum rules for axial GPDs given by Ji in [24]:

$$\begin{aligned}G_P(t) &= \int_{-1}^{1} dx\,\tilde{E}(x,\xi,t)\\ G_A(t) &= \int_{-1}^{1} dx\,\tilde{H}(x,\xi,t) \quad .\end{aligned} \tag{4.19}$$

However we like to remark about the sum rule in eq. 4.18 that it provides an observable for the second class form factor $G_T(t)$:

$$G_T(t) = \xi\left[\Big(\int_{-1}^{1} dx\tilde{E}(x,\xi,t)\Big) - G_P(t)\right] \quad ,$$

which is an interesting result in itself.

[4] This is only true because we assume a non zero $G_T(t)$.

The $N \to \Delta$ transition form factors can be treated along the same lines. The $p \to \Delta^+$ transition amplitudes are parameterized via

$$F^{+(p\to\Delta^+)}_{V,\lambda'\lambda} = \frac{1}{\sqrt{6P'^+P^+}}\bar{u}_\nu(P',\lambda')\Big[\kappa_1^{\mu\nu}G_1(t) + \kappa_2^{\mu\nu}G_2(t) + \kappa_3^{\mu\nu}G_3(t)\Big]u(P,\lambda) \quad .$$

The covariants are the same as in eq. 4.7. We find

$$\begin{aligned}
F^{+(p\to\Delta^+)}_{V,\frac{3}{2}\uparrow} =& \frac{\Delta_x}{\sqrt{3}}G_1(t) + \frac{\Delta_x(M_\Delta - M_N)}{2\sqrt{3}}G_2(t) \\
F^{+(p\to\Delta^+)}_{V,\frac{1}{2}\uparrow} =& -\frac{\Delta_x^2}{3M_\Delta}G_1(t) - \frac{\Delta_x^2}{6}G_2(t) + \frac{(M_\Delta - M_N)\Delta_x^2}{3M_\Delta}G_3(t) \\
F^{+(p\to\Delta^+)}_{V,\frac{1}{2}\downarrow} =& \frac{M_N\Delta_x}{3M_\Delta}G_1(t) - \frac{(M_\Delta - M_N)\Delta_x}{6}G_2(t) - \frac{\Delta_x^3}{3M_\Delta}G_3(t) \\
F^{+(p\to\Delta^+)}_{V,\frac{3}{2}\downarrow} =& -\frac{\Delta_x^2}{2\sqrt{3}}G_2(t) \quad .
\end{aligned}$$

The formulae have the same structure as the expressions for the $G^+_{\lambda'\lambda}$ in eq. 4.8 with $\xi = 0$. Therefore the form factors $G_i(t)$ can be obtained (ambiguously) in the same manner as the GPDs $H_i(x,\xi,t)$. Again we use the following prescriptions:

- I: Using $F^+_{\frac{3}{2}\uparrow}$, $F^+_{\frac{1}{2}\uparrow}$ and $F^+_{\frac{1}{2}\downarrow}$ and inverting the relations above we find:

$$\begin{aligned}
G_1(t) &= \frac{\sqrt{3}M_\Delta\Big[\Delta_x^2 + (M_\Delta - M_N)^2\Big]F^+_{\frac{3}{2}\uparrow} + 3\Delta_x M_\Delta(M_\Delta - M_N)F^+_{\frac{1}{2}\uparrow} + 3M_\Delta(M_\Delta - M_N)^2F^+_{\frac{1}{2}\downarrow}}{\Delta_x\Big[\Delta_x^2 M_N + (M_\Delta - M_N)^2(M_\Delta + M_N)\Big]} \\
G_2(t) &= \frac{2\sqrt{3}\Big[M_N(M_\Delta - M_N) - \Delta_x^2\Big]F^+_{\frac{3}{2}\uparrow} - 6\Delta_x M_\Delta F^+_{\frac{1}{2}\uparrow} - 6M_\Delta(M_\Delta - M_N)F^+_{\frac{1}{2}\downarrow}}{\Delta_x\Big[\Delta_x^2 M_N + (M_\Delta - M_N)^2(M_\Delta + M_N)\Big]} \\
G_3(t) &= \frac{\sqrt{3}\Delta_x M_\Delta^2 F^+_{\frac{3}{2}\uparrow} + 3M_\Delta(M_\Delta^2 - M_N^2)F^+_{\frac{1}{2}\uparrow} - 3\Delta_x M_\Delta M_N F^+_{\frac{1}{2}\downarrow}}{\Delta_x^2\Big[\Delta_x^2 M_N + (M_\Delta - M_N)^2(M_\Delta + M_N)\Big]} \quad .
\end{aligned} \tag{4.20}$$

- II: Using $F^+_{\frac{3}{2}\uparrow}$, $F^+_{\frac{1}{2}\uparrow}$ and $F^+_{\frac{3}{2}\downarrow}$ we have:

$$\begin{aligned}
G_1(t) &= \frac{\sqrt{3}}{\Delta_x}F^+_{\frac{3}{2}\uparrow} + \frac{\sqrt{3}(M_\Delta - M_N)}{\Delta_x^2}F^+_{\frac{3}{2}\downarrow} \\
G_2(t) &= -\frac{2\sqrt{3}}{\Delta_x^2}F^+_{\frac{3}{2}\downarrow} \\
G_3(t) &= \frac{\sqrt{3}}{\Delta_x(M_\Delta - M_N)}F^+_{\frac{3}{2}\uparrow} + \frac{3M_\Delta}{\Delta_x^2(M_\Delta - M_N)}F^+_{\frac{1}{2}\uparrow} - \frac{\sqrt{3}M_N}{\Delta_x^2(M_\Delta - M_N)}F^+_{\frac{3}{2}\downarrow} \quad .
\end{aligned} \tag{4.21}$$

The relations between the $G_i(t)$ are the same[5] as for the GPDs with $\xi = 0$. The physically intuitive transition form factors $G^\star_M(t)$, $G^\star_E(t)$ and $G^\star_C(t)$ are likewise obtained from the $G_i(t)$ along the lines of eq. 4.11 and eq. 4.12.

Since for the vectorial transition form factors we have the same covariants as for the respective GPDs the evaluation of the generic sum rules reveals:

$$\begin{aligned}\int_{-1}^{1} dx\, H^\star_M(x,\xi,t) &= 2\, G^\star_M(t)\\ \int_{-1}^{1} dx\, H^\star_E(x,\xi,t) &= 2\, G^\star_E(t)\\ \int_{-1}^{1} dx\, H^\star_C(x,\xi,t) &= 2\, G^\star_C(t) \quad .\end{aligned}$$

The factor 2 stems from the different definition of the transition amplitudes $F^{\mu\,(p\to\Delta^+)}_{A,\,\lambda'\lambda}$ and $G^{\mu\,(p\to\Delta^+)}_{A,\,\lambda'\lambda}$ concerning isospin. For details c.f. chapter 2.

For the axial transition the situation is different again. The transition amplitudes are parameterized by

$$F^{\mu(p\to\Delta^+)}_{A,\lambda'\lambda} = \frac{1}{2\sqrt{P'^+P^+}}\bar{u}_\nu(P',\lambda')\Big[\tilde{\kappa}^{\mu\nu}_1 C_5(t) + \tilde{\kappa}^{\mu\nu}_2 C_6(t) + \tilde{\kappa}^{\mu\nu}_3 C_3(t) + \tilde{\kappa}^{\mu\nu}_4 C_4(t)\Big]u(P,\lambda) \quad . \tag{4.22}$$

The form factors are named $C_5(t)$, $C_6(t)$, $C_3(t)$ and $C_4(t)$ for historical reasons. Here we have four form factors in contrast to three leading twist GPDs. With only three independent good LF transition amplitudes[6] a bad transition amplitude is required additionally. We choose[7] $\tilde{F}^{x\,(p\to\Delta^+)}_{A,\,\frac{3}{2}\uparrow}$. The evaluation of the transition amplitudes reveals

$$\begin{aligned}
F^{+\,(p\to\Delta^+)}_{A,\,\frac{3}{2}\uparrow} &= -\frac{\Delta_x}{\sqrt{2}M_N}C_3(t) - \frac{\Delta_x(M_\Delta+M_N)}{\sqrt{2}M_N^2}C_4(t)\\
F^{+\,(p\to\Delta^+)}_{A,\,\frac{1}{2}\uparrow} &= \frac{M_\Delta+M_N}{\sqrt{6}M_\Delta}C_5(t) + \frac{\Delta_x^2}{\sqrt{6}M_\Delta M_N}C_3(t) + \frac{(2M_\Delta+M_N)\Delta_x^2}{\sqrt{6}M_\Delta M_N^2}C_4(t)\\
F^{+\,(p\to\Delta^+)}_{A,\,\frac{1}{2}\downarrow} &= \frac{\Delta_x}{\sqrt{6}M_\Delta}C_5(t) - \frac{\Delta_x}{\sqrt{6}M_\Delta}C_3(t) + \frac{\Delta_x\Big[\Delta_x^2 - M_\Delta(M_\Delta+M_N)\Big]}{\sqrt{6}M_\Delta M_N^2}C_4(t)\\
F^{+\,(p\to\Delta^+)}_{A,\,\frac{3}{2}\downarrow} &= -\frac{\Delta_x^2}{\sqrt{2}M_N^2}C_4(t)\\
\tilde{F}^{x\,(p\to\Delta^+)}_{A,\,\frac{3}{2}\uparrow} &= -\frac{M_\Delta+M_N}{\sqrt{2}}C_5(t) + \frac{(M_\Delta+M_N)\Delta_x^2}{\sqrt{2}M_N^2}C_6(t) - \frac{M_\Delta^2-M_N^2}{\sqrt{2}M_N}C_3(t)\\
&\quad - \frac{(M_\Delta-M_N)(M_\Delta+M_N)^2}{\sqrt{2}M_N^2}C_4(t) \quad .
\end{aligned}$$

[5] up to an overall factor 2.

[6] The resulting amplitude relation will be dealt with in the following section.

[7] We define $\tilde{F}^x = 2\bar{P}^+F^x$ in order to suppress kinematical factors of $2\bar{P}^+$.

Our aim concerning the application of the relations between form factors and amplitudes is to evaluate the form factors in a quark model calculation. In order to get an estimate for covariance breaking effects in this particular model calculation we need two distinct reasonable prescriptions of how to get form factors from the transition amplitudes. we use the prescriptions

- I: Using $F^+_{\frac{3}{2}\uparrow}$, $F^+_{\frac{1}{2}\uparrow}$, $F^+_{\frac{1}{2}\downarrow}$ and $\tilde{F}^x_{\frac{3}{2}\uparrow}$ and inverting the relations above we find

$$
\begin{aligned}
C_5(t) =& \frac{\sqrt{2}\Delta_x(\Delta_x^2 - M_\Delta^2 + M_\Delta M_N + M_N^2)F^+_{\frac{3}{2}\uparrow} + \sqrt{6}M_\Delta(\Delta_x^2 - M_\Delta^2 + M_N^2)F^+_{\frac{1}{2}\uparrow} - \sqrt{6}M_\Delta^2\Delta_x F^+_{\frac{1}{2}\downarrow}}{\Delta_x^2 M_N - (M_\Delta - M_N)(M_\Delta + M_N)^2} \\
C_6(t) =& \frac{\sqrt{2}M_N^2\Big[\Delta_x^4 - \Delta_x^2 M_\Delta^2 + M_\Delta^4 + 2(\Delta_x^2 - M_\Delta^2)M_N^2 + M_N^4\Big]}{\Delta_x^3\Big[\Delta_x^2 M_N - (M_\Delta - M_N)(M_\Delta + M_N)^2\Big]}F^+_{\frac{3}{2}\uparrow} \\
&+ \frac{\sqrt{6}M_\Delta M_N^2(\Delta_x^2 - M_\Delta^2 + M_N^2)}{\Delta_x^2\Big[\Delta_x^2 M_N - (M_\Delta - M_N)(M_\Delta + M_N)^2\Big]}F^+_{\frac{1}{2}\uparrow} \\
&- \frac{\sqrt{6}M_\Delta^2 M_N^2}{\Delta_x\Big[\Delta_x^2 M_N - (M_\Delta - M_N)(M_\Delta + M_N)^2\Big]}F^+_{\frac{1}{2}\downarrow} + \frac{\sqrt{2}M_N^2}{\Delta_x^2(M_\Delta + M_N)}\tilde{F}^x_{\frac{3}{2}\uparrow} \\
C_3(t) =& \frac{\sqrt{2}M_\Delta M_N\Big[\Delta_x^2 + (M_\Delta + M_N)^2\Big]F^+_{\frac{3}{2}\uparrow} + \sqrt{6}M_\Delta M_N(M_\Delta + M_N)\Delta_x F^+_{\frac{1}{2}\uparrow}}{\Delta_x\Big[\Delta_x^2 M_N - (M_\Delta - M_N)(M_\Delta + M_N)^2\Big]} \\
&- \frac{\sqrt{6}M_\Delta M_N(M_\Delta + M_N)^2 F^+_{\frac{1}{2}\downarrow}}{\Delta_x\Big[\Delta_x^2 M_N - (M_\Delta - M_N)(M_\Delta + M_N)^2\Big]} \\
C_4(t) =& -\frac{\sqrt{2}M_N^2\left(\Big[\Delta_x^2 + M_N(M_\Delta + M_N)\Big]F^+_{\frac{3}{2}\uparrow} + \sqrt{3}M_\Delta\Delta_x F^+_{\frac{1}{2}\uparrow} - \sqrt{3}M_\Delta(M_\Delta + M_N)F^+_{\frac{1}{2}\downarrow}\right)}{\Delta_x\Big[\Delta_x^2 M_N - (M_\Delta - M_N)(M_\Delta + M_N)^2\Big]} \quad .
\end{aligned}
\tag{4.23}
$$

- II: Using $F^+_{\frac{3}{2}\uparrow}$, $F^+_{\frac{1}{2}\uparrow}$, $F^+_{\frac{3}{2}\downarrow}$ and $F^x_{\frac{3}{2}\uparrow}$ we have

$$
\begin{aligned}
C_5(t) &= \frac{\sqrt{2}\Delta_x F^+_{\frac{3}{2}\uparrow} + \sqrt{6}M_\Delta F^+_{\frac{1}{2}\uparrow} + \sqrt{2}M_\Delta F^+_{\frac{3}{2}\downarrow}}{M_\Delta + M_N} \\
C_6(t) &= \frac{\sqrt{2}M_N^2\Big[(\Delta_x^2 - M_\Delta^2 + M_N^2)F^+_{\frac{3}{2}\uparrow} + \sqrt{3}M_\Delta\Delta_x F^+_{\frac{1}{2}\uparrow} + M_\Delta\Delta_x F^+_{\frac{3}{2}\downarrow} + \Delta_x\tilde{F}^x_{\frac{3}{2}\uparrow}\Big]}{\Delta_x^3(M_\Delta + M_N)} \\
C_3(t) &= \frac{\sqrt{2}M_N\Big[-\Delta_x F^+_{\frac{3}{2}\uparrow} + (M_\Delta + M_N)F^+_{\frac{3}{2}\downarrow}\Big]}{\Delta_x^2} \\
C_4(t) &= -\frac{\sqrt{2}M_N^2}{\Delta_x^2}F^+_{\frac{3}{2}\downarrow} \quad .
\end{aligned}
\tag{4.24}
$$

Now the sum rules for the axial GPDs also look different. We start from the generic sum rule (eq. 4.2). As for the $N \to N$ transition the ξ dependence drops out in this equation due to Lorentz covariance. Using the parameterizations 4.22 for $\tilde{F}^{+}_{\lambda'\lambda}$ and 4.13 for $\tilde{G}^{+}_{\lambda'\lambda}$ we obtain

$$\begin{aligned}
&\frac{1}{4\sqrt{1-\xi^2}\bar{P}^+}\int_{-1}^{1} dx\, \bar{u}_\nu(P',\lambda')\Big(C_1(x,\xi,t)\tilde{\kappa}_1^{+\nu} + C_3(x,\xi,t)\tilde{\kappa}_3^{+\nu} + C_4(x,\xi,t)\tilde{\kappa}_4^{+\nu}\Big)u(P,\lambda) \\
&= \frac{1}{2\sqrt{P'^+P^+}}\bar{u}_\nu(P',\lambda')\Big(C_5(t)\tilde{\kappa}_1^{+\nu} + C_6(t)\tilde{\kappa}_2^{+\nu} + C_3(t)\tilde{\kappa}_3^{+\nu} + C_4(t)\tilde{\kappa}_4^{+\nu}\Big)u(P,\lambda)
\end{aligned}$$

Using eq. 4.14 we can reexpress $\tilde{\kappa}_4^{+\nu}$ and find

$$\begin{aligned}
&\frac{1}{2}\int_{-1}^{1} dx\, \bar{u}_\nu(P',\lambda')\Bigg(\Big[C_1(x,\xi,t) + \frac{M_\Delta^2 - M_N^2}{M_N^2}C_4(x,\xi,t)\Big]\tilde{\kappa}_1^{+\nu} + \frac{1}{\xi}C_4(x,\xi,t)\tilde{\kappa}_2^{+\nu} \\
&+ C_3(x,\xi,t)\tilde{\kappa}_3^{+\nu}\Bigg)u(P,\lambda) \\
&= \bar{u}_\nu(P',\lambda')\Bigg(\Big[C_5(t) + \frac{M_\Delta^2 - M_N^2}{M_N^2}C_4(t)\Big]\tilde{\kappa}_1^{+\nu} + \Big[C_6(t) + \frac{1}{\xi}C_4(t)\Big]\tilde{\kappa}_2^{+\nu} + C_3(t)\tilde{\kappa}_3^{+\nu}\Bigg)u(P,\lambda)
\end{aligned}$$

Since the covariants $\tilde{\kappa}_1^{+\nu}$, $\tilde{\kappa}_2^{+\nu}$ and $\tilde{\kappa}_3^{+\nu}$ are independent we can compare their contributions separately. We read off from the above expression:

$$\begin{aligned}
\int_{-1}^{1} dx\, C_1(x,\xi,t) &= 2C_5(t) - 2\xi\frac{M_\Delta^2 - M_N^2}{M_N^2}C_6(t) \\
\int_{-1}^{1} dx\, C_3(x,\xi,t) &= 2C_3(t) \\
\int_{-1}^{1} dx\, C_4(x,\xi,t) &= 2C_4(t) + 2\xi C_6(t) \quad .
\end{aligned} \tag{4.25}$$

We like to comment the appearance on ξ on the r.h.s. of the sum rules in 4.25. The ξ independence due to Lorentz covariance is generally valid for generic sum rules of the type $F^{\mu}_{\lambda'\lambda}(t) = \int dx\, \frac{1}{1-\xi^2}\, G^{\mu}_{\lambda'\lambda}(x,\xi,t)$. For $H(x,\xi,t)$ and $E(x,\xi,t)$ this property is inherited as DVCS and elastic scattering transition amplitudes are parameterized by the same covariants. The ξ dependence in 4.25 on the other hand roots in the different number of covariants which parameterize $F^{\mu}_{\lambda'\lambda}$ and $G^{+}_{\lambda'\lambda}$.

Finally for the $N \to \Delta$ transition the moments of GPDs do not have to satisfy a polynomiality condition. The latter arises for the $N \to N$ transition by considering towers of higher spin twist 2 local operators which allow for an ordering pattern leading to the polynomiality condition. There exists no analog for the $N \to \Delta$ transition.

We remark a similarity to the axial $N \to N$ transition. It is possible to obtain $G_P(t)$ from good LF DVCS transition amplitudes only.

$$G_P(t) = \int_{-1}^{1} dx\, \tilde{E}(x,\xi,t) = \frac{2\sqrt{1-\xi^2}M_N}{\xi\Delta_x}\int_{-1}^{1} dx\, G^{+(N\to N)}_{A,\downarrow\uparrow}$$

The sum rules in eq. 4.25 likewise provide a possibility to extract all Adler form factors from good LF $N \to \Delta$ DVCS transition amplitudes alone. We read off the expressions

$$C_6(t) = \frac{\int_{-1}^{1} dx\, C_4(x,\xi,t) - C_4(t)}{\xi}$$
$$C_6(t) = \frac{M_N^2}{\xi(M_\Delta^2 - M_N^2)} \left(\int_{-1}^{1} dx\, C_1(x,\xi,t) - C_5(t) \right) \quad .$$

4.4 Amplitude relations

In the last two sections we have given the expressions for the good components of vectorial and axial $N \to N$ and $N \to \Delta$ transition amplitudes. Even when we restricted ourselves to these good components we could observe an ambiguity in case of the $N \to \Delta$ transition. This indicates the existence of a constraint equation among these amplitudes. This holds true the more as we allow for other transition amplitudes, i.e. $F^{\mu}_{\lambda'\lambda}$ with $\mu \in \{x, y, -\}$. The number of independent amplitudes for a given transition can never exceed the number of physical GPDs or form factors.

The formalism which we develop here holds for the transition amplitudes $F^{\mu}_{\lambda'\lambda}$ as well as for the DVCS transition amplitudes $G^{\mu}_{\lambda'\lambda}$. However since DVCS transition amplitudes with different Lorentz indices μ are parameterized by GPDs with different twists there exist maximally relations between the amplitudes with the same Lorentz index[8] e.g. between the amplitudes $G^{+}_{\lambda'\lambda}$. In the following we will only speak about transition amplitudes and form factors in order to be concise - obviously GPDs can be treated similarly in the above mentioned sense.

The resulting constraint equations can be understand as consistency relations which have to hold if the amplitudes obey relativistic covariance[9]. In order to simplify the calculation of these consistency relations we introduce a generalized notation:

Let T^i with $i \in I$ denote the form factors for a given transition. Further let G^j with $j \in J$ enumerate all possible amplitudes for this transition. The respective coefficients C^{ij} which relate these form factors shall be defined by

$$G^j = \sum_{i \in I} C^{ij} T^i$$

with the shortcut notation

$$G = C^T \cdot T \quad .$$

As an example consider the elastic vectorial $N \to N$ transition. Here we have

$$\begin{aligned} T =& \{T^i\}_{i \in I = \{1,2\}} \text{ with } T^1 = F_1(t) \text{ and } T^2 = F_2(t) \\ G =& \{G^j\}_{j \in J = \{1,\ldots,8\}} \text{ with } G^1 = F_{V,\uparrow\uparrow}^{+(N\to N)},\ G^2 = F_{V,\uparrow\downarrow}^{+(N\to N)},\ G^3 = F_{V,\uparrow\uparrow}^{x(N\to N)} \\ G^4 =& F_{V,\uparrow\downarrow}^{x(N\to N)},\ G^5 = F_{V,\uparrow\uparrow}^{y(N\to N)},\ G^6 = F_{V,\uparrow\downarrow}^{y(N\to N)},\ G^7 = F_{V,\uparrow\uparrow}^{-(N\to N)},\ G^8 = F_{V,\uparrow\downarrow}^{-(N\to N)} \quad . \end{aligned} \tag{4.26}$$

[8] There exist relations between $G^{x}_{\lambda'\lambda}$ and $G^{y}_{\lambda'\lambda}$ as well.

[9] In the physical world they do of course. In model calculations relativistic covariance may be violated though.

As an example for the coefficients we mention

$$C^{22} = -\frac{\Delta_x}{2M_N} \quad .$$

Now for a subset $K \subseteq J$ with $\#K = \#I$ and

$$Det\{(C^{ik})\}_{i\in I, k\in K} \neq 0$$

the form factors are expressed by

$$T^i = \sum_{k\in K} (C^{-1})^{ik} G^k \qquad\qquad \forall i \in I$$

Now for any $l \in J$ with $l \notin K$ one obtains

$$\begin{aligned} G^l &= \sum_{i\in I} (C^{il})^T T^i \\ &= \sum_{i\in I} \sum_{k\in K} (C^{il})^T (C^{-1})^{ik} G^k \\ &\equiv \sum_{k\in K} (\tilde{C})^{lk} G^k \end{aligned} \tag{4.27}$$

which is the desired consistency relation between the amplitudes $\{G^k\}_{k\in K}$ and G^l.

Before applying this prescription to the various processes we like to remind the reader of the parameterizations for the various transition amplitudes

$$\begin{aligned} F^{\mu\,(N\to N)}_{V,\,\lambda'\lambda} &= \frac{1}{2\sqrt{P'^+P^+}} \bar{u}(P',\lambda') \Big[\gamma^\mu F_1(t) + \frac{i\sigma^{\mu\nu}\Delta_\nu}{2M_N} F_2(t) \Big] u(P,\lambda) \\ F^{\mu\,(N\to N)}_{A,\,\lambda'\lambda} &= \frac{1}{2\sqrt{P'^+P^+}} \bar{u}(P',\lambda') \Big[\gamma^\mu\gamma_5 G_A(t) + \frac{\Delta^\mu\gamma_5}{2M_N} G_P(t) + \frac{i\sigma^{\mu\nu}\Delta_\nu}{2M_N}\gamma_5 G_T(t) \Big] u(P,\lambda) \\ F^{\mu\,(p\to\Delta^+)}_{V,\,\lambda'\lambda} &= \frac{1}{\sqrt{6P'^+P^+}} \bar{u}_\nu(P',\lambda') \Big[\kappa_1^{\mu\nu} G_1(t) + \kappa_2^{\mu\nu} G_2(t) + \kappa_3^{\mu\nu} G_3(t) \Big] u(P,\lambda) \\ F^{\mu\,(p\to\Delta^+)}_{A,\,\lambda'\lambda} &= \frac{1}{2\sqrt{P'^+P^+}} \bar{u}_\nu(P',\lambda') \Big[\tilde{\kappa}_1^{\mu\nu} C_5(t) + \tilde{\kappa}_2^{\mu\nu} C_6(t) + \tilde{\kappa}_3^{\mu\nu} C_3(t) + \tilde{\kappa}_4^{\mu\nu} C_4(t) \Big] u(P,\lambda) \quad . \end{aligned}$$

For convenience we introduce the notation $\tilde{F}^\mu$ for the transition amplitudes with

$$\begin{aligned} \tilde{F}^+ &= F^+ \\ \tilde{F}^x &= 2\bar{P}^+ F^x \\ \tilde{F}^y &= 2\bar{P}^+ F^y \\ \tilde{F}^- &= (2\bar{P}^+)^2 F^- \quad . \end{aligned}$$

in order to suppress various factors $2\bar{P}^+$ in the following relations. From now on we will apply this convention for the DVCS amplitudes $\tilde{G}^\mu$ as well. Finally we can apply eq. 4.27 in order to gain amplitude relations.

For the vectorial $N \to N$ transition we choose to express all other amplitudes in terms of

$$\tilde{F}^{q,+\,(N\to N)}_{V,\uparrow\uparrow} \quad \text{and} \quad \tilde{F}^{q,+\,(N\to N)}_{V,\downarrow\uparrow} \quad .$$

The consistency relations then read

$$\begin{aligned}
\tilde{F}^{x}_{\downarrow,\uparrow} &= 0 \\
\tilde{F}^{x}_{\uparrow,\uparrow} &= 0 \\
\tilde{F}^{y}_{\downarrow,\uparrow} &= 0 \\
\tilde{F}^{y}_{\uparrow,\uparrow} &= i(2M_N\tilde{F}^{+}_{\downarrow,\uparrow} + \Delta_x\tilde{F}^{+}_{\uparrow,\uparrow}) \\
\tilde{F}^{-}_{\downarrow,\uparrow} &= (\Delta_x^2 - 4M_N^2)\tilde{F}^{+}_{\downarrow,\uparrow} - 4M_N\Delta_x\tilde{F}^{+}_{\uparrow,\uparrow} \\
\tilde{F}^{-}_{\uparrow,\uparrow} &= -4M_N\Delta_x\tilde{F}^{+}_{\downarrow,\uparrow} + (4M_N^2 - \Delta_x^2)\tilde{F}^{+}_{\uparrow,\uparrow} \quad .
\end{aligned} \tag{4.28}$$

The same can be done for the axial $N \to N$ transition. Here we choose to express the other amplitudes in terms of

$$\begin{aligned}
&\tilde{F}^{q,+\,(N\to N)}_{V,\uparrow\uparrow} \\
&\tilde{F}^{q,+\,(N\to N)}_{V,\downarrow\uparrow} \\
&\tilde{F}^{q,x\,(N\to N)}_{V,\downarrow\uparrow} \quad .
\end{aligned}$$

Then the consistency relations read

$$\begin{aligned}
\tilde{F}^{x}_{\uparrow\uparrow} &= 0 \\
\tilde{F}^{y}_{\uparrow,\uparrow} &= i\Delta_x\tilde{F}^{+}_{\uparrow,\uparrow} \\
\tilde{F}^{y}_{\downarrow,\uparrow} &= 2iM_N\tilde{F}^{+}_{\uparrow,\uparrow} \\
\tilde{F}^{-}_{\uparrow,\uparrow} &= -(\Delta_x^2 + 4M_N^2)\tilde{F}^{+}_{\uparrow,\uparrow} \\
\tilde{F}^{-}_{\downarrow,\uparrow} &= (\Delta_x^2 + 4M_N^2)\tilde{F}^{+}_{\downarrow,\uparrow} \quad .
\end{aligned} \tag{4.29}$$

Finally let us state that with the assumption of vanishing $G_T(Q^2)$ one can obtain as additional constraints

$$\begin{aligned}
\tilde{F}^{+}_{\downarrow,\uparrow} &= 0 \\
\tilde{F}^{-}_{\downarrow,\uparrow} &= 0 \quad .
\end{aligned}$$

This relation should be approximately fulfilled since as mentioned before $G_T(Q^2)$ is a second class form factor and hence suppressed.

In fact since quark masses for different flavors are assumed equal in quark models no quark model calculation is sensitive to $G_T(Q^2)$. Consequently we find numerically that $\tilde{F}^{-}_{\downarrow,\uparrow}$ vanishes.

As next process we consider the vectorial $N \to \Delta$ transition. Here we can express all other

amplitudes in terms of $\tilde{F}^+_{\frac{3}{2}\uparrow}$, $\tilde{F}^+_{\frac{1}{2}\uparrow}$ and $\tilde{F}^+_{\frac{1}{2}\downarrow}$. We find

$$\tilde{F}^+_{\frac{3}{2},\downarrow} = \frac{\Delta_x\Big[\big[\Delta_x^2 + M_N(M_N-M_\Delta)\big]\tilde{F}^+_{\frac{3}{2},\uparrow} + \sqrt{3}M_\Delta\big(\Delta_x\tilde{F}^+_{\frac{1}{2},\uparrow} + (M_\Delta - M_N)\tilde{F}^+_{\frac{1}{2},\downarrow}\big)\Big]}{\Delta_x^2 M_N + (M_\Delta - M_N)^2(M_\Delta + M_N)}$$

$$\tilde{F}^x_{\frac{3}{2},\uparrow} = \frac{M_\Delta^2 - M_N^2}{\Delta_x}\tilde{F}^+_{\frac{3}{2},\uparrow}$$

$$\tilde{F}^x_{\frac{1}{2},\uparrow} = \frac{M_\Delta^2 - M_N^2}{\Delta_x}\tilde{F}^+_{\frac{1}{2},\uparrow}$$

$$\tilde{F}^x_{\frac{1}{2},\downarrow} = \frac{M_\Delta^2 - M_N^2}{\Delta_x}\tilde{F}^+_{\frac{1}{2},\downarrow}$$

$$\begin{aligned}\tilde{F}^x_{\frac{3}{2},\downarrow} &= \frac{M_\Delta^2 - M_N^2}{\Delta_x}\tilde{F}^+_{\frac{3}{2},\downarrow}\\ &= \frac{(M_\Delta^2 - M_N^2)\Big[\big[\Delta_x^2 + M_N(M_N-M_\Delta)\big]\tilde{F}^+_{\frac{3}{2},\uparrow} + \sqrt{3}M_\Delta\big(\Delta_x\tilde{F}^+_{\frac{1}{2},\uparrow} + (M_\Delta - M_N)\tilde{F}^+_{\frac{1}{2},\downarrow}\big)\Big]}{\Delta_x^2 M_N + (M_\Delta - M_N)^2(M_\Delta + M_N)}\end{aligned}$$

$$\begin{aligned}\tilde{F}^y_{\frac{3}{2},\uparrow} &= -i\frac{\Big[(M_\Delta - M_N)^3(M_\Delta + M_N)^2 - \Delta_x^4 M_N\Big]\tilde{F}^+_{\frac{3}{2},\uparrow}}{\Delta_x\Big[\Delta_x^2 M_N + (M_\Delta - M_N)^2(M_\Delta + M_N)\Big]}\\ &\quad - i\frac{\Big[\Delta_x^2(M_\Delta - M_N)(-2M_\Delta^2 + M_\Delta M_N + 2M_N^2)\Big]\tilde{F}^+_{\frac{3}{2},\uparrow}}{\Delta_x\Big[\Delta_x^2 M_N + (M_\Delta - M_N)^2(M_\Delta + M_N)\Big]}\\ &\quad - i\frac{-\Big[\sqrt{3}M_\Delta(M_\Delta - M_N)^2(M_\Delta + M_N)\Big]\tilde{F}^+_{\frac{1}{2},\uparrow} + \Big[\sqrt{3}\Delta_x M_\Delta M_N(M_\Delta - M_N)\Big]\tilde{F}^+_{\frac{1}{2},\downarrow}}{\Delta_x^2 M_N + (M_\Delta - M_N)^2(M_\Delta + M_N)}\end{aligned}$$

$$\tilde{F}^y_{\frac{1}{2},\uparrow} = i\left[\sqrt{3}M_\Delta\tilde{F}^+_{\frac{3}{2},\uparrow} + \Delta_x\tilde{F}^+_{\frac{1}{2},\uparrow} + (2M_\Delta - M_N)\tilde{F}^+_{\frac{1}{2},\downarrow}\right]$$

$$\begin{aligned}\tilde{F}^y_{\frac{1}{2},\downarrow} &= i\frac{\Big[\sqrt{3}\Delta_x M_\Delta\big(\Delta_x^2 + M_N(M_N - M_\Delta)\big)\Big]\tilde{F}^+_{\frac{3}{2},\uparrow}}{\Delta_x^2 M_N + (M_\Delta - M_N)^2(M_\Delta + M_N)}\\ &\quad - i\left[M_N + M_\Delta\Big(2 - \frac{3\Delta_x^2 M_\Delta}{\Delta_x^2 M_N + (M_\Delta - M_N)^2(M_\Delta + M_N)}\Big)\right]\tilde{F}^+_{\frac{1}{2},\uparrow}\\ &\quad - i\frac{(M_\Delta - M_N)\left[(M_\Delta^2 - M_N^2)^2 + \Delta_x^2(M_N^2 + M_\Delta M_N - 3M_\Delta^2)\right]}{\Delta_x\Big[\Delta_x^2 M_N + (M_\Delta - M_N)^2(M_\Delta + M_N)\Big]}\tilde{F}^+_{\frac{1}{2},\downarrow}\end{aligned}$$

$$\begin{aligned}\tilde{F}^y_{\frac{3}{2},\downarrow} &= i\frac{\Big[(M_\Delta - M_N)^2(M_\Delta + M_N)M_N + \Delta_x^4 - \Delta_x^2(2M_\Delta^2 + M_\Delta M_N - 2M_N^2)\Big]\tilde{F}^+_{\frac{3}{2},\uparrow}}{\Delta_x^2 M_N + (M_\Delta - M_N)^2(M_\Delta + M_N)}\\ &\quad + i\frac{\sqrt{3}M_\Delta\left(\Delta_x(\Delta_x^2 - 2M_\Delta^2 + 2M_N^2)\tilde{F}^+_{\frac{1}{2},\uparrow} + \Big[\Delta_x^2 M_\Delta - (M_\Delta - M_N)^2(M_\Delta + M_N)\Big]\tilde{F}^+_{\frac{1}{2},\downarrow}\right)}{\Delta_x^2 M_N + (M_\Delta - M_N)^2(M_\Delta + M_N)}\end{aligned}$$

$$
\begin{aligned}
\tilde{F}^{-}_{\frac{3}{2},\uparrow} &= \left[4M_\Delta^2 - 2M_N^2 - \Delta_x^2\Big(1 + \frac{6M_\Delta^3}{\Delta_x^2 M_N + (M_\Delta - M_N)^2(M_\Delta + M_N)}\Big)\right]\tilde{F}^{+}_{\frac{3}{2},\uparrow} \\
&+ \frac{2\sqrt{3}M_\Delta}{\Delta_x}\left[M_\Delta^2 - M_N^2 + \frac{3\Delta_x^2 M_\Delta(M_N^2 - M_\Delta^2)}{\Delta_x^2 M_N + (M_\Delta - M_N)^2(M_\Delta + M_N)}\right]\tilde{F}^{+}_{\frac{1}{2},\uparrow} \\
&+ 2\sqrt{3}M_\Delta\left[M_\Delta\Big(\frac{3\Delta_x^2 M_N}{\Delta_x^2 M_N + (M_\Delta - M_N)^2(M_\Delta + M_N)} - 2\Big) - M_N\right]\tilde{F}^{+}_{\frac{1}{2},\downarrow} \\
\tilde{F}^{-}_{\frac{1}{2},\uparrow} &= \frac{2\sqrt{3}M_\Delta(M_\Delta^2 - M_N^2 - \Delta_x^2)\Big[\Delta_x^2(M_N - 2M_\Delta) + (M_\Delta - M_N)^2(M_\Delta + M_N)\Big]}{\Delta_x\Big[\Delta_x^2 M_N + (M_\Delta - M_N)^2(M_\Delta + M_N)\Big]}\tilde{F}^{+}_{\frac{3}{2},\uparrow} \\
&+ \Big[\frac{2(M_\Delta^2 - M_N^2)^2}{\Delta_x^2} - \Delta_x^2 - 12M_\Delta^2 - 8M_\Delta M_N + \frac{12\Delta_x^2 M_\Delta^2(M_\Delta + M_N)}{\Delta_x^2 M_N + (M_\Delta - M_N)^2(M_\Delta + M_N)}\Big]\tilde{F}^{+}_{\frac{1}{2},\uparrow} \\
&+ \Big[2\Delta_x(M_N - 2M_\Delta) - \frac{2(M_\Delta^2 - M_N^2)(2M_\Delta + M_N)}{\Delta_x}\Big]\tilde{F}^{+}_{\frac{1}{2},\downarrow} \\
&+ \frac{12\Delta_x M_\Delta^2(M_\Delta^2 - M_N^2)}{\Delta_x^2 M_N + (M_\Delta - M_N)^2(M_\Delta + M_N)}\tilde{F}^{+}_{\frac{1}{2},\downarrow}
\end{aligned}
$$

$$
\begin{aligned}
\tilde{F}^{-}_{\frac{1}{2},\downarrow} &= -\frac{2\sqrt{3}M_\Delta(\Delta_x^2 - M_\Delta^2 + M_N^2)(\Delta_x^2 - 2M_\Delta^2 + M_\Delta M_N + M_N^2)}{\Delta_x^2 M_N + (M_\Delta - M_N)^2(M_\Delta + M_N)}\tilde{F}^{+}_{\frac{3}{2},\uparrow} \\
&- 2(M_\Delta + M_N)(\Delta_x^2 - 2M_\Delta^2 + M_\Delta M_N + M_N^2) \\
&\cdot \frac{\big(\Delta_x^2(3M_\Delta - M_N) - (M_\Delta - M_N)^2(M_\Delta + M_N)\big)}{\Delta_x\Big[\Delta_x^2 M_N + (M_\Delta - M_N)^2(M_\Delta + M_N)\Big]}\tilde{F}^{+}_{\frac{1}{2},\uparrow} \\
&+ \Big[\Delta_x^2 + 6M_\Delta^2 + 8M_\Delta M_N - \frac{6\Delta_x^2 M_\Delta^2(M_\Delta + 2M_N)}{\Delta_x^2 M_N + (M_\Delta - M_N)^2(M_\Delta + M_N)}\Big]\tilde{F}^{+}_{\frac{1}{2},\downarrow} \\
\tilde{F}^{-}_{\frac{3}{2},\downarrow} &= \frac{\Delta_x\Big[\Delta_x^2(4M_\Delta - 3M_N)(M_\Delta + M_N) - \Delta_x^4\Big]}{\Delta_x^2 M_N + (M_\Delta - M_N)^2(M_\Delta + M_N)}\tilde{F}^{+}_{\frac{3}{2},\uparrow} \\
&- \frac{2\Delta_x(M_\Delta - M_N)\big(3M_\Delta^3 + 2M_\Delta^2 M_N - M_N^3\big)}{\Delta_x^2 M_N + (M_\Delta - M_N)^2(M_\Delta + M_N)}\tilde{F}^{+}_{\frac{3}{2},\uparrow} \\
&- \frac{\sqrt{3}M_\Delta\Big[\Delta_x^4 + 2(M_\Delta^2 - M_N^2)^2 - 4\Delta_x^2(M_\Delta^2 + M_\Delta M_N - M_N^2)\Big]}{\Delta_x^2 M_N + (M_\Delta - M_N)^2(M_\Delta + M_N)}\tilde{F}^{+}_{\frac{1}{2},\uparrow} \\
&- \frac{\sqrt{3}\Delta_x M_\Delta\Big[\Delta_x^2(M_\Delta + M_N) - 2M_\Delta(M_\Delta - M_N)(M_\Delta + 3M_N)\Big]}{\Delta_x^2 M_N + (M_\Delta - M_N)^2(M_\Delta + M_N)}\tilde{F}^{+}_{\frac{1}{2},\downarrow} \quad . \qquad (4.30)
\end{aligned}
$$

Of course the relation for $\tilde{F}^{+}_{\frac{3}{2},\downarrow}$ is the angular condition. The relations for $\tilde{F}^{x}_{\lambda',\lambda}$ can be understood as gauge invariance conditions which are (unlike for the nucleon nucleon transition) non trivial since $\Delta^- \neq 0$ for the $N \to \Delta$ transition.

For the axial $N \to \Delta$ transition we express all other amplitudes through $\tilde{F}^{+}_{\frac{3}{2},\uparrow}$, $\tilde{F}^{+}_{\frac{1}{2},\uparrow}$,$\tilde{F}^{+}_{\frac{1}{2},\downarrow}$

and $\tilde{F}^x_{\frac{3}{2},\uparrow}$. We find

$$
\begin{aligned}
\tilde{F}^+_{\frac{3}{2}\downarrow} =& \frac{\Delta_x\Big[\Delta_x^2 + M_N(M_\Delta + M_N)\Big]}{\Delta_x^2 M_N - (M_\Delta - M_N)(M_\Delta + M_N)^2}\tilde{F}^+_{\frac{3}{2}\uparrow} + \frac{\sqrt{3}\Delta_x^2 M_\Delta}{\Delta_x^2 M_N - (M_\Delta - M_N)(M_\Delta + M_N)^2}\tilde{F}^+_{\frac{1}{2}\uparrow} \\
& - \frac{\sqrt{3}\Delta_x M_\Delta(M_\Delta + M_N)}{\Delta_x^2 M_N - (M_\Delta - M_N)(M_\Delta + M_N)^2}\tilde{F}^+_{\frac{1}{2}\downarrow} \\
\tilde{F}^x_{\frac{1}{2}\uparrow} =& \frac{(M_\Delta - M_N)\Big[(2M_\Delta + M_N)\Delta_x^2 - (M_\Delta - M_N)(M_\Delta + M_N)^2\Big]}{\sqrt{3}\Delta_x^2 M_\Delta}\tilde{F}^+_{\frac{3}{2}\uparrow} + \frac{M_\Delta^2 - M_N^2}{\Delta_x}\tilde{F}^+_{\frac{1}{2}\uparrow} \\
& - \frac{\Big[(2M_\Delta + M_N)\Delta_x^2 - (M_\Delta - M_N)(M_\Delta + M_N)^2\Big]}{\sqrt{3}\Delta_x M_\Delta(M_\Delta + M_N)}\tilde{F}^x_{\frac{3}{2}\uparrow} \\
\tilde{F}^x_{\frac{1}{2}\downarrow} =& \frac{(M_\Delta - M_N)\Big[\Delta_x^2 - (M_\Delta + M_N)(2M_\Delta - M_N)\Big]}{\sqrt{3}\Delta_x M_\Delta}\tilde{F}^+_{\frac{3}{2}\uparrow} + \frac{M_\Delta^2 - M_N^2}{\Delta_x}\tilde{F}^+_{\frac{1}{2}\downarrow} \\
& - \frac{\Big[\Delta_x^2 - (M_\Delta + M_N)(2M_\Delta - M_N)\Big]}{\sqrt{3}M_\Delta(M_\Delta + M_N)}\tilde{F}^x_{\frac{3}{2}\uparrow} \\
\tilde{F}^x_{\frac{3}{2}\downarrow} =& -\frac{(M_\Delta - M_N)M_\Delta\Big[\Delta_x^2 + (M_\Delta + M_N)^2\Big]}{(M_\Delta - M_N)(M_\Delta + M_N)^2 - \Delta_x^2 M_N}\tilde{F}^+_{\frac{3}{2}\uparrow} + \frac{\sqrt{3}\Delta_x M_\Delta(M_\Delta^2 - M_N^2)}{\Delta_x^2 M_N - (M_\Delta - M_N)(M_\Delta + M_N)^2}\tilde{F}^+_{\frac{1}{2}\uparrow} \\
& - \frac{\sqrt{3}M_\Delta(M_\Delta^2 - M_N^2)(M_\Delta + M_N)}{\Delta_x^2 M_N - (M_\Delta - M_N)(M_\Delta + M_N)^2}\tilde{F}^+_{\frac{1}{2}\downarrow} + \frac{\Delta_x}{M_\Delta + M_N}\tilde{F}^x_{\frac{3}{2}\uparrow} \\
\tilde{F}^y_{\frac{3}{2}\uparrow} =& i\frac{\Big[\Delta_x^4 M_N + (M_\Delta - M_N)^2(M_\Delta + M_N)^3 - \Delta_x^2(M_\Delta + M_N)(2M_\Delta^2 + M_\Delta M_N - 2M_N^2)\Big]}{\Delta_x\Big[\Delta_x^2 M_N - (M_\Delta - M_N)(M_\Delta + M_N)^2\Big]}\tilde{F}^+_{\frac{3}{2}\uparrow} \\
& + i\frac{\sqrt{3}M_\Delta(M_\Delta - M_N)(M_\Delta + M_N)^2}{(M_\Delta - M_N)(M_\Delta + M_N)^2 - \Delta_x^2 M_N}\tilde{F}^+_{\frac{1}{2}\uparrow} - i\frac{\sqrt{3}M_\Delta M_N(M_\Delta + M_N)}{(M_\Delta - M_N)(M_\Delta + M_N)^2 - \Delta_x^2 M_N}\tilde{F}^+_{\frac{1}{2}\downarrow} \\
\tilde{F}^y_{\frac{1}{2}\uparrow} =& i\Big[\sqrt{3}M_\Delta\tilde{F}^+_{\frac{3}{2}\uparrow} + \Delta_x\tilde{F}^+_{\frac{1}{2}\uparrow} - (2M_\Delta + M_N)\tilde{F}^+_{\frac{1}{2}\downarrow}\Big] \\
\tilde{F}^y_{\frac{1}{2}\downarrow} =& \frac{i}{\Delta_x^2 M_N - (M_\Delta - M_N)(M_\Delta + M_N)^2}\Bigg[\Big(\sqrt{3}\Delta_x M_\Delta\Big[\Delta_x^2 + M_N(M_\Delta + M_N)\Big]\Big)\tilde{F}^+_{\frac{3}{2}\uparrow} \\
& + \Big((2M_\Delta - M_N)\Big[\Delta_x^2 M_N - (M_\Delta - M_N)(M_\Delta + M_N)^2\Big] + 3\Delta_x^2 M_\Delta\Big)\tilde{F}^+_{\frac{1}{2}\uparrow} \\
& + (M_\Delta + M_N)\Big[(M_\Delta^2 - M_N^2)^2 - (3M_\Delta^2 + M_\Delta M_N - M_N^2)\Delta_x^2\Big]\tilde{F}^+_{\frac{1}{2}\downarrow} \\
\tilde{F}^y_{\frac{3}{2}\downarrow} =& i\frac{\Delta_x^4 - (2M_\Delta^2 - M_\Delta M_N - 2M_N^2)\Delta_x^2 - (M_\Delta - M_N)(M_\Delta + M_N)^2 M_N}{\Delta_x^2 M_N - (M_\Delta - M_N)(M_\Delta + M_N)^2}\tilde{F}^+_{\frac{3}{2}\uparrow} \\
& + i\frac{\sqrt{3}\Delta_x M_\Delta(\Delta_x^2 - 2M_\Delta^2 + 2M_N^2)}{\Delta_x^2 M_N - (M_\Delta - M_N)(M_\Delta + M_N)^2}\tilde{F}^+_{\frac{1}{2}\uparrow} \\
& + i\frac{\sqrt{3}M_\Delta\Big[(M_\Delta - M_N)(M_\Delta + M_N)^2 - \Delta_x^2 M_\Delta)\Big]}{\Delta_x^2 M_N - (M_\Delta - M_N)(M_\Delta + M_N)^2}\tilde{F}^+_{\frac{1}{2}\uparrow}
\end{aligned}
$$

$$
\begin{aligned}
\tilde{F}^{-}_{\frac{3}{2}\uparrow} =& \left(4M_\Delta^2 - 2M_N^2 - \Delta_x^2 - \frac{2(M_\Delta^2 - M_N^2)^2}{\Delta_x^2} + \frac{6\Delta_x^2 M_\Delta^3}{\Delta_x^2 M_N - (M_\Delta^2 - M_N^2)(M_\Delta + M_N)}\right)\tilde{F}^{+}_{\frac{3}{2}\uparrow} \\
&+ \frac{2\sqrt{3}M_\Delta}{\Delta_x}\left(M_\Delta^2 - M_N^2 + \frac{3M_\Delta(M_\Delta^2 - M_N^2)\Delta_x^2}{M_N\Delta_x^2 - (M_\Delta^2 - M_N^2)(M_\Delta + M_N)}\right)\tilde{F}^{+}_{\frac{1}{2}\uparrow} \\
&+ 2\sqrt{3}M_\Delta\left((2M_\Delta - M_N) - \frac{3M_N M_\Delta \Delta_x^2}{M_N\Delta_x^2 - (M_\Delta^2 - M_N^2)(M_\Delta + M_N)}\right)\tilde{F}^{+}_{\frac{1}{2}\downarrow} \\
&+ \frac{2(M_\Delta^2 - M_N^2)}{\Delta_x}\tilde{F}^{x}_{\frac{3}{2}\uparrow} \\
\tilde{F}^{-}_{\frac{1}{2}\uparrow} =& \frac{2\Big[(2M_\Delta + M_N)\Delta_x^2 - (M_\Delta - M_N)(M_\Delta + M_N)^2\Big]}{\sqrt{3}\Delta_x^3 M_\Delta\Big[(M_\Delta - M_N)(M_\Delta + M_N)^2 - \Delta_x^2 M_N\Big]}\Big[(M_\Delta^2 - M_N^2)^3 + 3\Delta_x^4 M_\Delta^2 \\
&- (M_\Delta^2 - M_N^2)(3M_\Delta^2 + M_\Delta M_N - M_N^2)\Delta_x^2\Big]\tilde{F}^{+}_{\frac{3}{2}\uparrow} + \Big[8M_\Delta M_N - \frac{12M_\Delta^3}{M_N} - \Delta_x^2 \\
&+ \frac{2(M_\Delta^2 - M_N^2)^2}{\Delta_x^2} - \frac{12M_\Delta^2(M_\Delta^2 - M_N^2)^2}{M_N\Big[M_N\Delta_x^2 - (M_\Delta - M_N)(M_\Delta + M_N)^2\Big]}\Big]\tilde{F}^{+}_{\frac{1}{2}\uparrow} + \Big[2(2M_\Delta + M_N)\Delta_x \\
&+ \frac{2(M_\Delta^2 - M_N^2)(2M_\Delta - M_N)}{\Delta_x} + \frac{12M_\Delta^2\Delta_x(M_\Delta^2 - M_N^2)}{M_N\Delta_x^2 - (M_\Delta - M_N)(M_\Delta + M_N)^2}\tilde{F}^{+}_{\frac{1}{2}\downarrow} \\
&+ \frac{2\Big[(M_\Delta^2 - M_N^2)^2 - (2M_\Delta^2 - M_\Delta M_N - M_N^2)\Delta_x^2\Big]}{\sqrt{3}\Delta_x^2 M_\Delta}\tilde{F}^{x}_{\frac{3}{2}\uparrow} \\
\tilde{F}^{-}_{\frac{1}{2}\downarrow} =& \frac{2\Big[(M_\Delta + M_N)(2M_\Delta - M_N) - \Delta_x^2\Big]}{\sqrt{3}\Delta_x^2 M_\Delta\Big[\Delta_x^2 M_N - (M_\Delta - M_N)(M_\Delta + M_N)^2\Big]} \\
&\cdot\Big[(M_\Delta^2 - M_N^2)^3 - (M_\Delta^2 - M_N^2)(3M_\Delta^2 + M_\Delta M_N - M_N^2)\Delta_x^2 + 3M_\Delta^2\Delta_x^4\Big]\tilde{F}^{+}_{\frac{3}{2}\uparrow} \\
&- \frac{2(M_\Delta - M_N)\Big[\Delta_x^2 - (2M_\Delta - M_N)(M_\Delta + M_N)\Big]}{\Delta_x\Big[\Delta_x^2 M_N - (M_\Delta - M_N)(M_\Delta + M_N)^2\Big]} \\
&\cdot\Big[(M_\Delta + M_N)^2(M_N - M_\Delta) + (3M_\Delta + M_N)\Delta_x^2\Big]\tilde{F}^{+}_{\frac{1}{2}\uparrow} \\
&+ \Big[\Delta_x^2 + 6M_\Delta^2 - 8M_\Delta M_N + \frac{6M_\Delta^2(M_\Delta - 2M_N)\Delta_x^2}{\Delta_x^2 M_N - (M_\Delta - M_N)(M_\Delta + M_N)^2}\Big]\tilde{F}^{+}_{\frac{1}{2}\downarrow}\Bigg) \\
&- \frac{2(M_\Delta - M_N)\Big[\Delta_x^2 - (2M_\Delta - M_N)(M_\Delta + M_N)\Big]}{\sqrt{3}\Delta_x M_\Delta}\tilde{F}^{x}_{\frac{3}{2}\uparrow}
\end{aligned}
$$

$$\begin{aligned}\tilde{F}^{-}_{\frac{3}{2}\downarrow} =&2(M_\Delta - M_N)\tilde{F}^{x}_{\frac{3}{2}\uparrow} + \frac{1}{\Delta_x\Big[\Delta_x^2 M_N - (M_\Delta - M_N)(M_\Delta + M_N)^2\Big]}\Bigg(\Bigg[2(M_\Delta^2 - M_N^2)^3 \\ &-2(M_\Delta + M_N)^2(3M_\Delta^2 - 4M_\Delta M_N + 2M_N^2)\Delta_x^2 + (4M_\Delta^2 - M_\Delta M_N - 3M_N^2)\Delta_x^4 - \Delta_x^6\Bigg]\tilde{F}^{+}_{\frac{3}{2}\uparrow} \\ &- \sqrt{3}\Delta_x M_\Delta\Bigg[2(M_\Delta^2 - M_N^2)^2 - 4(M_\Delta^2 - M_\Delta M_N - M_N^2)\Delta_x^2 + \Delta_x^4\Bigg]\tilde{F}^{+}_{\frac{1}{2}\uparrow} \\ &+ \sqrt{3}\Delta_x^2 M_\Delta\Bigg[2M_\Delta(M_\Delta + M_N)(3M_N - M_\Delta) + (M_\Delta - M_N)\Delta_x^2\Bigg]\tilde{F}^{+}_{\frac{1}{2}\downarrow}\Bigg) \quad . \end{aligned} \tag{4.31}$$

Again one might call the relation among the good LF component transition amplitudes angular condition.

For the DVCS amplitudes we can also write down relations among the $G^+_{\lambda'\lambda}$ for the $p \to \Delta^+$ transition. For the vectorial transition we find

$$\begin{aligned}G^{+}_{\frac{3}{2}\downarrow} =&\frac{\Delta_x\Bigg[\Big(\Delta_x^2 - (1-\xi)M_N A\Big)G^{+}_{\frac{3}{2}\uparrow} + \sqrt{3}(1+\xi)M_\Delta\Delta_x G^{+}_{\frac{1}{2}\uparrow}\Bigg]}{M_N(1-\xi)\Big[\Delta_x^2 + M_N^2(1-\xi)^2\Big] - (1-\xi^2)M_\Delta M_N B + (1+\xi)^3 M_\Delta^3} \\ &+\frac{\sqrt{3}(1+\xi)M_\Delta\Delta_x A G^{+}_{\frac{1}{2}\downarrow}}{M_N(1-\xi)\Big[\Delta_x^2 + M_N^2(1-\xi)^2\Big] - (1-\xi^2)M_\Delta M_N B + (1+\xi)^3 M_\Delta^3}\end{aligned} \tag{4.32}$$

and for the axial transition we find

$$\begin{aligned}G^{+}_{\frac{3}{2}\downarrow} =&\frac{\Delta_x\Bigg[\Big(\Delta_x^2 + (1-\xi)M_N B\Big)G^{+}_{\frac{3}{2}\uparrow} + \sqrt{3}(1+\xi)M_\Delta\Delta_x G^{+}_{\frac{1}{2}\uparrow}\Bigg]}{(1-\xi)M_N\Big[\Delta_x^2 + (1-\xi)^2 M_N^2\Big] - (1-\xi^2)M_\Delta M_N A - (1+\xi)^3 M_\Delta^3} \\ &-\frac{\sqrt{3}(1+\xi)M_\Delta\Delta_x B G^{+}_{\frac{1}{2}\downarrow}}{(1-\xi)M_N\Big[\Delta_x^2 + (1-\xi)^2 M_N^2\Big] - (1-\xi^2)M_\Delta M_N A - (1+\xi)^3 M_\Delta^3}\end{aligned} \tag{4.33}$$

Again we have made use of the convenient shortcut notations in eqs. 4.9 and 4.15. Both relations have the same structure for $\xi = 0$ as the angular conditions for the respective amplitudes $F^+_{\lambda'\lambda}$.

4.5 Higher Twist GPDs

Higher twists are related to bad LF transition amplitudes. Having much freedom for the choice of covariant sets to parameterize these transition amplitudes we choose the covariants which are known from the twist 2 parametrization. Additionally we allow for another covariant, which is suppressed in leading twist due to either the analog to the gauge condition or the suppression of second class terms. Of course we would have the freedom to choose them at

leading twist as well but this is not favorable because of the relation to the form factors. So when we parameterize e.g. the vectorial $N \to N$ transition amplitude we choose to do so by:

$$\begin{aligned} G^{\perp}_{\lambda'\lambda} =& \frac{1}{2\bar{P}^+}\bar{u}(P',\lambda')\Big[\gamma^{\perp}\Big(H(x,\xi,t) + H_{(3)}(x,\xi,t)\Big) + \frac{i\sigma^{\perp\nu}\Delta_\nu}{2M_N}E(x,\xi,t) \\ &+ \frac{\Delta^{\perp}}{2M_N}X_{(3)}(x,\xi,t)\Big]u(P,\lambda) \\ G^{-}_{\lambda'\lambda} =& \frac{1}{2\bar{P}^+}\bar{u}(P',\lambda')\Big[\gamma^{-}\Big(H(x,\xi,t) + H_{(3)}(x,\xi,t) + H_{(4)}(x,\xi,t)\Big) \\ &+ \frac{i\sigma^{-\nu}\Delta_\nu}{2M_N}\Big(E(x,\xi,t) + E_{(4)}(x,\xi,t)\Big) + \frac{\Delta^{-}}{2M_N}X_{(3)}(x,\xi,t)\Big]u(P,\lambda) \quad . \end{aligned}$$

Then we call $H_{(3)}$ and $X_{(3)}$ the genuine twist 3 GPDs and $H_{(4)}$ and $E_{(4)}$ the genuine twist 4 GPDs. There is no choice about whether the covariant $\frac{\Delta^\mu}{2M_N}$ contributes at twist 3 or at twist 4 level. The reason is that one can express $\kappa_1^{\perp} = \kappa_2^{\perp}$ while $\kappa_3^{\perp}$ is independent.

For the sum rules we have

$$\begin{aligned} \int_{-1}^{1} dx\, H(x,\xi,t) &= F_1(t) \\ \int_{-1}^{1} dx\, E(x,\xi,t) &= F_2(t) \\ \int_{-1}^{1} dx\, H_{(3)}(x,\xi,t) &= 0 \\ \int_{-1}^{1} dx\, X_{(3)}(x,\xi,t) &= 0 \\ \int_{-1}^{1} dx\, H_{(4)}(x,\xi,t) &= 0 \\ \int_{-1}^{1} dx\, E_{(4)}(x,\xi,t) &= 0 \quad . \end{aligned} \tag{4.34}$$

We should mention that there exist only 2 twist 3 GPDs, although the number of corresponding transition amplitudes might suggest 4 at first glance. The transition amplitudes $G^x_{\lambda'\lambda}$ in a given reference frame can be related to the $G^y_{\lambda'\lambda}$ in another reference frame. Since the GPDs by which the transition amplitudes are parameterized are frame independent they must be the same objects. So the same twist 3 GPDs which parameterize $G^x_{\lambda'\lambda}$ do the same job for the $G^y_{\lambda'\lambda}$. And with the four vectors in the game one cannot build other independent covariants.

Of course this argument relies on the LF rotation $L_f(\omega_z)$ being a kinematical Lorentz transformation. This explains why the same argument cannot be used to relate e.g. $G^+_{\lambda'\lambda}$ and $G^x_{\lambda'\lambda}$. With the same kinematics as in the previous section these amplitude relations read

$$\begin{aligned} G^y_{\uparrow\uparrow} &= i\frac{\Delta_x}{\xi(\Delta_x^2 + 4M_N^2)}\Big(2M_N G^x_{\downarrow\uparrow} + \Delta_x G^x_{\uparrow\uparrow}\Big) \\ G^y_{\downarrow\uparrow} &= i\frac{2M_N}{\Delta_x^2 + 4M_N^2}\Big(2M_N G^x_{\downarrow\uparrow} + \Delta_x G^x_{\uparrow\uparrow}\Big) \quad . \end{aligned} \tag{4.35}$$

We like to remark that these relations are derived without assuming a certain number of twist 3 GPDs. Hence this example illustrates the argument above.

The behavior of these amplitude relations for small values of ξ is obviously in agreement with the amplitude relations for the form factor related amplitudes. Finally let us provide the expressions for the different twist GPDs in terms of transition amplitudes

$$
\begin{aligned}
H(x,\xi,t) =& \frac{1}{1-\xi^2}\tilde{G}^{+}_{\uparrow\uparrow} + \frac{2\xi^2 M_N}{\sqrt{1-\xi^2}\Delta_x}\tilde{G}^{+}_{\downarrow\uparrow} \\
E(x,\xi,t) =& \frac{2\sqrt{1-\xi^2}M_N}{\Delta_x}\tilde{G}^{+}_{\downarrow\uparrow} \\
X_{(3)}(x,\xi,t) =& \frac{4\sqrt{1-\xi^2}M_N^2\tilde{G}^{x}_{\uparrow\uparrow} - 2\sqrt{1-\xi^2}M_N\Delta_x\tilde{G}^{x}_{\downarrow\uparrow}}{\Delta_x(4M_N^2+\Delta_x^2)} \\
H_{(3)}(x,\xi,t) =& -\frac{1}{\sqrt{1-\xi^2}}\tilde{G}^{+}_{\uparrow\uparrow} - \frac{2M_N\tilde{G}^{+}_{\downarrow\uparrow}}{\sqrt{1-\xi^2}\Delta_x} + \frac{\sqrt{1-\xi^2}}{\xi(4M_N^2+\Delta_x^2)}\Big(2M_N\tilde{G}^{x}_{\downarrow\uparrow} + \Delta_x\tilde{G}^{x}_{\uparrow\uparrow}\Big) \\
H_{(4)}(x,\xi,t) =& \frac{2\sqrt{1-\xi^2}M_N}{\Delta_x}\tilde{G}^{+}_{\downarrow\uparrow} - \frac{\sqrt{1-\xi^2}\big[\Delta_x^2+4\xi^2M_N^2\big]}{\xi\Delta_x(4M_N^2+\Delta_x^2)}\tilde{G}^{x}_{\uparrow\uparrow} - \frac{2\sqrt{1-\xi^2}M_N}{\xi(4M_N^2+\Delta_x^2)}\tilde{G}^{x}_{\downarrow\uparrow} \\
&+ \frac{8(1-\xi^2)^{\frac{3}{2}}M_N^2}{(4M_N^2+\Delta_x^2)^2}\tilde{G}^{-}_{\uparrow\uparrow} + \frac{2(1-\xi^2)^{\frac{3}{2}}M_N(4M_N^2-\Delta_x^2)}{\Delta_x(4M_N^2+\Delta_x^2)^2}\tilde{G}^{-}_{\downarrow\uparrow} \\
E_{(4)}(x,\xi,t) =& -\frac{2\sqrt{1-\xi^2}M_N}{\Delta_x}\tilde{G}^{+}_{\downarrow\uparrow} + \frac{4\xi\sqrt{1-\xi^2}M_N^2}{\Delta_x(4M_N^2+\Delta_x^2)}\tilde{G}^{x}_{\uparrow\uparrow} - \frac{2\xi\sqrt{1-\xi^2}M_N}{4M_N^2+\Delta_x^2}\tilde{G}^{x}_{\downarrow\uparrow} \\
&- \frac{\sqrt{1-\xi^2}\big[\Delta_x^2+4(3-2\xi^2)M_N^2\big]}{(4M_N^2+\Delta_x^2)^2}\tilde{G}^{-}_{\uparrow\uparrow} \\
&- \frac{2\sqrt{1-\xi^2}M_N\big[4(2-\xi^2)M_N^2+\xi^2\Delta_x^2\big]}{\Delta_x(4M_N^2+\Delta_x^2)^2}\tilde{G}^{-}_{\downarrow\uparrow}.
\end{aligned}
\tag{4.36}
$$

For the axial $N \to N$ transition we find

$$
\begin{aligned}
G^{\perp}_{\lambda'\lambda} =& \frac{1}{2\bar{P}^+}\bar{u}(P',\lambda')\Big[\gamma^{\perp}\gamma_5\Big(\tilde{H}(x,\xi,t)+\tilde{H}_{(3)}(x,\xi,t)\Big) \\
&+ \frac{\Delta^{\perp}}{2M_N}\gamma_5\Big(\tilde{E}(x,\xi,t)+\tilde{E}_{(3)}(x,\xi,t)\Big)\Big]u(P,\lambda) \\
G^{-}_{\lambda'\lambda} =& \frac{1}{2\bar{P}^+}\bar{u}(P',\lambda')\Big[\gamma^{-}\gamma_5\Big(\tilde{H}(x,\xi,t)+\tilde{H}_{(3)}(x,\xi,t)+\tilde{H}_{(4)}(x,\xi,t)\Big) \\
&+ \frac{\Delta^{-}}{2M_N}\gamma_5\Big(\tilde{E}(x,\xi,t)+\tilde{E}_{(3)}(x,\xi,t)\Big) + \frac{i\sigma^{-\nu}\Delta_\nu}{2M_N}\gamma_5\Big(\tilde{X}_{(4)}(x,\xi,t)\Big)\Big]u(P,\lambda) \quad .
\end{aligned}
$$

Again there is no choice whether $\tilde{\kappa}^{\mu}_3$ contributes at twist 3 or twist 4 level. Here one finds $\tilde{\kappa}^{\perp}_3 = 0$ and hence it cannot contribute at twist 3 level. We have the sum rules

$$
\begin{aligned}
\int_{-1}^{1} dx\, \tilde{H}(x,\xi,t) &= G_A(t) \\
\int_{-1}^{1} dx\, \tilde{E}(x,\xi,t) &= G_P(t) + \frac{1}{\xi}G_T(t)
\end{aligned}
$$

$$\begin{aligned}
&\int_{-1}^{1} dx\, \tilde{H}_{(3)}(x,\xi,t) = 0 \\
&\int_{-1}^{1} dx\, \tilde{E}_{(3)}(x,\xi,t) = -\frac{1}{\xi} G_T(t) \\
&\int_{-1}^{1} dx\, \tilde{H}_{(4)}(x,\xi,t) = 0 \\
&\int_{-1}^{1} dx\, \tilde{X}_{(4)}(x,\xi,t) = G_T(t) \quad .
\end{aligned} \tag{4.37}$$

The argument for only 2 independent GPDs at twist 3 is the same as for the vector transition. In the given kinematics the respective amplitude relations read

$$\begin{aligned}
G^{y}_{A,\uparrow\uparrow} &= i\frac{\Delta_x}{\xi(\Delta_x^2 + 4M_N^2)}\Big(2\xi M_N G^{x}_{A,\downarrow\uparrow} + \Delta_x G^{x}_{A,\uparrow\uparrow}\Big) \\
G^{y}_{A,\downarrow\uparrow} &= i\frac{2M_N}{\xi(\Delta_x^2 + 4M_N^2)}\Big(2\xi M_N G^{x}_{A,\downarrow\uparrow} + \Delta_x G^{x}_{A,\uparrow\uparrow}\Big) \quad .
\end{aligned} \tag{4.38}$$

Again the behavior for small values of ξ agrees with the respective amplitude relations for the form factor related amplitudes. Next let us provide the expressions for the different twist GPDs in terms of transition amplitudes

$$\begin{aligned}
\tilde{H}(x,\xi,t) =& \frac{1}{\sqrt{1-\xi^2}}\tilde{G}^{+}_{\uparrow\uparrow} + \frac{2\xi M_N}{\sqrt{1-\xi^2}\Delta_x}\tilde{G}^{+}_{\downarrow\uparrow} \\
\tilde{E}(x,\xi,t) =& \frac{2\sqrt{1-\xi^2}M_N}{\xi\Delta_x}\tilde{G}^{+}_{\downarrow\uparrow} \\
\tilde{H}_{(3)}(x,\xi,t) =& -\frac{1}{\sqrt{1-\xi^2}}\tilde{G}^{+}_{\uparrow\uparrow} - \frac{2\xi M_N}{\sqrt{1-\xi^2}\Delta_x}\tilde{G}^{+}_{\downarrow\uparrow} + \frac{\sqrt{1-\xi^2}\Delta_x}{\xi(4M_N^2+\Delta_x^2)}\tilde{G}^{x}_{\uparrow\uparrow} + \frac{2\sqrt{1-\xi^2}M_N}{4M_N^2+\Delta_x^2}\tilde{G}^{x}_{\downarrow\uparrow} \\
\tilde{E}_{(3)}(x,\xi,t) =& -\frac{2\sqrt{1-\xi^2}M_N}{\xi\Delta_x}\tilde{G}^{+}_{\downarrow\uparrow} + \frac{4\sqrt{1-\xi^2}M_N^2}{\xi\Delta_x(4M_N^2+\Delta_x^2)}\tilde{G}^{x}_{\uparrow\uparrow} - \frac{2\sqrt{1-\xi^2}M_N}{4M_N^2+\Delta_x^2}\tilde{G}^{x}_{\downarrow\uparrow} \\
\tilde{H}_{(4)}(x,\xi,t) =& -\frac{\sqrt{1-\xi^2}\Delta_x}{\xi(4M_N^2+\Delta_x^2)}\tilde{G}^{x}_{\uparrow\uparrow} - \frac{2\sqrt{1-\xi^2}M_N}{4M_N^2+\Delta_x^2}\tilde{G}^{x}_{\downarrow\uparrow} \\
&- \frac{\sqrt{1-\xi^2}}{4M_N^2+\Delta_x^2}\tilde{G}^{-}_{\uparrow\uparrow} - \frac{2\sqrt{1-\xi^2}\xi M_N}{\Delta_x(4M_N^2+\Delta_x^2)}\tilde{G}^{-}_{\downarrow\uparrow} \\
\tilde{X}_{(4)}(x,\xi,t) =& \frac{4\sqrt{1-\xi^2}M_N^2}{\Delta_x(4M_N^2+\Delta_x^2)}\tilde{G}^{x}_{\uparrow\uparrow} - \frac{2\xi\sqrt{1-\xi^2}M_N}{4M_N^2+\Delta_x^2}\tilde{G}^{x}_{\downarrow\uparrow} + \frac{2(1-\xi^2)^{\frac{3}{2}}M_N}{\Delta_x(4M_N^2+\Delta_x^2)}\tilde{G}^{-}_{\downarrow\uparrow} \quad .
\end{aligned} \tag{4.39}$$

For the $N \to \Delta$ transition we can parameterize the bad amplitudes as follows:

$$\begin{aligned}
G^{+\,(p\to\Delta^+)}_{V,\lambda'\lambda} =& \frac{1}{2\sqrt{6}\bar{P}^+}\bar{u}_\nu(P',\lambda')\Big[\kappa_1^{+\nu}H_1(x,\xi,t) + \kappa_2^{+\nu}H_2(x,\xi,t) + \kappa_3^{+\nu}H_3(x,\xi,t)\Big]u(P,\lambda) \\
G^{\perp\,(p\to\Delta^+)}_{V,\lambda'\lambda} =& \frac{1}{2\sqrt{6}\bar{P}^+}\bar{u}_\nu(P',\lambda')\Big[\kappa_1^{\perp\nu}\Big(H_1(x,\xi,t) + H_1^{(3)}(x,\xi,t)\Big) + \kappa_2^{\perp\nu}\Big(H_2(x,\xi,t) \\
&+ H_2^{(3)}(x,\xi,t)\Big) + \kappa_3^{\perp\nu}\Big(H_3(x,\xi,t) + H_3^{(2)}(x,\xi,t)\Big)\Big]u(P,\lambda) \\
G^{-\,(p\to\Delta^+)}_{V,\lambda'\lambda} =& \frac{1}{2\sqrt{6}\bar{P}^+}\bar{u}_\nu(P',\lambda')\Big[\kappa_1^{-\nu}\Big(H_1(x,\xi,t) + H_1^{(3)}(x,\xi,t) + H_1^{(4)}(x,\xi,t)\Big)
\end{aligned}$$

$$+\kappa_2^{-\nu}\Big(H_2(x,\xi,t)+H_2^{(3)}(x,\xi,t)+H_2^{(4)}(x,\xi,t)\Big)$$
$$+\kappa_3^{-\nu}\Big(H_3(x,\xi,t)+H_3^{(3)}(x,\xi,t)+H_3^{(4)}(x,\xi,t)\Big)\Big]u(P,\lambda) \quad .$$

One may wonder why we do not use the fourth independent covariant $\kappa_4^{\mu\nu}$ in order to parameterize at least a higher twist amplitude with. Actually this is just a matter of taste. Of course one could choose to parameterize e.g.

$$G_{V,\,\lambda'\lambda}^{\perp\,(p\to\Delta^+)} = \frac{1}{2\sqrt{6}\bar{P}^+}\bar{u}_\nu(P',\lambda')\Big[\kappa_1^{\perp\nu}\Big(H_1(x,\xi,t)+H_1^{(3)}(x,\xi,t)\Big)+\kappa_2^{\perp\nu}\Big(H_2(x,\xi,t)$$
$$+H_2^{(3)}(x,\xi,t)\Big)+\kappa_3^{\perp\nu}H_3(x,\xi,t)+\kappa_4^{\perp\nu}H_4^{(4)}(x,\xi,t)\Big]u(P,\lambda) \quad .$$

But then there is nothing gained by doing so. The covariant $\kappa_4^{\mu\nu}$ bears no physical intuition. There is no fourth form factor to which it could be related (due to current conservation). Thus we choose not to use it. The arising sum rules for the genuine higher twist vectorial $N\to\Delta$ GPDs are trivial:

$$\begin{aligned}
\int_{-1}^{1} dx\, H_1(x,\xi,t) &= 2\,G_1(t)\\
\int_{-1}^{1} dx\, H_2(x,\xi,t) &= 2\,G_2(t)\\
\int_{-1}^{1} dx\, H_3(x,\xi,t) &= 2\,G_3(t)\\
\int_{-1}^{1} dx\, H_1^{(3)}(x,\xi,t) &= 0\\
\int_{-1}^{1} dx\, H_2^{(3)}(x,\xi,t) &= 0\\
\int_{-1}^{1} dx\, H_3^{(3)}(x,\xi,t) &= 0\\
\int_{-1}^{1} dx\, H_1^{(4)}(x,\xi,t) &= 0\\
\int_{-1}^{1} dx\, H_2^{(4)}(x,\xi,t) &= 0\\
\int_{-1}^{1} dx\, H_3^{(4)}(x,\xi,t) &= 0 \quad .
\end{aligned} \tag{4.40}$$

From the perpendicular transition amplitudes we obtain expressions for the sum of twist 2 and twist 3 GPDs. Combining these results with the expressions for the twist 2 GPDs (eq. 4.10) we find the formulae for the genuine twist 3 GPDs in terms of transition amplitudes. For example we find (using prescription II)

$$H_1^{(3)}(x,\xi,t) = 2\sqrt{\frac{3(1-\xi)}{1+\xi}}\Bigg(-\frac{1}{\Delta_x}\tilde{G}^+_{\frac{3}{2}\uparrow}-\frac{(1+\xi)M_\Delta-(1-\xi)M_N}{\Delta_x^2}\tilde{G}^+_{\frac{3}{2}\downarrow}$$
$$+\frac{1-\xi^2}{(1+\xi)^2M_\Delta^2-(1-\xi)^2M_N^2+\xi^2\Delta_x^2}\Big[\tilde{G}^x_{\frac{3}{2}\uparrow}+\frac{(1+\xi)M_\Delta-(1-\xi)M_N}{\Delta_x}\tilde{G}^x_{\frac{3}{2}\downarrow}\Big]\Bigg) \quad . \tag{4.41}$$

We will not provide the results for $H_2^{(3)}(x,\xi,t)$, $H_3^{(3)}(x,\xi,t)$, $H_1^{(4)}(x,\xi,t)$, $H_2^{(4)}(x,\xi,t)$ and $H_3^{(4)}(x,\xi,t)$ here for lack of space[10].

The angular conditions for the x and $-$ component[11] transition amplitudes read

$$\begin{aligned}
\tilde{G}^x_{\frac{3}{2}\downarrow} =& \frac{\Delta_x\Big(\Delta_x^2\tilde{G}^x_{\frac{3}{2}\uparrow} + \sqrt{3}(1+\xi)\Delta_x M_\Delta \tilde{G}^x_{\frac{1}{2}\uparrow} + A\big[\sqrt{3}(1+\xi)M_\Delta\tilde{G}^x_{\frac{1}{2}\downarrow} - (1-\xi)M_N\tilde{G}^x_{\frac{3}{2}\uparrow}\big]\Big)}{(1-\xi)\big[(1-\xi)^2M_N^2+\Delta_x^2\big]M_N - (1-\xi^2)M_N M_\Delta B + (1+\xi)^3M_\Delta^3} \quad . \\
\tilde{G}^-_{\frac{3}{2}\downarrow} =& \frac{\Delta_x\Big(\sqrt{3}\big[\Delta_x^2 - (1-\xi)M_N A\big]\tilde{G}^-_{\frac{3}{2}\uparrow} + 3(1+\xi)M_\Delta\big[\Delta_x\tilde{G}^-_{\frac{1}{2}\uparrow} + \xi A\tilde{G}^-_{\frac{1}{2}\downarrow}\big]\Big)}{(1-\xi)\big[(1-\xi)^2M_N^2+\Delta_x^2\big]M_N - (1-\xi^2)M_N M_\Delta B + (1+\xi)^3M_\Delta^3} \quad . \qquad (4.42)
\end{aligned}$$

Once more we have used eqs. 4.9 and 4.15. Finally the kinematical Lorentz rotation $L_f(\omega_z)$ provides further amplitude relations of the type

$$\tilde{G}^y_{\lambda'\lambda} = a\,\tilde{G}^x_{\frac{3}{2}\uparrow} + b\,\tilde{G}^x_{\frac{1}{2}\uparrow} + c\,\tilde{G}^x_{\frac{1}{2}\downarrow} \quad .$$

As an example we mention

$$\tilde{G}^y_{\frac{1}{2}\uparrow} = i\frac{\Delta_x\Big(\sqrt{3}(1+\xi)M_\Delta\tilde{G}^x_{\frac{3}{2}\uparrow} + \Delta_x\tilde{G}^x_{\frac{1}{2}\uparrow} + \big[2(1+\xi)M_\Delta - (1-\xi)M_N\big]\tilde{G}^x_{\frac{1}{2}\downarrow}\Big)}{(1+\xi)^2M_\Delta^2 + (1-\xi)^2M_N^2 + \xi\Delta_x^2} \quad . \qquad (4.43)$$

Again the situation changes when we consider the axial $N \to \Delta$ GPDs. Here exist four form factors and we like to reflect this fact in the parametrization of the DVCS amplitudes. Here they are:

$$\begin{aligned}
G^{+\,(p\to\Delta^+)}_{A,\,\lambda'\lambda} =& \frac{1}{4\bar{P}^+}\bar{u}_\nu(P',\lambda')\Big[\tilde{\kappa}_1^{+\nu}C_1(x,\xi,t) + \tilde{\kappa}_3^{+\nu}C_3(x,\xi,t) + \tilde{\kappa}_4^{+\nu}C_4(x,\xi,t)\Big]u(P,\lambda) \\
G^{\perp\,(p\to\Delta^+)}_{A,\,\lambda'\lambda} =& \frac{1}{4\bar{P}^+}\bar{u}_\nu(P',\lambda')\Big[\tilde{\kappa}_1^{\perp\nu}\Big(C_1(x,\xi,t) + C_1^{(3)}(x,\xi,t)\Big) + \tilde{\kappa}_2^{\perp\nu}C_2^{(3)}(x,\xi,t) \\
&+\tilde{\kappa}_3^{\perp\nu}\Big(C_3(x,\xi,t) + C_3^{(3)}(x,\xi,t)\Big) + \tilde{\kappa}_4^{\perp\nu}C_4(x,\xi,t)\Big]u(P,\lambda) \\
G^{-\,(p\to\Delta^+)}_{A,\,\lambda'\lambda} =& \frac{1}{4\bar{P}^+}\bar{u}_\nu(P',\lambda')\Big[\tilde{\kappa}_1^{-\nu}\Big(C_1(x,\xi,t) + C_1^{(3)}(x,\xi,t) + C_1^{(4)}(x,\xi,t)\Big) \\
&+ \tilde{\kappa}_2^{-\nu}C_2^{(3)}(x,\xi,t) + \tilde{\kappa}_3^{-\nu}\Big(C_3(x,\xi,t) + C_3^{(3)}(x,\xi,t) + C_3^{(4)}(x,\xi,t)\Big) \\
&+ \tilde{\kappa}_4^{-\nu}\Big(C_4(x,\xi,t) + C_4^{(4)}(x,\xi,t)\Big)\Big]u(P,\lambda) \quad .
\end{aligned}$$

Again we have no choice whether the covariant $\kappa_4^{\mu\nu}$ contributes at twist 3 or not. The argument is the same as for the vectorial $N \to \Delta$ transition.

[10] Actually we have chosen $H_1^{(3)}(x,\xi,t)$ given in prescription II as example since this result is comparatively concise. Generally the expressions tend to be rather lengthy.

[11] The y component is too lengthy to be written down here.

The sum rules for the axial higher twist GPDs read

$$\int_{-1}^{1} dx\, C_1(x,\xi,t) = 2\Big(C_5(t) - \frac{\xi(M_\Delta^2 - M_N^2)}{M_N^2} C_6(t)\Big) \tag{4.44}$$

$$\int_{-1}^{1} dx\, C_3(x,\xi,t) = 2\, C_3(t) \tag{4.45}$$

$$\int_{-1}^{1} dx\, C_4(x,\xi,t) = 2\Big(C_4(t) + \xi C_6(t)\Big) \tag{4.46}$$

$$\int_{-1}^{1} dx\, C_1^{(3)}(x,\xi,t) = 0$$

$$\int_{-1}^{1} dx\, C_2^{(3)}(x,\xi,t) = 2C_6(t) \tag{4.47}$$

$$\int_{-1}^{1} dx\, C_3^{(3)}(x,\xi,t) = 0$$

$$\int_{-1}^{1} dx\, C_1^{(4)}(x,\xi,t) = 2\Big(\frac{\xi(M_\Delta^2 - M_N^2)}{M_N^2} C_6(t)\Big)$$

$$\int_{-1}^{1} dx\, C_3^{(4)}(x,\xi,t) = 0$$

$$\int_{-1}^{1} dx\, C_4^{(4)}(x,\xi,t) = -2\xi C_6(t) \quad .$$

One remark is in order here. The genuine higher twist GPD $C_2^{(3)}(x,\xi,t)$ can not be considered negligible if $C_6(t)$ is finite.

The parametrization for the perpendicular transition amplitudes allows us to express the genuine twist 3 GPDs in terms of good and perpendicular transition amplitudes just as in the case of the vectorial $N \to \Delta$ transition. In order to access the axial genuine twist 4 GPDs from +, x and - transition amplitudes we have to make additional use of the relation

$$\tilde{\kappa}_4^{-\nu} = \frac{M_\Delta^2 - M_N^2}{M_N^2} \tilde{\kappa}_1^{-\nu} - \frac{1}{\xi} \tilde{\kappa}_2^{-\nu} \quad .$$

As an example we provide the result for $C_2^{(3)}(x,\xi,t)$:

$$\begin{aligned} C_2^{(3)}(x,\xi,t) =& \frac{2\sqrt{2(1-\xi^2)}(1-\xi)M_N^2 \left(\Delta_x \tilde{G}^x_{\frac{3}{2}\uparrow} + \sqrt{3}(1+\xi)M_\Delta \tilde{G}^x_{\frac{1}{2}\uparrow}\right)}{\Delta_x\big[(1+\xi)M_\Delta + (1-\xi)M_N\big]\Big[(1+\xi)^2 M_\Delta^2 - (1-\xi)^2 M_N^2 + \xi\Delta_x^2\Big]} \\ &+ \frac{2\sqrt{2(1-\xi^2)}(1-\xi)M_N^2\big[(1+\xi)^2 M_\Delta + \xi(1-\xi)M_N\big]\tilde{G}^x_{\frac{3}{2}\downarrow}}{\Delta_x\big[(1+\xi)M_\Delta + (1-\xi)M_N\big]\Big[(1+\xi)^2 M_\Delta^2 - (1-\xi)^2 M_N^2 + \xi\Delta_x^2\Big]} \quad . \end{aligned} \tag{4.48}$$

The angular conditions for the x and - component amplitudes read

$$\tilde{G}^{x}_{\frac{3}{2}\downarrow} = \frac{\Delta_x\Big(\Delta_x^2\tilde{G}^{x}_{\frac{3}{2}\uparrow} + \sqrt{3}(1+\xi)M_\Delta\Delta_x\tilde{G}^{x}_{\frac{1}{2}\uparrow} + B\big[(1-\xi)M_N\tilde{G}^{x}_{\frac{3}{2}\uparrow} - \sqrt{3}(1+\xi)M_\Delta\tilde{G}^{x}_{\frac{1}{2}\downarrow}\big]\Big)}{(1-\xi)M_N\big[(1-\xi)^2M_N^2+\Delta_x^2\big] - (1-\xi^2)M_NM_\Delta A - (1+\xi)^3M_\Delta^3}$$

$$\tilde{G}^{-}_{\frac{3}{2}\downarrow} = \frac{\Delta_x\Big(\big[\Delta_x^2 + (1-\xi)M_N\big]B\tilde{G}^{-}_{\frac{3}{2}\uparrow} + \sqrt{3}(1+\xi)M_\Delta\big[\Delta_x\tilde{G}^{-}_{\frac{1}{2}\uparrow} - B\tilde{G}^{-}_{\frac{1}{2}\downarrow}\big]\Big)}{(1-\xi)M_N\big[(1-\xi)^2M_N^2+\Delta_x^2\big] - (1-\xi^2)M_NM_\Delta A - (1+\xi)^3M_\Delta^3} \quad . \tag{4.49}$$

Finally as an example for an amplitude relation of the type

$$\tilde{G}^{y}_{\lambda'\lambda} = a\,\tilde{G}^{x}_{\frac{3}{2}\uparrow} + b\,\tilde{G}^{x}_{\frac{1}{2}\uparrow} + c\,\tilde{G}^{x}_{\frac{1}{2}\downarrow}$$

we give

$$\tilde{G}^{y}_{\frac{1}{2}\uparrow} = i\frac{\Delta_x\Big(\Delta_x\tilde{G}^{x}_{\frac{1}{2}\uparrow} + \sqrt{3}(1+\xi)M_\Delta\tilde{G}^{x}_{\frac{3}{2}\uparrow} - \big[(1-\xi)M_N + 2(1+\xi)M_\Delta\big]\tilde{G}^{x}_{\frac{1}{2}\downarrow}}{(1+\xi)^2M_\Delta^2 - (1-\xi)^2M_N^2 + \xi\Delta_x^2} \quad . \tag{4.50}$$

4.6 "Mixed Twist GPDs"

In this section we try to establish a link between the treatment of form factors and GPDs concerning non "+" transition amplitudes. This will turn out to be useful in order to apply the spurious covariants formalism which will be explored for form factors in the following chapter. Under mixed twists we understand an approximation in which we assume that some "mixed twist GPDs" can be accessed from any set of DVCS transition amplitudes, independently of the Lorentz component μ. This means we simply parameterize DVCS amplitudes by the maximal set of independent covariants, i.e.

$$G^{q,\,\mu\,(N\to N)}_{V,\,\lambda'\lambda} = \frac{1}{2\bar{P}^+}\bar{u}(P',\lambda')\Big[\gamma^\mu H^q_{(*)}(x,\xi,t) + \frac{i\sigma^{\mu\nu}\Delta_\nu}{2M_N}E^q_{(*)}(x,\xi,t) + \frac{\Delta^\mu}{2M_N}X^q_{(*)}(x,\xi,t)\Big]u(P,\lambda) \tag{4.51}$$

$$G^{q,\,\mu\,(N\to N)}_{A,\,\uparrow\uparrow} = \frac{1}{2\bar{P}^+}\bar{u}(P',\lambda')\Big[\gamma^\mu\gamma_5\tilde{H}^q_{(*)}(x,\xi,t) + \frac{\Delta^\mu\gamma_5}{2M_N}\tilde{E}^q_{(*)}(x,\xi,t) + \frac{i\sigma^{\mu\nu}\Delta_\nu}{2M_N}\tilde{X}^q_{(*)}(x,\xi,t)\Big]u(P,\lambda) \tag{4.52}$$

$$\begin{aligned} G^{\mu\,(p\to\Delta^+)}_{V,\,\lambda'\lambda} =& \frac{1}{2\sqrt{6}\bar{P}^+}\bar{u}_\nu(P',\lambda')\Big[\kappa_1^{\mu\nu}H^1_{(*)}(x,\xi,t) + \kappa_2^{\mu\nu}H^2_{(*)}(x,\xi,t) + \kappa_3^{\mu\nu}H^3_{(*)}(x,\xi,t) \\ &+ \kappa_4^{\mu\nu}H^4_{(*)}(x,\xi,t)\Big]u(P,\lambda) \\ G^{\mu\,(p\to\Delta^+)}_{A,\,\lambda'\lambda} =& \frac{1}{4\bar{P}^+}\bar{u}_\nu(P',\lambda')\Big[\tilde{\kappa}_1^{\mu\nu}C^1_{(*)}(x,\xi,t) + \tilde{\kappa}_2^{\mu\nu}C^2_{(*)}(x,\xi,t) + \tilde{\kappa}_3^{\mu\nu}C^3_{(*)}(x,\xi,t) \\ &+ \tilde{\kappa}_4^{\mu\nu}C^4_{(*)}(x,\xi,t)\Big]u(P,\lambda) \quad . \end{aligned}$$

We name these objects $GPD_{(*)}(x,\xi,t)$ mixed twist GPDs since one needs at least one non plus component transition amplitude in order to access them. (As for each process there is

one GPD more than there are independent twist 2 GPDs).

Now we have to address the question what kind of approximation these objects imply, and whether it is a reasonable approximation. This issue can be discussed by comparing the expressions above with the properly defined higher twist GPDs from the last section. Starting with the vectorial $N \to N$ transition we firstly remark that the covariant κ_1^μ can be expressed by the others for a given μ. We find

$$\begin{aligned}
\kappa_1^+ &= -\frac{1}{\xi}\kappa_3^+ + \kappa_2^+ \\
\kappa_1^\perp &= \kappa_2^\perp \\
\kappa_1^- &= \frac{1}{\xi}\kappa_3^- + \kappa_2^- \quad .
\end{aligned}$$

This way we can compare the parameterizations of higher twist GPDs with those for mixed twist GPDs for the transition amplitudes. We get

$$\begin{aligned}
\Big(E_{(*)} + H_{(*)}\Big)\kappa_2^+ + \Big(X_{(*)} - \frac{1}{\xi}H_{(*)}\Big)\kappa_3^+ =& (E+H)\kappa_2^+ - \frac{1}{\xi}H\kappa_3^+ \\
\Big(E_{(*)} + H_{(*)}\Big)\kappa_2^\perp + X_{(*)}\kappa_3^\perp =& \Big(H + H_3 + E\Big)\kappa_2^\perp + X_3\kappa_3^\perp \\
\Big(E_{(*)} + H_{(*)}\Big)\kappa_2^- + \Big(X_{(*)} + \frac{1}{\xi}H_{(*)}\Big)\kappa_3^- =& \Big(H + H_3 + H_4 + E + E_4\Big)\kappa_2^- \\
&+ \Big(X_3 + \frac{1}{\xi}(H + H_3 + H_4)\Big)\kappa_3^- \quad .
\end{aligned}$$

The implications of comparing all components μ are:

$$\begin{aligned}
H_{(*)} &= H + \xi X_3 \\
E_{(*)} &= E - \xi X_3 \\
X_{(*)} &= X_3 \\
H_3 &= 0 \\
H_4 &= \xi X_3 \\
E_4 &= -\xi X_3 \quad .
\end{aligned}$$

In short, if all genuine higher twist GPDs are very small this approximation is quite ok. There is no a priori reason why these higher twist GPDs should be small (they are kinematically suppressed, but not necessarily small quantities in themselves). A little hope for the higher twist GPDs being small comes from the sum rules (eq. 4.34) which guarantee at least that their integral over x must vanish.

For the "mixed" GPDs the sum rules again become very intuitive:

$$\begin{aligned}
\int_{-1}^{1} dx\, H_{(*)}(x,\xi,t) &= F_1(t) \\
\int_{-1}^{1} dx\, E_{(*)}(x,\xi,t) &= F_2(t) \\
\int_{-1}^{1} dx\, X_{(*)}(x,\xi,t) &= 0 \quad .
\end{aligned}$$

Finally we provide the formulae for the mixed GPDs in terms of the amplitudes $G^+_{\uparrow\uparrow}$, $G^+_{\downarrow\uparrow}$ and $G^x_{\uparrow\uparrow}$:

$$\begin{aligned}
H_{(*)}(x,\xi,t) =& \sqrt{1-\xi^2}\tilde{G}^+_{\uparrow\uparrow} + \frac{\xi\sqrt{1-\xi^2}}{\Delta_x}\tilde{G}^x_{\uparrow\uparrow} \\
E_{(*)}(x,\xi,t) =& \frac{\xi^2}{\sqrt{1-\xi^2}}\tilde{G}^+_{\uparrow\uparrow} + \frac{2M_N}{\sqrt{1-\xi^2}\Delta_x}\tilde{G}^+_{\downarrow\uparrow} - \frac{\xi\sqrt{1-\xi^2}}{\Delta_x}\tilde{G}^x_{\uparrow\uparrow} \\
X_{(*)}(x,\xi,t) =& -\frac{\xi}{\sqrt{1-\xi^2}}\tilde{G}^+_{\uparrow\uparrow} - \frac{2\xi M_N}{\sqrt{1-\xi^2}\Delta_x}\tilde{G}^+_{\downarrow\uparrow} + \frac{\sqrt{1-\xi^2}}{\Delta_x}\tilde{G}^x_{\uparrow\uparrow} \quad .
\end{aligned} \tag{4.53}$$

For the axial $N \to N$ transition we can go through similar steps. We find

$$\begin{aligned}
\tilde{H}_{(*)} &= \tilde{H} \\
\tilde{E}_{(*)} &= \tilde{E} + \tilde{E}_3 \\
\tilde{X}_{(*)} &= -\xi\tilde{E}_3 \\
\tilde{H}_3 &= 0 \\
\tilde{H}_4 &= 0 \\
\tilde{X}_4 &= -\xi\tilde{E}_3 \quad .
\end{aligned}$$

Therefore we find again that the introduction of mixed twist GPDs is reasonable if one can assume the genuine higher twist GPDs to be small. Likewise the sum rules again become very intuitive:

$$\begin{aligned}
\int_{-1}^{1} dx\, \tilde{H}_{(*)}(x,\xi,t) &= G_A(t) \\
\int_{-1}^{1} dx\, \tilde{E}_{(*)}(x,\xi,t) &= G_P(t) \\
\int_{-1}^{1} dx\, \tilde{X}_{(*)}(x,\xi,t) &= G_T \quad .
\end{aligned}$$

Finally the mixed GPDs in terms of the amplitudes $G^+_{\uparrow\uparrow}$, $G^+_{\downarrow\uparrow}$ and $G^x_{\downarrow\uparrow}$:

$$\begin{aligned}
\tilde{H}_{(*)}(x,\xi,t) =& \frac{1}{\sqrt{1-\xi^2}}\tilde{G}^+_{\uparrow\uparrow} + \frac{2\xi M_N}{\sqrt{1-\xi^2}\Delta_x}\tilde{G}^+_{\downarrow\uparrow} \\
\tilde{E}_{(*)}(x,\xi,t) =& \frac{4M_N^2}{\sqrt{1-\xi^2}\Delta_x^2}\tilde{G}^+_{\uparrow\uparrow} + \frac{8\xi M_N^3}{\sqrt{1-\xi^2}\Delta_x^3}\tilde{G}^+_{\downarrow\uparrow} - \frac{2\sqrt{1-\xi^2}M_N}{\Delta_x^2}\tilde{G}^x_{\downarrow\uparrow} \\
\tilde{X}_{(*)}(x,\xi,t) =& -\frac{4\xi M_N^2}{\sqrt{1-\xi^2}\Delta_x^2}\tilde{G}^+_{\uparrow\uparrow} + \frac{2M_N\left[(1-\xi^2)\Delta_x^2 - 4\xi^2 M_N^2\right]}{\sqrt{1-\xi^2}\Delta_x^3}\tilde{G}^+_{\downarrow\uparrow} + \frac{2\xi\sqrt{1-\xi^2}M_N}{\Delta_x^2}\tilde{G}^x_{\downarrow\uparrow} \quad .
\end{aligned} \tag{4.54}$$

For the vectorial $N \to \Delta$ transition we have to express the covariant $\kappa_4^{\mu\nu}$ by the other three. We find

$$\begin{aligned}
\kappa_4^{+\nu} &= A^+\kappa_2^{+\nu} + B^+\kappa_3^{+\nu} \\
\kappa_4^{\perp\nu} &= A^\perp\kappa_2^{\perp\nu} + B^\perp\kappa_3^{\perp\nu} \\
\kappa_4^{-\nu} &= A^-\kappa_2^{-\nu} + B^-\kappa_3^{-\nu} \quad .
\end{aligned}$$

Here we have used the shortcut notations

$$
\begin{aligned}
A^+ &= -\frac{2\xi}{t+\xi(M_\Delta^2-M_N^2)} \\
B^+ &= -\frac{1-\xi}{t+\xi(M_\Delta^2-M_N^2)} \\
A^\perp &= \frac{1}{M_\Delta^2-M_N^2} \\
B^\perp &= -\frac{2}{M_\Delta^2-M_N^2} \\
A^- &= \frac{4(1-\xi)M_N^2+2\xi t-4(1+\xi)M_\Delta^2}{t^2-(2-\xi)M_N^2t+2(1-\xi)M_N^4+2(1+\xi)M_\Delta^4-\Big[4M_N^2+(2+\xi)t\Big]M_\Delta^2} \\
B^- &= \frac{(4+2\xi)M_\Delta^2+2\xi M_N^2-(1+\xi)t}{t^2-(2-\xi)M_N^2t+2(1-\xi)M_N^4+2(1+\xi)M_\Delta^4-\Big[4M_N^2+(2+\xi)t\Big]M_\Delta^2} \quad .
\end{aligned}
$$

Comparing the expressions for the amplitudes we find

$$
\begin{aligned}
H_1^{(*)} &= H_1 \\
H_2^{(*)} &= H_2 - \frac{A^+}{A^\perp-A^+}H_2^{(3)} \\
H_3^{(*)} &= H_3 - \frac{A^+(B^\perp-B^+)}{A^\perp-A^+}H_3^{(3)} \\
H_4^{(*)} &= \frac{H_2^{(3)}}{A^\perp-A^+} \\
H_1^{(3)} &= 0 \\
H_1^{(4)} &= 0 \quad .
\end{aligned}
$$

Again as long as $H_4^{(*)}$ and thus all genuine higher twist GPDs are small this approximation is ok and in this case the concept of mixed GPDs is sensible.

Finally we consider the axial $N \to \Delta$ transition. Here we can express the superfluous covariants in terms of others as following:

$$
\begin{aligned}
\tilde{\kappa}_2^{+\nu} &= \xi\left(\tilde{\kappa}_4^{+\nu} - \frac{M_\Delta^2-M_N^2}{M_N^2}\tilde{\kappa}_1^{+\nu}\right) \\
\tilde{\kappa}_4^{\perp\nu} &= \frac{M_\Delta^2-M_N^2}{M_N^2}\tilde{\kappa}_1^{\perp\nu} \\
\tilde{\kappa}_2^{-\nu} &= \xi\left(\frac{M_\Delta^2-M_N^2}{M_N^2}\tilde{\kappa}_1^{+\nu} - \tilde{\kappa}_4^{+\nu}\right)
\end{aligned}
$$

These expressions lead to

$$\begin{aligned}
C_1^{(*)} &= C_1 + \frac{\xi(M_\Delta^2 - M_N^2)}{M_N^2} C_2^{(3)} \\
C_2^{(*)} &= C_2^{(3)} \\
C_3^{(*)} &= C_3 \\
C_4^{(*)} &= C_4 - \xi C_2^{(3)} \\
C_1^{(3)} &= C_3^{(3)} = C_3^{(4)} = 0 \\
C_1^{(4)} &= \frac{\xi(M_\Delta^2 - M_N^2)}{M_N^2} C_2^{(3)} \\
C_4^{(4)} &= -\xi C_2^{(3)} \quad .
\end{aligned}$$

And again this is a reasonable approximation as long as the genuine higher twist GPDs are small. As mentioned in the last section however the existence of a finite $C_6(t)$ forbids the genuine higher twist axial GPDs to vanish. Luckily the factors ξ in the above expressions seem to save the merit of introducing mixed GPDs for the axial $N \to \Delta$ transition at least for small values of ξ.

For all the mixed twist GPDs we can now give consistency relations which have to hold if the approximations are reasonable. This works along the same lines as the derivation of the consistency relations among the amplitudes which correspond to the form factors. This means that we can apply 4.27 in order to gain amplitude relations.

For the vectorial $N \to N$ transition we choose to express all other amplitudes in terms of

$$\begin{aligned}
&\tilde{G}_{V,\uparrow\uparrow}^{q,+\,(N\to N)} \\
&\tilde{G}_{V,\downarrow\uparrow}^{q,+\,(N\to N)} \\
&\tilde{G}_{V,\uparrow\uparrow}^{q,x\,(N\to N)} \quad .
\end{aligned}$$

Then the consistency relations read[12]

$$\begin{aligned}
\tilde{G}^x_{\downarrow,\uparrow} =& \frac{\xi(4M_N^2 + \Delta_x^2)(2M_N\tilde{G}^+_{\downarrow,\uparrow} + \Delta_x\tilde{G}^+_{\uparrow,\uparrow}) - (1-\xi^2)\Delta_x^2\tilde{G}^x_{\uparrow,\uparrow}}{2(1-\xi^2)M_N\Delta_x} \\
\tilde{G}^y_{\uparrow,\uparrow} =& \frac{i\left[2M_N\tilde{G}^+_{\downarrow,\uparrow} + \Delta_x\tilde{G}^+_{\uparrow,\uparrow}\right]}{1-\xi^2} \\
\tilde{G}^y_{\downarrow,\uparrow} =& \frac{2i\xi M_N(2M_N\tilde{G}^+_{\downarrow,\uparrow} + \Delta_x\tilde{G}^+_{\uparrow\uparrow})}{(1-\xi^2)\Delta_x}
\end{aligned}$$

[12] Whenever the meaning is clear from the context we will drop the indices q,A or V and $N \to N$ or $N \to \Delta$.

$$\begin{aligned}
\tilde{G}^{-}_{\uparrow,\uparrow} =& \frac{\Big[4(1-3\xi^2)M_N^2\Delta_x - (1+\xi^2)\Delta_x^3\Big]\tilde{G}^{+}_{\uparrow,\uparrow} - \Big[4M_N\Delta_x^2 + 16\xi^2 M_N^3\Big]\tilde{G}^{+}_{\downarrow,\uparrow}}{(1-\xi^2)^2\Delta_x} \\
&+ \frac{2\xi(\Delta_x^2 + 4M_N^2)\tilde{G}^{x}_{\uparrow,\uparrow}}{(1-\xi^2)\Delta_x} \\
\tilde{G}^{-}_{\downarrow,\uparrow} =& \frac{\Big[\xi^2\Delta_x^3 - 4(1-2\xi^2)M_N^2\Delta_x\Big]\tilde{G}^{+}_{\uparrow,\uparrow} + \Big[(1+\xi^2)M_N\Delta_x^2 - 4(1-3\xi^2)M_N^3\Big]\tilde{G}^{+}_{\downarrow,\uparrow}}{(1-\xi^2)^2 M_N} \\
&- \frac{\xi(1-\xi^2)(\Delta_x^2 + 4M_N^2)\tilde{G}^{x}_{\uparrow,\uparrow}}{(1-\xi^2)^2 M_N} \quad .
\end{aligned} \tag{4.55}$$

One can nicely observe the reduction in case of the form factor corresponding amplitudes $\tilde{F}^{\mu}_{\lambda'\lambda}$ by setting $\xi = 0$.

For the axial $N \to N$ transition we express the other amplitudes in terms of

$$\begin{aligned}
&\tilde{G}^{q,+\,(N\to N)}_{A,\uparrow\uparrow} \\
&\tilde{G}^{q,+\,(N\to N)}_{A,\downarrow\uparrow} \\
&\tilde{G}^{q,x\,(N\to N)}_{A,\downarrow\uparrow} \quad .
\end{aligned}$$

We find the relations

$$\begin{aligned}
\tilde{G}^{x}_{\uparrow,\uparrow} =& \frac{\xi\left[(4M_N^2\Delta_x + \Delta_x^3)\tilde{G}^{+}_{\uparrow,\uparrow} + 2\xi M_N(\Delta_x^2 + 4M_N^2)\tilde{G}^{+}_{\downarrow,\uparrow} - 2(1-\xi^2)\Delta_x M_N\tilde{G}^{x}_{\downarrow,\uparrow}\right]}{(1-\xi^2)\Delta_x^2} \\
\tilde{G}^{y}_{\uparrow,\uparrow} =& \frac{i(\Delta_x\tilde{G}^{+}_{\uparrow\uparrow} + 2\xi M_N\tilde{G}^{+}_{\downarrow\uparrow})}{1-\xi^2} \\
\tilde{G}^{y}_{\downarrow,\uparrow} =& \frac{2iM_N(\Delta_x\tilde{G}^{+}_{\uparrow,\uparrow} + 2\xi M_N\tilde{G}^{+}_{\downarrow\uparrow})}{(1-\xi^2)\Delta_x} \\
\tilde{G}^{-}_{\uparrow,\uparrow} =& \frac{\Delta_x^2 + 4M_N^2}{(1-\xi^2)^2\Delta_x^3}\Bigg(\Big[8\xi^2 M_N^2\Delta_x - (1-\xi^2)\Delta_x^3\Big]\tilde{G}^{+}_{\uparrow\uparrow} \\
&+\Big[16\xi^3 M_N^3 - 4\xi(1-\xi^2)M_N\Delta_x^2\Big]\tilde{G}^{+}_{\downarrow\uparrow} - \Big[4\xi^2(1-\xi^2)\Delta_x M_N\Big]\tilde{G}^{x}_{\downarrow\uparrow}\Bigg) \\
\tilde{G}^{-}_{\downarrow,\uparrow} =& -\frac{(\Delta_x^2 + 4M_N^2)\left[\Big(8\xi^2 M_N^2 - (1-\xi^2)\Delta_x^2\Big)\tilde{G}^{+}_{\downarrow\uparrow} + 2\xi\Delta_x\Big(2M_N\tilde{G}^{+}_{\uparrow\uparrow} - (1-\xi^2)\tilde{G}^{x}_{\downarrow\uparrow}\Big)\right]}{(1-\xi^2)^2\Delta_x^2} \quad .
\end{aligned} \tag{4.56}$$

The consistency relations for both axial and vectorial $N \to \Delta$ amplitudes as derived using the expressions for mixed twist GPDs are lengthy and thus will not be given here for lack of space. We have derived and implemented them numerically though, so they are evaluated in the subsequent section numerically. However we provide one example each. For the vectorial

$N \to \Delta$ transition one of the relations reads

$$\begin{aligned}\tilde{G}^x_{\frac{1}{2}\downarrow} =& \frac{\sqrt{3}(1-\xi^2)\Delta_x\big[\Delta_x^2 + (1-\xi^2)M_N^2 - 2(1+\xi)^2 M_\Delta^2 + (1-\xi^2)M_N M_\Delta\big]\tilde{G}^x_{\frac{3}{2}\uparrow}}{3(1+\xi)(1-\xi^2)\Delta_x M_\Delta A} \\ & - \frac{\big[(1+\xi)^2 M_\Delta^2 - (1-\xi)^2 M_N^2 + \xi\Delta_x^2\big]}{3(1+\xi)(1-\xi^2)\Delta_x M_\Delta A} \\ & \cdot \big[\sqrt{3}\Big(\Delta_x^2 + (1-\xi)^2 M_N^2 - 2(1+\xi)^2 M_\Delta^2 + (1-\xi^2)M_N M_\Delta\Big)\tilde{G}^+_{\frac{3}{2}\uparrow} - 3(1+\xi)M_\Delta A\tilde{G}^+_{\frac{1}{2}\downarrow}\big]\end{aligned} \tag{4.57}$$

and for the axial $N \to \Delta$ transition one relation is given by

$$\begin{aligned}\tilde{G}^x_{\frac{1}{2}\uparrow} =& \frac{(1-\xi^2)\Delta_x\Big(AB^2 - \Delta_x^2\big[(1-\xi)M_N + 2(1+\xi)M_\Delta\big]\Big)\tilde{G}^x_{\frac{3}{2}\uparrow}}{\sqrt{3}(1+\xi)(1-\xi^2)\Delta_x^2 M_\Delta B} \\ & + \frac{(1+\xi)^2 M_\Delta^2 - (1-\xi)^2 M_N^2 + \xi\Delta_x^2}{\sqrt{3}(1+\xi)(1-\xi^2)\Delta_x^2 M_\Delta B} \\ & \cdot \left(\sqrt{3}(1+\xi)\Delta_x M_\Delta B\tilde{G}^+_{\frac{1}{2}\uparrow} + \Big(\Delta_x^2\big[(1-\xi)M_N + 2(1+\xi)M_\Delta\big] - AB^2\Big)\tilde{G}^+_{\frac{3}{2}\uparrow}\right) .\end{aligned} \tag{4.58}$$

4.7 Results

We will conclude this chapter with the application of the formulae derived in the previous sections to the amplitudes which we have obtained in the model calculation. In the following 4 subsections we will present the plots for the different transitions and discuss the results.

4.7.1 Vectorial $N \to N$ transition

In fig. 4.1 we explore how well the form factor related amplitudes satisfy covariance in our model calculation. Obviously the shape of all curves is very similar between the predicted results and the direct calculation. The amplitude relations for the perpendicular amplitudes are satisfied at 30% level. This is a reasonable result. For the $-$ component transition amplitudes the deviations are much higher. We would like to understand them as 30% agreement between $\perp$ and $-$ component transition amplitudes. In fact that is the size of the error for amplitude relations with $-$ amplitudes in terms of $\perp$ amplitudes. (Not displayed here for lack of space). Particularly for $F^-_{\uparrow\uparrow}$ the error is much smaller. This seems to be coincidence.

In fig. 4.2 we display the DVCS amplitude relations which connect the x and y component amplitudes. These amplitude relations therefore provide a measure for the covariance-consistency of amplitudes which are associated with the same twist. Since for $\xi = 0$ the amplitudes $\tilde{G}^x_{\uparrow\uparrow}$ and $\tilde{G}^x_{\downarrow\uparrow}$ vanish the amplitude relations can only be verified for finite values of ξ[13]. We find

[13] Choosing very small values for ξ requires too much computer time to produce a statistical error which is small enough for our purpose.

that the amplitude relations are satisfied at 30% level or better.

The amplitude relations in eq. 4.55 not only require covariance for the model amplitudes. They also assume that genuine higher twist GPDs are negligible. In fig. 4.3 these predictions are tested. We have confined ourselves to showing only the $p \to p$ amplitude relations here. The amplitude relations for $\tilde{G}^{y}_{\uparrow\uparrow}$, $\tilde{G}^{-}_{\uparrow\uparrow}$ and $\tilde{G}^{-}_{\downarrow\uparrow}$ are consistent with the findings in fig. 4.1. The amplitude relations for $\tilde{G}^{x}_{\downarrow\uparrow}$ and $\tilde{G}^{y}_{\downarrow\uparrow}$ however look very bad. Since they scale with $\mathcal{O}(\xi)$ the numerical extraction of the amplitudes for very small values of ξ is again impossible. These amplitudes also enter in the expressions for the twist 3 GPDs.

In fig. 4.4 we show the leading twist GPDs for $t = -0.5\,GeV^2$ and different values of skewedness ξ. The value for t which we chose here is small enough and thus within the application range of quark models. As discussed in chapter 3 the valence quark picture only provides results in the kinematical range $x \geq \xi$. For large values of x the valence quark contribution is dominant and hence the GPDs which we show here are predictive in this regime.

Twist 3 GPDs are presented in fig. 4.5. The non satisfaction of the amplitude relations which we showed in fig. 4.55 already casts serious doubts on the predictive power of quark models for observables that are extracted from bad LF component amplitudes in general (and higher twist GPDs in particular). In fact the genuine twist 3 GPDs $H_{(3)}$ and $X_{(3)}$ do not satisfy the sum rules in eq. 4.34. Likewise they are not small which would be the necessary condition in order to apply the concept of mixed twist GPDs. While we provided a formalism to extract higher twist GPDs from bad LF amplitudes the quark model is not able to provide the required covariance consistency in the amplitudes to be predictive for higher twist GPDs.

In fig. 4.6 we give the vectorial $N \to N$ form factors. The results look quite reasonable compared to the experimental data. However we have to emphasize that $G^{p}_{M}(Q^2)$ was used to fit the spatial quark model wave function (eq. 3.14). Nevertheless $G^{p}_{E}(Q^2)$ and $G^{n}_{M}(Q^2)$ are quite well described by the model. Although our model calculation only takes s-waves into account $G^{n}_{E}(Q^2)$ does not vanish as one should expect from $SU(6)$ arguments. The finite result stems from the Melosh rotation which mixes different spin states. While the experimental data for $G^{n}_{E}(Q^2)$ is not described by the model, the order of magnitude and the shape of this form factor are reproduced correctly even without taking into account d-waves. The deviation from the sum rules for finite values of ξ stems from covariance breaking effects as we discussed in chapter 3.

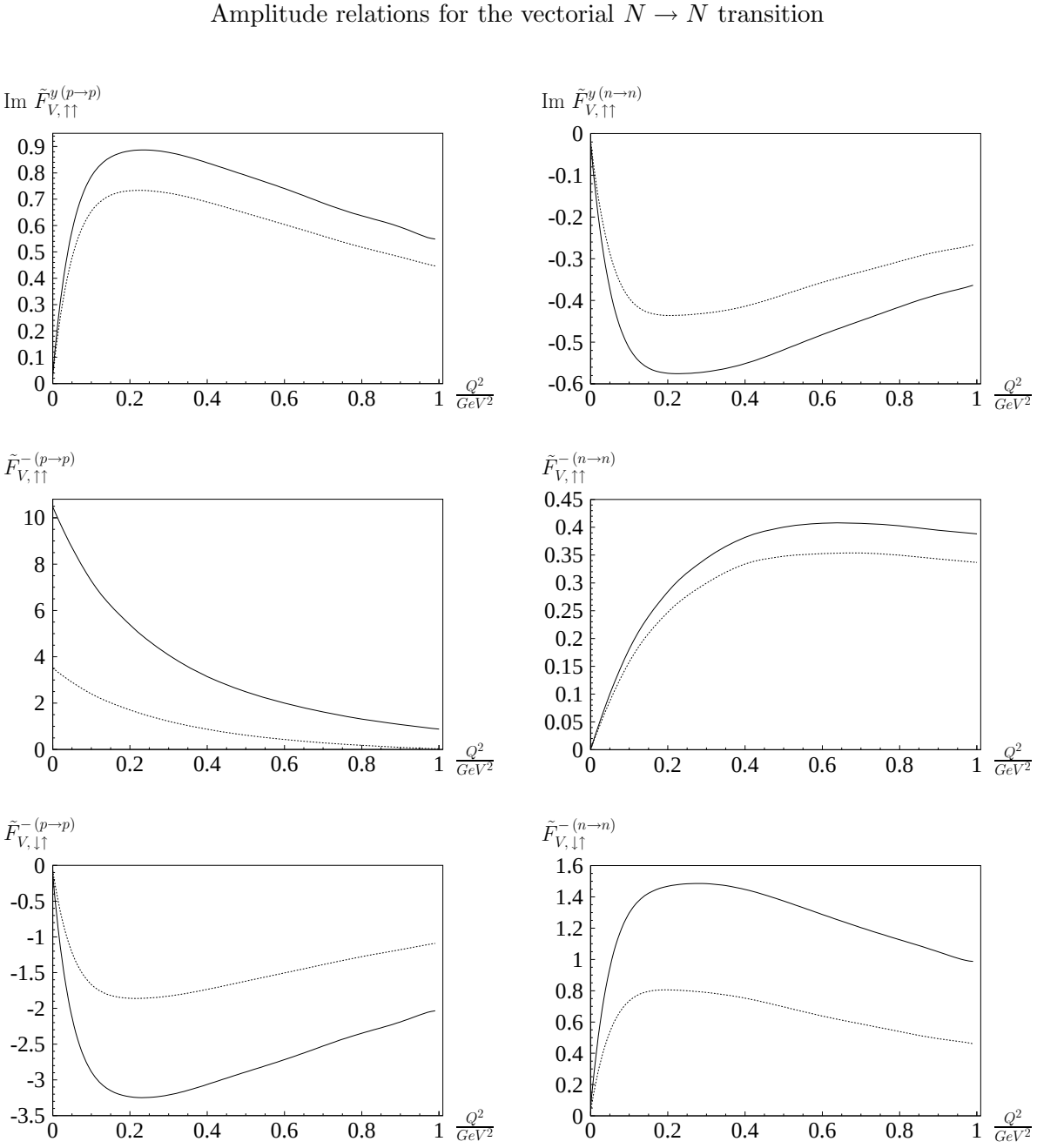

Figure 4.1: *Solid lines: Direct model calculation for the respective amplitudes. Dotted lines: Expected result if the respective amplitude relation (eq. 4.28) holds.*

Amplitude relations for the vectorial $N \to N$ transition (eq. 4.35)

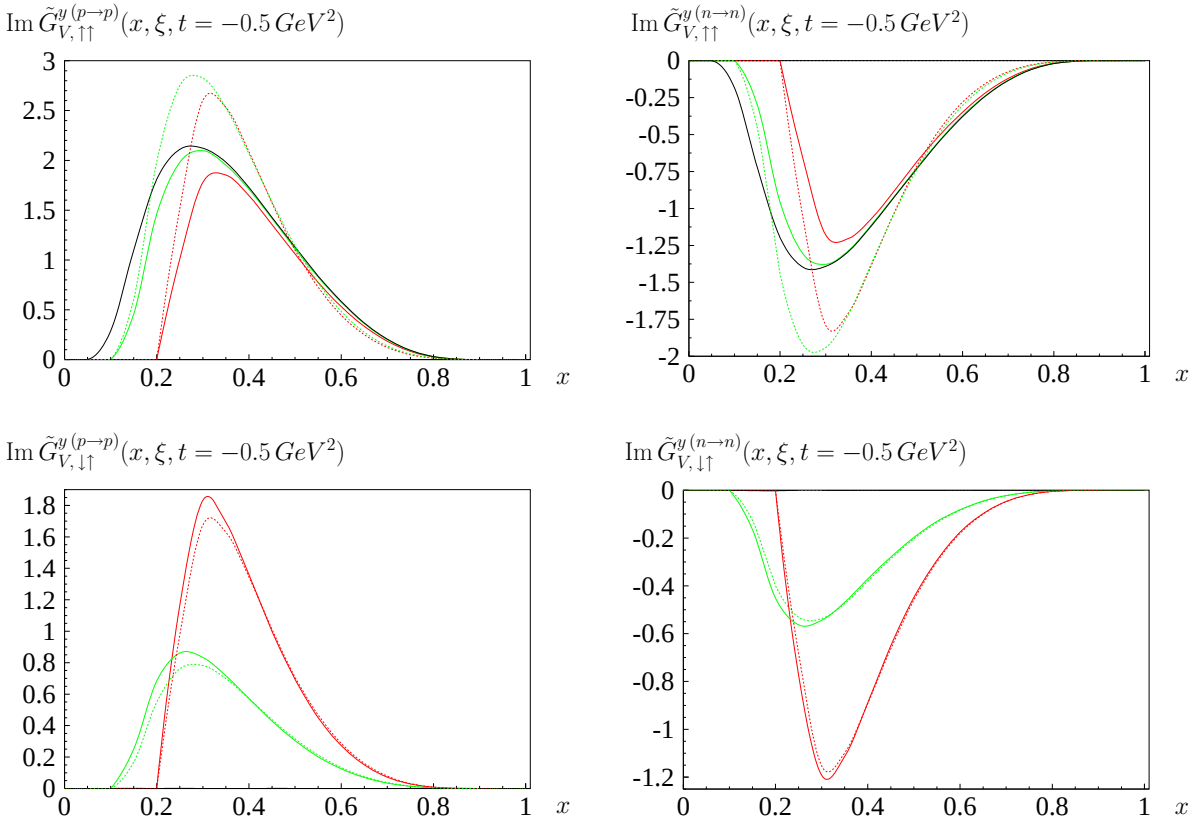

Figure 4.2: *Solid lines: Direct model calculation for the respective amplitude. Dotted lines: Expected result if the respective amplitude relation (eq. 4.35) holds. Black curve: Results for* $\xi = 0$*; Green curve: Results for* $\xi = 0.1$*; Red curve: Results for* $\xi = 0.2$*.*

Amplitude relations for the vectorial $N \to N$ transition (eq. 4.55)

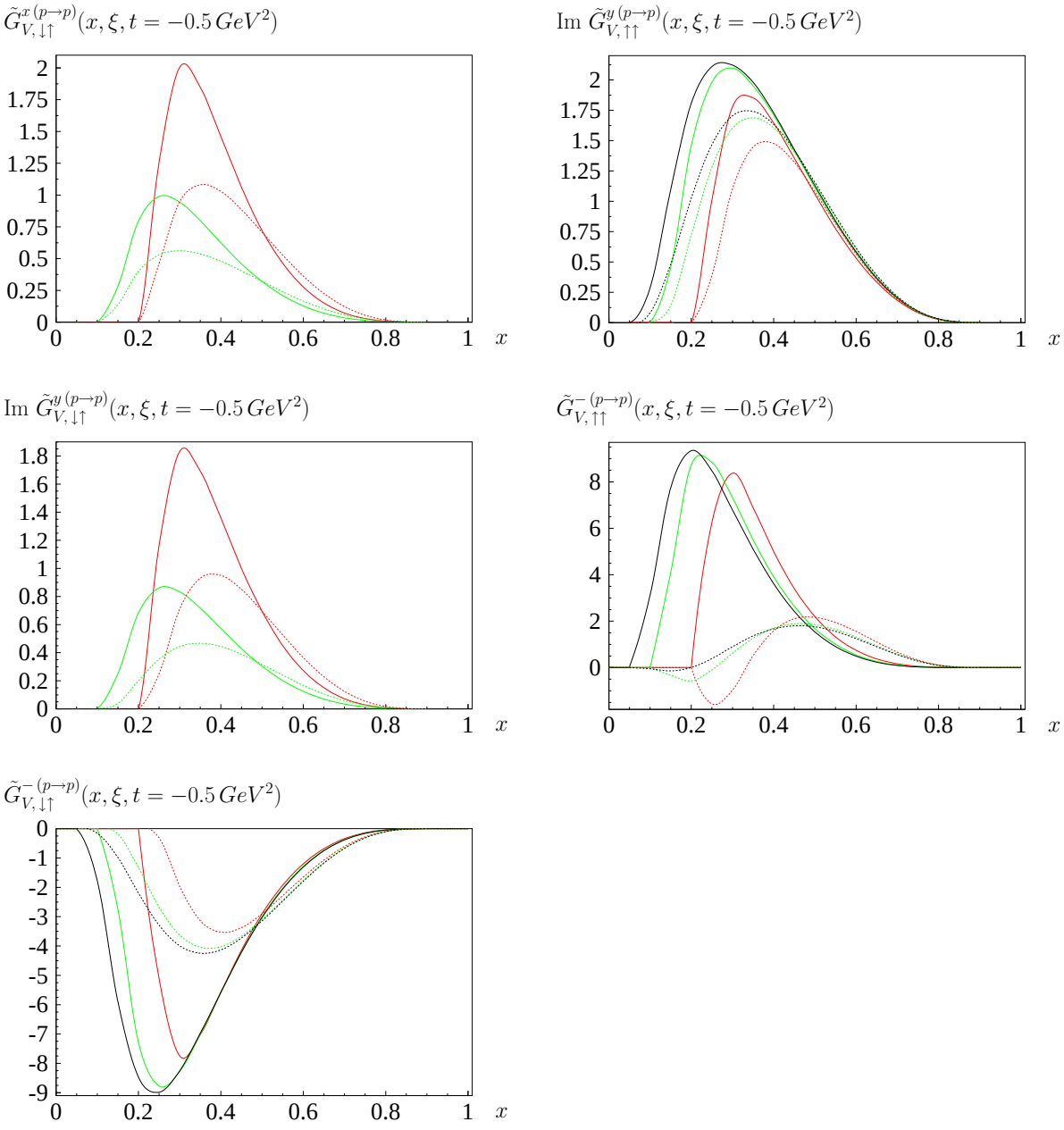

Figure 4.3: *Solid lines: Direct model calculation for the respective amplitude. Dotted lines: Expected result if the respective amplitude relation (eq. 4.55) holds. Black curve: Results for $\xi = 0$; Green curve: Results for $\xi = 0.1$; Red curve: Results for $\xi = 0.2$.*

Leading twist GPDs for the vectorial $N \to N$ transition

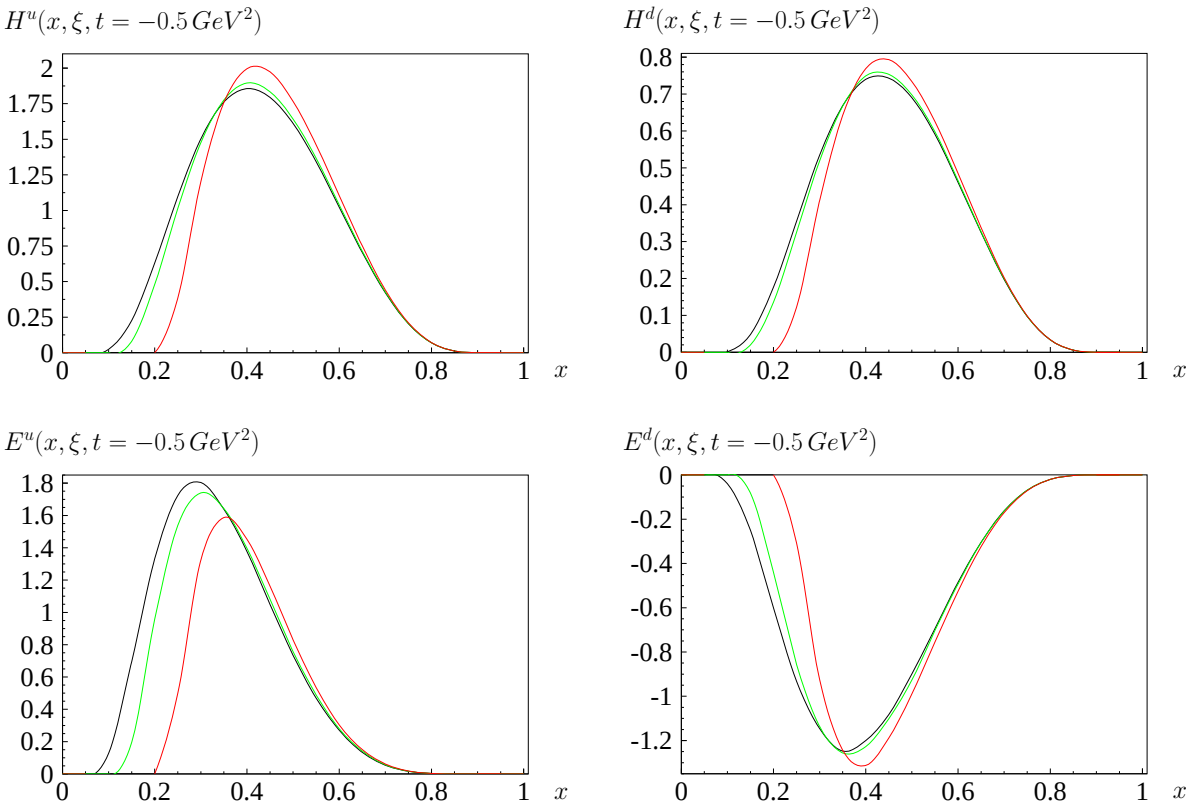

Figure 4.4: *Black curve: $\xi = 0$; Green curve: $\xi = 0.1$; Red curve: $\xi = 0.2$. The GPDs are extracted from the good LF component amplitudes (eq. 4.3).*

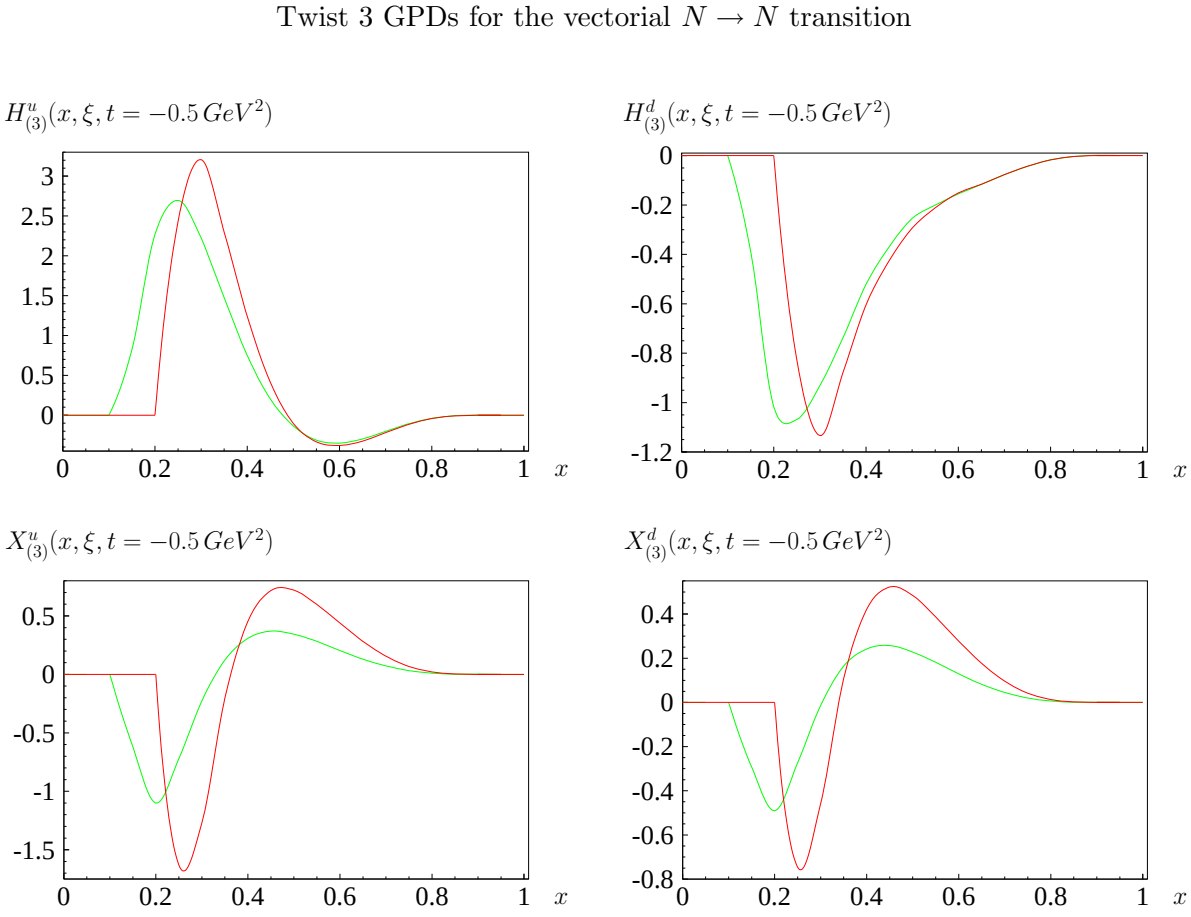

Figure 4.5: *Green curve:* $\xi = 0.1$*; Red curve:* $\xi = 0.2$.
The GPDs are extracted using the perpendicular LF component amplitudes (eq. 4.36).

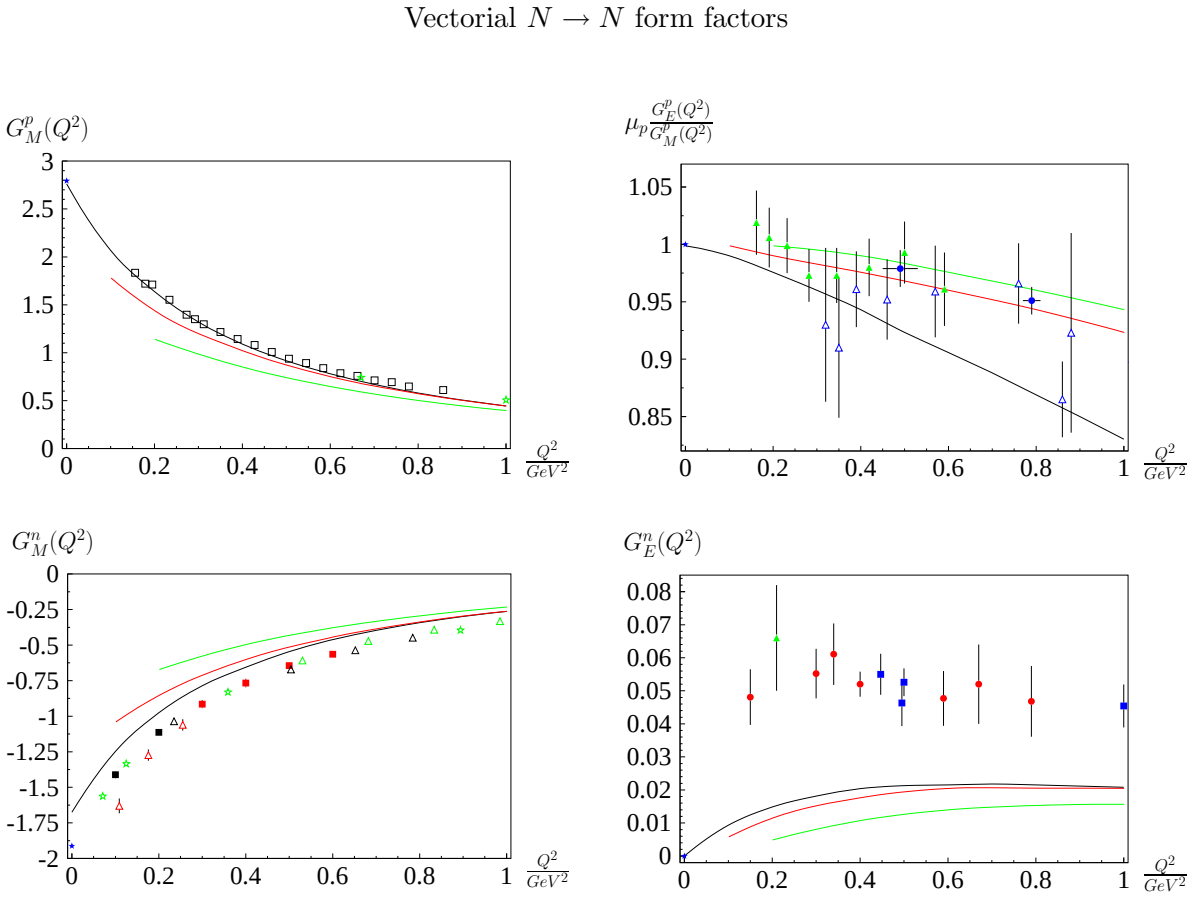

Figure 4.6: *The vectorial nucleon form factors. Calculated from the good LF amplitudes directly (black curve), evaluated using the sum rules for $\xi = 0$ (on top of the black curve), $\xi = 0.1$ (red curve) and $\xi = 0.2$ (green curve). The experimental data are taken from the following references:*
Upper left panel: green star: [82], black square: [83].
Upper right panel: blue triangle: [84], blue circle: [85], green triangle: [86].
Lower left panel: green triangle: [87], green star: [88], black triangle: [89], black square: [90], red triangle: [91], red square: [92].
Lower right panel: blue square: [93] [94] [95], red circle: [96] [97] [98] [99] [100] [101], green triangle: [102].
The black star in each panel denotes the experimental value for $Q^2 = 0\ GeV^2$.

4.7.2 Axial $N \to N$ transition

In fig. 4.7 we explore how well the form factor related amplitudes satisfy covariance in our model calculation. We have confined ourselves to presenting the isovectorial amplitudes only. Like for the vectorial $N \to N$ transition the shape of all curves is very similar between the predicted results and the direct calculation. The amplitude relations for the perpendicular amplitudes are satisfied at 30% level and again for the $-$ component transition amplitudes the deviations are much higher.

In fig. 4.8 we display the DVCS amplitude relations which connect the x and y component amplitudes. These amplitude relations therefore provide a measure for the covariance-consistency of amplitudes which are associated with the same twist. For $\xi \to 0$ the expression $\frac{\tilde{G}^x_{\uparrow\uparrow}}{\xi}$ becomes difficult to access numerically. Therefore the amplitude relations can only be verified for $\xi = 0.1$ and $\xi = 0.2$. We find that the amplitude relations are satisfied at 30% level or better.

The amplitude relations in eq. 4.56 not only require covariance for the model amplitudes. They also assume that genuine higher twist GPDs are negligible. In fig. 4.9 these predictions are tested. The amplitude relations for $\tilde{G}^y_{\uparrow\uparrow}$, $\tilde{G}^y_{\downarrow\uparrow}$ and $\tilde{G}^-_{\uparrow\uparrow}$ are consistent with the findings in fig. 4.7. Concerning $\tilde{G}^-_{\uparrow\uparrow}$ it is remarkable that the strong ξ dependence in the prediction for the amplitude is not followed by the directly calculated amplitude. The amplitude relations for $\tilde{G}^x_{\uparrow\uparrow}$ and $\tilde{G}^-_{\downarrow\uparrow}$ look quite bad. Since they scale with $\mathcal{O}(\xi)$ the numerical extraction of the amplitudes for very small values of ξ is again impossible. These amplitudes also enter in the expressions for the twist 3 GPDs.

In fig. 4.10 we show the leading twist GPDs for $t = -0.5\,GeV^2$ and different values of skewedness ξ. The value for t which we chose here is small enough and thus within the application range of quark models. As discussed in chapter 3 the valence quark picture only provides results in the kinematical range $x \geq \xi$. For large values of x the valence quark contribution is dominant and hence the GPDs which we show here are predictive in this regime. As discussed in section 4.2 the GPD $\tilde{E}(x,\xi,t)$ is obtained directly from the leading ξ behavior in $\tilde{G}^+_{\downarrow\uparrow}$ and is therefore to be trusted less than the results for $\tilde{H}(x,\xi,t)$. Apart from this covariance breaking effect which casts doubts on the reliability of the prediction for $\tilde{E}(x,\xi,t)$ there is a much more serious argument why the results for $\tilde{E}(x,\xi,t)$ are less predictive. In fact this GPD is dominated by the pion pole contribution, which is physically not accessible in a quark model calculation. This will become particularly obvious in the discussion of $G_P(t)$.

Twist 3 GPDs are presented in fig. 4.11. These genuine twist 3 GPDs $\tilde{H}_{(3)}$ and $\tilde{E}_{(3)}$ are not negligible. They do not satisfy the respective sum rules (eq. 4.37). Like for the vectorial $N \to N$ we only provide these twist 3 GPDs to show that we can treat them in our formalism. The predictive power of the quark model amplitudes for these GPDs is little.

In fig. 4.12 we give the axial $N \to N$ form factors. The results for $G_A(t)$ are reasonable compared to the experimental results which we have simply represented in the figure by a dipole fit. Concerning $G_P(t)$ we have a couple of comments to make. Firstly it is not amazing that the sum rule for $\xi = 0$ does not lie on top of the directly calculated curve for this form

factor. The reason is that $G_P(t)$ is extracted using $\tilde{G}^x_{\downarrow\uparrow}$ while the sum rules use the good LF component DVCS amplitudes only. Then the result for $G_P(t)$ is negative in our calculation while data shows a large positive $G_P(t)$. In fact the pseudoscalar form factor is dominated by the pion pole contribution

$$G_P(t) = \frac{4M_N^2}{M_\pi^2 - t} G_A(t) \quad .$$

This physics cannot be described using the valence quark picture. So our result has to be understood as valence quark contribution which should be added to the pion pole contribution. The deviation from the sum rules for finite values of ξ stems from covariance breaking effects as we discussed in chapter 3.

Amplitude relations for the axial $N \to N$ transition

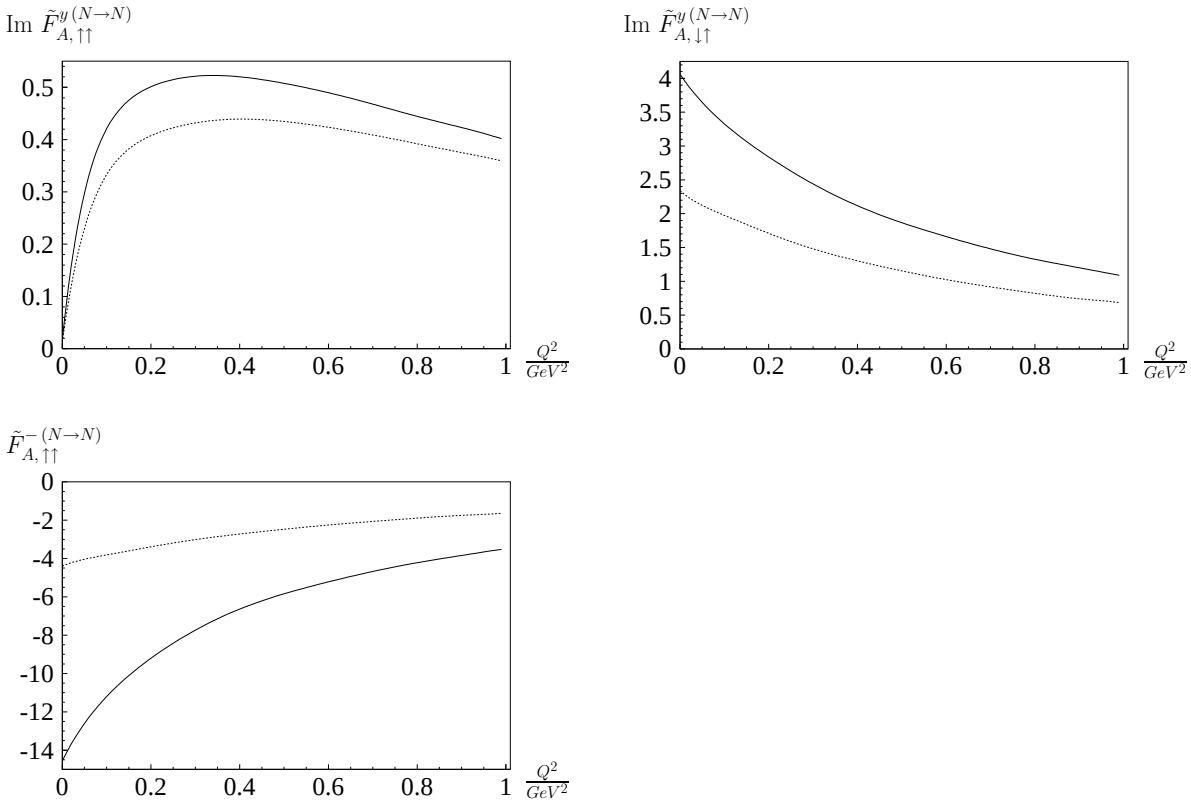

Figure 4.7: *Solid lines: Direct model calculation for the respective amplitudes. Dotted lines: Expected result if the respective amplitude relation (eq. 4.29) holds.*

Amplitude relations for the axial $N \to N$ transition (eq. 4.38)

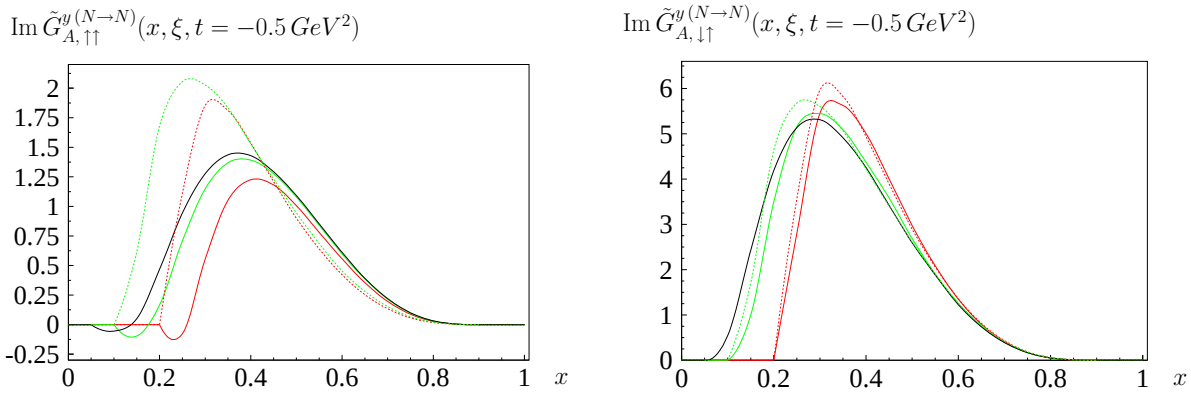

Figure 4.8: *Solid lines: Direct model calculation for the respective amplitude. Dotted lines: Expected result if the respective amplitude relation (eq. 4.38) holds. Black curve: Results for $\xi = 0$; Green curve: Results for $\xi = 0.1$; Red curve: Results for $\xi = 0.2$.*

Amplitude relations for the axial $N \to N$ transition (eq. 4.56)

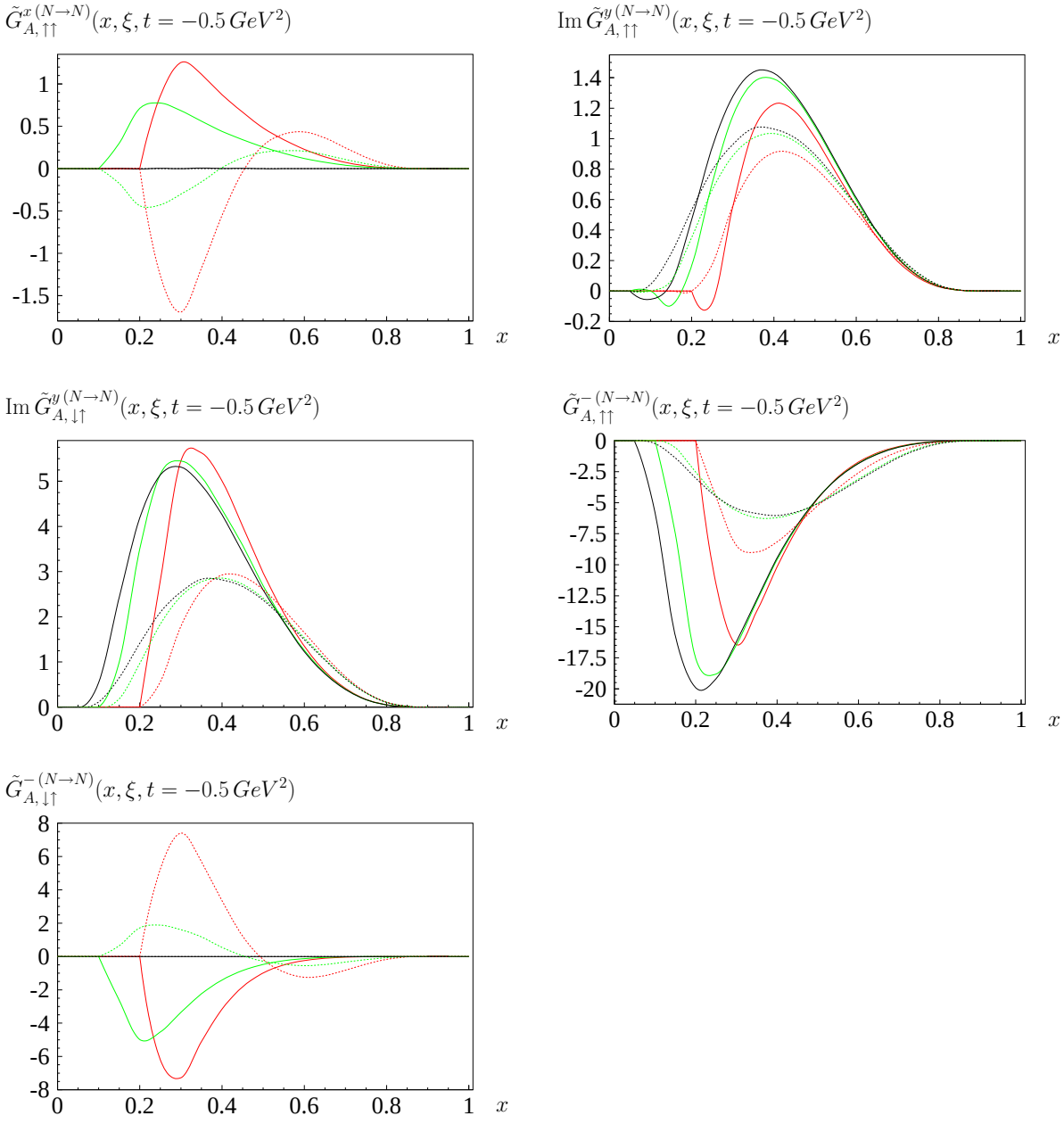

Figure 4.9: *Solid lines: Direct model calculation for the respective amplitude. Dotted lines: Expected result if the respective amplitude relation (eq. 4.56) holds. Black curve: Results for $\xi = 0$; Green curve: Results for $\xi = 0.1$; Red curve: Results for $\xi = 0.2$.*

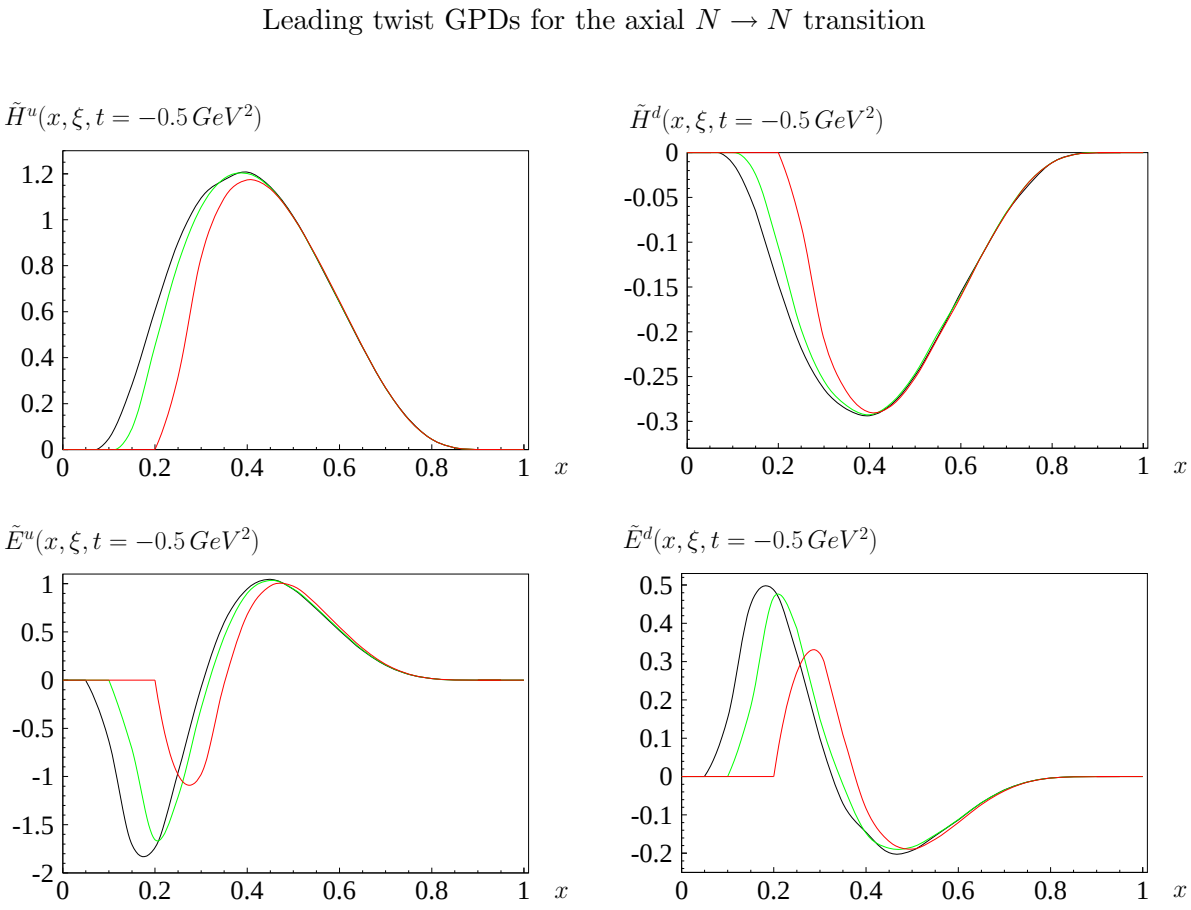

Figure 4.10: *Black curve: $\xi = 0$; Green curve: $\xi = 0.1$; Red curve: $\xi = 0.2$. The GPDs are extracted from the good LF component amplitudes (eq. 4.4).*

Twist 3 GPDs for the axial $N \to N$ transition

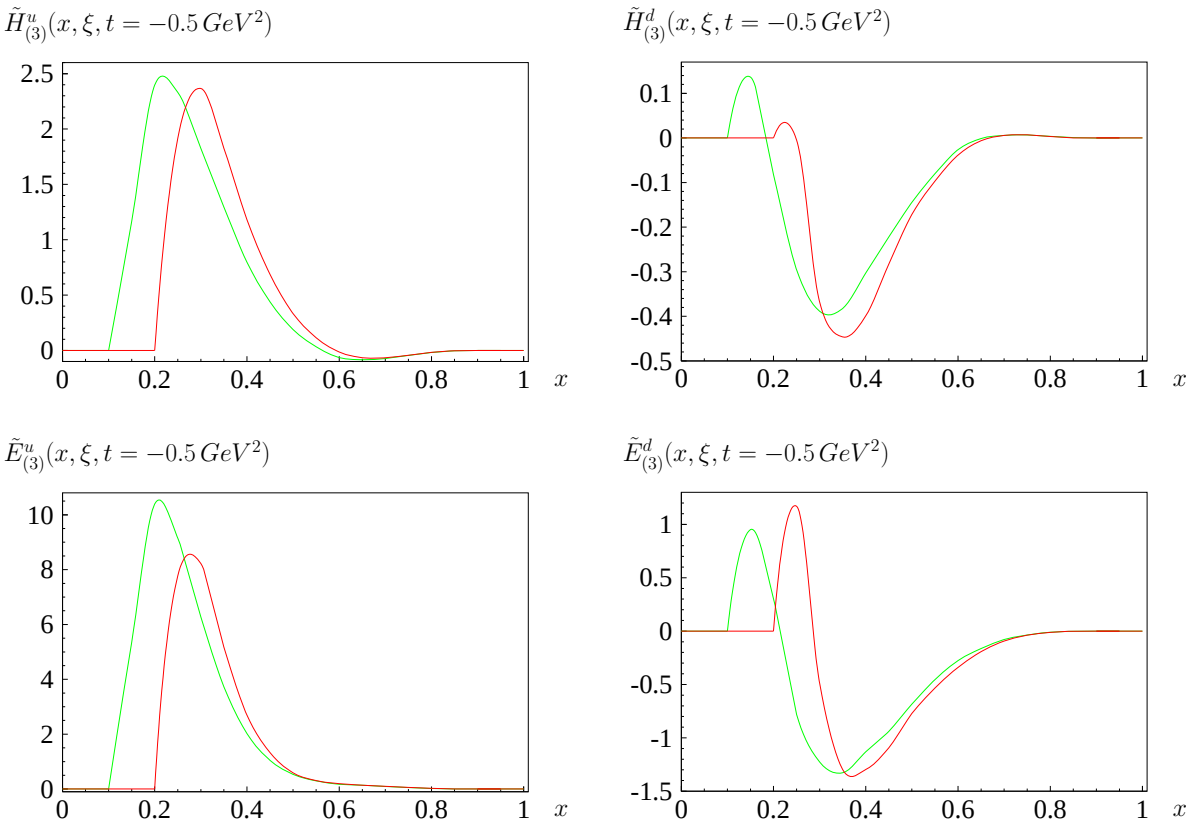

Figure 4.11: *Green curve:* $\xi = 0.1$*; Red curve:* $\xi = 0.2$.
The GPDs are extracted using the perpendicular LF component amplitudes (eq. 4.39).

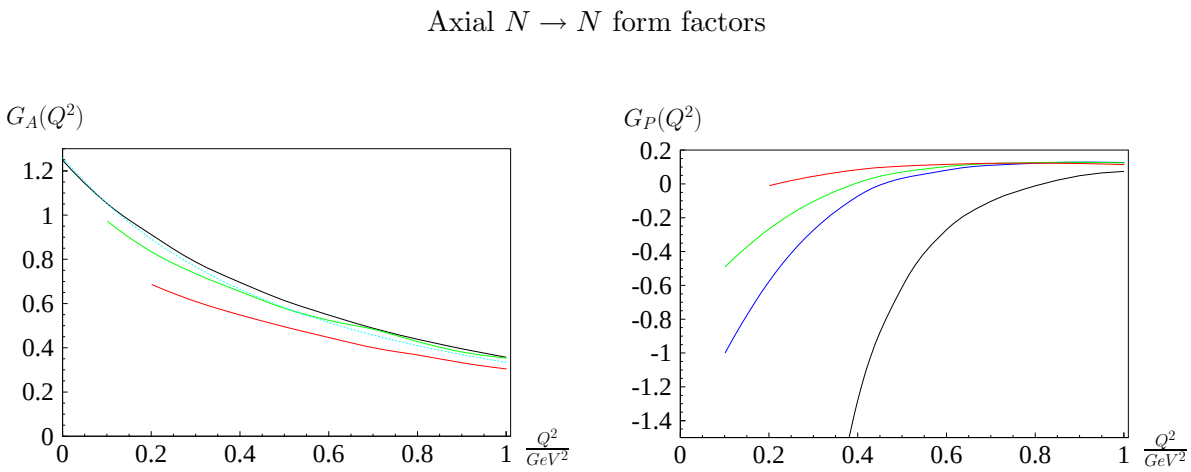

Figure 4.12: *The axial nucleon form factors. Calculated from good and bad LF amplitudes directly (black curve), evaluated using the sum rules for $\xi = 0$ (blue curve), $\xi = 0.1$ (green curve) and $\xi = 0.2$ (red curve). The dotted cyan curve is the dipole fit for $G_A(Q^2)$ with the dipole mass $M_A = 1.03\ GeV^2$.*

4.7.3 Vectorial $p \to \Delta^+$ transition

In fig. 4.13 the amplitude relations among the $\tilde{F}^{\mu}_{\lambda'\lambda}$ are tested. Our first remark concerns the angular condition ($\tilde{F}^{+}_{\frac{3}{2}\downarrow}$) which is broken. Actually the breaking of the angular condition is within 30% and thus not larger than other typical covariance breaking effects. However this inconsistency afflicts the predictability for $G^{\star}_{E}(t)$ and $G^{\star}_{C}(t)$ as will be discussed later. Another interesting feature for the $N \to \Delta$ transition is the possibility to check gauge invariance explicitly within the same kinematics. The consistency relations for $\tilde{F}^{x}_{\lambda'\lambda}$ can be understood as gauge (invariance) conditions:

$$\begin{aligned}
& \Delta_{\mu} F^{\mu}_{\lambda'\lambda} = 0 \\
\Leftrightarrow \quad & \frac{1}{2}\Delta^{+} F^{-}_{\lambda'\lambda} + \frac{1}{2}\Delta^{-} F^{+}_{\lambda'\lambda} - \Delta^{x} F^{x}_{\lambda'\lambda} - \Delta^{y} F^{y}_{\lambda'\lambda} = 0 \\
\Leftrightarrow \quad & \frac{1}{2}\Delta^{-} F^{+}_{\lambda'\lambda} = \Delta^{x} F^{x}_{\lambda'\lambda} \\
\Leftrightarrow \quad & \frac{M^2_{\Delta} - M^2_{N}}{2\bar{P}^{+}} F^{+}_{\lambda'\lambda} = \Delta^{x} F^{x}_{\lambda'\lambda} \\
\Leftrightarrow \quad & \tilde{F}^{x}_{\lambda'\lambda} = \frac{M^2_{\Delta} - M^2_{N}}{\Delta_{x}} \tilde{F}^{+}_{\lambda'\lambda}
\end{aligned}$$

which is the respective amplitude relation (eq. 4.30). The directly calculated amplitudes are non zero however they are quite small. Unfortunately it turns out that gauge invariance is very strongly broken. The other two amplitude relations which we chose to present are satisfied at within 30% error.

In fig. 4.14 we display the DVCS amplitude relations which connect the x and y component amplitudes. These amplitude relations therefore provide a measure for the covariance-consistency of amplitudes which are associated with the same twist. The angular conditions for DVCS amplitudes ($\tilde{G}^{+}_{\frac{3}{2}\downarrow}$ and $\tilde{G}^{x}_{\frac{3}{2}\downarrow}$) are satisfied at 30% level. The relation for $\tilde{G}^{y}_{\frac{1}{2}\uparrow}$ does not look very good. After the experience with the amplitudes $\tilde{F}^{x}_{\lambda'\lambda}$ this does not come as a big surprise. At least for higher values of ξ (where gauge invariance is broken strongly) the relation approaches the usual error of 30%. Finally the angular condition for the - component ($\tilde{G}^{-}_{\frac{3}{2}\downarrow}$) shows that twist 4 associated DVCS amplitudes are strongly inconsistent in the quark model. Even the shape of the calculated amplitude differs from the prediction. People who like reading tea leaves may fancy the fact that for large values of x where valence quark physics dominates this amplitude relation is roughly satisfied.

The amplitude relation in eq. 4.57 which requires covariance for the model amplitudes and assumes genuine higher twist GPDs to be negligible is presented in fig. 4.15. The result is discouraging concerning the possibility to obtain mixed twist GPDs from our model.

In fig. 4.16 we show the leading twist GPDs for $t = -0.5\,GeV^2$ and different values of skewedness ξ. The value for t which we chose here is small enough and thus within the application range of quark models. As discussed in chapter 3 the valence quark picture only provides results in the kinematical range $x \geq \xi$. For large values of x the valence quark contribution is dominant and hence the GPDs which we show here might be predictive in

this regime. This is the case for $H^\star_M(x,\xi,t)$ as we see from the fact that the breaking of the angular condition does not afflict this GPD. This can be understood from the fact that the different prescriptions to obtain $H^\star_M(x,\xi,t)$ from the good LF components provide the same results (within 2-3 % deviation). For $H^\star_E(x,\xi,t)$ and $H^\star_C(x,\xi,t)$ the situation is different. The breaking of covariance destroys the predictive power for these GPDs.

An example for a genuine twist 3 $N \to \Delta$ GPD is presented in fig. 4.17. Again we only provide it to demonstrate that we can treat higher twist GPDs in our formalism. There is little predictive power in the quark model amplitudes for this GPDs as one can see from the fact that the sum rule for this GPD (eq. 4.40) is not satisfied.

In fig. 4.18 we give the vectorial $N \to \Delta$ form factors. The magnetic form factor $G^\star_M(t)$ again is the only predictive result. However the value of $G^\star_M(0)$ is only 70% of the physical value. One may wonder how this is possible as simple SU(6) arguments already describe this value much better. Technically the deviation from the SU(6) result stems from the Melosh rotation (see chapter 3). The shape of $G^\star_M(t)$ follows a dipole behavior which is reasonable in this kinematical regime. The sum rule results for finite skewedness deviate from the direct calculation. The sign of this deviation is different for the $N \to N$ transition. This reveals that sea quark contributions have opposite sign for the $N \to \Delta$ transition as compared to the $N \to N$ transition. In the upper right panel we have displayed $R_{EM} = -\frac{G^\star_E(Q^2)}{G^\star_C(Q^2)}$. R_{SM} in the lower left panel is connected to the $N \to \Delta$ transition form factors via [103]

$$R_{SM} = -\frac{\sqrt{\left[Q^2 + (M_\Delta + M_N)^2\right]\left[Q^2 + (M_\Delta - M_N)^2\right]}}{4M^2_\Delta}\frac{G^\star_C(Q^2)}{G^\star_M(Q^2)} \quad .$$

We remark that our various predictions for R_{EM} and R_{SM} are in the correct order of magnitude. Apart from this observation we have to state that the covariance breaking effects severely afflict the predictive power for these ratios. In fact different prescriptions even lead to different signs and shapes for these ratios. Unless covariance breaking effects are taken care of the light front quark model calculation is not predictive for these observables.

Next we like to report on other **LF** quark model calculations for $N \to \Delta$ transition form factors. The first such calculation was performed in [104]. In this paper only one prescription to extract $G^\star_M$, $G^\star_E$ and $G^\star_C$ was applied. Therefore the issue of inconsistent results for $G^\star_E$ and $G^\star_C$ was not addressed. The problem with the low predictions for $G^\star_M(0)$ has been remarked of course. The author introduced an additional "free" parameter C_Δ in order to orthogonalize the nucleon and Δ **LF** wave functions and thus to enforce the gauge condition. By doing so he obtained reasonable agreement with the $G^\star_M(Q^2)$ experimental data. On the other hand he pointed already out in his paper that this parameter C_Δ is not really free but the Melosh rotation requires $C_\Delta = 1$ which is in strong contrast to the ad hoc tuning $C_\Delta = -0.22355$ which ensures the gauge condition. To our knowledge this ansatz has not been applied subsequently as it lacks a sound theoretical justification. In [105] the authors apply a more sophisticated wave function (harmonic oscillator basis truncated such that d-waves are still included, parameters fitted to baryon spectrum). They consider two different prescriptions and find the same behavior for $G^\star_E(Q^2)$ and $G^\star_C(Q^2)$ as we do. Additionally they include constituent quark form factors which allows for a realistic description of the faster than dipole fall - off behavior of $G^\star_M(Q^2)$ at higher values of Q^2. The difficulty to predict $G^\star_E$ and $G^\star_C$ however remains.

Amplitude relations for the vectorial $p \to \Delta^+$ transition

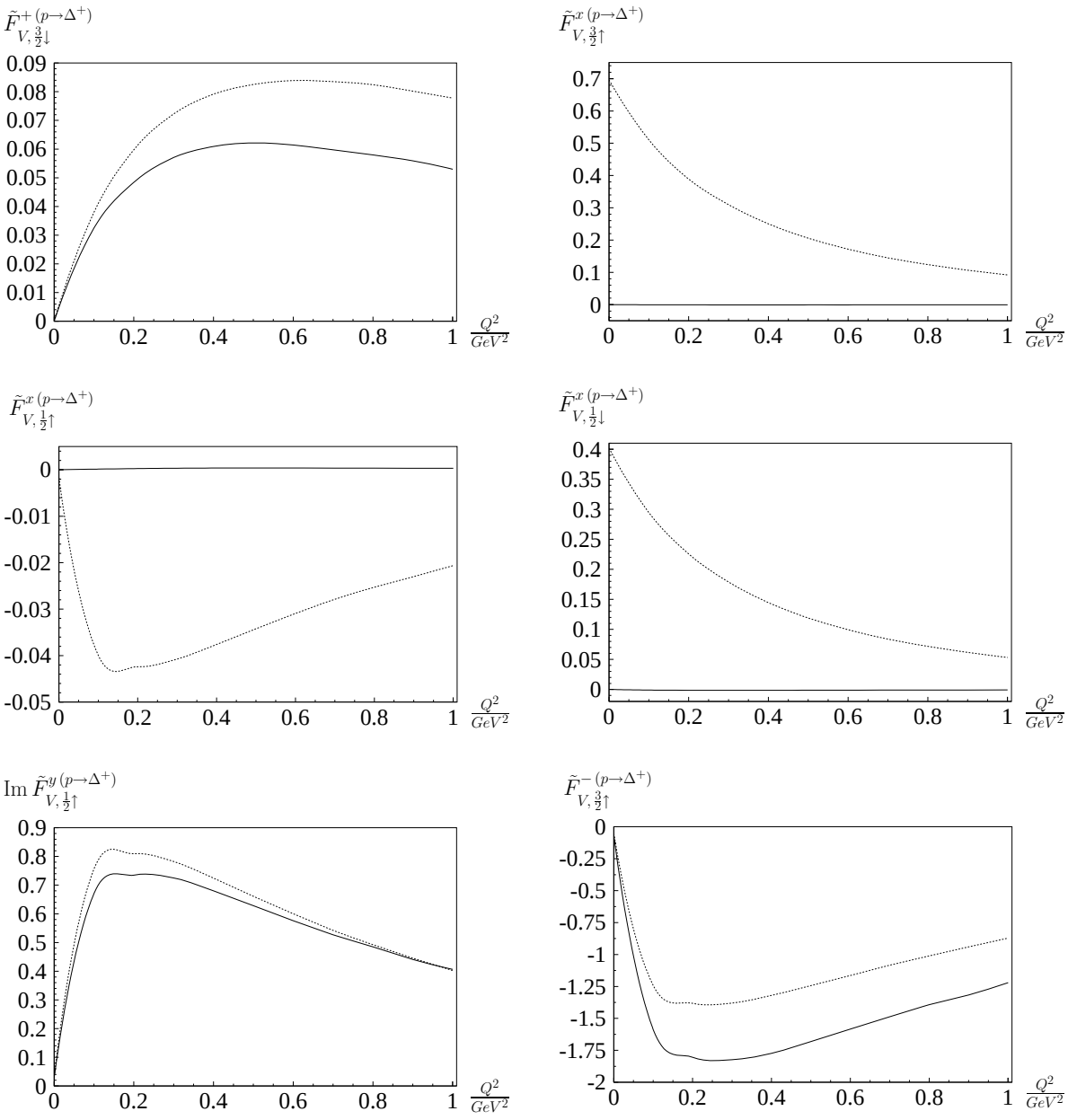

Figure 4.13: *Solid lines: Direct model calculation for the respective amplitudes. Dotted lines: Expected result if the respective amplitude relation (eq. 4.30) holds.*

Amplitude relations for the vectorial $p \to \Delta^+$ transition (eqs. 4.32, 4.42 and 4.43)

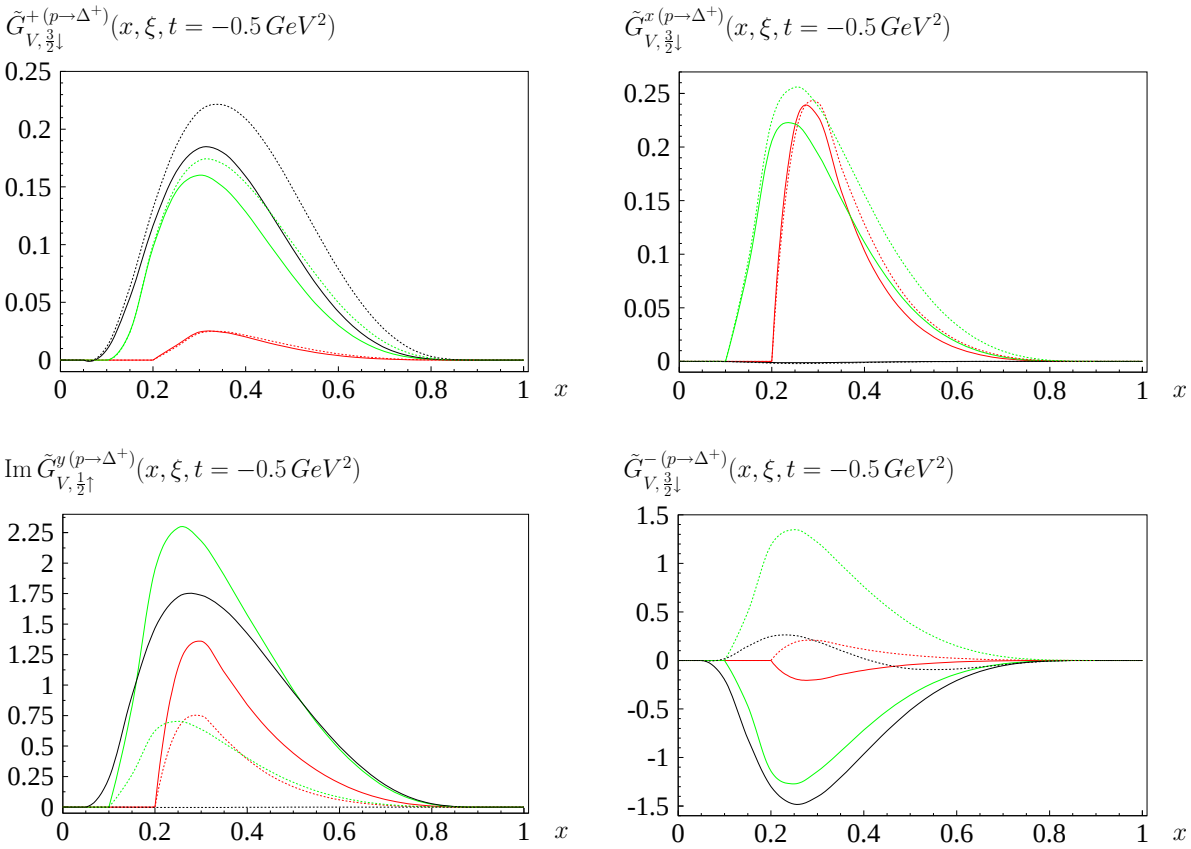

Figure 4.14: *Solid lines: Direct model calculation for the respective amplitude. Dotted lines: Expected result if the respective amplitude relations (eqs. 4.32, 4.42 and 4.43) hold.*
Black curve: Results for $\xi = 0$; Green curve: Results for $\xi = 0.1$; Red curve: Results for $\xi = 0.2$.

Amplitude relation for the vectorial $p \to \Delta^+$ transition (eq. 4.57)

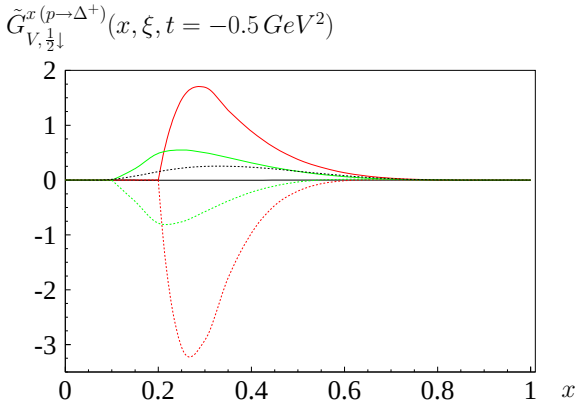

Figure 4.15: *Solid lines: Direct model calculation for* $\tilde{G}^{x\,(p\to\Delta^+)}_{V,\frac{1}{2}\downarrow}$.
Dotted lines: Expected result if the respective amplitude relation (eq. 4.57) holds.
Black curve: Results for $\xi = 0$*; Green curve: Results for* $\xi = 0.1$*; Red curve: Results for* $\xi = 0.2$.

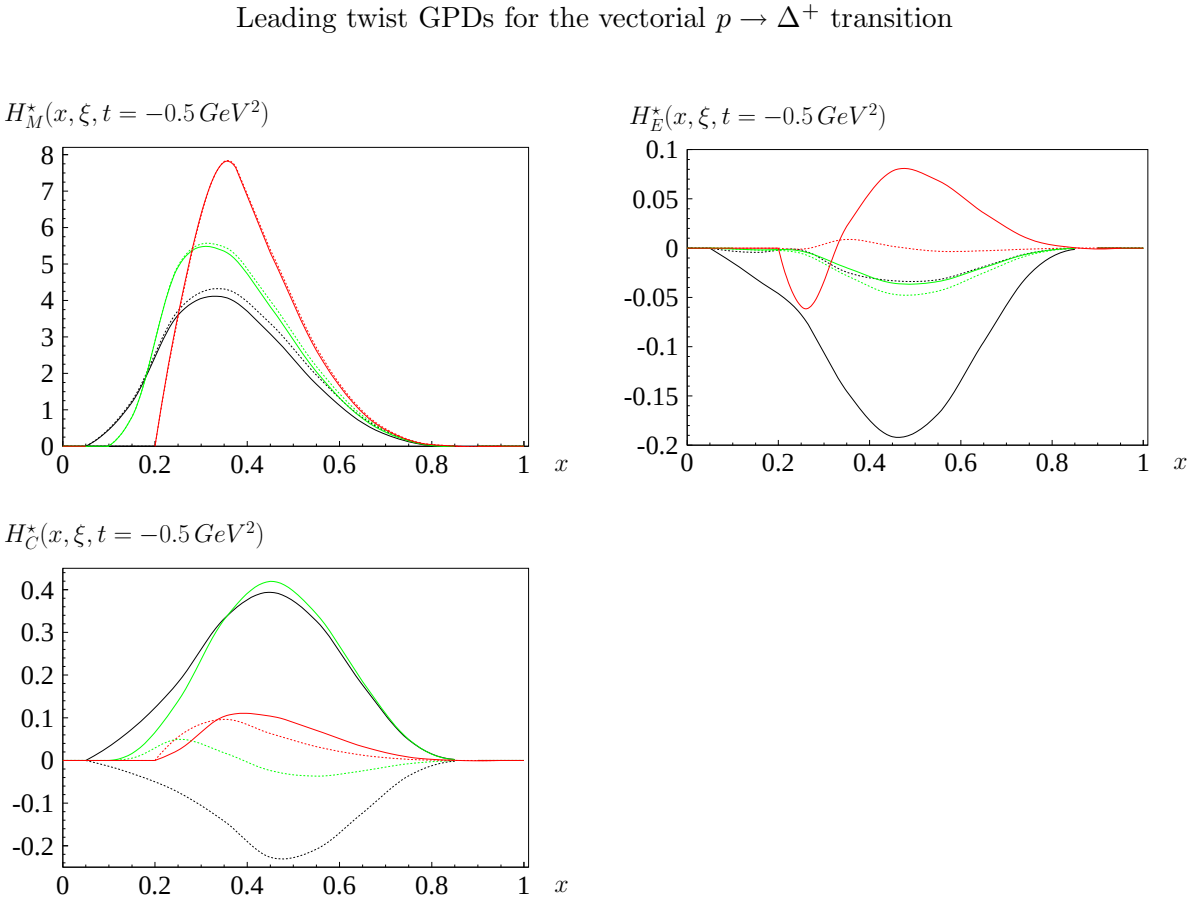

Figure 4.16: *Black curve: $\xi = 0$; Green curve: $\xi = 0.1$; Red curve: $\xi = 0.2$. The GPDs are extracted from the good LF component amplitudes using prescription I (dotted lines) and prescription II (solid lines) as described in sec. 4.2.*

Twist 3 GPD for the vectorial $p \to \Delta^+$ transition

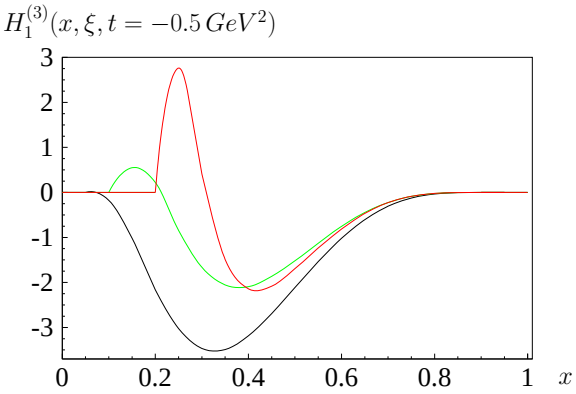

Figure 4.17: *Green curve:* $\xi = 0.1$*; Red curve:* $\xi = 0.2$.
This GPD is obtained using perpendicular LF component amplitudes (eq. 4.41). The result has been obtained using prescription II.

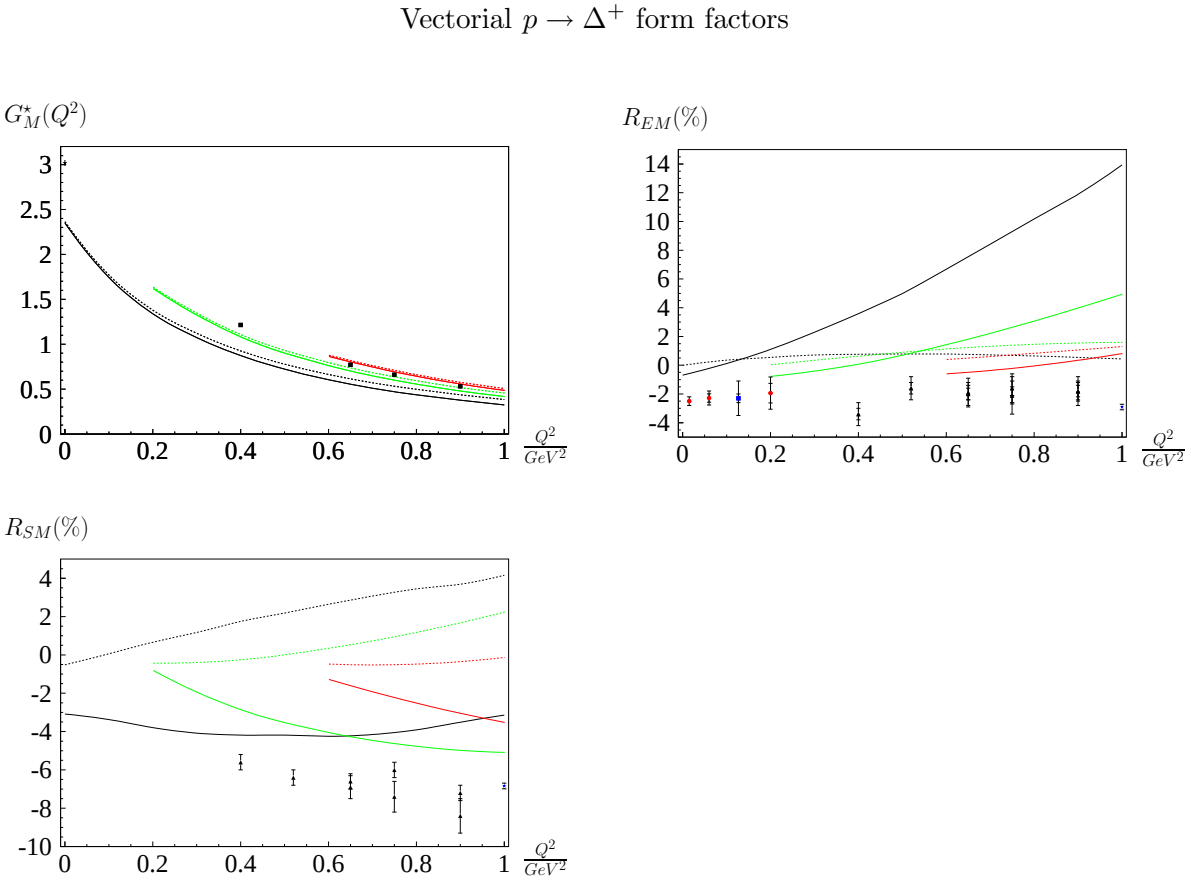

Figure 4.18: *The vectorial nucleon form factors calculated from the good LF amplitudes directly (black curve), evaluated using the sum rules for $\xi = 0$ (on top of the black curve), $\xi = 0.1$ (green curve) and $\xi = 0.2$ (red curve). The dotted curves are the results obtained using prescription I; Results from prescription II are given by solid curves. Experimental data points are extracted from the following references:*
Upper left panel: black star ($G_M^\star(Q^2 = 0\,GeV^2)$: see e.g. [48]), black square: [106].
Upper right panel: black triangle: [106], blue star: [107], blue square: [108], red circle: [109] [110] [111].
Lower left panel: black triangle: [106], blue star: [107].
The connection between the transition form factors and the ratios E/M and S/M is explained in the text.

4.7.4 Axial $p \to \Delta^+$ transition

In fig. 4.19 the amplitude relations among the $\tilde{F}^{\mu}_{\lambda'\lambda}$ are tested. Our first remark concerns the angular condition ($\tilde{F}^{+}_{\frac{3}{2}\downarrow}$). Unlike for the vectorial transition it is already strongly broken for the good LF component amplitude. Also the other amplitude relations which we show here are not satisfied. Only $\tilde{F}^{y}_{\frac{1}{2}\uparrow}$ is roughly (shape, 50% error) in agreement with the prediction. Partly one can understand this behavior since the predicted amplitudes here depend on $\tilde{F}^{x}_{\frac{3}{2}\uparrow}$. Following the experience with the gauge condition for the vectorial $N \to \Delta$ transition which affected the x component amplitudes one can think along the lines of PCAC here which explains the large deviations from the predictions. However $\tilde{F}^{x}_{\frac{3}{2}\uparrow}$ does not appear in the relations for $\tilde{F}^{+}_{\frac{3}{2}\downarrow}$ and $\tilde{F}^{y}_{\frac{1}{2}\uparrow}$. A physical explanation why the axial $N \to \Delta$ amplitudes suffer from much higher covariance breaking effects than the vectorial $N \to \Delta$ amplitudes could be rooted in the fact that the quark model is not adequate for describing pion pole physics. The latter is important for the axial $N \to \Delta$ transition (see e.g. [112]) since

$$C_6(t) = \frac{M_N^2}{M_\pi^2 - t} C_5(t) \quad .$$

In the language of the light front formalism the missing of important pionic contributions translates into the expectation of large higher Fock contributions. This again implies large covariance breaking effects.

In fig. 4.20 we display the DVCS amplitude relations which connect the x and y component amplitudes. These amplitude relations therefore provide a measure for the covariance-consistency of amplitudes which are associated with the same twist. The angular condition for $\tilde{G}^{x}_{\frac{3}{2}\downarrow}$ is satisfied at 30% level. The same can be said about the relation for $\tilde{G}^{y}_{\frac{1}{2}\uparrow}$. The other two amplitude relations are not satisfied (in agreement with the findings from fig. 4.19. We observe an interesting behavior at $\xi = 0.2$. For this value of skewedness the amplitude relations are well satisfied. The reason for this behavior can be found when one looks at the kinematics. For $\xi = 0.2$ and $t = -0.5 GeV^2$ the momentum transfer variable Δ_x is very small. This indicates that for vanishing Δ_x the covariance breaking effects become very small. In retrospect we find the same behavior for the vectorial $N \to \Delta$ DVCS amplitudes.

The amplitude relation in eq. 4.58 which requires covariance for the model amplitudes and assumes genuine higher twist GPDs to be negligible is presented in fig. 4.21. Like for the vectorial $N \to \Delta$ transition the result is discouraging concerning the possibility to obtain mixed twist GPDs from our model. The pole behavior in the predicted amplitude for the value $\xi = 0.2$ stems from the factor Δ_x^2 in the denominator of 4.58.

In fig. 4.22 we show the leading twist GPDs for $t = -0.5\, GeV^2$ and different values of skewedness ξ. The value for t which we chose here is small enough and thus within the application range of quark models. As discussed in chapter 3 the valence quark picture only provides results in the kinematical range $x \geq \xi$. For large values of x the valence quark contribution is dominant and hence the GPDs which we show here might be predictive in this regime. This is the case for $C_1(x, \xi, t)$ as we see from the fact that the breaking of the angular condition does not afflict this GPD. This can be understood from the fact that the

different prescriptions to obtain $C_1(x,\xi,t)$ from the good LF components provide the same results (within 2-3 % deviation). For $C_3(x,\xi,t)$ and $C_4(x,\xi,t)$ the situation is different. The breaking of covariance destroys the predictive power for these GPDs.

An example for a genuine twist 3 $N \to \Delta$ GPD is presented in fig. 4.23. Again we only provide it to demonstrate that we can treat higher twist GPDs in our formalism. There is little predictive power in the quark model amplitudes for this GPDs as one can see from the fact that the sum rule for this GPD is violated (c.f. the three black stars in the middle left panel of fig. 4.24).

In fig. 4.24 we give the axial $N \to \Delta$ form factors. The leading form factor $C_5(t)$ is the only reliable result. For higher values of Q^2 the predictive power of our calculation decreases a little bit. The two different prescriptions produce a slightly different slope in $C_5(t)$. The other axial $N \to \Delta$ form factors suffer from a large inconsistency between the different prescriptions. Additionally a similar remark as for $G_P(t)$ is in order for $C_6(t)$ which is dominated by pion pole physics.

Amplitude relations for the axial $p \to \Delta^+$ transition

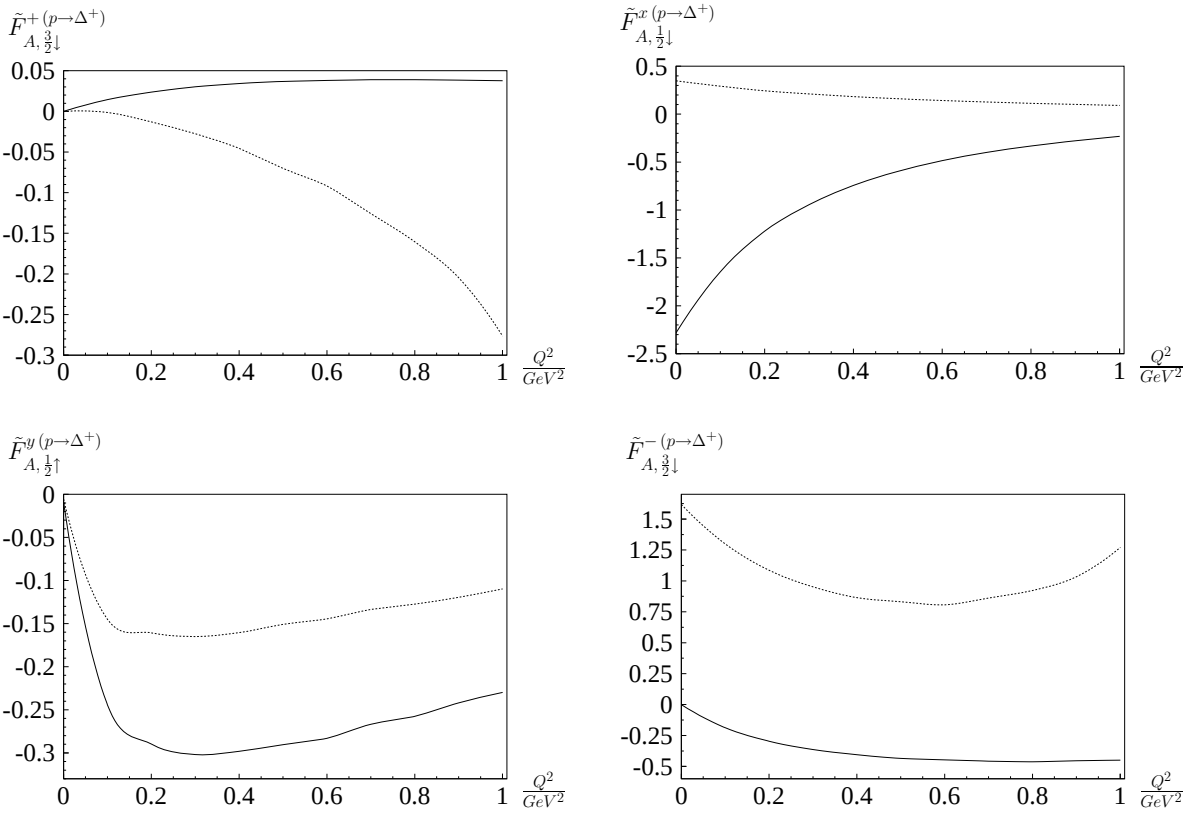

Figure 4.19: *Solid lines: Direct model calculation for the respective amplitudes. Dotted lines: Expected result if the respective amplitude relation (eq. 4.31) holds.*

Amplitude relations for the axial $p \to \Delta^+$ transition (eqs. 4.33, 4.49 and 4.50)

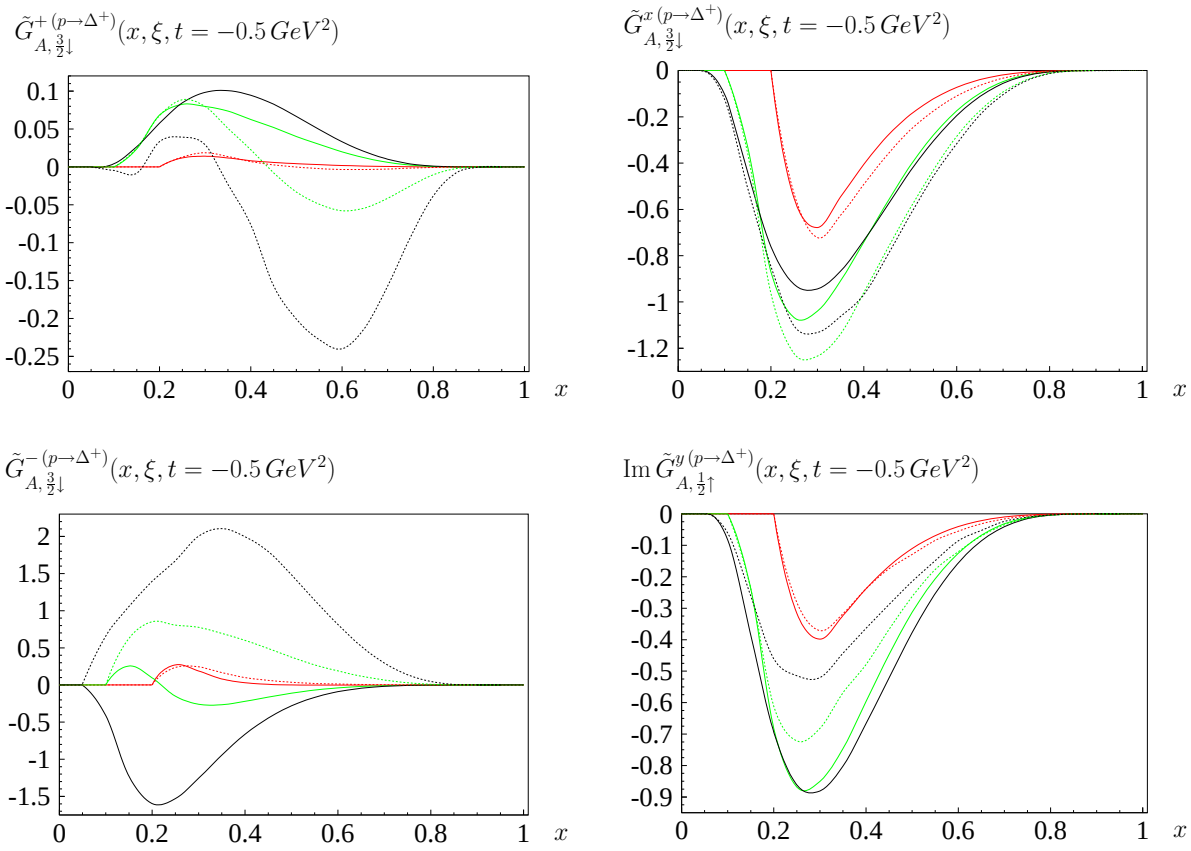

Figure 4.20: *Solid lines: Direct model calculation for the respective amplitude. Dotted lines: Expected result if the respective amplitude relations (eqs. 4.33, 4.49 and 4.50) hold.*
Black curve: Results for $\xi = 0$; Green curve: Results for $\xi = 0.1$; Red curve: Results for $\xi = 0.2$.

Amplitude relation for the axial $p \to \Delta^+$ transition (eq. 4.58)

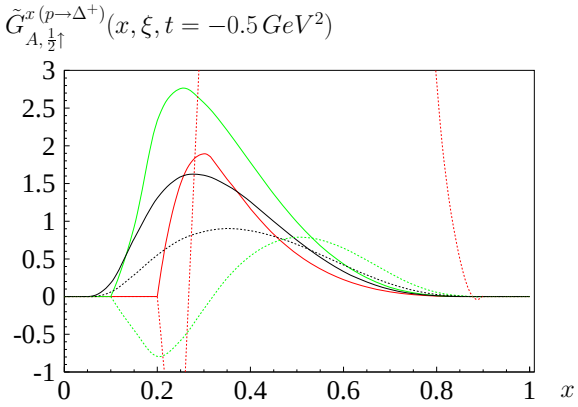

Figure 4.21: *Solid lines: Direct model calculation for* $\tilde{G}^{x\,(p\to\Delta^+)}_{A,\frac{1}{2}\uparrow}$.
Dotted lines: Expected result if the respective amplitude relation (eq. 4.58) holds.
Black curve: Results for $\xi = 0$*; Green curve: Results for* $\xi = 0.1$*; Red curve: Results for* $\xi = 0.2$.

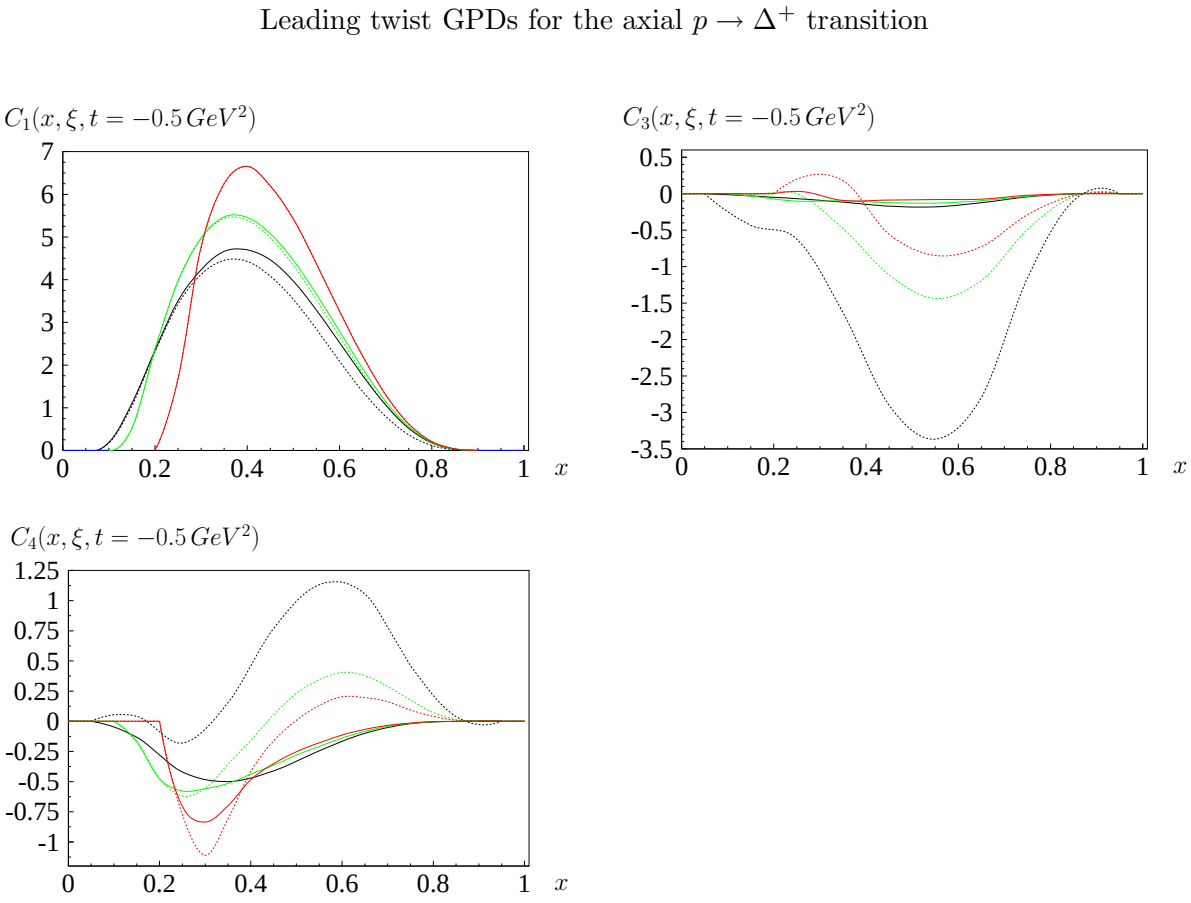

Figure 4.22: *Black curve: $\xi = 0$; Green curve: $\xi = 0.1$; Red curve: $\xi = 0.2$. The GPDs are extracted from the good LF component amplitudes using prescription I (dotted lines) and prescription II (solid lines) as described in sec. 4.2.*

Twist 3 GPDs for the axial $p \to \Delta^+$ transition

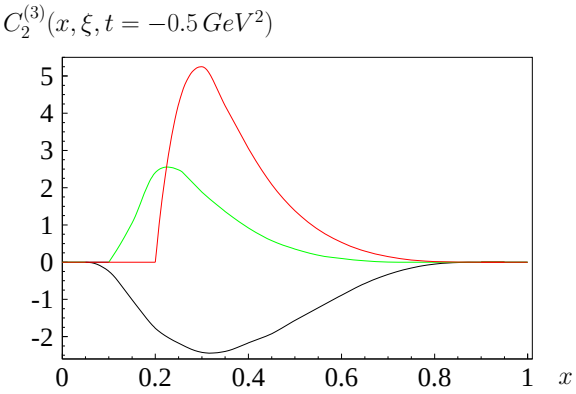

Figure 4.23: *Green curve:* $\xi = 0.1$*; Red curve:* $\xi = 0.2$*.*
This GPD is obtained using perpendicular LF component amplitudes (eq. 4.48). The result has been obtained using prescription II.

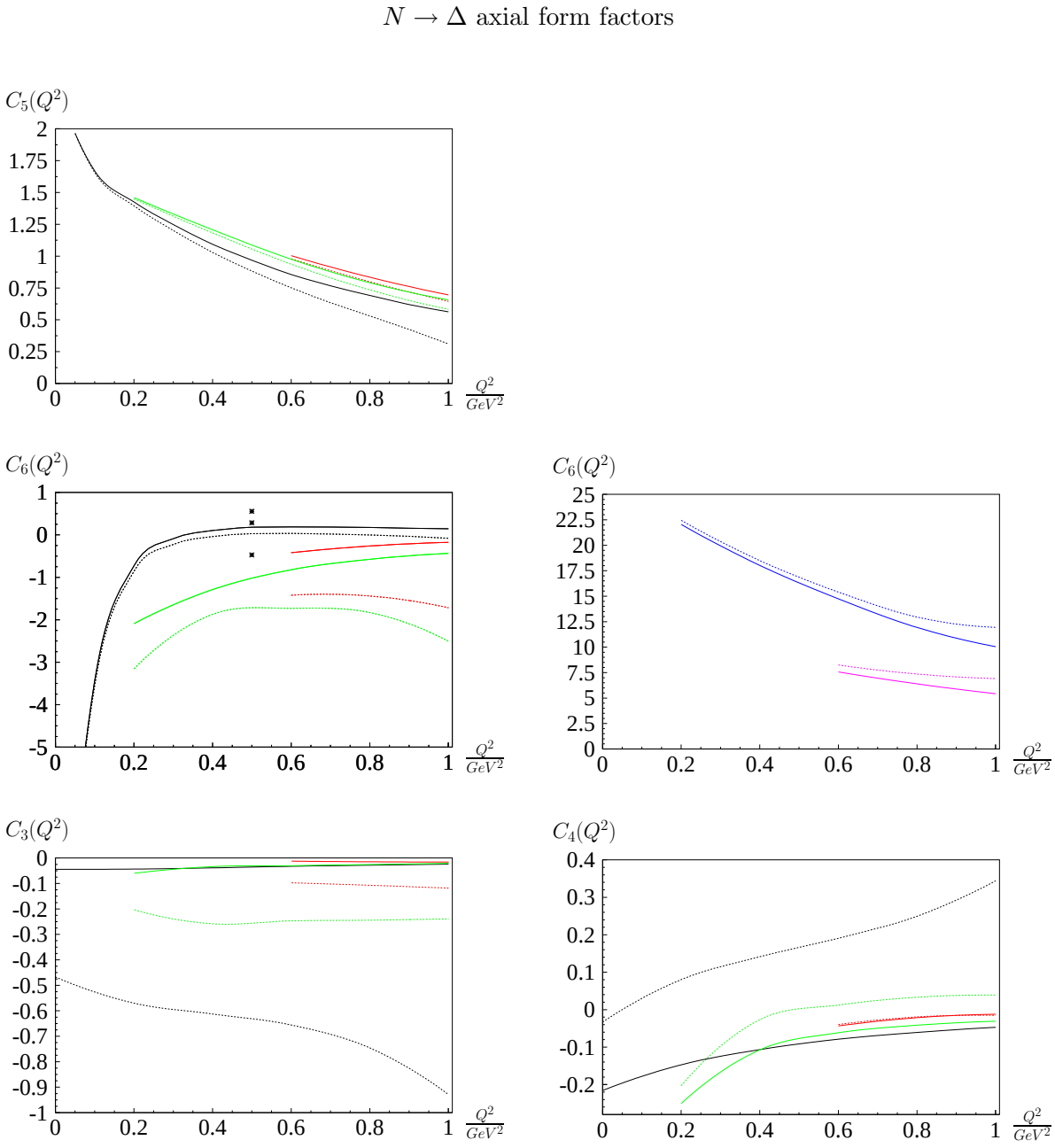

Figure 4.24: *The axial nucleon form factors. Calculated from the good LF amplitudes directly (black curve), evaluated using the sum rules (eqs. 4.44, 4.45 and 4.46) for $\xi = 0.1$ (green) and $\xi = 0.2$ (red). For the evaluation of $C_6(t)$ the sum rule (eq. 4.46) for $\xi = 0.1$ (green) and $\xi = 0.2$ (red) have been used. From the sum rule (eq. 4.44) one obtains curves for $\xi = 0.1$ (blue) and $\xi = 0.2$ (magenta). Finally the sum rule (eq. 4.47) provides three ($\xi = 0$; 0.1 and 0.2) values for $Q^2 = 0.5\,GeV^2$. In all panels the dotted curves are the results obtained using prescription I; Results from prescription II are given by solid curves.*

Chapter 5

Spurious covariants

5.1 Introduction

Whenever one breaks an important physical symmetry in a model calculation the resulting quantities suffer from an inconsistency. While in a fully covariant calculation the choice of the reference system for the model calculation does not influence the result this is no longer true if Lorentz covariance is violated. For instance the brickwall frame in an instant form model calculation (using the impulse approximation) is not only chosen because of its simple kinematics but mainly because covariance breaking effects get minimized in this framework.

Using a light front description one might think at first that this problem does not arise here since Lorentz boosts are kinematical in this Hamiltonian form. But due to the dynamical nature of Lorentz rotations the dependence on the reference frame gets manifest here.

A very convenient way to parameterize this reference frame dependence is to vary the direction of the so called null vector n^μ

$$\begin{aligned} n^\mu x_\mu &= 0 \\ n^2 &= 0 \end{aligned}$$

The conventional choice of this null vector is $n \propto (1, 0, 0, -1)$ which leads to $\tau = x + z$ playing the role of time in this theory, namely light front time. Another choice of the null plane direction can be achieved via a Lorentz rotation and due to relativistic covariance all observables must remain invariant under such a transformation. However in models which do not satisfy Lorentz covariance this is not the case.

In [22] the idea of spurious covariants, which consists of parameterizing the unphysical violation of Lorentz covariance in terms of new pseudo observables which depend on n^μ, was applied to the calculation of vectorial $N \to N$ form factors. This method requires the extension of the set of covariants which parameterize this process by allowing for an additional Lorentz vector in the construction of these covariants, the null vector n^μ.

To illustrate this argument let us start with the vector form factors for the nucleon-nucleon

elastic scattering. Allowing for spurious form factors the transition amplitude can now be parameterized as

$$\langle p' \mid J^\mu(0) \mid p\rangle = \frac{1}{2\sqrt{p'^+p^+}}\bar{u}(p')\left(\sum_i \kappa_i^\mu F^i(Q^2, n\cdot p, n\cdot p') + \sum_j \tilde{\kappa}_j^\mu B^j(Q^2, n\cdot p, n\cdot p')\right)u(p)$$

Here the usual covariants κ_1^μ and κ_2^μ are the structures for the electric and magnetic form factor. Additionally three new covariants $\tilde{\kappa}_j^\mu$ appear with their respective spurious form factors. They are built using the null plane vector e.g $\frac{\not{n}(p^\mu+p'^\mu)}{p\cdot n}$. In order to be on the safe side one must allow for the dependence of all form factors (original ones as well as spurious ones) on all possible invariants which can be built using the null vector. In this case that would be $n\cdot p$ and $n\cdot p'$. Of course if this dependence was a genuine one for the original form factors the introduction of spurious covariants would not be very useful since this would imply that the spurious contributions, i.e. the reference frame dependence due to covariance breaking, could not be separated from the physical ones in a clean way.

Fortunately one can argue without looking into the kinematics that the dependence on these two invariants must vanish: The direction of the null plane is fixed by the direction of the null vector only. n^μ may be multiplied with a scalar without altering the direction of the null plane. Thus the form factors can only depend on the ratio $\frac{n\cdot p}{n\cdot p'}$. However due to $n\cdot q = 0$ this ratio is one.

In order to clarify the relation between the one body current approximation, breaking of Lorentz covariance, reference frame dependence and restoration of reference frame independence in the context of spurious form factors we write the full current as a sum of its contributions each of which can be separated into the physical and the null plane dependent part.

$$\begin{aligned}
J^\mu &= \sum_i J_i^\mu \\
J_i^\mu &= F_i^\mu + B_i^\mu(n^\mu) \\
\langle p' \mid F_i^\mu(0) \mid p\rangle &= \frac{1}{2\sqrt{p'^+p^+}}\bar{u}(p')\Big(\sum_k \kappa_k^\mu F_i^k(Q^2)\Big)u(p) \\
\langle p' \mid B_i^\mu(0) \mid p\rangle &= \frac{1}{2\sqrt{p'^+p^+}}\bar{u}(p')\Big(\sum_k \tilde{\kappa}_k^\mu B_i^k(Q^2)\Big)u(p) \\
F_i(Q^2) &= \sum_k F_i^k(Q^2) \\
B_i(Q^2) &= \sum_k B_i^k(Q^2)
\end{aligned}$$

So now let J_1^μ denote the one body current while other J_i^μ stand for various many body contributions. Thinking of the many body contributions in terms of a Fock space expansion it is clear that when one considers all contributions to the current one has restored Lorentz covariance. Consequently the spurious form factors $B_i^k(Q^2)$ must add up to zero while they

will be non zero individually. On the other hand side the one body contribution $F_i^1(Q^2)$ is reference frame independent although it is still obtained from a one body approximation.

This method of introducing spurious covariants as it was presented in [22] in order to absorb the frame dependence from covariance breaking into spurious covariants can be extended towards axial $N \to N$ transition form factors as well as towards vectorial and axial $N \to \Delta$ form factors in a similar fashion by constructing appropriate spurious covariants for these transitions. We will provide these covariants in the next section.

In [113] the author proposed to apply this formalism to extract GPDs in a similar way. In order to proceed along these lines we have to discuss three special features of GPDs which are different from form factors.

Firstly in DVCS gauge invariance does not impose a constraint on the number of possible covariants. This increases both the number of physical and spurious covariants which are required to parameterize the soft transition amplitude. Secondly we have to reconsider the possible dependence of GPDs on the invariants $n \cdot p$ and $n \cdot p'$ since unlike for the form factors $n \cdot \Delta$ is different from zero. The scaling argument which we gave for elastic scattering still holds. Hence the spurious GPDs can only depend on the ratio $\frac{n \cdot \Delta}{n \cdot \bar{P}}$. The null vector n always projects out the + component of a four vector, even if "+" eventually bears the meaning of e.g. $A^+ = A^0 + A^x$. Hence the ratio above can always be expressed by

$$\frac{n \cdot \Delta}{n \cdot \bar{P}} = \frac{\Delta^+}{\bar{P}^+} = -2\xi \quad .$$

Therefore the spurious GPDs have no additional kinematical- or null plane dependence since they can depend on x, ξ and t anyway.

Finally the extraction of physical and spurious form factors involves bad **LF** transition amplitudes, e.g. $\langle P' \mid J^x(0) \mid P \rangle$. If we want to match the number of possible (physical and spurious) DVCS covariants with transition amplitudes it is obvious that the calculation of physical GPDs also involves such bad **LF** transition amplitudes. However in DVCS twist 2 GPDs are related to good **LF** transition amplitudes; GPDs of twist 3 are connected with perpendicular **LF** transition amplitudes and twist 4 GPDs are obtained from "−" **LF** transition amplitudes. Therefore in order to extract GPDs using the spurious covariants formalism we have to work with mixed twist GPDs. These GPDs have been introduced in 4.6. We have to emphasize that working with mixed twist GPDs implies the assumption that higher twist GPDs are small. To put this statement in a different way this implies that using spurious covariants for GPDs implies two approximations - the covariance breaking approximation (i.e. the impulse approximation in our model) and the assumption that higher twist GPDs are small.

As we have discussed in the last chapter there is no a priori argument why higher twist GPDs should be small compared to the leading twist GPDs. The only indication that nourishes such a hope is that their respective sum rules (mostly) give 0. Our model calculation for selected examples of higher twist GPDs (figs. 4.5, 4.11, 4.17 and 4.23) lead to sizable higher twist GPDs. On the one hand side this casts serious doubts on the applicability of mixed twist GPDs in the framework of a **LF** quark model calculation. On the other hand

side we realized in sec. 4.7 that these higher twist GPDs do not respect their sum rules due to covariance breaking. Therefore we conclude that the chance of higher twist GPDs being small is not generally ruled out and the spurious covariants for mixed twist GPDs might be useful in other model calculations. Thus we pursue the evaluation of mixed twist GPDs for light front quark model amplitudes in the spirit of a toy model calculation.

This restriction does not concern the spurious form factors which we also discuss in this chapter as for them we do not have to imply any additional assumptions.

We point out that in [113] the GPDs under consideration are conceptionally identical with what we have called mixed twist GPDs. The issue of different twists is simply not discussed there. Also additional spurious covariants which only appear for GPDs are not considered in that work.

5.2 Construction of spurious covariants

The construction of spurious covariants follows the same procedure as the construction of any set of covariants. First one has to write down all possible covariants involving momenta, gamma matrices and the null plane vector n^μ which can appear in the transition under consideration. Then one can use symmetries (like time reversal invariance and gauge invariance) and the equations of motions in order to get rid of superfluous covariants.

It is useful to use symmetry arguments to count the number of possible independent transition amplitudes beforehand since the number of covariants that parameterize a transition has to match the number of independent transition amplitudes. Then one only has to ensure that the chosen covariants form a complete set. We use the notation introduced in 4.4

$$G^j = \sum_i C^{ij} T^j$$

where this time G^j enumerates both physical and spurious form factors or GPDs, T^j denotes the independent transition amplitudes (e.g. $G^{+(N\to N)}_{\downarrow\downarrow}$ or $\tilde{G}^{y(N\to N)}_{\uparrow\uparrow}$) and C^{ij} are the kinematical dependent coefficients which connect them. Then considering the matrix (C^{ij}) the criterium for a complete set of covariants is a non vanishing determinant

$$\det C \neq 0 \quad .$$

The next subsections provide our results for the different transition amplitudes.

5.2.1 Vectorial $N \to N$ transition

Counting the number of independent DVCS transition amplitudes we end up with 8 since parity relate the amplitudes $G^{\mu(N\to N)}_{V,\uparrow\uparrow}$ with $G^{\mu(N\to N)}_{V,\downarrow\downarrow}$ and $G^{\mu(N\to N)}_{V,\downarrow\uparrow}$ with $G^{\mu(N\to N)}_{V,\uparrow\downarrow}$. A possible

complete set of covariants reads

$$\begin{aligned}
\kappa_1^\mu &= \gamma^\mu \\
\kappa_2^\mu &= \frac{i\sigma^{\mu\nu}}{2M_N}\Delta_\nu \\
\kappa_3^\mu &= \frac{\Delta^\mu}{2M_N} \\
\tilde{\kappa}_1^\mu &= \frac{\not{n}\bar{P}^\mu}{n\cdot\bar{P}} \\
\tilde{\kappa}_2^\mu &= \frac{2M_N\, n^\mu}{n\cdot\bar{P}} \\
\tilde{\kappa}_3^\mu &= \frac{4M_N^2\, \not{n} n^\mu}{(n\cdot\bar{P})^2} \\
\tilde{\kappa}_4^\mu &= \frac{2iM_N\, \sigma^{\mu\nu} n_\nu}{n\cdot\bar{P}} \\
\tilde{\kappa}_5^\mu &= \frac{\Delta^\mu \not{n}}{n\cdot\bar{P}}
\end{aligned}$$

We have evaluated the respective determinant in eq. 5.1 using Mathematica. Since it does not vanish we have found a complete set of physical and spurious covariants which parameterizes the vectorial soft amplitude $G_{V,\lambda'\lambda}^{\mu(N\to N)}$.

The first three covariants are physical. They correspond to the mixed twist GPDs introduced in eq. 4.51. The other five covariants are spurious. Note that we have chosen to compensate each appearance of the null vector n^μ in the numerator by a factor $n\cdot\bar{P}$ in the denominator in order to avoid arbitrary scaling factors from the null plane vector in the coefficients C^{ij}.

For elastic scattering gauge invariance gives two additional constraints so we expect to find 2 physical gauge invariant covariants, one non contributing non gauge invariant covariant (κ_3^μ), 4 gauge invariant spurious covariants and two non gauge invariant covariants. In fact although neither $\tilde{\kappa}_4^\mu$ nor $\tilde{\kappa}_5^\mu$ satisfy current conservation one can construct a current conserving covariant from κ_3^μ, $\tilde{\kappa}_4^\mu$ and $\tilde{\kappa}_5^\mu$ namely

$$\tilde{\kappa}^\mu = \kappa_3^\mu - \frac{1}{2}\tilde{\kappa}_4^\mu - \frac{t}{8M_N^2}\tilde{\kappa}_5^\mu \quad .$$

Since the violation of gauge invariance is a possible consequence of covariance breaking one should involve all eight covariants in the extraction of the physical form factors. However for the $N\to N$ transition we are in the lucky situation that gauge invariance is satisfied on the level of amplitude relations

$$\begin{aligned}
F_{\uparrow\uparrow}^x &= 0 \\
F_{\downarrow\uparrow}^x &= 0 \quad .
\end{aligned}$$

Therefore for elastic scattering using only κ_1^μ, κ_2^μ, $\tilde{\kappa}_1^\mu$, $\tilde{\kappa}_2^\mu$ and $\tilde{\kappa}_3^\mu$ produces the same result as using all eight covariants.

The spurious covariants $\tilde{\kappa}_1^\mu$, $\tilde{\kappa}_2^\mu$ and $\tilde{\kappa}_3^\mu$ were already given in [22][1]. $\tilde{\kappa}_4^\mu$ and $\tilde{\kappa}_5^\mu$ only appear in DVCS where we find five spurious GPDs.

5.2.2 Axial $N \to N$ transition

Counting the number of independent DVCS transition amplitudes again yields 8 due to parity. A possible complete set of covariants reads

$$\begin{aligned}
\kappa_1^\mu &= \gamma^\mu \gamma_5 \\
\kappa_2^\mu &= \frac{\Delta^\mu}{2M_N} \gamma_5 \\
\kappa_3^\mu &= \frac{i\sigma^{\mu\nu}}{2M_N} \Delta_\nu \gamma_5 \\
\tilde{\kappa}_1^\mu &= \frac{4M_N^2 \, \not{n} n^\mu}{(n \cdot \bar{P})^2} \gamma_5 \\
\tilde{\kappa}_2^\mu &= \frac{2iM_N \, \sigma^{\mu\nu} n_\nu}{n \cdot \bar{P}} \gamma_5 \\
\tilde{\kappa}_3^\mu &= \frac{\not{n} \bar{P}^\mu}{n \cdot \bar{P}} \gamma_5 \\
\tilde{\kappa}_4^\mu &= \frac{2M_N \, n^\mu}{n \cdot \bar{P}} \gamma_5 \\
\tilde{\kappa}_5^\mu &= \frac{\Delta^\mu \not{n}}{n \cdot \bar{P}} \gamma_5 \quad .
\end{aligned}$$

Completeness of this set follows from the counting argument above. We have verified linear independence of this covariant set by evaluating the respective determinant in eq. 5.1 using Mathematica and finding a non zero result.

The first three covariants are physical. They correspond to the mixed twist GPDs introduced in eq. 4.52. The other five covariants are spurious. Again we have chosen to compensate each appearance of the null vector n^μ in the numerator by a factor $n \cdot \bar{P}$ in the denominator in order to avoid arbitrary scaling factors from the null plane vector in the coefficients C^{ij}.

For elastic scattering only $\tilde{\kappa}_1^\mu$, $\tilde{\kappa}_2^\mu$ and $\tilde{\kappa}_3^\mu$ have to be considered. $\tilde{\kappa}_4^\mu$ only contributes to the second class current while $\tilde{\kappa}_5^\mu$ does not have to be considered at all. It is only related to $\langle P', \uparrow | \; J^x \; | \; P, \uparrow \rangle$ which is zero. These statements follow no simple argument like in the case of the non gauge invariant spurious covariants for the vectorial transition. We refer to the following section where these statement will be proven.

5.2.3 Vectorial $N \to \Delta$ transition

Counting the number of independent DVCS transition amplitudes yields 16 since parity relates $G_{V,\frac{3}{2}\uparrow}^{\mu(N\to\Delta)}$ with $G_{V,-\frac{3}{2}\downarrow}^{\mu(N\to\Delta)}$, $G_{V,\frac{1}{2}\uparrow}^{\mu(N\to\Delta)}$ with $G_{V,-\frac{1}{2}\downarrow}^{\mu(N\to\Delta)}$, $G_{V,\frac{1}{2}\downarrow}^{\mu(N\to\Delta)}$ with $G_{V,-\frac{1}{2}\uparrow}^{\mu(N\to\Delta)}$ and $G_{V,\frac{3}{2}\downarrow}^{\mu(N\to\Delta)}$

[1] We have defined $\tilde{\kappa}_2^\mu$ and $\tilde{\kappa}_3^\mu$ such that the corresponding spurious from factors are dimensionless.

with $G_{V,-\frac{3}{2}\uparrow}^{\mu(N\to\Delta)}$. A possible complete set of covariants reads

$$
\begin{aligned}
\kappa_1^{\mu\nu} &= \Big(\gamma^\mu\Delta^\nu - g^{\mu\nu}\not{\Delta}\Big)\gamma_5 \\
\kappa_2^{\mu\nu} &= \Big(P'^\mu\Delta^\nu - (P'\cdot\Delta)g^{\mu\nu}\Big)\gamma_5 \\
\kappa_3^{\mu\nu} &= \Big(\Delta^\mu\Delta^\nu - tg^{\mu\nu}\Big)\gamma_5 \\
\kappa_4^{\mu\nu} &= g^{\mu\nu}\gamma_5 \\
\tilde{\kappa}_1^{\mu\nu} &= \frac{n^\mu\Delta^\nu\gamma_5}{n\cdot\bar{P}} \\
\tilde{\kappa}_2^{\mu\nu} &= \frac{n^\mu n^\nu\not{\Delta}\gamma_5}{(n\cdot\bar{P})^2} \\
\tilde{\kappa}_3^{\mu\nu} &= \frac{n^\mu n^\nu\not{n}\gamma_5}{(n\cdot\bar{P})^3} \\
\tilde{\kappa}_4^{\mu\nu} &= \frac{n^\mu\Delta^\nu\not{n}\gamma_5}{(n\cdot\bar{P})^2} \\
\tilde{\kappa}_5^{\mu\nu} &= \frac{\Big((P'\cdot\Delta)\Delta^\mu - tP'^\mu\Big)n^\nu\gamma_5}{n\cdot\bar{P}} \\
\tilde{\kappa}_6^{\mu\nu} &= \frac{\Big(t\gamma^\mu - \Delta^\mu\not{\Delta}\Big)n^\nu\gamma_5}{n\cdot\bar{P}} \\
\tilde{\kappa}_7^{\mu\nu} &= \frac{\Big(tg^{\mu\nu} - \Delta^\mu\Delta^\nu\Big)\not{n}\gamma_5}{n\cdot\bar{P}} \\
\tilde{\kappa}_8^{\mu\nu} &= \frac{\Big(tP'^\mu\Delta^\nu - (P'\cdot\Delta)\Delta^\mu\Delta^\nu\Big)\not{n}\gamma_5}{n\cdot\bar{P}} \\
\tilde{\kappa}_9^{\mu\nu} &= \frac{\Delta^\mu n^\nu\gamma_5}{n\cdot\bar{P}} \\
\tilde{\kappa}_{10}^{\mu\nu} &= \frac{P'^\mu n^\nu\not{n}\gamma_5}{(n\cdot\bar{P})^2} \\
\tilde{\kappa}_{11}^{\mu\nu} &= \frac{\gamma^\mu n^\nu\not{n}\gamma_5}{(n\cdot\bar{P})^2} \\
\tilde{\kappa}_{12}^{\mu\nu} &= \frac{\gamma^\mu\Delta^\nu\not{n}\gamma_5}{n\cdot\bar{P}} \quad .
\end{aligned}
$$

The first four covariants are physical. They correspond to the mixed twist GPDs $H_1(x,\xi,t)$, $H_2(x,\xi,t)$, $H_3(x,\xi,t)$ and $H_4(x,\xi,t)$. The other 12 covariants are spurious.

For the $N\to\Delta$ form factors only the first three covariants are physical. We have chosen $\tilde{\kappa}_1^{\mu\nu}$ .. $\tilde{\kappa}_8^{\mu\nu}$ such that they are manifestly gauge invariant. Using $\kappa_4^{\mu\nu}$, $\tilde{\kappa}_9^{\mu\nu}$, $\tilde{\kappa}_{10}^{\mu\nu}$, $\tilde{\kappa}_{11}^{\mu\nu}$ and $\tilde{\kappa}_{12}^{\mu\nu}$ one can construct another gauge invariant covariant. Hence we find a total of 12 gauge invariant covariants which agrees with the four constraints from gauge invariance

$$\Delta_\mu F^\mu_{\lambda'\lambda} = 0 \quad .$$

The first four spurious covariants $\tilde{\kappa}_1^{\mu\nu}$, $\tilde{\kappa}_2^{\mu\nu}$, $\tilde{\kappa}_3^{\mu\nu}$ and $\tilde{\kappa}_4^{\mu\nu}$ are chosen such that they only receive contributions from $\langle P' \mid J^- \mid P\rangle$. This reduces the algebraic effort considerably which is a

nice feature since even if we use Mathematica the inversion of 16*16 matrices is quite involved.

We point out that unlike in the $N \to N$ transition also the non gauge invariant covariants have to be taken into account in the extraction of the physical form factors. This will become clear in the next section.

5.2.4 Axial $N \to \Delta$ transition

Counting of the number of independent DVCS transition amplitudes again yields 16 due to parity. A possible complete set of covariants reads

$$
\begin{aligned}
\kappa_1^{\mu\nu} &= g^{\mu\nu} \\
\kappa_2^{\mu\nu} &= \frac{\Delta^\mu \Delta^\nu}{M_N^2} \\
\kappa_3^{\mu\nu} &= \frac{g^{\mu\nu} \not{\Delta} - \gamma^\mu \Delta^\nu}{M_N} \\
\kappa_4^{\mu\nu} &= \frac{2\Big[(\bar{P}\cdot\Delta) g^{\mu\nu} - \bar{P}^\mu \Delta^\nu\Big]}{M_N^2} \\
\tilde{\kappa}_1^{\mu\nu} &= \frac{n^\mu \Delta^\nu}{n\cdot\bar{P}} \\
\tilde{\kappa}_2^{\mu\nu} &= \frac{n^\mu n^\nu \not{\Delta}}{(n\cdot\bar{P})^2} \\
\tilde{\kappa}_3^{\mu\nu} &= \frac{n^\mu n^\nu \not{n}}{(n\cdot\bar{P})^3} \\
\tilde{\kappa}_4^{\mu\nu} &= \frac{n^\mu \Delta^\nu \not{n}}{(n\cdot\bar{P})^2} \\
\tilde{\kappa}_5^{\mu\nu} &= \frac{\Big((\bar{P}\cdot\Delta)\Delta^\mu - t\bar{P}^\mu\Big) n^\nu}{n\cdot\bar{P}} \\
\tilde{\kappa}_6^{\mu\nu} &= \frac{\Big(t\gamma^\mu - \Delta^\mu \not{\Delta}\Big) n^\nu}{n\cdot\bar{P}} \\
\tilde{\kappa}_7^{\mu\nu} &= \frac{\Big(t g^{\mu\nu} - \Delta^\mu \Delta^\nu\Big) \not{n}}{n\cdot\bar{P}} \\
\tilde{\kappa}_8^{\mu\nu} &= \frac{\Big(t\bar{P}^\mu \Delta^\nu - (\bar{P}\cdot\Delta)\Delta^\mu \Delta^\nu\Big) \not{n}}{n\cdot\bar{P}} \\
\tilde{\kappa}_9^{\mu\nu} &= \frac{\Delta^\mu n^\nu}{n\cdot\bar{P}} \\
\tilde{\kappa}_{10}^{\mu\nu} &= \frac{\bar{P}^\mu n^\nu \not{n}}{(n\cdot\bar{P})^2}
\end{aligned}
$$

$$\tilde{\kappa}_{11}^{\mu\nu} = \frac{\gamma^\mu n^\nu \not{n}}{(n\cdot\bar{P})^2}$$
$$\tilde{\kappa}_{12}^{\mu\nu} = \frac{\gamma^\mu \Delta^\nu \not{n}}{n\cdot\bar{P}} \quad .$$

The first four covariants are physical. They correspond to the mixed twist GPDs $C_1(x,\xi,t)$, $C_2(x,\xi,t)$, $C_3(x,\xi,t)$ and $C_4(x,\xi,t)$. The other 12 covariants are spurious.

For the $N \to \Delta$ form factors no simplifications arise since there is no obvious analogy to second class currents for the $N \to \Delta$ transition.

5.3 Orthogonalization of spurious covariants

Having the goal in mind to disentangle physical GPDs and form factors from spurious ones it is clear that the spurious covariants have to be orthogonal to the physical ones. First we have to specify what we mean by orthogonality between covariants. We call two covariants A^μ and B^μ orthogonal if

$$\sum_{\lambda'\lambda} \langle P',\lambda' \mid A^\mu \mid P,\lambda\rangle \langle P',\lambda' \mid B_\mu \mid P,\lambda\rangle^\star = 0 \quad . \tag{5.1}$$

In [22] orthogonality is defined by

$$Tr\left[(\not{P}' + m) A^\mu (\not{P} + m) \bar{B}_\mu\right] = 0 \tag{5.2}$$

with $\bar{B}^\mu := \gamma^0 (B^\mu)^\dagger \gamma^0$. Our definition in eq. 5.1 has the advantage that it can also be applied to the $N \to \Delta$ transition. In this case we call the covariants $A^{\mu\nu}$ and $B^{\mu\nu}$ orthogonal if

$$\sum_{\lambda'\lambda} \left[\bar{u}^\rho_{\lambda'}(P') A^\mu_\rho u_\lambda(P)\right] \left[\bar{u}^\kappa_{\lambda'}(P') B_{\mu\kappa} u_\lambda(P)\right]^\star = 0 \quad .$$

For the $N \to N$ transition we can show equivalence of these two expressions:

$$\begin{aligned}
& \sum_{\lambda',\lambda} \langle P',\lambda' \mid A^\mu \mid P,\lambda\rangle \langle P',\lambda' \mid B_\mu \mid P,\lambda\rangle^\star = 0 \\
\Leftrightarrow \quad & \sum_{\lambda',\lambda} \langle P',\lambda' \mid A^\mu \mid P,\lambda\rangle \langle P,\lambda \mid \bar{B}_\mu \mid P',\lambda'\rangle = 0 \\
\Leftrightarrow \quad & \sum_{\lambda'} \langle P',\lambda' \mid A^\mu \big(\not{P} + m\big) \bar{B}_\mu \mid P',\lambda'\rangle = 0 \\
\Leftrightarrow \quad & Tr\left(\not{P}' + m\right) A^\mu \big(\not{P} + m\big) \bar{B}_\mu = 0
\end{aligned}$$

Here two identities for spin sums have been used:

$$\sum_\lambda u_\lambda(P)\, \bar{u}_\lambda(P) = \not{P} + m$$

and

$$\sum_{\lambda}\Big[\bar{u}_{\lambda}(P)\,A\,u_{\lambda}(P)\Big] = Tr\Big[\big(\not{P}+m\big)A\Big]$$

with A being an arbitrary 4×4 matrix. The latter identity can be proven in a straight forward way by using a complete set of sixteen 4×4 matrices for A (e.g. $1,\gamma_5,\gamma^{\mu},\gamma_5\gamma^{\mu},\sigma^{\mu\nu}$) and verifying the identity for these matrices individually.

Now the orthogonalization procedure is as following. With the physical covariants κ_i^{μ} and the spurious covariants $\tilde{\kappa}_j^{\mu}$ we choose the ansatz

$$\tilde{\kappa}_j'^{\mu} := \tilde{\kappa}_j^{\mu} + \sum_i x_i \cdot \kappa_i^{\mu} \quad .$$

The requirement that $\tilde{\kappa}_j^{\mu}$ is orthogonal to all κ_i^{μ} then provides i equations from which the x_i can be determined.

Finally we can calculate the coefficients

$$\begin{aligned} C^{i\mu}_{\lambda'\lambda} =& \langle P',\lambda' \mid \kappa_i^{\mu} \mid P,\lambda\rangle \\ C^{j\mu}_{\lambda'\lambda} =& \langle P',\lambda' \mid \tilde{\kappa}_j'^{\mu} \mid P,\lambda\rangle \end{aligned}$$

and inverting the resulting matrix we obtain expressions for physical (and spurious) form factors and GPDs in terms of transition amplitudes.

Before we proceed with the orthogonalization procedure for the different processes we like to comment on a statement in [22]:

The authors state that the covariants which we denoted by $\tilde{\kappa}_2^{\mu}$ and $\tilde{\kappa}_3^{\mu}$ require no orthogonalization since unlike $\tilde{\kappa}_1^{\mu}$ they have no part that would not depend on the null vector. The reason why they claim not having to orthogonalize $\tilde{\kappa}_2$ and $\tilde{\kappa}_3$ roots in their procedure to obtain the form factors from the amplitudes. They contract the current operator with the null vector, in which case the latter covariants drop out. However the impact of these covariants should appear in another step in their calculations as can be seen from their equations (15-17).

Particularly if one used an orthogonalized form of the covariants $\tilde{\kappa}_2^{\mu}$ and $\tilde{\kappa}_3^{\mu}$ their coefficients c_4 and c_5 would change. Similarly the expressions for their equations (22-23) would change. We claim that although the argument given by the authors about the structure vanishing after contraction of the current with the null vector is correct they still should orthogonalize the other two spurious covariants in order to obtain correct results. To put this differently we claim that although the non orthogonalized covariants $\tilde{\kappa}_2^{\mu}$ and $\tilde{\kappa}_3^{\mu}$ bear no null vector independent contributions they can still afflict the physical form factors due to mixing effects with $\tilde{\kappa}_1^{\mu}$ which depends on both.

Just for the records we remark that if we work with only $\tilde{\kappa}_1^{\mu}$ being orthogonalized we find back the expressions that are given in equation (23) in [22]. But we do not agree with their neglecting of two spurious covariants in the orthogonalization procedure.

Next we perform the orthogonalization of the spurious covariants for the different transitions.

5.3.1 Vectorial $N \to N$ transition

With the ansatz

$$\begin{aligned}
\tilde{\kappa}_1'^{\mu} =& \tilde{\kappa}_1^{\mu} + x_1\kappa_1^{\mu} + y_1\kappa_2^{\mu} + z_1\kappa_3^{\mu} \\
\tilde{\kappa}_2'^{\mu} =& \tilde{\kappa}_2^{\mu} + x_2\kappa_1^{\mu} + y_2\kappa_2^{\mu} + z_2\kappa_3^{\mu} \\
\tilde{\kappa}_3'^{\mu} =& \tilde{\kappa}_3^{\mu} + x_3\kappa_1^{\mu} + y_3\kappa_2^{\mu} + z_3\kappa_3^{\mu} \\
\tilde{\kappa}_4'^{\mu} =& \tilde{\kappa}_4^{\mu} + x_4\kappa_1^{\mu} + y_4\kappa_2^{\mu} + z_4\kappa_3^{\mu} \\
\tilde{\kappa}_5'^{\mu} =& \tilde{\kappa}_5^{\mu} + x_5\kappa_1^{\mu} + y_5\kappa_2^{\mu} + z_5\kappa_3^{\mu}
\end{aligned}$$

the above described orthogonalization procedure yields

$$\begin{aligned}
x_1 =& -\frac{4m^2}{4m^2 - t} \\
y_1 =& \frac{4m^2}{4m^2 - t} \\
z_1 =& 0
\end{aligned}$$

$$\begin{aligned}
x_2 =& -\frac{8m^2}{4m^2 - t} \\
y_2 =& \frac{8m^2}{4m^2 - t} \\
z_2 =& \frac{8\xi m^2}{t}
\end{aligned}$$

$$\begin{aligned}
x_3 =& -\frac{8m^2\Big(4(2+\xi^2)m^2 + (1-\xi^2)t\Big)}{(4m^2 - t)^2} \\
y_3 =& \frac{32m^4\Big(4\xi^2 m^2 + (3-\xi^2)t\Big)}{(4m^2 - t)^2 t} \\
z_3 =& \frac{64\xi m^4}{(4m^2 - t)t}
\end{aligned}$$

$$\begin{aligned}
x_4 =& 0 \\
y_4 =& \frac{8\xi m^2}{t} \\
z_4 =& \frac{8m^2}{4m^2 - t}
\end{aligned}$$

$$\begin{aligned} x_5 =& 0 \\ y_5 =& 0 \\ z_5 =& -\frac{8m^2}{4m^2-t} \quad . \end{aligned} \tag{5.3}$$

Equipped with the orthogonalized set of spurious covariants we can now proceed and express the form factors in terms of all possible amplitudes. For DVCS these amplitudes can now be decomposed into

$$\begin{aligned} G^{\mu}_{\lambda',\lambda} &= \sum_i C^{(i)\mu}_{\lambda',\lambda} A^i(x,\xi,t) + \sum_k \tilde{C}^{(k)\mu}_{\lambda',\lambda} B^k(x,\xi,t) \\ C^{(i)\mu}_{\lambda',\lambda} &= \frac{1}{2\bar{P}^+}\bar{u}(P',\lambda')\kappa_i^{\mu} u(P,\lambda) \\ \tilde{C}^{(i)\mu}_{\lambda',\lambda} &= \frac{1}{2\bar{P}^+}\bar{u}(P',\lambda')\tilde{\kappa}_i'^{\mu} u(P,\lambda) \\ \Big\{A^i(x,\xi,t), B^k(x,\xi,t)\Big\} &= \big\{H_{(\star)}(x,\xi,t), E_{(\star)}(x,\xi,t), X_{(\star)}(x,\xi,t), B_1(x,\xi,t), B_2(x,\xi,t), \\ &\qquad B_3(x,\xi,t), B_4(x,\xi,t), B_5(x,\xi,t)\big\} \quad . \end{aligned}$$

By inverting this relation one obtains an unambiguous expression for both, physical and spurious GPDs. They can be expressed in terms of the amplitude relations. We find

$$\begin{aligned} H_{(\star)}(x,\xi,t) =& \frac{\sqrt{1-\xi^2}(\Delta_x^2+8M_N^2)}{4(\Delta_x^2+4M_N^2)}\tilde{G}^+_{\uparrow\uparrow} - \frac{\sqrt{1-\xi^2}\Delta_x M_N}{2(\Delta_x^2+4M_N^2)}\tilde{G}^+_{\downarrow\uparrow} + \frac{\xi\sqrt{1-\xi^2}\Delta_x}{2(\Delta_x^2+4M_N^2)}\tilde{G}^x_{\uparrow\uparrow} \\ &+ \frac{\xi\sqrt{1-\xi^2}M_N}{\Delta_x^2+4M_N^2}\tilde{G}^x_{\downarrow\uparrow} - i\frac{\sqrt{1-\xi^2}\Delta_x}{2(\Delta_x^2+4M_N^2)}\tilde{G}^y_{\uparrow\uparrow} - i\frac{\xi\sqrt{1-\xi^2}M_N}{\Delta_x^2+4M_N^2}\tilde{G}^y_{\downarrow\uparrow} \\ &+ \frac{(1-\xi^2)^{\frac{3}{2}}(8M_N^2-\Delta_x^2)}{4(\Delta_x^2+4M_N^2)^2}\tilde{G}^-_{\uparrow\uparrow} - \frac{3(1-\xi^2)^{\frac{3}{2}}\Delta_x M_N}{2(\Delta_x^2+4M_N^2)^2}\tilde{G}^-_{\downarrow\uparrow} \\ E_{(\star)}(x,\xi,t) =& \frac{\sqrt{1-\xi^2}}{(\Delta_x^2+4M_N^2)(\Delta_x^2+4\xi^2M_N^2)}\Bigg(-\big[(1+\xi^2)\Delta_x^2+8\xi^2M_N^2\big]M_N^2\tilde{G}^+_{\uparrow\uparrow} \\ &+ \Delta_x M_N\big[\Delta_x^2+2(1+\xi^2)M_N^2\big]\tilde{G}^+_{\downarrow\uparrow} + 2\xi(1-\xi^2)\Delta_x M_N^2\tilde{G}^x_{\uparrow\uparrow} \\ &+ 4\xi(1-\xi^2)M_N^3\tilde{G}^x_{\downarrow\uparrow} - 2i(1-\xi^2)\Delta_x M_N^2\tilde{G}^y_{\uparrow\uparrow} - 4i\xi(1-\xi^2)M_N^3\tilde{G}^y_{\downarrow\uparrow} \\ &- \frac{(1-\xi^2)M_N^2\big[(3-\xi^2)\Delta_x^2+8\xi^2M_N^2\big]}{\Delta_x^2+4M_N^2}\tilde{G}^-_{\uparrow\uparrow} \\ &- \frac{(1-\xi^2)\Delta_x M_N\big[(2-6\xi^2)M_N^2-\Delta_x^2\big]}{\Delta_x^2+4M_N^2}\tilde{G}^-_{\downarrow\uparrow}\Bigg) \\ X_{(\star)}(x,\xi,t) =& \frac{\sqrt{1-\xi^2}}{\Delta_x^2+4\xi^2M_N^2}\Bigg(-2\xi M_N^2\tilde{G}^+_{\uparrow\uparrow} + \xi\Delta_x M_N\tilde{G}^+_{\downarrow\uparrow} + \frac{4(1-\xi^2)\Delta_x M_N^2}{\Delta_x^2+4M_N^2}\tilde{G}^x_{\uparrow\uparrow} \\ &- \frac{2(1-\xi^2)\Delta_x^2 M_N}{\Delta_x^2+4M_N^2}\tilde{G}^x_{\downarrow\uparrow} + \frac{2\xi(1-\xi^2)M_N^2}{\Delta_x^2+4M_N^2}\tilde{G}^-_{\uparrow\uparrow} - \frac{\xi(1-\xi^2)\Delta_x M_N}{\Delta_x^2+4M_N^2}\tilde{G}^-_{\downarrow\uparrow}\Bigg) \quad . \end{aligned} \tag{5.4}$$

We note that if we introduce the consistency relations in eq. 4.55 we find back the expressions from eq. 4.53. This is obvious since if the consistency relations are satisfied there are no

covariance breaking effects which have to be absorbed into spurious GPDs.

For elastic scattering one can read off from eq. 5.3 that $\tilde{\kappa}_1'^{\mu}$, $\tilde{\kappa}_2'^{\mu}$ and $\tilde{\kappa}_3'^{\mu}$ are gauge non invariant covariants. The amplitudes can be decomposed into

$$\begin{aligned}
F^{\mu}_{\lambda',\lambda} &= \sum_i C^{(i)\mu}_{\lambda',\lambda} F^i(Q^2) + \sum_k \tilde{C}^{(k)\mu}_{\lambda',\lambda} B^k(Q^2) \\
C^{(i)\mu}_{\lambda',\lambda} &= \frac{1}{2\sqrt{P'^+P^+}} \bar{u}(P',\lambda') \kappa_i^{\mu} u(P,\lambda) \\
\tilde{C}^{(i)\mu}_{\lambda',\lambda} &= \frac{1}{2\sqrt{P'^+P^+}} \bar{u}(P',\lambda') \tilde{\kappa}_i'^{\mu} u(P,\lambda) \\
\Big\{ F^i(Q^2), B^k(Q^2) \Big\} &= \big\{ F_1(Q^2), F_2(Q^2), F_3(Q^2), B_1(Q^2), B_2(Q^2), B_3(Q^2), B_4(Q^2), B_5(Q^2) \big\} \quad .
\end{aligned}$$

For the time being we allow for the unphysical form factors $F_3(Q^2)$, $B_4(Q^2)$ and $B_5(Q^2)$ which are forbidden by gauge invariance. We will discuss this issue in a moment.

$\lambda' \lambda\, \mu$	$C^{1\mu}_{\lambda'\lambda}$	$C^{2\mu}_{\lambda'\lambda}$	$\tilde{C}^{1\mu}_{\lambda'\lambda}$	$\tilde{C}^{2\mu}_{\lambda'\lambda}$	$\tilde{C}^{3\mu}_{\lambda'\lambda}$	$C^{3\mu}_{\lambda'\lambda}$	$\tilde{C}^{4\mu}_{\lambda'\lambda}$	$\tilde{C}^{5\mu}_{\lambda'\lambda}$
$\uparrow\uparrow$ +	x		x					
$\downarrow\uparrow$ +		x						
$\uparrow\uparrow$ y	x	x						
$\uparrow\uparrow$ −	x	x	x	x	x			
$\downarrow\uparrow$ −	x	x		x				
$\uparrow\uparrow$ x						x		x
$\downarrow\uparrow$ x						x	x	
$\downarrow\uparrow$ y							x	

Figure 5.1: *The non vanishing coefficients for elastic $N \to N$ scattering are denoted by an x.*

From fig. 5.1 we see that κ_3^{μ}, $\tilde{\kappa}_4'^{\mu}$ and $\tilde{\kappa}_5'^{\mu}$ are not required for the extraction of the physical form factors. They can be obtained by inverting the corresponding 5*5 matrix. We emphasize that the reason why κ_3^{μ}, $\tilde{\kappa}_4'^{\mu}$ and $\tilde{\kappa}_5'^{\mu}$ are not required is neither that these covariants are not gauge invariant nor that they are orthogonal to the physical covariants. We find for the form factors expressed in terms of the amplitude relations:

$$\begin{aligned}
F_1(t) =& \frac{1}{4(\Delta_x^2 + 4M_N^2)^2} \Bigg((\Delta_x^4 + 12\Delta_x^2 M_N^2 + 32 M_N^4) \tilde{F}^+_{\uparrow\uparrow} - (8\Delta_x M_N^3 + 2\Delta_x^3 M_N) \tilde{F}^+_{\downarrow\uparrow} \\
& - i(8\Delta_x M_N^2 + 2\Delta_x^3) \tilde{F}^y_{\uparrow\uparrow} + (8M_N^2 - \Delta_x^2) \tilde{F}^-_{\uparrow\uparrow} - 6\Delta_x M_N \tilde{F}^-_{\downarrow\uparrow} \Bigg) \\
F_2(t) =& \frac{1}{(\Delta_x^3 + 4\Delta_x M_N^2)^2} \Bigg(-(\Delta_x^4 M_N^2 + 4\Delta_x^2 M_N^4) \tilde{F}^+_{\uparrow\uparrow} + (\Delta_x^5 M_N + 6\Delta_x^3 M_N^3 + 8\Delta_x M_N^5) \tilde{F}^+_{\downarrow\uparrow} \\
& - i(2\Delta_x^3 M_N^2 + 8\Delta_x M_N^4) \tilde{F}^y_{\uparrow\uparrow} - 3\Delta_x^2 M_N^2 \tilde{F}^-_{\uparrow\uparrow} + (\Delta_x^3 M_N - 2M_N^3 \Delta_x) \tilde{F}^-_{\downarrow\uparrow} \Bigg) \\
F_3(t) =& \frac{4M_N^2}{\Delta_x(\Delta_x^2 + 4M_N^2)} \tilde{F}^x_{\uparrow\uparrow} - \frac{2M_N}{\Delta_x^2 + 4M_N^2} \tilde{F}^x_{\downarrow\uparrow} \quad .
\end{aligned} \tag{5.5}$$

Again we remark that if we introduce the consistency relations in eq. 4.28 we find back the expressions from eq. 4.16. Additionally the only terms in $F_3(t)$ are $\tilde{F}^x_{\uparrow\uparrow}$ and $\tilde{F}^x_{\downarrow\uparrow}$ which are zero for elastic scattering.

5.3.2 Axial $N \to N$ transition

With the ansatz

$$\begin{aligned}
\tilde{\kappa}_1'^{\mu} =& \tilde{\kappa}_1^{\mu} + x_1\kappa_1^{\mu} + y_1\kappa_2^{\mu} + z_1\kappa_3^{\mu} \\
\tilde{\kappa}_2'^{\mu} =& \tilde{\kappa}_2^{\mu} + x_2\kappa_1^{\mu} + y_2\kappa_2^{\mu} + z_2\kappa_3^{\mu} \\
\tilde{\kappa}_3'^{\mu} =& \tilde{\kappa}_3^{\mu} + x_3\kappa_1^{\mu} + y_3\kappa_2^{\mu} + z_3\kappa_3^{\mu} \\
\tilde{\kappa}_4'^{\mu} =& \tilde{\kappa}_4^{\mu} + x_4\kappa_1^{\mu} + y_4\kappa_2^{\mu} + z_4\kappa_3^{\mu} \\
\tilde{\kappa}_5'^{\mu} =& \tilde{\kappa}_5^{\mu} + x_5\kappa_1^{\mu} + y_5\kappa_2^{\mu} + z_5\kappa_3^{\mu}
\end{aligned}$$

the orthogonalization procedure gives

$$\begin{aligned}
x_1 =& 8m^2\Big[\frac{1}{4m^2-t} + \frac{\xi^2}{t}\Big] \\
y_1 =& -\frac{32m^4\Big[(1-3\xi^2)t + 12\xi^2m^2\Big]}{(4m^2-t)t^2} \\
z_1 =& -\frac{64\xi m^4}{(4m^2-t)t}
\end{aligned}$$

$$\begin{aligned}
x_2 =& -\frac{8m^2}{4m^2-t} \\
y_2 =& \frac{8m^2}{4m^2-t} \\
z_2 =& \frac{8\xi m^2}{t}
\end{aligned}$$

$$\begin{aligned}
x_3 =& 0 \\
y_3 =& 0 \\
z_3 =& -\frac{4\xi m^2}{t}
\end{aligned}$$

$$\begin{aligned}
x_4 =& 0 \\
y_4 =& \frac{8\xi m^2}{t} \\
z_4 =& \frac{8m^2}{4m^2-t}
\end{aligned}$$

$$\begin{aligned} x_5 =& 0 \\ y_5 =& \frac{8\xi m^2}{t} \\ z_5 =& 0 \quad . \end{aligned}$$

Equipped with the orthogonalized set of spurious covariants we can now proceed and express the form factors in terms of all possible amplitudes. For DVCS these amplitudes can now be decomposed into

$$\begin{aligned} G^{\mu}_{\lambda',\lambda} &= \sum_i C^{(i)\mu}_{\lambda',\lambda} A^i(x,\xi,t) + \sum_k \tilde{C}^{(k)\mu}_{\lambda',\lambda} B^k(x,\xi,t) \\ C^{(i)\mu}_{\lambda',\lambda} &= \frac{1}{2\bar{P}^+} \bar{u}(P',\lambda') \kappa_i^{\mu} u(P,\lambda) \\ \tilde{C}^{(i)\mu}_{\lambda',\lambda} &= \frac{1}{2\bar{P}^+} \bar{u}(P',\lambda') \tilde{\kappa}_i'^{\mu} u(P,\lambda) \\ \Big\{ A^i(x,\xi,t), B^k(x,\xi,t) \Big\} &= \Big\{ \tilde{H}_{(\star)}(x,\xi,t), \tilde{E}_{(\star)}(x,\xi,t), \tilde{X}_{(\star)}(x,\xi,t), B_1(x,\xi,t), B_2(x,\xi,t), \\ &\qquad B_3(x,\xi,t), B_4(x,\xi,t), B_5(x,\xi,t) \} \quad . \end{aligned}$$

By inverting this relation one obtains an unambiguous expression for both, physical and spurious GPDs. They can be expressed in terms of the amplitude relations. We find

$$\begin{aligned} \tilde{H}_{(\star)}(x,\xi,t) =& \frac{\sqrt{1-\xi^2}\Delta_x^2}{4(\Delta_x^2+4\xi^2M_N^2)} \tilde{G}^+_{\uparrow\uparrow} + \frac{\xi\sqrt{1-\xi^2}\Delta_x M_N}{2(\Delta_x^2+4\xi^2M_N^2)} \tilde{G}^+_{\downarrow\uparrow} + \frac{\xi\sqrt{1-\xi^2}\Delta_x}{2(\Delta_x^2+4\xi^2M_N^2)} \tilde{G}^x_{\uparrow\uparrow} \\ &+ \frac{\xi^2\sqrt{1-\xi^2}M_N}{\Delta_x^2+4\xi^2M_N^2} \tilde{G}^x_{\downarrow\uparrow} - i\frac{\sqrt{1-\xi^2}\Delta_x}{2(\Delta_x^2+4M_N^2)} \tilde{G}^y_{\uparrow\uparrow} - i\frac{\sqrt{1-\xi^2}M_N}{\Delta_x^2+4M_N^2} \tilde{G}^y_{\downarrow\uparrow} \\ &- \frac{(1-\xi^2)^{\frac{3}{2}}\Delta_x^2}{4(\Delta_x^2+4M_N^2)(\Delta_x^2+4\xi^2M_N^2)} \tilde{G}^-_{\uparrow\uparrow} - \frac{\xi(1-\xi^2)^{\frac{3}{2}}\Delta_x M_N}{2(\Delta_x^2+4M_N^2)(\Delta_x^2+4\xi^2M_N^2)} \tilde{G}^-_{\downarrow\uparrow} \\ \tilde{E}_{(\star)}(x,\xi,t) =& \frac{\sqrt{1-\xi^2}}{(\Delta_x^2+4\xi^2M_N^2)} \Bigg(\frac{\big[(1-3\xi^2)\Delta_x^2 - 8\xi^2M_N^2\big]M_N^2}{\Delta_x^2+4\xi^2M_N^2} \tilde{G}^+_{\uparrow\uparrow} \\ &+ \frac{\xi\Delta_x M_N\big[\Delta_x^2+(6-2\xi^2)M_N^2\big]}{\Delta_x^2+4\xi^2M_N^2} \tilde{G}^+_{\downarrow\uparrow} + \frac{6\xi(1-\xi^2)\Delta_x M_N^2}{\Delta_x^2+4\xi^2M_N^2} \tilde{G}^x_{\uparrow\uparrow} \\ &- \frac{2(1-\xi^2)M_N(\Delta_x^2-2\xi^2M_N^2)}{\Delta_x^2+4\xi^2M_N^2} \tilde{G}^x_{\downarrow\uparrow} - i\frac{2(1-\xi^2)\Delta_x M_N^2}{\Delta_x^2+4M_N^2} \tilde{G}^y_{\uparrow\uparrow} \\ &- i\frac{4(1-\xi^2)M_N^3}{\Delta_x^2+4M_N^2} \tilde{G}^y_{\downarrow\uparrow} - \frac{(1-\xi^2)M_N\big[(1-3\xi^2)\Delta_x^2-8\xi^2M_N^2\big]}{(\Delta_x^2+4M_N^2)(\Delta_x^2+4\xi^2M_N^2)} \tilde{G}^-_{\uparrow\uparrow} \\ &- \frac{\xi(1-\xi^2)\Delta_x M_N\big[\Delta_x^2+(6-2\xi^2)M_N^2\big]}{(\Delta_x^2+4M_N^2)(\Delta_x^2+4\xi^2M_N^2)} \tilde{G}^-_{\downarrow\uparrow} \Bigg) \\ \tilde{X}_{(\star)}(x,\xi,t) =& \frac{\sqrt{1-\xi^2}M_N}{\Delta_x^2+4\xi^2M_N^2} \Bigg(-2\xi M_N \tilde{G}^+_{\uparrow\uparrow} + \Delta_x \tilde{G}^+_{\downarrow\uparrow} - \frac{2\xi(1-\xi^2)M_N}{\Delta_x^2+4M_N^2} \tilde{G}^-_{\uparrow\uparrow} \\ &+ \frac{(1-\xi^2)\Delta_x}{\Delta_x^2+4M_N^2} \tilde{G}^-_{\downarrow\uparrow} \Bigg) \quad . \end{aligned} \tag{5.6}$$

We note that if we introduce the consistency relations in eq. 4.56 we find back the expressions from eq. 4.54. This is obvious since if the consistency relations are satisfied there are no covariance breaking effects which have to be absorbed into spurious GPDs.

For elastic scattering the amplitudes can be decomposed into

$$\begin{aligned}
F^{\mu}_{\lambda',\lambda} &= \sum_i C^{(i)\mu}_{\lambda',\lambda} F^i(Q^2) + \sum_k \tilde{C}^{(k)\mu}_{\lambda',\lambda} B^k(Q^2) \\
C^{(i)\mu}_{\lambda',\lambda} &= \frac{1}{2\sqrt{P'^+P^+}} \bar{u}(P',\lambda') \kappa_i^{\mu} u(P,\lambda) \\
\tilde{C}^{(i)\mu}_{\lambda',\lambda} &= \frac{1}{2\sqrt{P'^+P^+}} \bar{u}(P',\lambda') \tilde{\kappa}_i'^{\mu} u(P,\lambda) \\
\Big\{F^i(Q^2), B^k(Q^2)\Big\} &= \big\{G_A(Q^2), G_P(Q^2), G_T(Q^2), B_1(Q^2), B_2(Q^2), B_3(Q^2), B_4(Q^2), B_5(Q^2)\big\} \quad .
\end{aligned}$$

$\lambda'\lambda\,\mu$	$C^{1\mu}_{\lambda'\lambda}$	$C^{2\mu}_{\lambda'\lambda}$	$\tilde{C}^{1\mu}_{\lambda'\lambda}$	$\tilde{C}^{2\mu}_{\lambda'\lambda}$	$\tilde{C}^{3\mu}_{\lambda'\lambda}$	$C^{3\mu}_{\lambda'\lambda}$	$\tilde{C}^{4\mu}_{\lambda'\lambda}$	$\tilde{C}^{5\mu}_{\lambda'\lambda}$
$\uparrow\uparrow\ +$	x				x			
$\downarrow\uparrow\ x$	x	x		x				
$\uparrow\uparrow\ y$	x							
$\downarrow\uparrow\ y$	x			x				
$\uparrow\uparrow\ -$	x		x	x				
$\downarrow\uparrow\ +$						x		
$\downarrow\uparrow\ -$						x	x	
$\uparrow\uparrow\ x$								x

Figure 5.2: *The non vanishing coefficients for the axial elastic $N \to N$ transition are denoted by an x.*

From fig. 5.2 we conclude that we can obtain $G_A(Q^2)$ and $G_P(Q^2)$ by inverting a 5*5 matrix and $G_T(Q^2)$ from the inversion of a 2*2 matrix. $\tilde{\kappa}_5^{\mu}$ is related to $\langle P',\uparrow|\ J^x\ |\ P,\uparrow\rangle$ which is zero. The form factors then can be expressed in terms of the amplitude relations. We find

$$\begin{aligned}
G_A(t) =& \frac{1}{4}\tilde{F}^+_{\uparrow\uparrow} - i\frac{\Delta_x}{2\Delta_x^2 + 8M_N^2}\tilde{F}^y_{\uparrow\uparrow} - i\frac{M_N}{\Delta_x^2 + 4M_N^2}\tilde{F}^y_{\downarrow\uparrow} - \frac{1}{4(\Delta_x^2 + 4M_N^2)}\tilde{F}^-_{\uparrow\uparrow} \\
G_P(t) =& \frac{M_N^2}{\Delta_x^2}\tilde{F}^+_{\uparrow\uparrow} - \frac{2M_N}{\Delta_x^2}\tilde{F}^x_{\downarrow\uparrow} - i\frac{2M_N^2}{\Delta_x^3 + 4\Delta_x M_N^2}\tilde{F}^y_{\uparrow\uparrow} - i\frac{4M_N^3}{\Delta_x^4 + 4\Delta_x^2 M_N^2}\tilde{F}^y_{\downarrow\uparrow} - \frac{M_N^2}{\Delta_x^4 + 4\Delta_x^2 M_N^2}\tilde{F}^-_{\uparrow\uparrow} \\
G_T(t) =& \frac{M_N}{\Delta_x}\tilde{F}^+_{\downarrow\uparrow} + \frac{M_N}{\Delta_x(\Delta_x^2 + 4M_N^2)}\tilde{F}^-_{\downarrow\uparrow} \quad . \qquad (5.7)
\end{aligned}$$

Again we remark that if we introduce the consistency relations in eq. 4.29 we find back the expressions from eq. 4.17. G_T vanishes in our model calculation since $\tilde{F}^+_{\downarrow\uparrow}$ and $\tilde{F}^-_{\downarrow\uparrow}$ are zero.

5.3.3 Vectorial $N \to \Delta$ transition

With the ansatz

$$\tilde{\kappa}_i'^{\mu\nu} = \tilde{\kappa}_i^{\mu\nu} + w_i\kappa_1^{\mu\nu} + x_i\kappa_2^{\mu\nu} + y_i\kappa_3^{\mu\nu} + z_i\kappa_4^{\mu\nu} \qquad \text{for } i = 1..12$$

and defining

$$N = \Delta_x^4 + 2\Delta_x^2\Big[(1+\xi)^2 M_\Delta^2 + (1-\xi)^2 M_N^2\Big] + \Big[(1-\xi)^2 M_N^2 - (1+\xi)^2 M_\Delta^2\Big]^2$$

the above described orthogonalization procedure yields

$$\begin{aligned}
w_1 =& 0\\
x_1 =& -\frac{4(1-\xi^2)\left(\Delta_x^2 + \xi\Big[(1+\xi)^2 M_\Delta^2 - (1-\xi)^2 M_N^2\Big]\right)}{N}\\
y_1 =& \frac{2(1-\xi)(1-\xi^2)\Big[\Delta_x^2 + (1-\xi)^2 M_N^2 - (1+\xi)^2 M_\Delta^2\Big]}{N}\\
z_1 =& 2\xi\\
\\
w_2 =& 0\\
x_2 =& \frac{4(1-\xi)(1-\xi^2)^2(M_\Delta + M_N)}{N^2}\left(\Delta_x^2\Big[(3-\xi)(1-\xi)^2 M_N^2 - (3-5\xi)(1+\xi)^2 M_\Delta^2\Big]\right.\\
&\left. + (3+\xi)\Delta_x^4 - 2\xi\Big[(1-\xi)^2 M_N^2 - (1+\xi)^2 M_\Delta^2\Big]^2\right)\\
y_2 =& -\frac{4(1-\xi)^4(1+\xi)^2(M_N + M_\Delta)}{N^2}\left(\Delta_x^4 + \Big[(1-\xi)^2 M_N^2 - (1+\xi)^2 M_\Delta^2\Big]^2\right.\\
&\left. - 2\Delta_x^2\Big[2(1+\xi)^2 M_\Delta^2 - (1-\xi)^2 M_N^2\Big]\right)\\
z_2 =& \frac{4\xi(1-\xi)(1-\xi^2)(M_N + M_\Delta)\Big[(1+\xi)^2 M_\Delta^2 - (1-\xi)^2 M_N^2 - \Delta_x^2\Big]}{N}\\
w_3 =& \frac{4(1-\xi)(1-\xi^2)^3\Delta_x^2\Big[(1+\xi)^2 M_\Delta^2 - (1-\xi)^2 M_N^2 - \Delta_x^2\Big]}{N^2}\\
x_3 =& -\frac{16(1-\xi)(1-\xi^2)^3}{\left(\Delta_x^2 + \Big[(1+\xi)M_\Delta + (1-\xi)M_N\Big]^2\right)^2\left(\Delta_x^2 + \Big[(1+\xi)M_\Delta - (1-\xi)M_N\Big]^2\right)^3}\\
&\cdot\left(\xi\Big[(1+\xi)M_\Delta + (1-\xi)M_N\Big]^2\Big[(1+\xi)M_\Delta - (1-\xi)M_N\Big]^3\right.\\
&- 2\Delta_x^2\Big[(1-\xi)^3 M_N^3 - (1-\xi)^3(1+\xi)M_N^2 M_\Delta + (1-\xi^2)^2 M_N M_\Delta^2 - (1-2\xi)(1+\xi)^3 M_\Delta^3\Big]\\
&\left. - \Delta_x^4\Big[3(1+\xi)M_\Delta - (2-\xi-\xi^2)M_N\Big]\right)
\end{aligned}$$

$$
\begin{aligned}
y_3 =& -\frac{8(1-\xi)^2(1-\xi^2)^3}{\left(\Delta_x^2+\Big[(1+\xi)M_\Delta+(1-\xi)M_N\Big]^2\right)^2\left(\Delta_x^2+\Big[(1+\xi)M_\Delta-(1-\xi)M_N\Big]^2\right)^3}\\
&\cdot\Bigg(\Big[(1+\xi)M_\Delta+(1-\xi)M_N\Big]^2\Big[(1+\xi)M_\Delta-(1-\xi)M_N\Big]^3\\
&+\Delta_x^4\Big[3(1+\xi)M_\Delta-(1-\xi)M_N\Big]-2\Delta_x^2\Big[3(1+\xi)^3M_\Delta^3\\
&-2(1-\xi)(1+\xi)^2M_NM_\Delta^2-2(1-\xi)(1-\xi^2)M_N^2M_\Delta+(1-\xi)^3M_N^3\Big]\Bigg)\\
z_3 =&\frac{8\xi(1-\xi)(1-\xi^2)^2}{\left(\Delta_x^2+\Big[(1+\xi)M_\Delta+(1-\xi)M_N\Big]^2\right)\left(\Delta_x^2+\Big[(1+\xi)M_\Delta-(1-\xi)M_N\Big]^2\right)^2}\\
&\cdot\Bigg(\Delta_x^2\Big[(1-\xi)M_N-2(1+\xi)M_\Delta\Big]+\Big[(1+\xi)M_\Delta+(1-\xi)M_N\Big]\\
&\cdot\Big[(1+\xi)M_\Delta-(1-\xi)M_N\Big]^2\Bigg)\\
w_4 =&\frac{2(1-\xi^2)^2\Delta_x^2}{N}\\
x_4 =& -\frac{4(1-\xi^2)^2}{\left(\Delta_x^2+\Big[(1+\xi)M_\Delta+(1-\xi)M_N\Big]^2\right)\left(\Delta_x^2+\Big[(1+\xi)M_\Delta-(1-\xi)M_N\Big]^2\right)^2}\\
&\cdot\Bigg(2\xi\Big[(1+\xi)M_\Delta+(1-\xi)M_N\Big]\Big[(1+\xi)M_\Delta-(1-\xi)M_N\Big]^2\\
&+\Delta_x^2\Big[(3+2\xi-\xi^2)M_\Delta-(3-2\xi-\xi^2)M_N\Big]\Bigg)\\
y_4 =& -\frac{4(1-\xi)(1-\xi^2)^2}{\left(\Delta_x^2+\Big[(1+\xi)M_\Delta+(1-\xi)M_N\Big]^2\right)\left(\Delta_x^2+\Big[(1+\xi)M_\Delta-(1-\xi)M_N\Big]^2\right)^2}\\
&\cdot\Bigg(\Delta_x^2\Big[(1-\xi)M_N-2(1+\xi)M_\Delta\Big]+\Big[(1+\xi)M_\Delta+(1-\xi)M_N\Big]\\
&\cdot\Big[(1+\xi)M_\Delta-(1-\xi)M_N\Big]^2\Bigg)\\
z_4 =&\frac{4\xi(1-\xi^2)\Big[(1+\xi)M_\Delta-(1-\xi)M_N\Big]}{\left(\Delta_x^2+\Big[(1+\xi)M_\Delta-(1-\xi)M_N\Big]^2\right)}
\end{aligned}
$$

$$
\begin{aligned}
w_5 =& 0 \\
x_5 =& \frac{2(1-\xi)}{N}\Bigg(\Delta_x^4 - (1-\xi)\Delta_x^2\Big[(1+\xi)M_\Delta^2 - (1-3\xi)M_N^2\Big] \\
& - 2\xi\Big[(1+\xi)^3 M_\Delta^4 - 2(1-\xi^2)M_\Delta^2 M_N^2 + (1-\xi)^3 M_N^4\Big]\Bigg) \\
y_5 =& -\frac{(1-\xi)}{N}\Bigg(\Delta_x^4 + (1-\xi)^4 M_N^4 - 2(1-\xi)^3(1+\xi)M_N^2 M_\Delta^2 + (1-\xi)(1+\xi)^3 M_\Delta^4 \\
& - 2(1-\xi)\Delta_x^2\Big[(1+\xi)M_\Delta^2 - (1-\xi)M_N^2\Big]\Bigg) \\
z_5 =& 0 \\
w_6 =& -\frac{2(1-\xi)}{N}\Bigg(\Delta_x^4 - (1-\xi)\Delta_x^2\Big[(1+\xi)M_\Delta^2 - (1-3\xi)M_N^2\Big] \\
& - 2\xi\Big[(1-\xi)^3 M_N^4 + (1+\xi)^3 M_\Delta^4 - 2(1-\xi^2)M_N^2 M_\Delta^2\Big]\Bigg) \\
x_6 =& 0 \\
y_6 =& -\frac{2(1-\xi)^2(1+\xi)(M_\Delta + M_N)\Big[\Delta_x^2 + (1-\xi)^2 M_N^2 - (1+\xi)^2 M_\Delta^2\Big]}{N} \\
z_6 =& 0 \\
w_7 =& 0 \\
x_7 =& 0 \\
y_7 =& -\frac{2(1-\xi^2)\Big[(1+\xi)M_\Delta - (1-\xi)M_N\Big]}{\Delta_x^2 + \Big[(1+\xi)M_\Delta - (1-\xi)M_N\Big]^2} \\
z_7 =& 0 \\
w_8 =& 0 \\
x_8 =& \frac{2\Big[(1+\xi)M_\Delta - (1-\xi)M_N\Big]\Bigg(\Delta_x^2 + 2\xi\Big[(1+\xi)M_\Delta^2 - (1-\xi)M_N^2\Big]\Bigg)}{\Delta_x^2 + \Big[(1+\xi)M_\Delta - (1-\xi)M_N\Big]^2} \\
y_8 =& -\frac{\Big[(1+\xi)M_\Delta - (1-\xi)M_N\Big]\Big[\Delta_x^2 + (1-\xi)^2 M_N^2 - (1-2\xi-3\xi^2)M_\Delta^2\Big]}{\Delta_x^2 + \Big[(1+\xi)M_\Delta - (1-\xi)M_N\Big]^2} \\
z_8 =& 0 \\
w_9 =& 0 \\
x_9 =& 0
\end{aligned}
$$

$$
\begin{aligned}
y_9 =& \frac{2(1+\xi)(1-\xi)^2\Big[\Delta_x^2+(1-\xi)^2M_N^2-(1+\xi)^2M_\Delta^2\Big]}{N}\\
z_9 =& -\frac{2(1-\xi)}{N}\Bigg(\Delta_x^4-(1-\xi)\Delta_x^2\Big[(1+\xi)M_\Delta^2-(1-3\xi)M_N^2\Big]\\
&-2\xi\Big[(1-\xi)^3M_N^4+(1+\xi)^3M_\Delta^4-2(1-\xi^2)M_NM_\Delta^2\Big]\Bigg)\\
w_{10} =& 0\\
x_{10} =& -\frac{4(1-\xi)(1-\xi^2)^2}{\Bigg(\Delta_x^2+\Big[(1+\xi)M_\Delta+(1-\xi)M_N\Big]^2\Bigg)\Bigg(\Delta_x^2+\Big[(1+\xi)M_\Delta-(1-\xi)M_N\Big]^2\Bigg)^2}\\
&\cdot\Bigg(\Delta_x^2\Big[(1-\xi)M_N-2(1+\xi)M_\Delta\Big]+\Big[(1+\xi)M_\Delta+(1-\xi)M_N\Big]\\
&\cdot\Big[(1+\xi)M_\Delta-(1-\xi)M_N\Big]^2\Bigg)\\
y_{10} =& 0\\
z_{10} =& -\frac{2(1-\xi)(1-\xi^2)}{\Bigg(\Delta_x^2+\Big[(1+\xi)M_\Delta+(1-\xi)M_N\Big]^2\Bigg)\Bigg(\Delta_x^2+\Big[(1+\xi)M_\Delta-(1-\xi)M_N\Big]^2\Bigg)^2}\\
&\cdot\Bigg(\Delta_x^4\Big[2(1+\xi)M_\Delta-(1-\xi)M_N\Big]+\Delta_x^2\Big[-2(1-\xi)^3M_N^3+2(1-\xi)^2(1+\xi)M_NM_\Delta^2\\
&-3(1-\xi^2)M_N^2M_\Delta-(3-5\xi)(1+\xi)^2M_\Delta^3\Big]-\Big[(1+\xi)M_\Delta-(1-\xi)M_N\Big]^2\\
&\cdot\Big[(1-\xi)^3M_N^3+(1-\xi^2)(1+\xi)M_\Delta M_N^2-(1-3\xi)(1+\xi)^2M_\Delta^3\\
&-(1-3\xi-\xi^2+3\xi^3)M_NM_\Delta^2\Big]\Bigg)\\
w_{11} =& \frac{4(1-\xi)(1-\xi^2)^2}{\Bigg(\Delta_x^2+\Big[(1+\xi)M_\Delta+(1-\xi)M_N\Big]^2\Bigg)^2\Bigg(\Delta_x^2+\Big[(1+\xi)M_\Delta-(1-\xi)M_N\Big]^2\Bigg)}\\
&\cdot\Bigg(\Big[(1+\xi)M_\Delta+(1-\xi)M_N\Big]^2\Big[(1+\xi)M_\Delta-(1-\xi)M_N\Big]\\
&-\Delta_x^2\Big[(1-\xi)M_N+2(1+\xi)M_\Delta\Big]\Bigg)\\
x_{11} =& \frac{8(1-\xi^2)^3}{N^2}\Bigg(2\Delta_x^4+\Delta_x^2\Big[(1-\xi)^2M_N^2+(1+\xi)^2M_\Delta^2\Big]-\Big[(1-\xi)^2M_N^2-(1+\xi)^2M_\Delta^2\Big]^2\Bigg)
\end{aligned}
$$

$$
\begin{aligned}
y_{11} =& 0 \\
z_{11} =& -\frac{4(1-\xi^2)^2}{\left(\Delta_x^2+\Big[(1+\xi)M_\Delta+(1-\xi)M_N\Big]^2\right)\left(\Delta_x^2+\Big[(1+\xi)M_\Delta-(1-\xi)M_N\Big]^2\right)^2} \\
& \cdot\Bigg(\Delta_x^4-2\xi M_\Delta\Big[(1+\xi)M_\Delta+(1-\xi)M_N\Big]\Big[(1+\xi)M_\Delta-(1-\xi)M_N\Big]^2 \\
& -(1-\xi)\Delta_x^2\Big[2(1+\xi)M_\Delta^2-(1-\xi)M_N^2-(1-\xi)M_NM_\Delta\Big]\Bigg) \\
w_{12} =& \frac{2(1-\xi^2)\Big[(1+\xi)M_\Delta+(1-\xi)M_N\Big]}{\Delta_x^2+\Big[(1+\xi)M_\Delta+(1-\xi)M_N\Big]^2} \\
x_{12} =& -\frac{4(1+\xi)(1-\xi^2)\Big[\Delta_x^2-(1-\xi^2)M_N^2+(1+\xi)^2M_\Delta^2\Big]}{N} \\
y_{12} =& 0 \\
z_{12} =& \frac{2(1+\xi)\left(\Delta_x^2+2\xi M_\Delta\Big[(1+\xi)M_\Delta-(1-\xi)M_N\Big]\right)}{\left(\Delta_x^2+\Big[(1+\xi)M_\Delta-(1-\xi)M_N\Big]^2\right)} \quad .
\end{aligned}
$$

Equipped with the orthogonalized set of spurious covariants we can now proceed and express the GPDs in terms of all possible amplitudes. For DVCS these amplitudes can now be decomposed into

$$
\begin{aligned}
G^\mu_{\lambda',\lambda} &= \sum_i C^{(i)\mu}_{\lambda',\lambda}A^i(x,\xi,t)+\sum_k \tilde{C}^{(k)\mu}_{\lambda',\lambda}B^k(x,\xi,t) \\
C^{(i)\mu}_{\lambda',\lambda} &= \frac{1}{2\bar{P}^+}\bar{u}_\nu(P',\lambda')\kappa_i^{\mu\nu}u(P,\lambda) \\
\tilde{C}^{(i)\mu}_{\lambda',\lambda} &= \frac{1}{2\bar{P}^+}\bar{u}_\nu(P',\lambda')\tilde{\kappa}_i'^{\mu\nu}u(P,\lambda) \\
\Big\{A^i(x,\xi,t),B^k(x,\xi,t)\Big\} &= \Big\{H^1_{(\star)}(x,\xi,t),H^2_{(\star)}(x,\xi,t),H^3_{(\star)}(x,\xi,t),H^4_{(\star)}(x,\xi,t),B_1(x,\xi,t), \\
&\quad B_2(x,\xi,t),B_3(x,\xi,t),B_4(x,\xi,t),B_5(x,\xi,t),B_6(x,\xi,t),B_7(x,\xi,t), \\
&\quad B_8(x,\xi,t),B_9(x,\xi,t),B_{10}(x,\xi,t),B_{11}(x,\xi,t),B_{12}(x,\xi,t)\Big\} \quad .
\end{aligned}
$$

By inverting this relation one obtains an unambiguous expression for both, physical and spurious GPDs. In principle they can be expressed in terms of the amplitude relations. However the analytical inversion of the 16*16 matrix is too involved even if we use Mathematica. Therefore we perform this inversion numerically.

The amplitudes $F^{\mu}_{\lambda',\lambda}$ can be decomposed into

$$
\begin{aligned}
F^{\mu}_{\lambda',\lambda} &= \sum_i C^{(i)\mu}_{\lambda',\lambda} F^i(Q^2) + \sum_k \tilde{C}^{(k)\mu}_{\lambda',\lambda} B^k(Q^2) \\
C^{(i)\mu}_{\lambda',\lambda} &= \frac{1}{2\sqrt{P'^+P^+}} \bar{u}_\nu(P',\lambda') \kappa_i^{\mu\nu} u(P,\lambda) \\
\tilde{C}^{(i)\mu}_{\lambda',\lambda} &= \frac{1}{2\sqrt{P'^+P^+}} \bar{u}_\nu(P',\lambda') \tilde{\kappa}_i'^{\mu\nu} u(P,\lambda) \\
\Big\{F^i(Q^2), B^k(Q^2)\Big\} &= \{G_1(t), G_2(t), G_3(t), G_4(t), B_1(t), B_2(t), B_3(t), B_4(t), B_5(t), \\
&\qquad B_6(t), B_7(t), B_8(t), B_9(t), B_{10}(t), B_{11}(t), B_{12}(t)\} \quad .
\end{aligned}
$$

Here no simplification arises from considering the coefficients $C^{(i)\mu}_{\lambda',\lambda}$ and $\tilde{C}^{(k)\mu}_{\lambda',\lambda}$. Therefore we have the interesting situation that the non gauge invariant spurious covariants have to be included in the extraction of the physical form factors. The form factors can be expressed analytically in terms of the amplitude relations. We find

$$
\begin{aligned}
G_1(t) =& \frac{1}{2\sqrt{2}\Big[(\Delta_x^2+M_\Delta^2)^2 + 2(\Delta_x - M_\Delta)(\Delta_x + M_\Delta)M_N^2 + M_N^4\Big]^2} \\
&\cdot \Bigg(\Delta_x M_\Delta \Big[(M_\Delta^2 - M_N^2)(M_\Delta - M_N) + \Delta_x^2(3M_\Delta + M_N)\Big]\Big[\Delta_x^2 + 2(M_\Delta^2 + M_N^2)\Big]\tilde{F}^+_{\frac{3}{2}\uparrow} \\
&- \sqrt{3}\Delta_x^2 M_\Delta(\Delta_x^2 - M_\Delta^2 + M_N^2)\Big[\Delta_x^2 + 2(M_\Delta^2 + M_N^2)\Big]\tilde{F}^+_{\frac{1}{2}\uparrow} \\
&- \sqrt{3}\Delta_x M_\Delta(M_\Delta - M_N)(\Delta_x^2 - M_\Delta^2 + M_N^2)\Big[\Delta_x^2 + 2(M_\Delta^2 + M_N^2)\Big]\tilde{F}^+_{\frac{1}{2}\downarrow} \\
&+ \Delta_x^2 M_\Delta(\Delta_x^2 + 3M_\Delta^2 - 4M_\Delta M_N + M_N^2)\Big[\Delta_x^2 + 2(M_\Delta^2 + M_N^2)\Big]\tilde{F}^+_{\frac{3}{2}\downarrow} \\
&+ 2M_\Delta(M_\Delta^2 - M_N^2)\Big[(M_\Delta - M_N)^2(M_\Delta + M_N) + \Delta_x^2(3M_\Delta + M_N)\Big]\tilde{F}^x_{\frac{3}{2}\uparrow} \\
&- 2\sqrt{3}\Delta_x M_\Delta(M_\Delta^2 - M_N^2)(\Delta_x^2 - M_\Delta^2 + M_N^2)\tilde{F}^x_{\frac{1}{2}\uparrow} \\
&- 2\sqrt{3}M_\Delta(M_\Delta - M_N)^2(M_\Delta + M_N)(\Delta_x^2 - M_\Delta^2 + M_N^2)\tilde{F}^x_{\frac{1}{2}\downarrow} \\
&+ 2\Delta_x M_\Delta(M_\Delta^2 - M_N^2)(\Delta_x^2 + 3M_\Delta^2 - 4M_\Delta M_N + M_N^2)\tilde{F}^x_{\frac{3}{2}\downarrow} \Bigg) \\
&+ i\frac{M_\Delta}{\sqrt{2}\Big[\Delta_x^2 + (M_\Delta - M_N)^2\Big]\Big[\Delta_x^2 + (M_\Delta + M_N)^2\Big]^2} \\
&\cdot \Bigg(\Big[(M_\Delta - M_N)(M_\Delta + M_N)^2 - \Delta_x^2(3M_\Delta + M_N)\Big]\tilde{F}^y_{\frac{3}{2}\uparrow} \\
&+ \sqrt{3}\Delta_x\Big[\Delta_x^2 - (3M_\Delta - M_N)(M_\Delta + M_N)\Big]\tilde{F}^y_{\frac{1}{2}\uparrow} \\
&+ \sqrt{3}\Big[(M_\Delta - M_N)(M_\Delta + M_N)^2 - \Delta_x^2(3M_\Delta + M_N)\Big]\tilde{F}^y_{\frac{1}{2}\downarrow} \\
&- \Delta_x\Big[\Delta_x^2 - (3M_\Delta - M_N)(M_\Delta + M_N)\Big]\tilde{F}^y_{\frac{3}{2}\downarrow} \Bigg)
\end{aligned}
$$

$$
\begin{aligned}
&+\frac{1}{2\sqrt{2}\Big[(\Delta_x^2+M_\Delta^2)^2+2(\Delta_x-M_\Delta)(\Delta_x+M_\Delta)M_N^2+M_N^4\Big]^2}\\
&\cdot\Bigg(-\Delta_x M_\Delta\Big[(M_\Delta-M_N)^2(M_\Delta+M_N)+\Delta_x^2(3M_\Delta+M_N)\Big]\tilde{F}^-_{\frac{3}{2}\uparrow}\\
&+\sqrt{3}\Delta_x^2 M_\Delta(\Delta_x^2-M_\Delta^2+M_N^2)\tilde{F}^-_{\frac{1}{2}\uparrow}\\
&+\sqrt{3}\Delta_x M_\Delta(M_\Delta-M_N)(\Delta_x^2-M_\Delta^2+M_N^2)\tilde{F}^-_{\frac{1}{2}\downarrow}\\
&-\Delta_x^2 M_\Delta(\Delta_x^2+3M_\Delta^2-4M_\Delta M_N+M_N^2)\tilde{F}^-_{\frac{3}{2}\downarrow}\Bigg)\\
G_2(t)=&\frac{1}{\sqrt{2}\Big[(\Delta_x^2+(M_\Delta-M_N)^2\Big]^3\Big[\Delta_x^2+(M_\Delta+M_N)^2\Big]^2}\\
&\cdot\Bigg(\Big[-\Delta_x^7M_N+2\Delta_x^5(M_\Delta-2M_N)(M_\Delta^2+M_N^2)+2\Delta_x(M_\Delta-M_N)^3(M_\Delta+M_N)\\
&\cdot(6M_\Delta^3+7M_\Delta^2M_N+M_N^3)+\Delta_x^3(M_\Delta-M_N)(4M_\Delta^4+M_\Delta^3M_N+7M_\Delta^2M_N^2-M_\Delta M_N^3\\
&+5M_N^4)\Big]\tilde{F}^+_{\frac{3}{2}\uparrow}\\
&+2\sqrt{3}M_\Delta\Big[-\Delta_x^6M_\Delta+2(M_\Delta-M_N)^4(M_\Delta+M_N)^3-2\Delta_x^2(2M_\Delta-M_N)(M_\Delta^2-M_N^2)^2\\
&-2\Delta_x^4M_\Delta(M_\Delta^2+M_N^2)\Big]\tilde{F}^+_{\frac{1}{2}\uparrow}\\
&+\sqrt{3}\Delta_xM_\Delta\Big[\Delta_x^6+4\Delta_x^4M_N^2-2(M_\Delta-M_N)^3(M_\Delta+M_N)(5M_\Delta^2+6M_\Delta M_N+3M_N^2)\\
&-\Delta_x^2(M_\Delta^2-M_N^2)(M_\Delta^2-2M_\Delta M_N+9M_N^2)\Big]\tilde{F}^+_{\frac{1}{2}\downarrow}\\
&-\Delta_x^2\Big[\Delta_x^6+\Delta_x^4(8M_\Delta^2-2M_\Delta M_N+4M_N^2)+2(M_\Delta-M_N)^2(9M_\Delta^4+12M_\Delta^3M_N\\
&+10M_\Delta^2M_N^2+M_N^4)+\Delta_x^2(15M_\Delta^4-10M_\Delta^3M_N+20M_\Delta^2M_N^2-6M_\Delta M_N^3+5M_N^4)\Big]\tilde{F}^+_{\frac{3}{2}\downarrow}\\
&-2(M_\Delta^2-M_N^2)\Big[\Delta_x^4M_N-(M_\Delta-M_N)^3M_N(M_\Delta+M_N)\\
&+2\Delta_x^2(M_\Delta-M_N)(5M_\Delta^2-M_N^2)\Big]\tilde{F}^x_{\frac{3}{2}\uparrow}\\
&+4\sqrt{3}\Delta_xM_\Delta(M_\Delta^2-M_N^2)\Big[\Delta_x^2(3M_\Delta-2M_N)-2(M_\Delta-M_N)^2(M_\Delta+M_N)\Big]\tilde{F}^x_{\frac{1}{2}\uparrow}\\
&-2\sqrt{3}M_\Delta(M_\Delta^2-M_N^2)\Big[3\Delta_x^4+(M_\Delta-M_N)^3(M_\Delta+M_N)\\
&-2\Delta_x^2(M_\Delta-M_N)(3M_\Delta+M_N)\Big]\tilde{F}^x_{\frac{1}{2}\downarrow}\\
&-2\Delta_x(M_\Delta^2-M_N^2)\Big[\Delta_x^4-2\Delta_x^2(3M_\Delta^2+M_\Delta M_N-M_N^2)\\
&+(M_\Delta-M_N)^2(3M_\Delta^2+M_N^2)\Big]\tilde{F}^x_{\frac{3}{2}\downarrow}\Bigg)
\end{aligned}
$$

$$
\begin{aligned}
&+ i\frac{1}{\Big[(\Delta_x^2+M_\Delta^2)^2+2(\Delta_x-M_\Delta)(\Delta_x+M_\Delta)M_N^2+M_N^4\Big]^2}\\
&\cdot\Bigg(\sqrt{2}\Big[\Delta_x^4M_N+M_N(M_\Delta^2-M_N^2)^2+2\Delta_x^2(M_\Delta^3-2M_\Delta^2M_N+M_N^3)\Big]\tilde{F}^y_{\frac{3}{2}\uparrow}\\
&+2\sqrt{6}\Delta_xM_\Delta\Big[\Delta_x^2M_N+(M_\Delta-M_N)^2(M_\Delta+M_N)\Big]\tilde{F}^y_{\frac{1}{2}\uparrow}\\
&-\sqrt{6}M_\Delta\Big[-\Delta_x^4-2\Delta_x^2M_\Delta(M_\Delta-M_N)+(M_\Delta^2-M_N^2)^2\Big]\tilde{F}^y_{\frac{1}{2}\downarrow}\\
&+\sqrt{2}\Delta_x\Big[\Delta_x^4-3M_\Delta^4+2(\Delta_x^2+M_\Delta^2)M_N^2+M_N^4\Big]\tilde{F}^y_{\frac{3}{2}\downarrow}\Bigg)\\
&+\frac{1}{\sqrt{2}\Big[(\Delta_x^2+(M_\Delta-M_N)^2\Big]^3\Big[\Delta_x^2+(M_\Delta+M_N)^2\Big]^2}\\
&\cdot\Bigg(\Delta_x\Big[\Delta_x^4M_N-(M_\Delta-M_N)^3M_N(M_\Delta+M_N)+2\Delta_x^2(M_\Delta-M_N)(5M_\Delta^2-M_N^2)\Big]\tilde{F}^-_{\frac{3}{2}\uparrow}\\
&-2\sqrt{3}\Delta_x^2M_\Delta\Big[\Delta_x^2(3M_\Delta-2M_N)-2(M_\Delta-M_N)^2(M_\Delta+M_N)\Big]\tilde{F}^-_{\frac{1}{2}\uparrow}\\
&+\sqrt{3}\Delta_xM_\Delta\Big[3\Delta_x^4+(M_\Delta-M_N)^3(M_\Delta+M_N)-2\Delta_x^2(M_\Delta-M_N)(3M_\Delta+M_N)\Big]\tilde{F}^-_{\frac{1}{2}\downarrow}\\
&+\Delta_x^2\Big[\Delta_x^4-2\Delta_x^2(3M_\Delta^2+M_\Delta M_N-M_N^2)+(M_\Delta-M_N)^2(3M_\Delta^2+M_N^2)\Big]\tilde{F}^-_{\frac{3}{2}\downarrow}\Bigg)
\end{aligned}
$$

$$
\begin{aligned}
G_3(t)=&\frac{1}{\sqrt{2}\Big[\Delta_x^2+(M_\Delta-M_N)^2\Big]^3\Big[\Delta_x^2+(M_\Delta+M_N)^2\Big]^2}\\
&\cdot\Bigg(2\Delta_xM_\Delta^2\Big[\Delta_x^4M_N-(M_\Delta-M_N)^2(M_\Delta+M_N)(7M_\Delta^2+M_N^2)\\
&+2\Delta_x^2M_\Delta(-M_\Delta^2+2M_\Delta M_N+M_N^2)\Big]\tilde{F}^+_{\frac{3}{2}\uparrow}\\
&-\sqrt{3}M_\Delta(M_\Delta-M_N)\Big[-\Delta_x^6-2\Delta_x^4(3M_\Delta^2+M_\Delta M_N+M_N^2)+4(M_\Delta^3-M_\Delta M_N^2)^2\\
&-\Delta_x^2(11M_\Delta^4+6M_\Delta^3M_N+4M_\Delta^2M_N^2+2M_\Delta M_N^3+M_N^4\Big]\tilde{F}^+_{\frac{1}{2}\uparrow}\\
&-\sqrt{3}\Delta_xM_\Delta\Big[\Delta_x^6+2\Delta_x^4(2M_\Delta^2+M_N^2)-2M_\Delta(M_\Delta-M_N)^2(M_\Delta+M_N)\\
&\cdot(5M_\Delta^2+2M_\Delta M_N+M_N^2)+\Delta_x^2(3M_\Delta^4+2M_\Delta^3M_N+4M_\Delta^2M_N^2-2M_\Delta M_N^3+M_N^4\Big]\tilde{F}^+_{\frac{1}{2}\downarrow}\\
&+2\Delta_x^2M_\Delta^2\Big[\Delta_x^4+\Delta_x^2M_\Delta(5M_\Delta-M_N)+(M_\Delta-M_N)\\
&\cdot(9M_\Delta^3+7M_\Delta^2M_N+3M_\Delta M_N^2+M_N^3)\Big]\tilde{F}^+_{\frac{3}{2}\downarrow}\\
&-2(M_\Delta-M_N)M_\Delta^2\Big[-3\Delta_x^4+(M_\Delta^2-M_N^2)^2-2\Delta_x^2(6M_\Delta^2+M_\Delta M_N+M_N^2)\Big]\tilde{F}^x_{\frac{3}{2}\uparrow}\\
&-2\sqrt{3}\Delta_xM_\Delta\Big[\Delta_x^4(2M_\Delta-M_N)-(M_\Delta-M_N)^2(M_\Delta+M_N)(6M_\Delta^2+M_\Delta M_N+M_N^2)\\
&+2\Delta_x^2(3M_\Delta^3-M_\Delta^2M_N+M_\Delta M_N^2-M_N^3)\Big]\tilde{F}^x_{\frac{1}{2}\uparrow}
\end{aligned}
$$

$$
\begin{aligned}
&+ 2\sqrt{3}M_\Delta\Big[\Delta_x^6 + M_\Delta(M_\Delta - M_N)^3(M_\Delta + M_N)^2 + \Delta_x^4(M_\Delta^2 + M_\Delta M_N + 2M_N^2)\\
&+ \Delta_x^2(-9M_\Delta^4 + 4M_\Delta^3 M_N + 4M_\Delta^2 M_N^2 + M_N^4)\Big]\tilde{F}^x_{\frac{1}{2}\downarrow}\\
&- 2\Delta_x M_\Delta^2\Big[3\Delta_x^4 - (M_\Delta - M_N)^2(M_\Delta + M_N)(3M_\Delta + M_N) + 2\Delta_x^2(5M_\Delta^2 + M_N^2)\Big]\tilde{F}^x_{\frac{3}{2}\downarrow}\Bigg)\\
&+ i\frac{1}{\Big[(\Delta_x^2 + M_\Delta^2)^2 + 2(\Delta_x - M_\Delta)(\Delta_x + M_\Delta)M_N^2 + M_N^4\Big]^2}\\
&\cdot\Bigg(-\sqrt{2}M_\Delta^2\Big[\Delta_x^2(3M_\Delta - M_N) + (M_\Delta - M_N)(M_\Delta + M_N)^2\Big]\tilde{F}^y_{\frac{3}{2}\uparrow}\\
&+ \sqrt{6}\Delta_x M_\Delta^2(\Delta_x^2 - M_\Delta^2 + M_N^2)\tilde{F}^y_{\frac{1}{2}\uparrow}\\
&+ \sqrt{6}M_\Delta^2(M_\Delta + M_N)(-\Delta_x^2 + M_\Delta^2 - M_N^2)\tilde{F}^y_{\frac{1}{2}\downarrow}\\
&+ \sqrt{2}\Delta_x M_\Delta^2\Big[\Delta_x^2 + (M_\Delta + M_N)(3M_\Delta + M_N)\Big]\tilde{F}^y_{\frac{3}{2}\downarrow}\Bigg)\\
&+ \frac{1}{\sqrt{2}\Big[\Delta_x^2 + (M_\Delta - M_N)^2\Big]^3\Big[\Delta_x^2 + (M_\Delta + M_N)^2\Big]^2}\\
&\cdot\Bigg(-2\Delta_x M_\Delta^2\Big[\Delta_x^2(3M_\Delta - 2M_N) - 2(M_\Delta - M_N)^2(M_\Delta + M_N)\Big]\tilde{F}^-_{\frac{3}{2}\uparrow}\\
&+ \sqrt{3}M_\Delta\Big[\Delta_x^4(3M_\Delta - M_N) + (M_\Delta - M_N)^3(M_\Delta + M_N)^2\\
&- 2\Delta_x^2(M_\Delta - M_N)(3M_\Delta^2 + M_\Delta M_N - M_N^2)\Big]\tilde{F}^-_{\frac{1}{2}\uparrow}\\
&- \sqrt{3}\Delta_x M_\Delta\Big[\Delta_x^4 + (M_\Delta - M_N)^2(M_\Delta + M_N)(3M_\Delta + M_N)\\
&+ 2\Delta_x^2(-3M_\Delta^2 + M_\Delta M_N + M_N^2)\Big]\tilde{F}^-_{\frac{1}{2}\downarrow}\\
&+ 2\Delta_x^2 M_\Delta^2(2\Delta_x^2 - 3M_\Delta^2 + M_\Delta M_N + 2M_N^2)\tilde{F}^-_{\frac{3}{2}\downarrow}\Bigg)\\
G_4(t) =&\frac{1}{\sqrt{2}\Big[\Delta_x^2 + (M_\Delta - M_N)^2\Big]^2 M_N\Big[\Delta_x^2 + (M_\Delta + M_N)^2\Big]}\\
&\cdot\Bigg(3\Delta_x M_\Delta^2(M_\Delta - M_N)\Big[(M_\Delta^2 - M_N^2)\tilde{F}^+_{\frac{3}{2}\uparrow} - \Delta_x\tilde{F}^x_{\frac{3}{2}\uparrow}\Big]\\
&- \sqrt{3}M_\Delta\Big[\Delta_x^2(2M_\Delta - M_N) - (M_\Delta - M_N)^2(M_\Delta + M_N)\Big]\Big[(M_\Delta^2 - M_N^2)\tilde{F}^+_{\frac{1}{2}\uparrow} - \Delta_x\tilde{F}^x_{\frac{1}{2}\uparrow}\Big]\\
&+ \sqrt{3}\Delta_x M_\Delta(\Delta_x^2 - 2M_\Delta^2 + M_\Delta M_N + M_N^2)\Big[(M_\Delta^2 - M_N^2)\tilde{F}^+_{\frac{1}{2}\downarrow} - \Delta_x\tilde{F}^x_{\frac{1}{2}\downarrow}\Big]\\
&- 3\Delta_x^2 M_\Delta^2\Big[(M_\Delta^2 - M_N^2)\tilde{F}^+_{\frac{3}{2}\downarrow} - \Delta_x\tilde{F}^x_{\frac{3}{2}\downarrow}\Big]\Bigg) \quad . \qquad (5.8)
\end{aligned}
$$

Again we remark that if we introduce the consistency relations in eq. 4.30 we find agreement

with the expressions in eq. 4.20. From the expression for $G_4(t)$ it is clear that if gauge invariance is satisfied at the level of transition amplitudes $G_4(t)$ vanishes. On the other hand side it is possible to break gauge invariance even if the transition amplitudes are covariantly consistent. The condition for gauge invariance after removing covariance breaking effects can be read off from the expression for $G_4(t)$. We will discuss the situation for our model calculation in the next section where we present the numerical results.

5.3.4 Axial $N \to \Delta$ transition

With the ansatz

$$\tilde{\kappa}_i'^{\mu\nu} = \tilde{\kappa}_i^{\mu\nu} + w_i\kappa_1^{\mu\nu} + x_i\kappa_2^{\mu\nu} + y_i\kappa_3^{\mu\nu} + z_i\kappa_4^{\mu\nu} \qquad \text{for } i = 1..12$$

and defining

$$N = \Delta_x^4 + 2\Delta_x^2\Big[(1+\xi)^2M_\Delta^2 + (1-\xi)^2M_N^2\Big] + \Big[(1+\xi)^2M_\Delta^2 - (1-\xi)^2M_N^2\Big]^2$$

the above described orthogonalization procedure yields

$$\begin{aligned}
w_1 =& -\frac{2(1-\xi^2)(M_\Delta^2 - M_N^2)\left(\Delta_x^2 + \xi\Big[(1+\xi)^2M_\Delta^2 - (1-\xi)^2M_N^2\Big]\right)}{N}\\
x_1 =& -\frac{2(1-\xi^2)M_N^2\Big[(1+\xi)^2M_\Delta^2 - (1-\xi)^2M_N^2 + \xi\Delta_x^2\Big]}{N}\\
y_1 =& 0\\
z_1 =& \frac{2(1-\xi^2)M_N^2\left(\Delta_x^2 + \xi\Big[(1+\xi)^2M_\Delta^2 - (1-\xi^2)M_N^2\Big]\right)}{N}
\end{aligned}$$

$$\begin{aligned}
w_2 =& \frac{2(1-\xi^2)^2(M_\Delta - M_N)}{N^2}\Bigg(\Delta_x^6 - 2\xi(1-\xi)(M_\Delta^2 - M_N^2)\Big[(1+\xi)^2M_\Delta^2 - (1-\xi)^2M_N^2\Big]^2\\
&+ \Delta_x^4\Big[(5+2\xi+\xi^2)M_\Delta^2 - (1+2\xi-3\xi^2)M_N^2\Big] - 2\Delta_x^2\Big[(1-\xi)^3M_N^4\\
&+ (1-5\xi+2\xi^2)(1+\xi)^2M_\Delta^4 - 2(1-3\xi+2\xi^2-\xi^3+\xi^4)M_\Delta^2M_N^2\Big]\Bigg)\\
x_2 =& -\frac{2(1-\xi)(1-\xi^2)^2M_N^2(M_\Delta - M_N)}{N^2}\Bigg(-(1+3\xi)\Delta_x^4 + 2\Big[(1+\xi)^2M_\Delta^2 - (1-\xi)^2M_N^2\Big]^2\\
&+ \Delta_x^2\Big[-(1+\xi)^2(5-3\xi)M_\Delta^2 + (1-3\xi)(1-\xi)^2M_N^2\Big]\Bigg)\Bigg)
\end{aligned}$$

$$
\begin{aligned}
y_2 =& 0\\
z_2 =& \frac{2(1-\xi)(1-\xi^2)^2 M_N^2 (M_\Delta - M_N)}{N^2}\Bigg(-(3+\xi)\Delta_x^4 + 2\xi\Big[(1+\xi)^2 M_\Delta^2 - (1-\xi)^2 M_N^2\Big]^2\\
&+ \Delta_x^2\Big[(3-5\xi)(1+\xi)^2 M_\Delta^2 - (3-\xi)(1-\xi)^2 M_N^2\Big]\Bigg)\\
w_3 =& \frac{8(1-\xi^2)^3}{\left(\Delta_x^2 + \Big[(1+\xi)M_\Delta + (1-\xi)M_N\Big]^2\right)^3 \left(\Delta_x^2 + \Big[(1+\xi)M_\Delta - (1-\xi)M_N\Big]^2\right)^2}\\
&\cdot\Bigg(\Delta_x^6\Big[\xi M_\Delta + (1-\xi)M_N\Big] - \xi(1-\xi)(M_\Delta^2 - M_N^2)\Big[(1+\xi)M_\Delta + (1-\xi)M_N\Big]^3\\
&\cdot\Big[(1+\xi)M_\Delta - (1-\xi)M_N\Big]^2 + \Delta_x^4\Big[-3\xi(1-\xi)^2 M_N^3 + (2-\xi-\xi^3)M_N M_\Delta^2\\
&+ (4+3\xi+\xi^3)M_\Delta^3 - (2-\xi+2\xi^2-3\xi^3)M_N^2 M_\Delta\Big] - \Delta_x^2\Big[(1-\xi)^4 M_N^4 M_\Delta\\
&+ (1+\xi)(1-\xi)^4 M_N^5 + (1-3\xi)(1-\xi^2)^2 M_N M_\Delta^4 - 2(1-\xi)^3(1+\xi^2)M_N^3 M_\Delta^2\\
&+ (1-7\xi+4\xi^2)(1+\xi)^3 M_\Delta^5 - 2(1-4\xi+2\xi^3-\xi^4+2\xi^5)M_N^2 M_\Delta^3\Big]\Bigg)\\
x_3 =& -\frac{8(1-\xi)(1-\xi^2)^3 M_N^2}{\left(\Delta_x^2 + \Big[(1+\xi)M_\Delta + (1-\xi)M_N\Big]^2\right)^3 \left(\Delta_x^2 + \Big[(1+\xi)M_\Delta - (1-\xi)M_N\Big]^2\right)^2}\\
&\cdot\Bigg(\Big[(1+\xi)M_\Delta + (1-\xi)M_N\Big]^3\Big[(1+\xi)M_\Delta - (1-\xi)M_N\Big]^2\\
&+ 2\Delta_x^2\Big[-\xi(1-\xi)^3 M_N^3 + (1-\xi)^3(1+\xi)M_N^2 M_\Delta - (2-\xi)(1+\xi)^3 M_\Delta^3\\
&- (1-\xi^2)^2 M_N M_\Delta^2\Big] + \Delta_x^4\Big[-3\xi(1+\xi)M_\Delta - (1+\xi-2\xi^2)M_N\Big]\Bigg)\\
y_3 =& \frac{4(1-\xi)(1-\xi^2)^3\Delta_x^2 M_N\Big[\Delta_x^2 + (1-\xi)^2 M_N^2 - (1+\xi)^2 M_\Delta^2\Big]}{N^2}\\
z_3 =& \frac{8(1-\xi)(1-\xi^2)^3 M_N^2}{\left(\Delta_x^2 + \Big[(1+\xi)M_\Delta + (1-\xi)M_N\Big]^2\right)^3 \left(\Delta_x^2 + \Big[(1+\xi)M_\Delta - (1-\xi)M_N\Big]^2\right)^2}\\
&\cdot\Bigg(\xi\Big[(1+\xi)M_\Delta + (1-\xi)M_N\Big]^3\Big[(1+\xi)M_\Delta - (1-\xi)M_N\Big]^2\\
&- 2\Delta_x^2\Big[(1-\xi)^3 M_N^3 + (1-\xi)^3(1+\xi)M_N^2 M_\Delta - (1-2\xi)(1+\xi)^3 M_\Delta^3 - (1-\xi^2)^2 M_N M_\Delta^2\Big]\\
&+ \Delta_x^4\Big[-3(1+\xi)M_\Delta - (2-\xi-\xi^2)M_N\Big]\Bigg)
\end{aligned}
$$

$$
\begin{aligned}
w_4 =& -\frac{2(1-\xi^2)^2(M_\Delta - M_N)}{\left(\Delta_x^2 + \Big[(1+\xi)M_\Delta + (1-\xi)M_N\Big]^2\right)^2\left(\Delta_x^2 + \Big[(1+\xi)M_\Delta - (1-\xi)M_N\Big]\right)}\\
&\cdot\Bigg(-\Delta_x^4 + 2\xi(M_\Delta + M_N)\Big[(1+\xi)M_\Delta + (1-\xi)M_N\Big]^2\Big[(1+\xi)M_\Delta - (1-\xi)M_N\Big]\\
&+ 2\Delta_x^2\Big[2M_\Delta M_N + (1-\xi^2)M_\Delta^2 + (1-\xi^2)M_N^2\Big]\Bigg)\\
x_4 =& -\frac{2(1-\xi^2)^2 M_N^2}{\left(\Delta_x^2 + \Big[(1+\xi)M_\Delta + (1-\xi)M_N\Big]^2\right)^2\left(\Delta_x^2 + \Big[(1+\xi)M_\Delta - (1-\xi)M_N\Big]\right)}\\
&\cdot\Bigg(2\Big[(1+\xi)M_\Delta + (1-\xi)M_N\Big]^2\Big[(1+\xi)M_\Delta - (1-\xi)M_N\Big]\\
&+ \Delta_x^2\Big[(1+2\xi-3\xi^2)M_N - (1-2\xi-3\xi^2)M_\Delta\Big]\Bigg)\\
y_4 =& -\frac{2(1-\xi^2)^2 M_N \Delta_x^2}{N}\\
z_4 =& \frac{2(1-\xi^2)^2 M_N^2}{\left(\Delta_x^2 + \Big[(1+\xi)M_\Delta + (1-\xi)M_N\Big]^2\right)^2\left(\Delta_x^2 + \Big[(1+\xi)M_\Delta - (1-\xi)M_N\Big]\right)}\\
&\cdot\Bigg(2\xi\Big[(1+\xi)M_\Delta + (1-\xi)M_N\Big]^2\Big[(1+\xi)M_\Delta - (1-\xi)M_N\Big]\\
&+ \Delta_x^2\Big[(3+2\xi-\xi^2)M_\Delta + (3-2\xi-\xi^2)M_N\Big]\Bigg)\\
w_5 =& \frac{(1-\xi)(1-\xi^2)(M_\Delta^2 - M_N^2)\Big[\Delta_x^2 - (1+\xi)^2 M_\Delta^2 + (1-\xi)^2 M_N^2\Big]}{N}\\
x_5 =& 0\\
y_5 =& 0\\
z_5 =& \frac{(1-\xi)(1-\xi^2)M_N^2\Big[(1+\xi)^2 M_\Delta^2 - (1-\xi)^2 M_N^2 - \Delta_x^2\Big]}{N}\\
w_6 =& \frac{2(1-\xi)(1-\xi^2)(M_\Delta - M_N)}{N}\left(\Delta_x^2 + (1-\xi)^2 M_N^2 - (1+\xi)^2 M_\Delta^2\right)\\
x_6 =& 0\\
y_6 =& -\frac{2(1-\xi)(1-\xi^2)M_N\Big[\Delta_x^2 + (1-\xi)^2 M_N^2 - (1+\xi)^2 M_\Delta^2\Big]}{N}\\
z_6 =& 0
\end{aligned}
$$

$$
\begin{aligned}
w_7 =& 0 \\
x_7 =& -\frac{2(1-\xi^2)M_N^2\Big[(1+\xi)^2M_\Delta+(1-\xi)M_N\Big]}{\Delta_x^2+\Big[(1+\xi)M_\Delta+(1-\xi)M_N\Big]^2} \\
y_7 =& 0 \\
z_7 =& 0 \\
w_8 =& -\frac{(1-\xi^2)(M_\Delta^2-M_N^2)\Big[(1+\xi)M_\Delta+(1-\xi)M_N\Big]}{\Delta_x^2+\Big[(1+\xi)M_\Delta+(1-\xi)M_N\Big]^2} \\
x_8 =& 0 \\
y_8 =& 0 \\
z_8 =& \frac{(1-\xi^2)M_N^2\Big[(1+\xi)M_\Delta+(1-\xi)M_N\Big]}{\Delta_x^2+\Big[(1+\xi)M_\Delta+(1-\xi)M_N\Big]^2} \\
w_9 =& 0 \\
x_9 =& \frac{2(1-\xi)(1-\xi^2)M_N^2\Big[\Delta_x^2+(1-\xi)^2M_N^2-(1+\xi)^2M_\Delta^2\Big]}{N} \\
y_9 =& 0 \\
z_9 =& 0 \\
w_{10} =& -\frac{2(1-\xi)(1-\xi^2)^2(M_\Delta^2-M_N^2)}{\left(\Delta_x^2+\Big[(1+\xi)M_\Delta+(1-\xi)M_N\Big]^2\right)^2\left(\Delta_x^2+\Big[(1+\xi)M_\Delta-(1-\xi)M_N\Big]^2\right)} \\
&\cdot\Bigg(\Big[(1+\xi)M_\Delta+(1-\xi)M_N\Big]^2\Big[(1+\xi)M_\Delta-(1-\xi)M_N\Big] \\
&-\Delta_x^2\Big[(1-\xi)M_N+2(1+\xi)M_\Delta\Big]\Bigg) \\
x_{10} =& 0 \\
y_{10} =& 0 \\
z_{10} =& \frac{2(1-\xi)(1-\xi^2)^2M_N^2}{\left(\Delta_x^2+\Big[(1+\xi)M_\Delta+(1-\xi)M_N\Big]^2\right)^2\left(\Delta_x^2+\Big[(1+\xi)M_\Delta-(1-\xi)M_N\Big]^2\right)} \\
&\cdot\Bigg(\Big[(1+\xi)M_\Delta+(1-\xi)M_N\Big]^2\Big[(1+\xi)M_\Delta-(1-\xi)M_N\Big] \\
&-\Delta_x^2\Big[2(1+\xi)M_\Delta+(1-\xi)M_N\Big]\Bigg)
\end{aligned}
$$

$$
\begin{aligned}
w_{11} =& \frac{4(1-\xi^2)^2}{N^2}\Bigg(\Delta_x^6 - 2\xi(1-\xi)M_N(M_\Delta - M_N)\Big[(1+\xi)^2M_\Delta^2 - (1-\xi)^2M_N^2\Big]^2 \\
&+ \Delta_x^4\Big[2(1+\xi)^2M_\Delta^2 + (3-2\xi-\xi^2)M_\Delta M_N - (1+2\xi-3\xi^2)M_N^2\Big] \\
&+ \Delta_x^2\Big[(1+\xi)^4M_\Delta^4 - 2(1-\xi)^3M_N^4 + (3-\xi)(1-\xi)^3M_\Delta M_N^3 \\
&+ (1+\xi)^2(1-4\xi+3\xi^2)M_N^2M_\Delta^2 - (3-8\xi+5\xi^2)(1+\xi)^2M_NM_\Delta^3\Big]\Bigg) \\
x_{11} =& -\frac{4(1-\xi^2)^3M_N^2}{N^2}\Bigg(-2\Delta_x^4 + \Big[(1-\xi)^2M_N^2 - (1+\xi)^2M_\Delta^2\Big]^2 \\
&- \Delta_x^2\Big[(1+\xi)^2M_\Delta^2 + (1-\xi)^2M_N^2\Big]\Bigg) \\
y_{11} =& -\frac{4(1-\xi)(1-\xi^2)^2M_N}{\left(\Delta_x^2 + \Big[(1+\xi)M_\Delta + (1-\xi)M_N\Big]^2\right)\left(\Delta_x^2 + \Big[(1+\xi)M_\Delta - (1-\xi)M_N\Big]^2\right)^2} \\
&\cdot\Bigg(\Delta_x^2\Big[(1-\xi)M_N - 2(1+\xi)M_\Delta\Big] \\
&+ \Big[(1+\xi)M_\Delta + (1-\xi)M_N\Big]\Big[(1+\xi)M_\Delta - (1-\xi)M_N\Big]^2\Bigg) \\
z_{11} =& \frac{4(1-\xi^2)^3M_N^2}{N^2}\Bigg(-2\Delta_x^4 + \Big[(1-\xi)^2M_N^2 - (1+\xi)^2M_\Delta^2\Big]^2 \\
&- \Delta_x^2\Big[(1+\xi)^2M_\Delta^2 + (1-\xi)^2M_N^2\Big]\Bigg) \\
w_{12} =& -\frac{4(1-\xi^2)M_N(M_\Delta - M_N)\left(\Delta_x^2 + \xi\Big[(1+\xi)^2M_\Delta^2 - (1-\xi)^2M_N^2\Big]\right)}{N} \\
x_{12} =& -\frac{2(1-\xi^2)(1+\xi)M_N^2\Big[\Delta_x^2 - (1-\xi)^2M_N^2 + (1+\xi)^2M_\Delta^2\Big]}{N} \\
y_{12} =& -\frac{2(1-\xi^2)M_N\Big[(1+\xi)M_\Delta - (1-\xi)M_N\Big]}{\Delta_x^2 + \Big[(1+\xi)M_\Delta - (1-\xi)M_N\Big]^2} \\
z_{12} =& \frac{2(1-\xi^2)(1+\xi)M_N^2\Big[\Delta_x^2 - (1-\xi)^2M_N^2 + (1+\xi)^2M_\Delta^2\Big]}{N} \quad .
\end{aligned}
$$

Equipped with the orthogonalized set of spurious covariants we can now proceed and express the GPDs in terms of all possible amplitudes. For DVCS these amplitudes can now be

decomposed into

$$
\begin{aligned}
G^{\mu}_{\lambda',\lambda} &= \sum_i C^{(i)\mu}_{\lambda',\lambda} A^i(x,\xi,t) + \sum_k \tilde{C}^{(k)\mu}_{\lambda',\lambda} B^k(x,\xi,t) \\
C^{(i)\mu}_{\lambda',\lambda} &= \frac{1}{2\bar{P}^+} \bar{u}_\nu(P',\lambda') \kappa_i^{\mu\nu} u(P,\lambda) \\
\tilde{C}^{(i)\mu}_{\lambda',\lambda} &= \frac{1}{2\bar{P}^+} \bar{u}_\nu(P',\lambda') \tilde{\kappa}_i'^{\mu\nu} u(P,\lambda) \\
\Big\{ A^i(x,\xi,t), B^k(x,\xi,t) \Big\} &= \{ C^1(x,\xi,t), C^2(x,\xi,t), C^3(x,\xi,t), C^4, B_1(x,\xi,t), \\
&\quad B_2(x,\xi,t), B_3(x,\xi,t), B_4(x,\xi,t), B_5(x,\xi,t), B_6(x,\xi,t), B_7(x,\xi,t), \\
&\quad B_8(x,\xi,t), B_9(x,\xi,t), B_{10}(x,\xi,t), B_{11}(x,\xi,t), B_{12}(x,\xi,t) \} \quad .
\end{aligned}
$$

By inverting this relation one obtains an unambiguous expression for both, physical and spurious GPDs. In principle they can be expressed in terms of the amplitude relations. However the analytical inversion of the 16*16 matrix is too involved even if we use Mathematica. Therefore we perform this inversion numerically.

The amplitudes $F^{\mu}_{\lambda',\lambda}$ can be decomposed into

$$
\begin{aligned}
F^{\mu}_{\lambda',\lambda} &= \sum_i C^{(i)\mu}_{\lambda',\lambda} F^i(Q^2) + \sum_k \tilde{C}^{(k)\mu}_{\lambda',\lambda} B^k(Q^2) \\
C^{(i)\mu}_{\lambda',\lambda} &= \frac{1}{2\sqrt{P'^+ P^+}} \bar{u}_\nu(P',\lambda') \kappa_i^{\mu\nu} u(P,\lambda) \\
\tilde{C}^{(i)\mu}_{\lambda',\lambda} &= \frac{1}{2\sqrt{P'^+ P^+}} \bar{u}_\nu(P',\lambda') \tilde{\kappa}_i'^{\mu\nu} u(P,\lambda) \\
\Big\{ F^i(Q^2), B^k(Q^2) \Big\} &= \{ C_5(t), C_6(t), C_3(t), C_4(t), B_1(t), B_2(t), B_3(t), B_4(t), B_5(t), \\
&\quad B_6(t), B_7(t), B_8(t), B_9(t), B_{10}(t), B_{11}(t), B_{12}(t) \} \quad .
\end{aligned}
$$

Again no simplification arises from considering the coefficients $C^{(i)\mu}_{\lambda',\lambda}$ and $\tilde{C}^{(k)\mu}_{\lambda',\lambda}$. Therefore we have to include all 16 covariants in the extraction of the physical form factors. The form factors can be expressed analytically in terms of the amplitude relations. We find

$$
\begin{aligned}
C_5(t) = & \frac{1}{2\sqrt{2}\Big[\Delta_x^2 + (M_\Delta - M_N)^2\Big]^2 \Big[\Delta_x^2 + (M_\Delta + M_N)^2\Big]^3} \Bigg(\Big[\Delta_x^9 M_N + 12 \Delta_x M_\Delta^2 (M_\Delta - M_N)^3 \\
& \cdot (M_\Delta + M_N)^4 + 2\Delta_x^3 (M_\Delta - M_N)(M_\Delta + M_N)^2 (4M_\Delta^2 - M_\Delta M_N - M_N^2) \\
& \cdot (M_\Delta^2 + M_N^2) + 2\Delta_x^7 (M_\Delta^3 + M_\Delta M_N^2 + 2M_N^3) + \Delta_x^5 (8M_\Delta^5 - M_\Delta^4 M_N + 2M_\Delta^3 M_N^2 \\
& - 4M_\Delta^2 M_N^3 + 6M_\Delta M_N^4 + 5M_N^5) \Big] \tilde{F}^+_{\frac{3}{2}\uparrow}
\end{aligned}
$$

$$
\begin{aligned}
&+ 2\sqrt{3}M_\Delta\Big[\Delta_x^8 M_N - 2\Delta_x^2(M_\Delta - 2M_N)(M_\Delta - M_N)^2(M_\Delta + M_N)^4 + 2(M_\Delta - M_N)^4 \\
&\cdot (M_\Delta + M_N)^5 + 2\Delta_x^6 M_N(M_\Delta^2 + M_\Delta M_N + 2M_N^2) + \Delta_x^4(M_\Delta + M_N) \\
&\cdot (M_\Delta^4 + 2M_\Delta^2 M_N^2 + 5M_N^4)\Big]\tilde{F}^+_{\frac{1}{2}\uparrow} \\
&+ \sqrt{3}\Delta_x M_\Delta\Big[\Delta_x^8 + 4(M_\Delta - M_N)^3(2M_\Delta - M_N)(M_\Delta + M_N)^4 + 4\Delta_x^6(M_\Delta^2 + M_N^2) \\
&+ 2\Delta_x^2(M_\Delta + M_N)^2(M_\Delta^4 + 4M_\Delta^2 M_N^2 - 8M_\Delta M_N^3 + 3M_N^4) + \Delta_x^4(7M_\Delta^4 + 2M_\Delta^3 M_N \\
&+ 4M_\Delta^2 M_N^2 - 2M_\Delta M_N^3 + 5M_N^4)\Big]\tilde{F}^+_{\frac{1}{2}\downarrow} \\
&+ \Delta_x^2\Big[\Delta_x^8 + 12M_\Delta^2(M_\Delta^2 - M_N^2)^3 + 2\Delta_x^6(2M_\Delta^2 + M_\Delta M_N + 2M_N^2) + 2\Delta_x^2(M_\Delta + M_N) \\
&\cdot (M_\Delta^2 + M_N^2)(3M_\Delta^3 - M_\Delta^2 M_N + M_\Delta M_N^2 + M_N^3) + \Delta_x^4(7M_\Delta^4 + 6M_\Delta^3 M_N + 8M_\Delta^2 M_N^2 \\
&+ 6M_\Delta M_N^3 + 5M_N^4\Big]\tilde{F}^+_{\frac{3}{2}\downarrow} \\
&+ 2\Delta_x^2(M_\Delta^2 - M_N^2)\Big[\Delta_x^4 M_N - (M_\Delta - M_N)(M_\Delta + M_N)^2(8M_\Delta^2 + M_\Delta M_N + M_N^2) \\
&+ 2\Delta_x^2(M_\Delta^3 - M_\Delta^2 M_N + M_\Delta M_N^2 + M_N^3)\Big]\tilde{F}^x_{\frac{3}{2}\uparrow} \\
&+ 4\sqrt{3}\Delta_x M_\Delta(M_\Delta^2 - M_N^2)\Big[\Delta_x^4 M_N + 2\Delta_x^2 M_\Delta(2M_\Delta - M_N)(M_\Delta + M_N) \\
&- (M_\Delta - M_N)^2(M_\Delta + M_N)^3\Big]\tilde{F}^x_{\frac{1}{2}\uparrow} \\
&+ 2\sqrt{3}\Delta_x^2 M_\Delta(M_\Delta^2 - M_N^2)\Big[\Delta_x^4 - (5M_\Delta - 3M_N)(M_\Delta - M_N)(M_\Delta + M_N)^2 \\
&+ \Delta_x^2(6M_\Delta^2 - 2M_N^2)\Big]\tilde{F}^x_{\frac{1}{2}\downarrow} \\
&+ 2\Delta_x^3(M_\Delta^2 - M_N^2)\Big[\Delta_x^4 - 9M_\Delta^4 + 2M_\Delta^3 M_N + 12M_\Delta^2 M_N^2 + 2M_\Delta M_N^3 + M_N^4 \\
&+ 2\Delta_x^2(M_\Delta^2 + M_\Delta M_N + M_N^2)\Big]\tilde{F}^x_{\frac{3}{2}\downarrow}\Bigg) \\
&+ \frac{i}{\sqrt{2}\Big[\Delta_x^2 + (M_\Delta - M_N)^2\Big]^2\Big[\Delta_x^2 + (M_\Delta + M_N)\Big]^2}\Bigg(-\Delta_x^2\Big[\Delta_x^4 M_N + (M_\Delta - M_N)^2 \\
&\cdot (M_\Delta + M_N)(2M_\Delta^2 + M_\Delta M_N + M_N^2) + 2\Delta_x^2(2M_\Delta^3 - M_\Delta^2 M_N + M_N^3)\Big]\tilde{F}^y_{\frac{3}{2}\uparrow} \\
&+ 2\sqrt{3}\Delta_x^3 M_\Delta(M_\Delta - M_N)\Big[\Delta_x^2 + M_N(M_\Delta + M_N)\Big]\tilde{F}^y_{\frac{1}{2}\uparrow} \\
&- \sqrt{3}\Delta_x^2 M_\Delta\Big[\Delta_x^4 + 4\Delta_x^2 M_\Delta M_N + (M_\Delta - M_N)^3(M_\Delta + M_N)\Big]\tilde{F}^y_{\frac{1}{2}\downarrow} \\
&- \Delta_x^3\Big[\Delta_x^4 + 3M_\Delta^4 - 8M_\Delta^3 M_N + 4M_\Delta^2 M_N^2 + M_N^4 + 2\Delta_x^2(M_\Delta^2 + M_N^2)\Big]\tilde{F}^y_{\frac{3}{2}\downarrow}\Bigg)
\end{aligned}
$$

$$
\begin{aligned}
&+\frac{1}{2\sqrt{2}\Big[\Delta_x^2+(M_\Delta-M_N)^2\Big]^2\Big[\Delta_x^2+(M_\Delta+M_N)^2\Big]^3}\Bigg(-\Delta_x^3\Big[\Delta_x^4M_N-(M_\Delta-M_N)\\
&\cdot(M_\Delta+M_N)^2(8M_\Delta^2+M_\Delta M_N+M_N^2)+2\Delta_x^2(M_\Delta^3-M_\Delta^2M_N+M_\Delta M_N^2+M_N^3)\Big]\tilde{F}^-_{\frac{3}{2}\uparrow}\\
&-2\sqrt{3}\Delta_x^2M_\Delta\Big[\Delta_x^4M_N+2\Delta_x^2M_\Delta(2M_\Delta-M_N)(M_\Delta+M_N)\\
&-(M_\Delta-M_N)^2(M_\Delta+M_N)^3\Big]\tilde{F}^-_{\frac{1}{2}\uparrow}-\sqrt{3}\Delta_x^3M_\Delta\Big[\Delta_x^4-(5M_\Delta-3M_N)(M_\Delta-M_N)\\
&\cdot(M_\Delta+M_N)^2+\Delta_x^2(6M_\Delta^2-2M_N^2)\Big]\tilde{F}^-_{\frac{1}{2}\downarrow}-\Delta_x^4\Big[\Delta_x^4-9M_\Delta^4+2M_\Delta^3M_N+12M_\Delta^2M_N^2\\
&+2M_\Delta M_N^3+M_N^4+2\Delta_x^2(M_\Delta^2+M_\Delta M_N+M_N^2)\Big]\tilde{F}^-_{\frac{3}{2}\downarrow}\Bigg)\\
C_6(t)=&\frac{1}{2\sqrt{2}\Big[\Delta_x^2+(M_\Delta-M_N)^2\Big]^2\Big[\Delta_x^2+(M_\Delta+M_N)^2\Big]^3}\Bigg(\Delta_xM_N^2\Big[\Delta_x^2+2(M_\Delta^2+M_N^2)\Big]\\
&\cdot\Big[\Delta_x^4M_N-(M_\Delta-M_N)(M_\Delta+M_N)^2(8M_\Delta^2+M_\Delta M_N+M_N^2)+2\Delta_x^2(M_\Delta^3-M_\Delta^2M_N\\
&+M_\Delta M_N^2+M_N^3)\Big]\tilde{F}^+_{\frac{3}{2}\uparrow}\\
&+2\sqrt{3}M_\Delta M_N^2\Big[\Delta_x^4M_N+2\Delta_x^2M_\Delta(2M_\Delta-M_N)(M_\Delta+M_N)\\
&-(M_\Delta-M_N)^2(M_\Delta+M_N)^3\Big]\Big[\Delta_x^2+2(M_\Delta^2+M_N^2)\Big]\tilde{F}^+_{\frac{1}{2}\uparrow}\\
&+\sqrt{3}\Delta_xM_\Delta M_N^2\Big[\Delta_x^4-(5M_\Delta-3M_N)(M_\Delta-M_N)(M_\Delta+M_N)^2\\
&+\Delta_x^2(6M_\Delta^2-2M_N^2)\Big]\tilde{F}^+_{\frac{1}{2}\downarrow}\\
&+\Delta_x^2M_N^2\Big[\Delta_x^2+2(M_\Delta^2+M_N^2)\Big]\Bigg[\Delta_x^4-9M_\Delta^4+2M_\Delta^3M_N+12M_\Delta^2M_N^2+2M_\Delta M_N^3\\
&+M_N^4+2\Delta_x^2(M_\Delta^2+M_\Delta M_N+M_N^2)\Big]\tilde{F}^+_{\frac{3}{2}\downarrow}\\
&-2M_N^2(M_\Delta+M_N)\Big[\Delta_x^4(M_N^2-6M_\Delta^2-M_\Delta M_N)+(M_\Delta^2-M_N^2)^2\\
&\cdot(2M_\Delta^2+M_\Delta M_N+M_N^2)-2\Delta_x^2(7M_\Delta^4-2M_\Delta^3M_N+8M_\Delta^2M_N^2-M_N^4)\Big]\tilde{F}^x_{\frac{3}{2}\uparrow}\\
&-4\sqrt{3}\Delta_xM_\Delta M_N^2\Big[\Delta_x^4(2M_\Delta+M_N)-(M_\Delta-M_N)(M_\Delta+M_N)^2\\
&\cdot(4M_\Delta^2-M_\Delta M_N+3M_N^2)+\Delta_x^2(3M_\Delta^3+5M_\Delta M_N^2+4M_N^3)\Big]\tilde{F}^x_{\frac{1}{2}\uparrow}\\
&-2\sqrt{3}M_\Delta M_N^2\Big[2\Delta_x^6-\Delta_x^4(M_\Delta^2+2M_\Delta M_N-7M_N^2)+(M_\Delta^2-M_N^2)^3\\
&-4\Delta_x^2(3M_\Delta^4+M_\Delta^3M_N+M_\Delta M_N^3-M_N^4)\Big]\tilde{F}^x_{\frac{1}{2}\downarrow}\\
&-2\Delta_xM_N^2\Big[\Delta_x^4(M_N^2-7M_\Delta^2)-2\Delta_x^2(7M_\Delta^4+M_\Delta^3M_N+6M_\Delta^2M_N^2-M_\Delta M_N^3-M_N^4)\\
&+(M_\Delta+M_N)^2(3M_\Delta^4-8M_\Delta^3M_N+4M_\Delta^2M_N^2+M_N^4)\Big]\tilde{F}^x_{\frac{3}{2}\downarrow}\Bigg)
\end{aligned}
$$

$$
\begin{aligned}
&+\frac{i}{\sqrt{2}\Big[\Delta_x^2+(M_\Delta-M_N)^2\Big]^2\Big[\Delta_x^2+(M_\Delta+M_N)^2\Big]^2}\Bigg(-M_N^2\Big[\Delta_x^4M_N+(M_\Delta-M_N)^2\\
&\cdot(M_\Delta+M_N)(2M_\Delta^2+M_\Delta M_N+M_N^2)+2\Delta_x^2(2M_\Delta^3-M_\Delta^2M_N+M_N^3)\Big]\tilde{F}^y_{\frac{3}{2}\uparrow}\\
&-\sqrt{3}M_\Delta M_N^2\Big[\Delta_x^4+4\Delta_x^2M_\Delta M_N+(M_\Delta-M_N)^3(M_\Delta+M_N)\Big]\tilde{F}^y_{\frac{1}{2}\downarrow}\\
&-\Delta_xM_N^2\Big[\Delta_x^4+3M_\Delta^4-8M_\Delta^3M_N+4M_\Delta^2M_N^2+M_N^4+2\Delta_x^2(M_\Delta^2+M_N^2)\Big]\tilde{F}^y_{\frac{3}{2}\downarrow}\Bigg)\\
&+\frac{i\sqrt{6}\Delta_xM_\Delta(M_\Delta-M_N)M_N^2\Big[\Delta_x^2+M_N(M_\Delta+M_N)\Big]}{\Big[(\Delta_x^2+M_\Delta^2)^2+2(\Delta_x-M_\Delta)(\Delta_x+M_\Delta)M_N^2+M_N^4\Big]^2}\tilde{F}^y_{\frac{1}{2}\uparrow}\\
&+\frac{1}{2\sqrt{2}\Big[\Delta_x^2+(M_\Delta-M_N)^2\Big]^2\Big[\Delta_x^2+(M_\Delta+M_N)^2\Big]^3}\Bigg(-\Delta_xM_N^2\Big[\Delta_x^4M_N-(M_\Delta-M_N)\\
&\cdot(M_\Delta+M_N)^2(8M_\Delta^2+M_\Delta M_N+M_N^2)+2\Delta_x^2(M_\Delta^3-M_\Delta^2M_N+M_\Delta M_N^2+M_N^3)\Big]\tilde{F}^-_{\frac{3}{2}\uparrow}\\
&+2\sqrt{3}M_\Delta M_N^2\Big[-\Delta_x^4M_N-2\Delta_x^2M_\Delta(2M_\Delta-M_N)(M_\Delta+M_N)+(M_\Delta-M_N)^2\\
&\cdot(M_\Delta+M_N)^3\Big]\tilde{F}^-_{\frac{1}{2}\uparrow}\\
&-\sqrt{3}\Delta_xM_\Delta M_N^2\Big[\Delta_x^4-(5M_\Delta-3M_N)(M_\Delta-M_N)(M_\Delta+M_N)^2\\
&+\Delta_x^2(6M_\Delta^2-2M_N^2)\Big]\tilde{F}^-_{\frac{1}{2}\downarrow}\\
&-\Delta_x^2M_N^2\Big[\Delta_x^4-9M_\Delta^4+2M_\Delta^3M_N+12M_\Delta^2M_N^2+2M_\Delta M_N^3+M_N^4\\
&+2\Delta_x^2(M_\Delta^2+M_\Delta M_N+M_N^2)\Big]\tilde{F}^-_{\frac{3}{2}\downarrow}\Bigg)\\
C_3(t)=&\frac{1}{2\sqrt{2}\Big[(\Delta_x^2+M_\Delta^2)^2+2(\Delta_x-M_\Delta)(\Delta_x+M_\Delta)M_N^2+M_N^4\Big]^2}\Bigg(-\Delta_xM_\Delta M_N\\
&\cdot\Big[\Delta_x^2(3M_\Delta-M_N)+(M_\Delta-M_N)(M_\Delta+M_N)^2\Big]\Big[\Delta_x^2+2(M_\Delta^2+M_N^2)\Big]\tilde{F}^+_{\frac{3}{2}\uparrow}\\
&-\sqrt{3}\Delta_xM_\Delta M_N(M_\Delta+M_N)(\Delta_x^2-M_\Delta^2+M_N^2)\Big[\Delta_x^2+2(M_\Delta^2+M_N^2)\Big]\tilde{F}^+_{\frac{1}{2}\downarrow}\\
&+\Delta_x^2M_\Delta M_N\Big[\Delta_x^2+(M_\Delta+M_N)(3M_\Delta+M_N)\Big]\Big[\Delta_x^2+2(M_\Delta^2+M_N^2)\Big]\tilde{F}^+_{\frac{3}{2}\downarrow}\\
&+2\sqrt{3}M_\Delta(M_\Delta-M_N)M_N(M_\Delta+M_N)^2(M_\Delta^2-M_N^2-\Delta_x^2)\tilde{F}^x_{\frac{1}{2}\downarrow}\\
&+2\Delta_xM_\Delta M_N(M_\Delta^2-M_N^2)\Big[\Delta_x^2+(M_\Delta+M_N)(3M_\Delta+M_N)\Big]\tilde{F}^x_{\frac{3}{2}\downarrow}\\
&+\sqrt{3}\Delta_xM_\Delta M_N(M_\Delta+M_N)(\Delta_x^2-M_\Delta^2+M_N^2)\tilde{F}^-_{\frac{1}{2}\downarrow}\Bigg)
\end{aligned}
$$

$$
\begin{aligned}
&+\frac{1}{2\sqrt{2}\Big[\Delta_x^2+(M_\Delta-M_N)^2\Big]^2\Big[\Delta_x^2+(M_\Delta+M_N)^2\Big]^2}\Bigg(\sqrt{3}\Delta_x^2 M_\Delta M_N\\
&\cdot(\Delta_x^2-M_\Delta^2+M_N^2)\Big[\Delta_x^2+2(M_\Delta^2+M_N^2)\Big]\tilde{F}^+_{\frac{1}{2}\uparrow}\\
&-2M_\Delta(M_\Delta^2-M_N^2)M_N\Big[\Delta_x^2(3M_\Delta-M_N)+(M_\Delta-M_N)(M_\Delta+M_N)^2\Big]\tilde{F}^x_{\frac{3}{2}\uparrow}\\
&+2\sqrt{3}\Delta_x M_\Delta M_N(M_\Delta^2-M_N^2)(\Delta_x^2-M_\Delta^2+M_N^2)\tilde{F}^x_{\frac{1}{2}\uparrow}\\
&+\frac{i}{\sqrt{2}\Big[\Delta_x^2+(M_\Delta-M_N)^2\Big]^2\Big[\Delta_x^2+(M_\Delta+M_N)^2\Big]}\Bigg(-M_\Delta M_N\Big[\Delta_x^2(M_N-3M_\Delta)\\
&+(M_\Delta-M_N)^2(M_\Delta+M_N)\Big]\tilde{F}^y_{\frac{3}{2}\uparrow}\\
&-\sqrt{3}\Delta_x M_\Delta M_N(\Delta_x^2-3M_\Delta^2+2M_\Delta M_N+M_N^2)\tilde{F}^y_{\frac{1}{2}\uparrow}\\
&+\sqrt{3}M_\Delta M_N\Big[\Delta_x^2(M_N-3M_\Delta)+(M_\Delta-M_N)^2(M_\Delta+M_N)\Big]\tilde{F}^y_{\frac{1}{2}\downarrow}\\
&-\Delta_x M_\Delta M_N(\Delta_x^2-3M_\Delta^2+2M_\Delta M_N+M_N^2)\tilde{F}^y_{\frac{3}{2}\downarrow}\Bigg)\\
&+\frac{1}{2\sqrt{2}\Big[\Delta_x^2+(M_\Delta-M_N)^2\Big]^2\Big[\Delta_x^2+(M_\Delta+M_N)^2\Big]^2}\Bigg(\Delta_x M_\Delta M_N\Big[\Delta_x^2(3M_\Delta-M_N)\\
&+(M_\Delta-M_N)(M_\Delta+M_N)^2\Big]\tilde{F}^-_{\frac{3}{2}\uparrow}\\
&-\sqrt{3}\Delta_x^2 M_\Delta M_N(\Delta_x^2-M_\Delta^2+M_N^2)\tilde{F}^-_{\frac{1}{2}\uparrow}\\
&-\Delta_x^2 M_\Delta M_N\Big[\Delta_x^2+(M_\Delta+M_N)(3M_\Delta+M_N)\Big]\tilde{F}^-_{\frac{3}{2}\downarrow}\Bigg)\\
C_4(t)=&\frac{1}{2\sqrt{2}\Big[\Delta_x^2+(M_\Delta-M_N)^2\Big]^2\Big[\Delta_x^2+(M_\Delta+M_N)^2\Big]^3}\Bigg(-\Delta_x M_N^2\Big[\Delta_x^6 M_N\\
&+2\Delta_x^4(M_\Delta+2M_N)(M_\Delta^2+M_N^2)+2(M_\Delta-M_N)(M_\Delta+M_N)^3\\
&\cdot(6M_\Delta^3-7M_\Delta^2M_N-M_N^3)+\Delta_x^2(M_\Delta+M_N)(4M_\Delta^4-M_\Delta^3M_N+7M_\Delta^2M_N^2\\
&+M_\Delta M_N^3+5M_N^4\Big]\tilde{F}^+_{\frac{3}{2}\uparrow}\\
&-2\sqrt{3}M_\Delta M_N^2\Big[-\Delta_x^6 M_\Delta+2(M_\Delta-M_N)^3(M_\Delta+M_N)^4-2\Delta_x^2(2M_\Delta+M_N)\\
&\cdot(M_\Delta^2-M_N^2)^2-2\Delta_x^4 M_\Delta(M_\Delta^2+M_N^2)\Big]\tilde{F}^+_{\frac{1}{2}\uparrow}
\end{aligned}
$$

$$
\begin{aligned}
&+\sqrt{3}\Delta_x M_\Delta M_N^2\Big[\Delta_x^6+4\Delta_x^4M_N^2-2(M_\Delta-M_N)(M_\Delta+M_N)^3\\
&\cdot(5M_\Delta^2-6M_\Delta M_N+3M_N^2)-\Delta_x^2(M_\Delta^2-M_N^2)(M_\Delta^2+2M_\Delta M_N+9M_N^2)\Big]\tilde{F}^+_{\frac{1}{2}\downarrow}\\
&-\Delta_x^2M_N^2\Big[\Delta_x^6+2\Delta_x^4(4M_\Delta^2+M_\Delta M_N+2M_N^2)+2(M_\Delta+M_N)^2(9M_\Delta^4-12M_\Delta^3M_N\\
&+10M_\Delta^2M_N^2+M_N^4)+\Delta_x^2(15M_\Delta^4+10M_\Delta^3M_N+20M_\Delta^2M_N^2+6M_\Delta M_N^3+5M_N^4)\Big]\tilde{F}^+_{\frac{3}{2}\downarrow}\\
&+2M_N^2(M_N^2-M_\Delta^2)\Big[\Delta_x^4M_N-M_N(M_\Delta-M_N)(M_\Delta+M_N)^3-2\Delta_x^2(M_\Delta+M_N)\\
&\cdot(5M_\Delta^2-M_N^2)\Big]\tilde{F}^x_{\frac{3}{2}\uparrow}\\
&-4\sqrt{3}\Delta_x M_\Delta M_N^2(M_\Delta^2-M_N^2)\Big[-2(M_\Delta-M_N)(M_\Delta+M_N)^2+\Delta_x^2(3M_\Delta+2M_N)\Big]\tilde{F}^x_{\frac{1}{2}\uparrow}\\
&-2\sqrt{3}M_\Delta M_N^2(M_\Delta^2-M_N^2)\Big[3\Delta_x^4-2\Delta_x^2(3M_\Delta-M_N)(M_\Delta+M_N)+(M_\Delta-M_N)\\
&\cdot(M_\Delta+M_N)^3\Big]\tilde{F}^x_{\frac{1}{2}\downarrow}\\
&+2\Delta_x M_N^2(M_N^2-M_\Delta^2)\Big[\Delta_x^4+(M_\Delta+M_N)^2(3M_\Delta^2+M_N^2)\\
&+2\Delta_x^2(M_N^2+M_\Delta M_N-3M_\Delta^2)\Big]\tilde{F}^x_{\frac{3}{2}\downarrow}\Bigg)\\
&+\frac{i}{\sqrt{2}\Big[\Delta_x^2+(M_\Delta-M_N)^2\Big]^2\Big[\Delta_x^2+(M_\Delta+M_N)^2\Big]^2}\Bigg(M_N^2\Big[\Delta_x^4M_N+M_N(M_\Delta^2-M_N^2)^2\\
&-2\Delta_x^2(M_\Delta^3+2M_\Delta^2M_N-M_N^3)\Big]\tilde{F}^y_{\frac{3}{2}\uparrow}\\
&+\sqrt{3}M_\Delta M_N^2\Big[\Delta_x^4+2\Delta_x^2M_\Delta(M_\Delta+M_N)-(M_\Delta^2-M_N^2)^2\Big]\tilde{F}^y_{\frac{1}{2}\downarrow}\Bigg)\\
&+\frac{i}{\sqrt{2}\Big[(\Delta_x^2+M_\Delta^2)^2+2(\Delta_x-M_\Delta)(\Delta_x+M_\Delta)M_N^2+M_N^4\Big]^2}\Bigg(2\sqrt{3}\Delta_x M_\Delta M_N^2\\
&\cdot\Big[\Delta_x^2M_N-(M_\Delta-M_N)(M_\Delta+M_N)^2\Big]\tilde{F}^y_{\frac{1}{2}\uparrow}\\
&+\Delta_x M_N^2\Big[\Delta_x^4-3M_\Delta^4+2(\Delta_x^2+M_\Delta^2)M_N^2+M_N^4\Big]\tilde{F}^y_{\frac{3}{2}\downarrow}\Bigg)\\
&+\frac{1}{2\sqrt{2}\Big[\Delta_x^2+(M_\Delta-M_N)^2\Big]^2\Big[\Delta_x^2+(M_\Delta+M_N)^2\Big]^3}\Bigg(\Delta_x M_N^2\Big[\Delta_x^4M_N-(M_\Delta-M_N)M_N\\
&\cdot(M_\Delta+M_N)^3-2\Delta_x^2(M_\Delta+M_N)(5M_\Delta^2-M_N^2)\Big]\tilde{F}^-_{\frac{3}{2}\uparrow}
\end{aligned}
$$

$$+ 2\sqrt{3}\Delta_x^2 M_\Delta M_N^2 \Big[-2(M_\Delta - M_N)(M_\Delta + M_N)^2 + \Delta_x^2(3M_\Delta + 2M_N)\Big]\tilde{F}^-_{\frac{1}{2}\uparrow}$$
$$+ \sqrt{3}\Delta_x M_\Delta M_N^2 \Big[3\Delta_x^4 - 2\Delta_x^2(3M_\Delta - M_N)(M_\Delta + M_N) + (M_\Delta - M_N)$$
$$\cdot (M_\Delta + M_N)^3\Big]\tilde{F}^-_{\frac{1}{2}\downarrow}$$
$$+ \Delta_x^2 M_N^2 \Big[\Delta_x^4 + (M_\Delta + M_N)^2(3M_\Delta^2 + M_N^2) + 2\Delta_x^2(M_N^2 - 3M_\Delta^2 + M_\Delta M_N)\Big]\tilde{F}^-_{\frac{3}{2}\downarrow}\Bigg) \quad . \quad (5.9)$$

Again we remark that if we introduce the consistency relations in eq. 4.31 we find back the expressions in eq. 4.23.

5.4 Results and discussion

In this section we apply the previously explored spurious covariants formalism to calculate the form factors and mixed GPDs and hence hope to overcome covariance breaking effects from the impulse approximation. To be more precise using spurious covariants allows us to restore reference frame independence for form factors and GPDs which was previously violated due to covariance breaking.

In fig. 5.3 we see that the curves for the $N \to N$ form factors which we obtained using spurious covariants (red) are similar in shape to the curves which we calculated from the good component of the transition amplitudes alone (black). Actually the black curve is obtained by evaluating eq. 5.5 where we use the consistency relations to obtain the bad component transition amplitudes from the good **LF** component model transition amplitudes. The black curves coincide with fig. 4.6 which illustrates the consistency of 4.28 and 4.16 with 5.5[2].

However the red curves are quantitatively different from the black curves and hence differ considerably from the experimental data.

Consequently we have to address the question why our new results are numerically poorer than the results from the simple approach. We had rather expected the opposite beforehand as spurious covariants were introduced in order to deal with frame dependence due to covariance breaking.

Firstly we remark that the free parameters of the spatial wave function (see eq. 3.14) have been chosen such that $G_M^p(Q^2)$ is best described if it is extracted from the good components of the transition amplitudes alone. By introducing spurious covariants more transition amplitudes get involved and the interplay among them causes trouble. This is particularly the case as we know that the "$\perp$" and "$-$" components of the transition amplitudes suffer from sizable inconsistencies as we have discussed in sec. 4.7. Unfortunately the obvious consequence of this observation namely to readjust the free parameters in the quark model wave functions for the use of spurious covariants does not work. We have scanned the parameter space from $m_q = 100$ MeV... 500 MeV and $\alpha = 0.3$ GeV^2... 0.7 GeV^2 and found that while the use of spurious covariants leads to good results for $G_M^p(Q^2)$ for a wide range of (m_q, α), $G_E^p(Q^2)$

[2]We have also verified this consistency analytically.

does not even get close to being described successfully. So we perform our calculations with the given parameters for the sake of comparability.

Secondly we like to remind the reader that a small error in some of the amplitudes can lead to a sizable error in the form factors due to the interplay among the different amplitudes. As an example for such a behavior we recall the violation of the angular condition (eq. 4.30). Here a 30% effect lead to a total loss of predictive power in the extraction of $G_E^\star(Q^2)$ and $G_C^\star(Q^2)$. In this example $G_M^\star(Q^2)$ proved to be robust against small deviations from the angular condition while $G_E^\star(Q^2)$ and $G_C^\star(Q^2)$ did not. The question now arises which properties our model amplitudes should have in order to guarantee robust results for the form factors that are obtained using spurious covariants.

We will address this question by focussing on a discussion about $F_1^p(Q^2)$ (upper left panel in fig. 5.3). In the spurious covariants approach we obtain $F_1^p(Q^2 = 0) \sim 2$ and thus find a strong deviation from the physical value $F_1^p(Q^2 = 0) = 1$. Physically this means that the charge is not conserved. Therefore we now explore where this strong deviation stems from. The expression for $F_1^p(Q^2)$ in eq. 5.5 reduces in the limit $Q^2 \to 0$ to

$$F_1(0) = \frac{1}{2}\tilde{F}^+_{\uparrow\uparrow} + \frac{1}{8M_N^2}\tilde{F}^-_{\uparrow\uparrow} \quad .$$

The expression for $F_1(0)$ extracted from the good **LF** component transition amplitudes alone reads

$$F_1(0) = \tilde{F}^+_{\uparrow\uparrow} \quad .$$

These expressions agree if

$$\tilde{F}^-_{\uparrow\uparrow} = 4M_N^2\tilde{F}^+_{\uparrow\uparrow} \quad . \tag{5.10}$$

This is one of the consistency relations for respecting Poincare covariance (c.f. eq. 4.28) in the limit $Q^2 \to 0$.The inconsistency of our model amplitude $\tilde{F}^-_{\uparrow\uparrow}$ with eq. 5.10 thus causes $F_1^p(0)$ to deviate from unity.

Charge non conservation is clearly a major drawback. We emphasize that using spurious covariants only the effects of covariance breaking on the frame dependence are resolved. Other inconsistencies due to covariance breaking are not necessarily removed. Nevertheless it is still frustrating that using good **LF** component transition amplitudes alone the proton charge is conserved while employing a more elaborated approach charge conservation is violated[3]. Therefore we take a closer look on how charge conservation comes about in the former case and what difference appears in the latter. For $Q^2 = 0$ the Melosh rotation becomes unity (c.f. eq. 3.6). For the relevant current components $Q^2 = 0$ leads to (see eq. 3.16)

$$\langle p', \lambda' \mid J^+ \mid p, \lambda\rangle = \chi^\dagger_{\lambda'}\chi_\lambda \tag{5.11}$$

$$\langle p', \lambda' \mid J^- \mid p, \lambda\rangle = \frac{m^2 + \vec{p}_\perp^{\,2}}{(p^+)^2}\chi^\dagger_{\lambda'}\chi_\lambda \quad . \tag{5.12}$$

[3]In [22] the charge of the proton is conserved. However this stems from the authors default to orthogonalize all spurious covariants. We have already discussed why this is mandatory and where the argument provided in [22] to not having to orthogonalize $\tilde{\kappa}_2^\mu$ and $\tilde{\kappa}_3^\mu$ fails.

For the spin flavor portion we find unity in both cases for the non flip amplitude. Thus the normalization of the spatial wave function enforces $\tilde{F}_{\uparrow\uparrow}^{+(p\to p)} = 1$ while the kinematical factor in the integrand from eq. 5.12 certainly does not enforce $\tilde{F}_{\uparrow\uparrow}^{-(p\to p)} = 4M_N^2$.

The other three panels in fig. 5.3 show that the reference frame dependence at least is not for all form factors of the order 100%. We have already mentioned in the previous section that a possible non physical form factor $F_3(t)$ is zero if gauge invariance is satisfied. In fact eq. 5.5 allows for the weaker condition that

$$2M_N\tilde{F}_{\uparrow\uparrow}^{x} = \Delta_x\tilde{F}_{\downarrow\uparrow}^{x} \tag{5.13}$$

has to be satisfied in order to guarantee vanishing of $F_3(t)$ in the spurious covariants formalism. We note that our model satisfies this condition.

In fig. 5.4 the black curves coincide with fig. 4.12 which illustrates the consistency of 4.29 and 4.17 with 5.7[4]. Just as for $F_1^p(Q^2)$ we find that the reference frame independent results (red) for $G_A(Q^2)$ and $G_P(Q^2)$ differ strongly from the respective results in chapter 4. For $G_A(Q^2)$ the new result moves far away from the experimental data while $G_P(Q^2)$ switches sign. As our quark model does not describe pion physics we consider the sign correction as a fortunate coincidence.

In figs. 5.5 and 5.6 the situation is similar. The black curves agree with the results from prescription I in figs. 4.18 and 4.24. In the case of the vectorial $N \to \Delta$ transition this result roots in the smallness of $G_4^\star(t)$ in the spurious covariants formalism. In the lower left panels the statistical errors from the MC integration add up to an effect that is visible with the bare eye. This is not the case for most other results. The numerical results for $H_E^\star(Q^2)$ and $H_C^\star(Q^2)$ are not impressive. On the other hand the ambiguity due to different possible prescriptions how to extract the $N \to \Delta$ transition form factors from the amplitudes has been resolved. The uniqueness of the $N \to \Delta$ transition form factors is a positive consequence of the spurious covariants formalism applied to the $N \to \Delta$ transition.

Unlike for the $N \to N$ transition gauge invariance is not satisfied for the $N \to \Delta$ transition amplitudes in our model. Eq. 5.8 reveals that again a weaker condition than gauge invariance

$$\Big[(M_\Delta^2 - M_N^2)\tilde{F}_{\lambda'\lambda}^{+} - \Delta_x\tilde{F}_{\lambda'\lambda}^{x}\Big] = 0$$

is sufficient in the spurious covariants formalism to ensure $G_4^\star(Q^2)$ to vanish:

$$\begin{aligned}
0 = \Bigg(& 3\Delta_x M_\Delta^2(M_\Delta - M_N)\Big[(M_\Delta^2 - M_N^2)\tilde{F}_{\frac{3}{2}\uparrow}^{+} - \Delta_x\tilde{F}_{\frac{3}{2}\uparrow}^{x}\Big] \\
& - \sqrt{3}M_\Delta\Big[\Delta_x^2(2M_\Delta - M_N) - (M_\Delta - M_N)^2(M_\Delta + M_N)\Big]\Big[(M_\Delta^2 - M_N^2)\tilde{F}_{\frac{1}{2}\uparrow}^{+} - \Delta_x\tilde{F}_{\frac{1}{2}\uparrow}^{x}\Big] \\
& + \sqrt{3}\Delta_x M_\Delta(\Delta_x^2 - 2M_\Delta^2 + M_\Delta M_N + M_N^2)\Big[(M_\Delta^2 - M_N^2)\tilde{F}_{\frac{1}{2}\downarrow}^{+} - \Delta_x\tilde{F}_{\frac{1}{2}\downarrow}^{x}\Big] \\
& - 3\Delta_x^2 M_\Delta^2\Big[(M_\Delta^2 - M_N^2)\tilde{F}_{\frac{3}{2}\downarrow}^{+} - \Delta_x\tilde{F}_{\frac{3}{2}\downarrow}^{x}\Big]\Bigg) \quad .
\end{aligned} \tag{5.14}$$

[4]We have also verified this consistency analytically.

The result for $G_4^\star(t)$ shows that our model satisfies this relation to good accuracy while gauge invariance is strongly violated.

About figs. 5.7, 5.8, 5.9 and 5.10 we have not much to say. However one observation requires a remark. The spurious covariants formalism absorbs reference frame dependence into non physical form factors and GPDs. The dependence of

$$\int_{-1}^{1} dx\, GPD(x,\xi,t) \tag{5.15}$$

on ξ obviously does not decrease if the reference dependence is eliminated. The neglect of non valence contributions seems to be the dominant cause for the sum rule violation. We mention that for $H_C^\star(Q^2)$ (lower left panel in fig. 5.9) and particularly for $C_3^\star(Q^2)$ (lower left panel in fig. 5.10) numerical uncertainties play a big role which show up as wiggles in the curves.

In conclusion we like to address the reason for the poor numerical findings in this chapter. Firstly we remark that already the amplitude relations which we discussed in the last chapter were badly satisfied. Certainly this effects are handed down to the form factors and mixed twist GPDs which we have calculated here. In order to understand why the non plus LF component transition amplitudes are described so badly in the quark model we recall the expression for the bad **LF** component from chapter 3

$$\chi = \frac{1}{\partial^+}\Big[\vec{\alpha}^\perp(\vec{\partial}^\perp - ig\vec{A}^\perp)\phi - im\gamma^0\phi\Big] \quad .$$

In the quark model we have neglected the gluon contribution. This influences the bad **LF** component transition amplitudes, but not the + components. We had the hope that the quark model might be capable of providing at least a good approximation for the bad LF component transition amplitudes. This is clearly not the case. One needs a better model (that treats higher Fock states) in order to reasonably access the bad LF component amplitudes.

The spurious covariants which we have discussed in this chapter are model independent. So the results in this chapter have a use beyond the specific model context discussed here for illustrative purpose. We have demonstrated in the framework of a LF quark model that reference frame dependencies can be absorbed into spurious form factors and GPDs. It would be interesting to employ a more involved model like [115] to exploit this formalism.

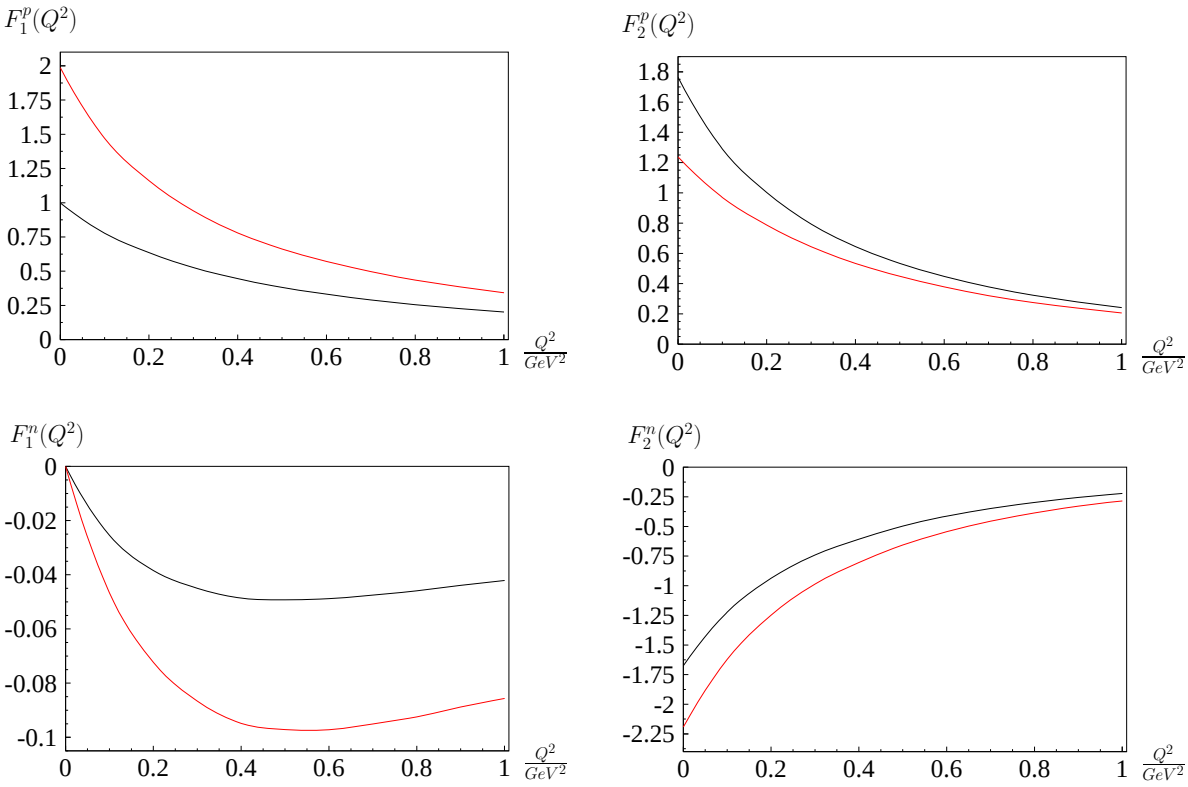

Figure 5.3: *The vectorial nucleon form factors calculated using the spurious covariants formalism (eq. 5.5). The red curve is obtained using all amplitudes from our LF quark model calculation. The black curve uses $\tilde{F}^+_{\uparrow\uparrow}$ and $\tilde{F}^+_{\downarrow\uparrow}$ from the model while the other amplitudes that we use are obtained using eq. 4.28.*

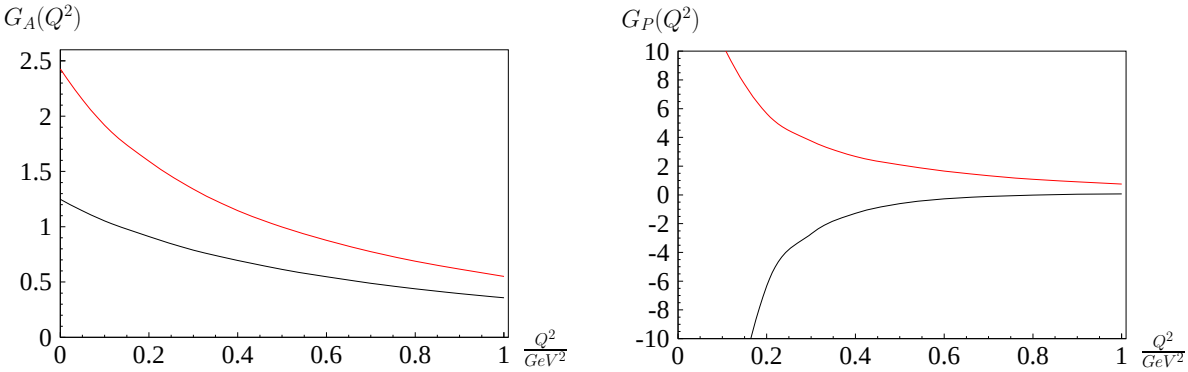

Figure 5.4: *The axial nucleon form factors calculated using the spurious covariants formalism (eq. 5.7). The red curve is obtained using all amplitudes from our LF quark model calculation. The black curve uses $\tilde{F}^+_{\uparrow\uparrow}$ and $\tilde{F}^x_{\downarrow\uparrow}$ from the model while the other amplitudes that we use are obtained using eq. 4.29.*

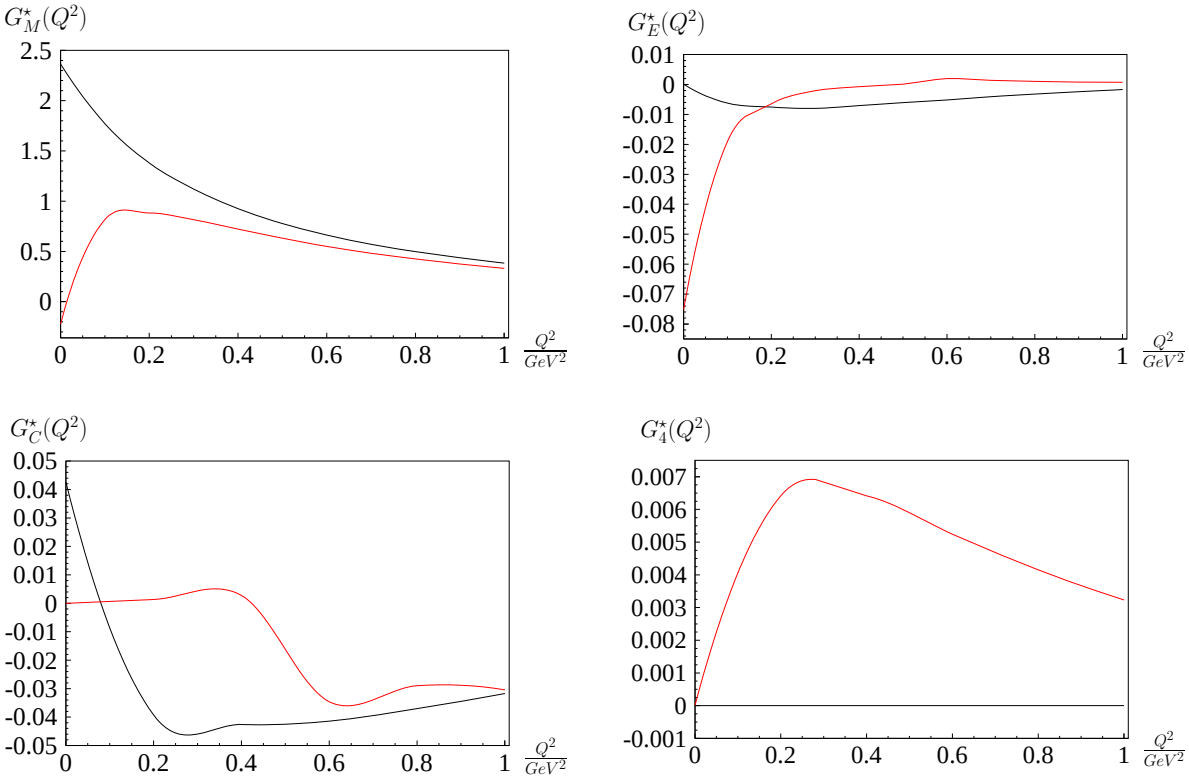

Figure 5.5: *The vectorial $N \to \Delta$ transition form factors calculated using the spurious covariants formalism (eq. 5.8). The red curve is obtained using all amplitudes from our LF quark model calculation. The black curve uses $\tilde{F}^+_{\frac{3}{2}\uparrow}$, $\tilde{F}^+_{\frac{1}{2}\uparrow}$ and $\tilde{F}^+_{\frac{1}{2}\downarrow}$ from the model while the other amplitudes that we use are obtained using eq. 4.30.*

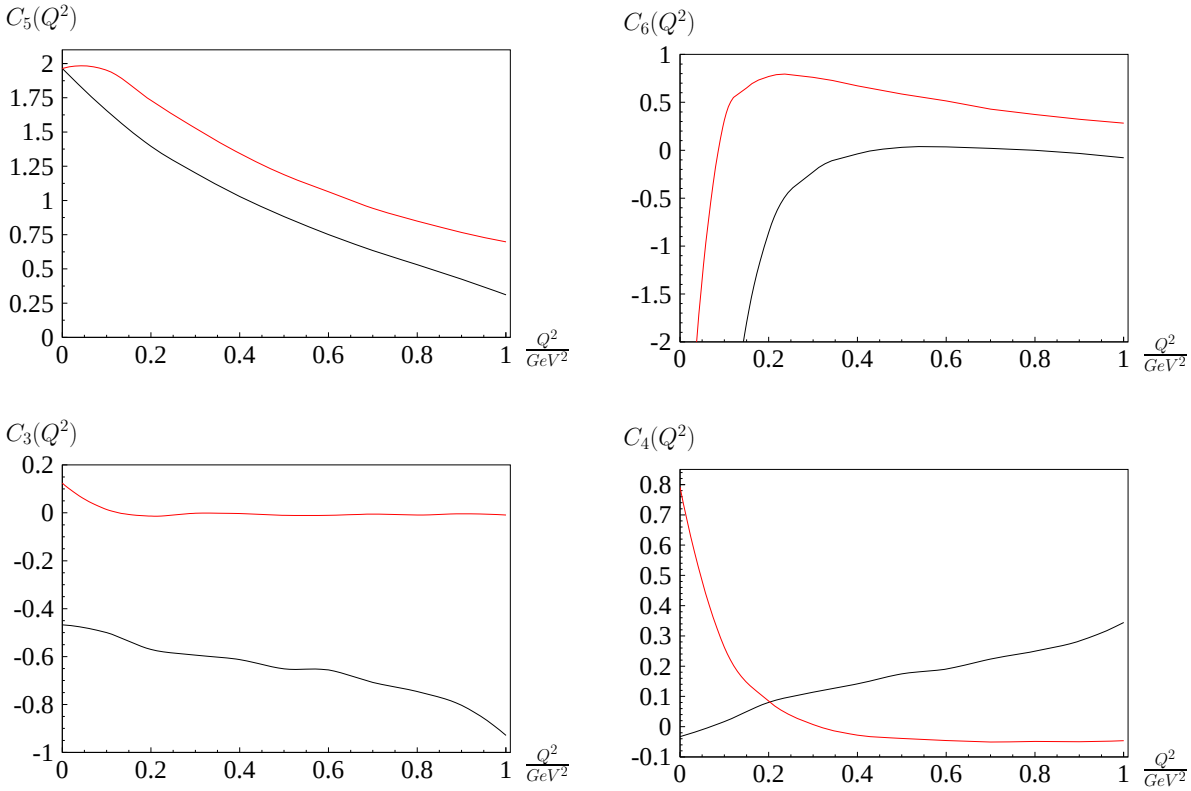

Figure 5.6: *The axial $N \to \Delta$ transition form factors calculated using the spurious covariants formalism (eq. 5.9). The red curve is obtained using all amplitudes from our LF quark model calculation. The black curve uses $\tilde{F}^+_{\frac{3}{2}\uparrow}$, $\tilde{F}^+_{\frac{1}{2}\uparrow}$, $\tilde{F}^+_{\frac{1}{2}\downarrow}$ and $\tilde{F}^x_{\frac{3}{2}\uparrow}$ from the model while the other amplitudes that we use are obtained using eq. 4.31.*

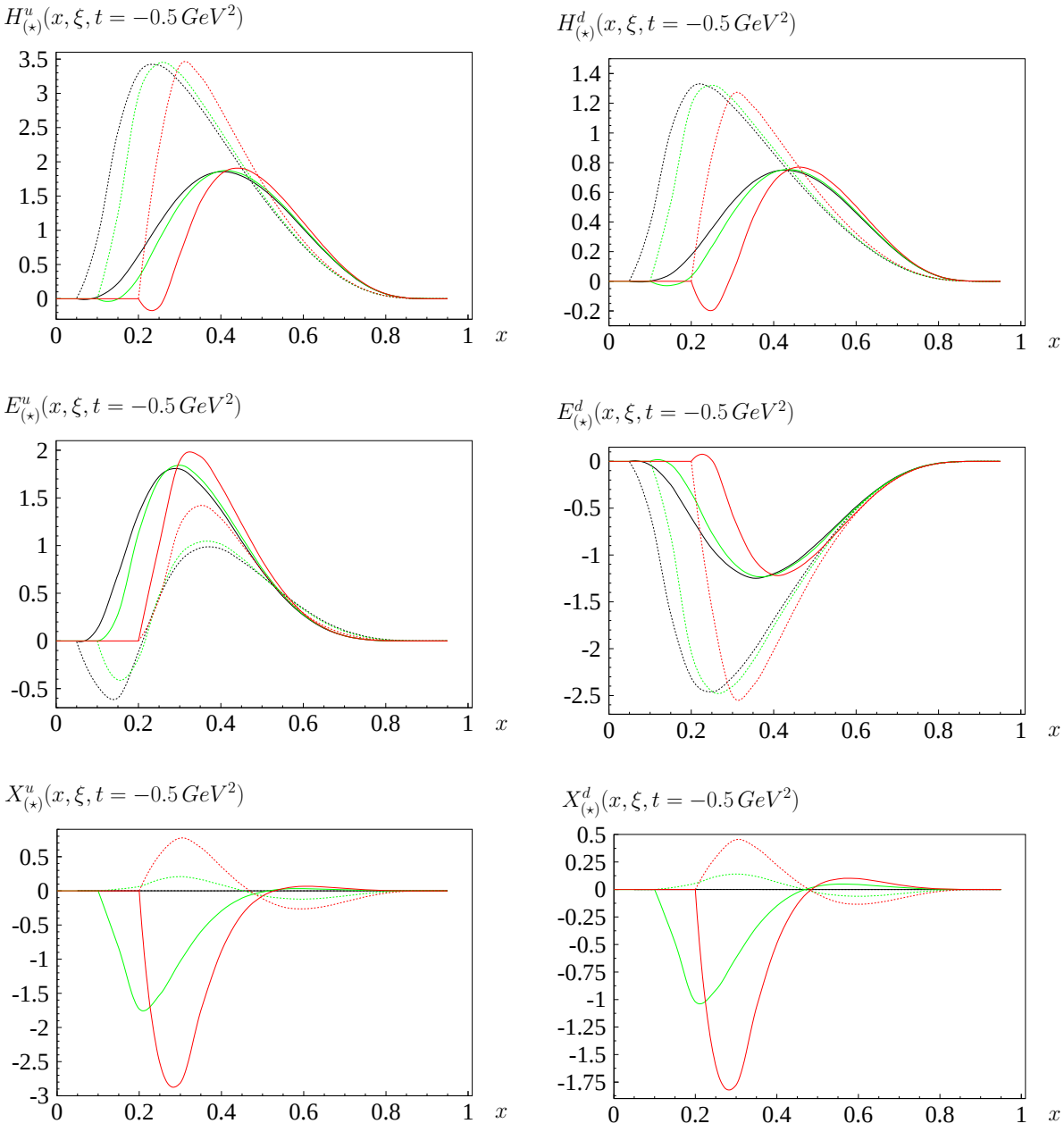

Figure 5.7: *The mixed vectorial nucleon GPDs calculated using the spurious covariants formalism (eq. 5.4). The solid curve is obtained using all amplitudes from our LF quark model calculation. The dotted curve uses $\tilde{G}^+_{\uparrow\uparrow}$, $\tilde{G}^+_{\downarrow\uparrow}$ and $\tilde{G}^x_{\uparrow\uparrow}$ from the model while the other amplitudes that we use are obtained using eq. 4.55. Results for $\xi = 0$ are given in black; $\xi = 0.1$ corresponds to the green curves and $\xi = 0.2$ to the red curves.*

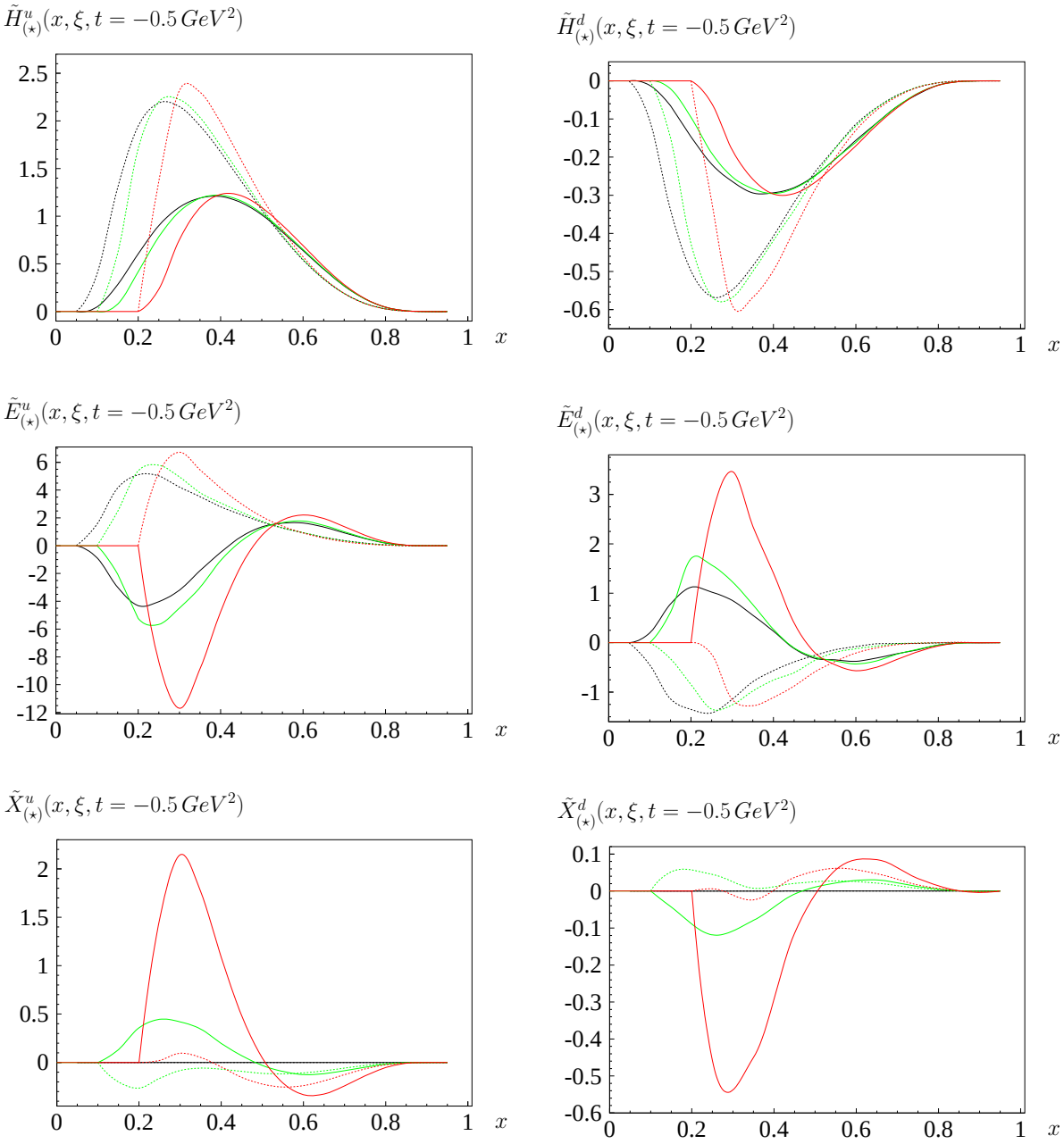

Figure 5.8: *The mixed axial nucleon GPDs calculated using the spurious covariants formalism (eq. 5.6). The solid curve is obtained using all amplitudes from our LF quark model calculation. The dotted curve uses $\tilde{G}^+_{\uparrow\uparrow}$, $\tilde{G}^+_{\downarrow\uparrow}$ and $\tilde{G}^x_{\downarrow\uparrow}$ from the model while the other amplitudes that we use are obtained using eq. 4.56. Results for $\xi = 0$ are given in black; $\xi = 0.1$ corresponds to the green curves and $\xi = 0.2$ to the red curves.*

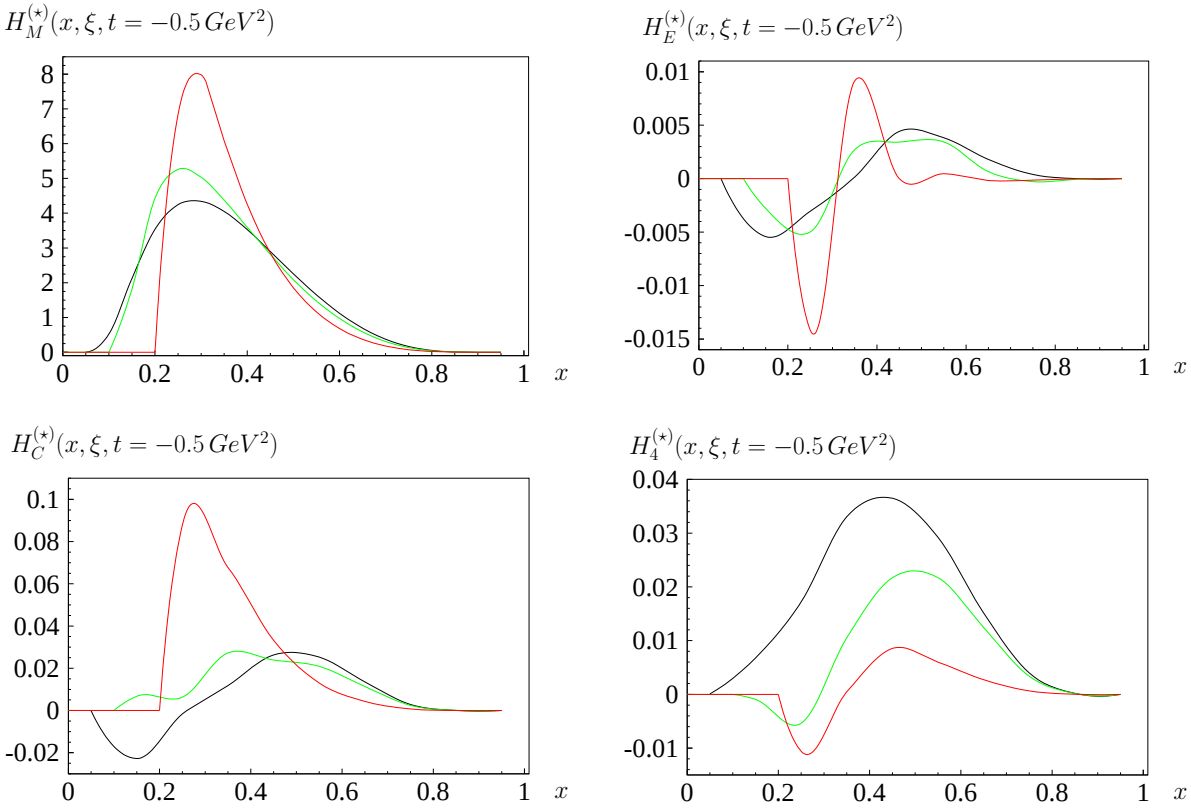

Figure 5.9: *The mixed twist vectorial $N \to \Delta$ transition GPDs calculated using the spurious covariants formalism. The results are obtained numerically using all amplitudes from our LF quark model calculation. Results for $\xi = 0$ are given in black; $\xi = 0.1$ corresponds to the green curves and $\xi = 0.2$ to the red curves.*

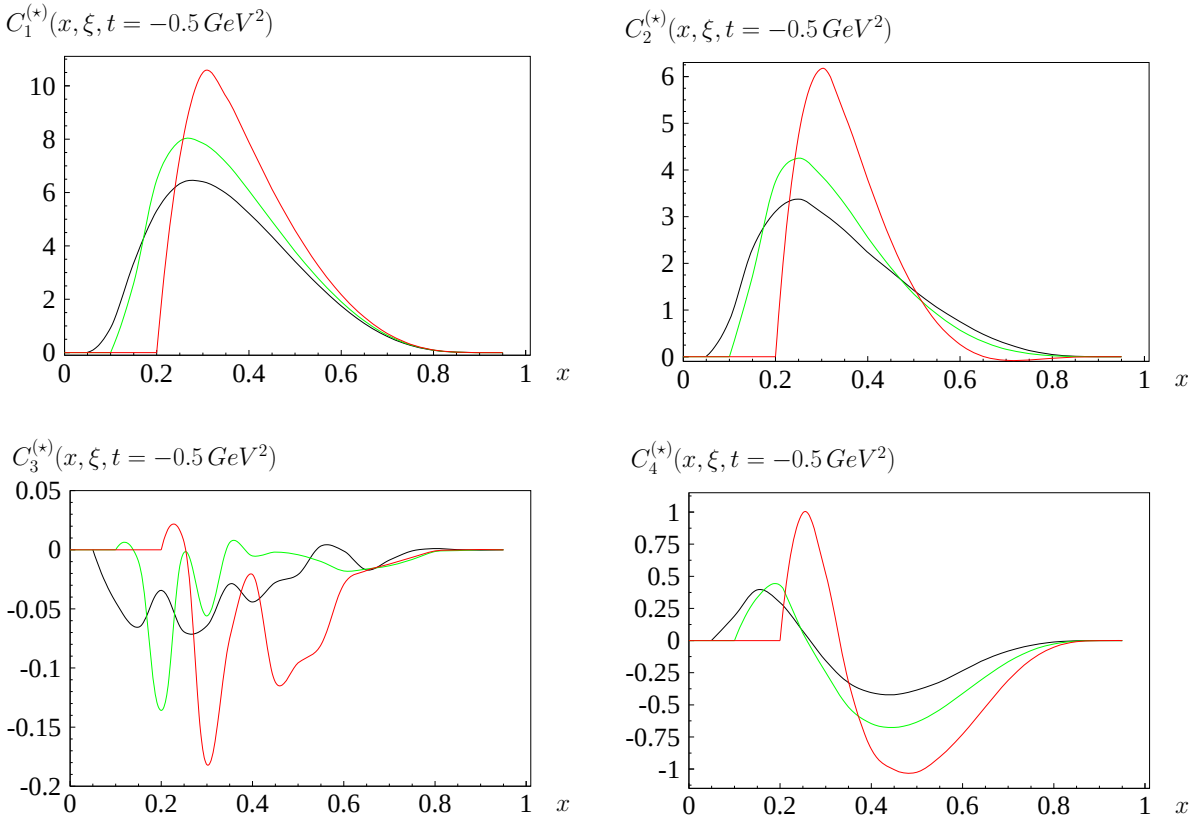

Figure 5.10: *The mixed twist axial $N \to \Delta$ transition GPDs calculated using the spurious covariants formalism. The results are obtained numerically using all amplitudes from our LF quark model calculation. Results for $\xi = 0$ are given in black; $\xi = 0.1$ corresponds to the green curves and $\xi = 0.2$ to the red curves.*

Chapter 6

Conclusions

Before concluding this thesis we like to provide some additional results that did not fit in the flow of the last chapters but which are interesting in themselves. On the one hand side we apply the large N_C relations from eqs. 2.6 and 2.7 to our model results. As can be seen from fig. 6.1 we find good agreement for the leading GPDs $H^\star_M(x,\xi,t)$ and $C_1(x,\xi,t)$ for $\xi = 0$ and decreasing agreement for higher values of ξ. The reason is that the skewedness effect for $N \to N$ has opposite sign compared to $N \to \Delta$ in our model calculation. Since we get no conclusive results for $H^\star_E(x,\xi,t)$ and $H^\star_C(x,\xi,t)$ in the direct model calculation we are happy to state that the large N_C results provide the same order of magnitude as the different prescriptions for these GPDs.

Another quantity that we like to discuss is the evaluation of Ji's sum rule (eq. 2.4). From the nucleon GPDs evaluated from the good LF components for $\xi = 0$ we get

$$\begin{aligned} J^u =& 0.265 \pm 0.001 \\ J^d =& -0.029 \pm 0.001 \end{aligned} \tag{6.1}$$

which is in fair agreement with the findings of lattice QCD [114]

$$\begin{aligned} J^u =& 0.37 \pm 0.06 \\ J^d =& -0.04 \pm 0.04 \quad . \end{aligned} \tag{6.2}$$

This implies that our model prediction for the quark contribution to the total nucleon spin is 47.2%. The deviation from the SU(6) prediction (100%) originates in relativistic effects which in the framework of the **LF** quark model enter via the Melosh rotation.

After this side remark we highlight the results of this thesis. We have applied a LF quark model using the overlap representation to calculate amplitudes for vectorial and axial $N \to N$ and $N \to \Delta$ transitions. So far in the literature the amplitudes in table 6.1 have been calculated in the framework of a LF quark model. In this thesis the missing slots have been filled.

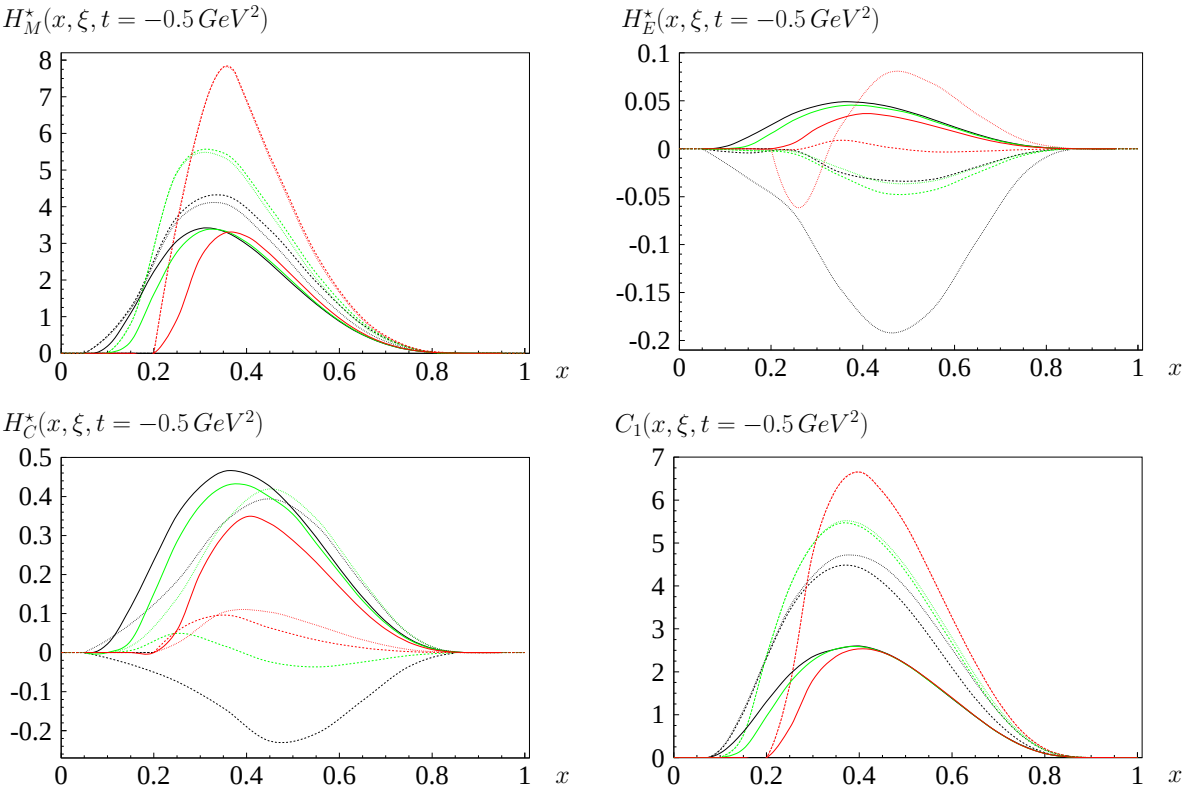

Figure 6.1: *The large N_C relations from eqs. 2.6 and 2.7 applied to the results from the quark model. The solid lines are the large N_C predictions using the nucleon GPD results from the quark model calculation as input. The dashed and dotted curves are the direct calculation for the $N \to \Delta$ GPDs in the two prescriptions which we use. The color of the curves indicates the value of the skewedness variable: $\xi = 0$ (black), $\xi = 0.1$ (green) and $\xi = 0.2$ (red).*

amplitude	$V, N \to N$	$A, N \to N$	$V, N \to \Delta$	$A, N \to \Delta$
$\tilde{F}^+_{\lambda'\lambda}$	x	x	x	
$\tilde{F}^\perp_{\lambda'\lambda}$	x		x	
$\tilde{F}^-_{\lambda'\lambda}$	x			
$\tilde{G}^+_{\lambda'\lambda}$	x	x		
$\tilde{G}^\perp_{\lambda'\lambda}$				
$\tilde{G}^-_{\lambda'\lambda}$				

Table 6.1: *Amplitudes that have been calculated in a* **LF** *model so far.*

We have established the connection between the transition amplitudes and the respective form factors and GPDs. These conversions are model independent and can be applied for future model calculations as well. Among the new results in this context are

- $N \to \Delta$ GPDs
- Adler form factors
- Sum rules for the $N \to \Delta$ GPDs without overparameterization of this DVCS process
- First toy model results for higher twist GPDs

We have presented a way to obtain model independent amplitude relations which have to be satisfied due to Poincare covariance. Among them we found back the angular condition. Additionally we presented dozens of new covariance consistency relations. All these relations are model independent.

We have worked out how bad LF component DVCS soft amplitudes and higher twist GPDs are related. For the latter we chose convenient sets of covariants and showed completeness. We have introduced "mixed twist" GPDs and have explored under which assumptions such a concept is sensible.

We have picked up the spurious covariants formalism which facilitated the reference frame independent extraction of form factors and (mixed twist) GPDs. In particular this formalism was extended towards axial transitions, the $N \to \Delta$ transition, and GPDs.

Numerically satisfying observables which have not been calculated before in a **LF** quark model were

- the magnetic $N \to \Delta$ transition GPD $H^\star_M(x, \xi, t)$
- the Adler form factor $C_5(Q^2)$
- the corresponding GPD $C_1(x, \xi, t)$

Most of our numerical results however can hardly be considered predictive as they suffer strongly from the consequences of the impulse approximation and the restrictions of the quark model. Fortunately the analytical results in the chapters 4 and 5 are model independent and therefore have a scope beyond the quark model calculation in this thesis.

Appendix A

Conventions and spinors

For the gamma matrices we use the conventions of Bjorken/Drell

$$\gamma^0 = \begin{pmatrix} 1 & 0 \\ 0 & -1 \end{pmatrix} \qquad \vec{\gamma} = \begin{pmatrix} 0 & \vec{\sigma} \\ -\vec{\sigma} & 0 \end{pmatrix}$$
$$\gamma_5 = i\gamma^0\gamma^1\gamma^2\gamma^3 = \begin{pmatrix} 0 & 1 \\ 1 & 0 \end{pmatrix} \qquad \sigma^{\mu\nu} = \frac{i}{2}\left[\gamma^\mu, \gamma^\nu\right] \quad .$$

The normalization of the (canonical) spinors for a particle with mass M is chosen to be

$$\bar{u}(p,s)\, u(p,s') = 2M\delta_{s,s'}$$

hence

$$u(p,s) = \frac{1}{\sqrt{p_0 + M}} \begin{pmatrix} (p_0 + M)\,\chi(s) \\ -(\vec{\sigma}\cdot\vec{p})\,\chi(s) \end{pmatrix} \quad .$$

For the LF vectors we choose the convention

$$A^\pm = A^0 \pm A^3 \quad .$$

Therefore one has

$$A^\mu B_\mu = \frac{1}{2}\Big(A^+B^- + A^-B^+\Big) - \vec{A}^\perp \cdot \vec{B}^\perp \quad .$$

The LF spinors are normalized by

$$\bar{u}_{LF}(p,\lambda) u_{LF}(p,\lambda') = 2M\delta_{\lambda'\lambda} \quad .$$

and read

$$
\begin{aligned}
u_{LF}(p,\uparrow) =& \frac{1}{\sqrt{2p^+}} \begin{pmatrix} M+p^+ \\ p^R \\ p^+ - M \\ p^R \end{pmatrix} \\
u_{LF}(p,\downarrow) =& \frac{1}{\sqrt{2p^+}} \begin{pmatrix} -p^L \\ p^+ + M \\ p^L \\ M - p^+ \end{pmatrix} \\
\bar{u}_{LF}(p,\uparrow) =& \frac{1}{\sqrt{2p^+}} \Big(M+p^+,\, p^L,\, M-p^+,\, -p^L \Big) \\
\bar{u}_{LF}(p,\downarrow) =& \frac{1}{\sqrt{2p^+}} \Big(-p^R,\, p^+ + M,\, -p^R,\, p^+ - M \Big) \quad .
\end{aligned}
$$

Massive spin 1 particles are described by polarization vectors. On the **LF** they explicitly read

$$
\begin{aligned}
\epsilon^\mu_{+1}(p) =& -\sqrt{2} \begin{pmatrix} 0 \\ 1 \\ 0 \\ \frac{p^R}{p^+} \end{pmatrix} \\
\epsilon^\mu_{0}(p) =& \frac{1}{M} \begin{pmatrix} p^+ \\ p^L \\ p^R \\ \frac{\vec{p}_\perp^{\,2} - M^2}{p^+} \end{pmatrix} \\
\epsilon^\mu_{-1}(p) =& \sqrt{2} \begin{pmatrix} 0 \\ 0 \\ 1 \\ \frac{p^L}{p^+} \end{pmatrix} \quad .
\end{aligned}
$$

Now the Rarita-Schwinger spinors which describe spin $\frac{3}{2}$ particles can be constructed using a Clebsch Gordon construction. They read

$$
\begin{aligned}
u^\mu_{3/2}(p) =& \epsilon^\mu_{+1}(p)\, u(p,\uparrow) \\
u^\mu_{1/2}(p) =& \sqrt{\frac{2}{3}} \epsilon^\mu_{0}(p)\, u(p,\uparrow) + \sqrt{\frac{1}{3}} \epsilon^\mu_{+1}(p)\, u(p,\downarrow) \\
u^\mu_{-1/2}(p) =& \sqrt{\frac{2}{3}} \epsilon^\mu_{0}(p)\, u(p,\downarrow) + \sqrt{\frac{1}{3}} \epsilon^\mu_{-1}(p)\, u(p,\uparrow) \\
u^\mu_{-3/2}(p) =& \epsilon^\mu_{-1}(p)\, u(p,\downarrow) \quad .
\end{aligned}
$$

These spinors have to satisfy the equations of motion

$$
\begin{aligned}
(\not{p} - M) u^\mu_\lambda(p) =& 0 \\
p_\mu\, u^\mu_\lambda(p) =& 0 \quad .
\end{aligned}
\tag{A.1}
$$

Appendix B

Kinematics for the $N \to \Delta$ transition

The kinematics for the $N \to \Delta$ transition is contained in eq. 2.5. Here we will give useful invariants which can be built from the respective four vectors. Naturally they do not depend on ξ. We find

$$\begin{aligned}
\Delta^2 =& t \\
\bar{P}^2 =& \bar{M}^2 = \frac{1}{2}(M_\Delta^2 + M_N^2) - \frac{t}{4} \\
P'^2 =& M_\Delta^2 \\
P^2 =& M_N^2 \\
\bar{P} \cdot \Delta =& \frac{1}{2}(M_\Delta^2 - M_N^2) \quad .
\end{aligned} \tag{B.1}$$

Appendix C

Covariant structures for the $N \to \Delta$ transition

In this section we provide some useful relations among $N \to \Delta$ covariants and then establish a connection between the sets of covariants which are used to parameterize the vectorial soft transition amplitude. Relations which we frequently apply in the subsequent calculations are the eqs. of motion for the RS spinor (eq. A.1) and the Dirac equation, which is the eq. of motion for the nucleon spinor.

We find the following relations:

$$\begin{aligned}
\langle \Delta \mid \gamma_5 \bar{\not{P}} \not{\Delta} \mid N \rangle &= \langle \Delta \mid \gamma_5 \Big[\frac{1}{2}(\not{P}'^2 - \not{P}^2) - \frac{1}{2}\not{P}'\not{P} + \frac{1}{2}\not{P}\not{P}' \Big] \mid N \rangle \\
&= \langle \Delta \mid \gamma_5 \Big[\frac{1}{2}(P'^2 - P^2) + P \cdot P' - P' \not{P} \Big] \mid N \rangle \\
&= \langle \Delta \mid \Big[M_\Delta^2 - \frac{t}{2} + \not{P}' M_N \Big] \gamma_5 \mid N \rangle \\
&= \langle \Delta \mid \Big[M_\Delta (M_\Delta + M_N) - \frac{t}{2} \Big] \gamma_5 \mid N \rangle
\end{aligned} \tag{C.1}$$

$$\begin{aligned}
\langle \Delta \mid \gamma_5 \gamma_\mu \bar{\not{P}} \mid N \rangle &= \langle \Delta \mid \frac{1}{2} \gamma_5 \gamma_\mu (\not{P}' + \not{P}) \mid N \rangle \\
&= \langle \Delta \mid \frac{1}{2} \gamma_5 \gamma_\mu M_N + \frac{1}{2} P'^\alpha \gamma_5 \gamma_\mu \gamma_\alpha \mid N \rangle \\
&= \langle \Delta \mid -\frac{1}{2} \gamma_\mu \gamma_5 M_N + \frac{1}{2} P'^\alpha \Big[2 g_{\mu\alpha} - \gamma_\alpha \gamma_\mu \Big] \gamma_5 \mid N \rangle \\
&= \langle \Delta \mid -\frac{1}{2} M_N \gamma_\mu \gamma_5 + P'_\mu \gamma_5 - \frac{1}{2} \not{P}' \gamma_\mu \gamma_5 \mid N \rangle \\
&= \langle \Delta \mid -\frac{1}{2} (M_N + M_\Delta) \gamma_\mu \gamma_5 + P'_\mu \gamma_5 \mid N \rangle
\end{aligned} \tag{C.2}$$

$$\begin{aligned}
\langle \Delta \mid \gamma_5 \gamma_\mu \not{\Delta} \mid N \rangle &= \langle \Delta \mid \gamma_5 \gamma_\mu (\not{P}' - \not{P}) \mid N \rangle \\
&= \langle \Delta \mid M_N \gamma_\mu \gamma_5 + 2 P'_\mu \gamma_5 - M_\Delta \gamma_\mu \gamma_5 \mid N \rangle
\end{aligned} \tag{C.3}$$

$$\begin{aligned}
\langle \Delta \mid \gamma_5\gamma_\mu\gamma_\nu \bar{\not{P}} \cdot \not{\Delta} \mid N\rangle &= \langle \Delta \mid \gamma_5\gamma_\mu\gamma_\nu \Big[M_\Delta^2 - \frac{t}{2} - \not{P}' M_N\Big] \mid N\rangle \\
&= \langle \Delta \mid (M_\Delta^2 - \frac{t}{2})\gamma_\mu\gamma_\nu\gamma_5 + \gamma_\mu\gamma_\nu\gamma_\alpha P'^\alpha\gamma_5 \mid N\rangle \\
&= \langle \Delta \mid (M_\Delta^2 - \frac{t}{2})\gamma_\mu\gamma_\nu\gamma_5 + \Big[2\gamma_\mu P'_\nu - \gamma_\mu\gamma_\alpha\gamma_\nu P'^\alpha\Big]\gamma_5 M_N \mid N\rangle \\
&= \langle \Delta \mid (M_\Delta^2 - \frac{t}{2})\gamma_\mu\gamma_\nu\gamma_5 + \Big[2P'_\nu\gamma_\mu\gamma_5 - 2P'_\mu\gamma_\nu\gamma_5 + \not{P}'\gamma_\mu\gamma_\nu\gamma_5\Big] M_N \mid N\rangle \\
&= \langle \Delta \mid \Big[M_\Delta(M_\Delta + M_N) - \frac{t}{2}\Big]\gamma_\mu\gamma_\nu\gamma_5 + 2M_N\Big[P'_\nu\gamma_\mu - P'_\mu\gamma_\nu\Big]\gamma_5 \mid N\rangle
\end{aligned} \tag{C.4}$$

$$\begin{aligned}
\langle \Delta \mid \not{\Delta}\gamma_5 \mid N\rangle &= \langle \Delta \mid (\not{P}' - \not{P})\gamma_5 \mid N\rangle \\
&= \langle \Delta \mid (M_\Delta + M_N)\gamma_5 \mid N\rangle
\end{aligned} \tag{C.5}$$

Another useful identity is:

$$\epsilon_{\alpha\beta\gamma\delta}\epsilon_{\alpha'\beta'\gamma'\delta'} = -\det\begin{pmatrix} g_{\alpha\alpha'} & g_{\alpha\beta'} & g_{\alpha\gamma'} & g_{\alpha\delta'} \\ g_{\beta\alpha'} & g_{\beta\beta'} & g_{\beta\gamma'} & g_{\beta\delta'} \\ g_{\gamma\alpha'} & g_{\gamma\beta'} & g_{\gamma\gamma'} & g_{\gamma\delta'} \\ g_{\delta\alpha'} & g_{\delta\beta'} & g_{\delta\gamma'} & g_{\delta\delta'} \end{pmatrix} \tag{C.6}$$

which can be proven by exploiting the total antisymmetry of the determinant and fixing the indices to find a possible constant factor. Another identity involving the totally antisymmetric tensor reads [116]

$$\begin{aligned}
\epsilon_{\mu\nu\alpha\beta} =& i\gamma_5\Big[\gamma_\mu\gamma_\nu\gamma_\alpha\gamma_\beta - g_{\mu\nu}\gamma_\alpha\gamma_\beta - g_{\alpha\beta}\gamma_\mu\gamma_\nu - g_{\mu\beta}\gamma_\nu\gamma_\alpha - g_{\nu\alpha}\gamma_\mu\gamma_\beta \\
&+ g_{\mu\alpha}\gamma_\nu\gamma_\beta + g_{\nu\beta}\gamma_\mu\gamma_\alpha + g_{\mu\nu}g_{\alpha\beta} - g_{\mu\alpha}g_{\nu\beta} + g_{\mu\beta}g_{\nu\alpha}\Big] \quad .
\end{aligned} \tag{C.7}$$

With the relations above at hand we can proceed to evaluate the structures which appear in the covariant sets

$$\begin{aligned}
\kappa_M^{\mu\nu} =& i\frac{3(M_\Delta + M_N)}{2M_N\big[(M_\Delta + M_N)^2 - t\big]}\epsilon^{\mu\nu\rho\lambda}\bar{P}_\rho\Delta_\lambda \\
\kappa_E^{\mu\nu} =& -\kappa_M^{\mu\nu} - \frac{6(M_\Delta + M_N)}{M_N\big[(M_\Delta - M_N)^2 - t\big]\big[(M_\Delta + M_N)^2 - t\big]}\epsilon^{\mu\kappa\alpha\beta}\bar{P}_\alpha\Delta_\beta\,\epsilon_\kappa^{\ \nu\ \alpha'\beta'}\bar{P}_{\alpha'}\Delta_{\beta'}\gamma_5 \\
\kappa_C^{\mu\nu} =& \frac{3(M_\Delta + M_N)}{M_N\big[(M_\Delta - M_N)^2 - t\big]\big[(M_\Delta + M_N)^2 - t\big]}\Big[(\bar{P}\cdot\Delta)\,\Delta^\mu\Delta^\nu - t\bar{P}^\mu\Delta^\nu\Big]\gamma_5
\end{aligned} \tag{C.8}$$

and

$$\begin{aligned}
\kappa_1^{\mu\nu} &= (\gamma^\mu\Delta^\nu - \not{\Delta}g^{\mu\nu})\gamma_5 \\
\kappa_2^{\mu\nu} &= (P'^\mu\Delta^\nu - (P'\cdot\Delta)g^{\mu\nu})\gamma_5 \\
\kappa_3^{\mu\nu} &= (\Delta^\mu\Delta^\nu - \Delta^2 g^{\mu\nu})\gamma_5 \quad .
\end{aligned} \tag{C.9}$$

We find

$$
\begin{aligned}
\langle \Delta \mid \epsilon_{\mu\nu\alpha\beta}\bar{P}^\alpha \Delta^\beta \mid N\rangle =& \langle \Delta \mid i\gamma_5 \Big[\gamma_\mu\gamma_\nu\gamma_\alpha\gamma_\beta - g_{\mu\nu}\gamma_\alpha\gamma_\beta - g_{\alpha\beta}\gamma_\mu\gamma_\nu - g_{\mu\beta}\gamma_\nu\gamma_\alpha - g_{\nu\alpha}\gamma_\mu\gamma_\beta \\
& + g_{\mu\alpha}\gamma_\nu\gamma_\beta + g_{\nu\beta}\gamma_\mu\gamma_\alpha + g_{\mu\nu}g_{\alpha\beta} - g_{\mu\alpha}g_{\nu\beta} + g_{\mu\beta}g_{\nu\alpha} \Big] \bar{P}^\alpha \Delta^\beta \mid N\rangle \\
=& \langle \Delta \mid i\gamma_5 \Big[\gamma_\mu\gamma_\nu \bar{\not{P}} \not{\Delta} - g_{\mu\nu}\bar{\not{P}}\not{\Delta} - (\bar{P}\cdot\Delta)\gamma_\mu\gamma_\nu - \Delta_\mu\gamma_\nu\bar{\not{P}} - \gamma_\mu\bar{P}_\nu\not{\Delta} \\
& + \bar{P}_\mu\gamma_\nu\not{\Delta} + \gamma_\mu\Delta_\nu\bar{\not{P}} + g_{\mu\nu}(\bar{P}\cdot\Delta) - \bar{P}_\mu\Delta_\nu + \Delta_\mu\bar{P}_\nu \Big] \mid N\rangle \\
=& \langle \Delta \mid i\gamma_5 \Big[-g_{\mu\nu}\bar{\not{P}}\not{\Delta} - \Delta_\mu\gamma_\nu\bar{\not{P}} - \frac{1}{2}\Delta_\mu\gamma_\nu\not{\Delta} + g_{\mu\nu}(\bar{P}\cdot\Delta) \\
& + \frac{1}{2}\Delta_\mu\Delta_\nu + \Delta_\mu\bar{P}_\nu \Big] \mid N\rangle \\
=& i\langle \Delta \mid \Bigg(\Big[\frac{t}{2} - M_\Delta(M_\Delta + M_N) \Big] g_{\mu\nu} - \Delta_\mu \Big[P'_\nu - \frac{1}{2}(M_N + M_\Delta)\gamma_\nu \Big] \\
& - \frac{1}{2}\Delta_\mu \Big[(M_N - M_\Delta)\gamma_\nu + 2P'_\nu \Big] + \frac{1}{2} g_{\mu\nu}(M_\Delta^2 - M_N^2) \\
& + \frac{1}{2}\Delta_\mu\Delta_\nu + \Delta_\mu\bar{P}_\nu \Bigg) \gamma_5 \mid N\rangle \\
=& i\langle \Delta \mid \Bigg(\frac{1}{2}\Big[t - (M_\Delta + M_N)^2 \Big] g_{\mu\nu} + M_\Delta\Delta_\mu\gamma_\nu \\
& - \frac{1}{2}\Delta_\mu\Delta_\nu - \Delta_\mu\bar{P}_\nu \Bigg) \gamma_5 \mid N\rangle \quad . \qquad \text{(C.10)}
\end{aligned}
$$

On the other hand we obtain

$$
\begin{aligned}
& \langle \Delta \mid M_\Delta \kappa^1_{\mu\nu} - \kappa^2_{\mu\nu} \Big] \mid N\rangle \\
=& \langle \Delta \mid \Big[M_\Delta\Delta_\mu\gamma_\nu - M_\Delta \not{\Delta} g_{\mu\nu} - \Delta_\mu\bar{P}_\nu + (\bar{P}\cdot\Delta)g_{\mu\nu} - \frac{1}{2}\Delta_\mu\Delta_\nu + \frac{t}{2}g_{\mu\nu} \Big] \gamma_5 \mid N\rangle \\
=& \langle \Delta \mid \Bigg(\frac{1}{2}\Big[t - (M_\Delta + M_N)^2 \Big] g_{\mu\nu} + M_\Delta\Delta_\mu\gamma_\nu - \frac{1}{2}\Delta_\mu\Delta_\nu - \Delta_\mu\bar{P}_\nu \Bigg) \gamma_5 \mid N\rangle \quad . \qquad \text{(C.11)}
\end{aligned}
$$

Comparing both expressions we get ($\mu \leftrightarrow \nu$ produces a minus sign in the antisymmetric tensor)

$$
\kappa^{\mu\nu}_M = \frac{3(M_\Delta + M_N)}{2M_N\big[(M_\Delta + M_N)^2 - t\big]} \Big(M_\Delta \kappa_1^{\mu\nu} - \kappa_2^{\mu\nu} \Big) \quad . \qquad \text{(C.12)}
$$

Next we find

$$
\begin{aligned}
\epsilon_{\mu\kappa\alpha\beta}\bar{P}^{\alpha}\Delta^{\beta}\epsilon_{\nu}{}^{\kappa}{}_{\alpha'\beta'}\bar{P}^{\alpha'}\Delta^{\beta'}\gamma_5 &= -\det\begin{pmatrix} g_{\mu\nu} & g_{\mu}^{\kappa} & g_{\mu\alpha'} & g_{\mu\beta'} \\ g_{\kappa\nu} & g_{\kappa}^{\kappa} & g_{\kappa\alpha'} & g_{\kappa\beta'} \\ g_{\alpha\nu} & g_{\alpha}^{\kappa} & g_{\alpha\alpha'} & g_{\alpha\beta'} \\ g_{\beta\nu} & g_{\beta}^{\kappa} & g_{\beta\alpha'} & g_{\beta\beta'} \end{pmatrix}\bar{P}^{\alpha}\Delta^{\beta}\bar{P}^{\alpha'}\Delta^{\beta'}\gamma_5 \\
&= -\det\begin{pmatrix} g_{\mu\nu} & g_{\mu}^{\kappa} & g_{\mu\alpha'} & g_{\mu\beta'} \\ g_{\kappa\nu} & g_{\kappa}^{\kappa} & g_{\kappa\alpha'} & g_{\kappa\beta'} \\ \bar{P}_{\nu} & \bar{P}^{\kappa} & \bar{P}_{\alpha'} & \bar{P}_{\beta'} \\ \Delta_{\nu} & \Delta^{\kappa} & \Delta_{\alpha'} & \Delta_{\beta'} \end{pmatrix}\bar{P}^{\alpha'}\Delta^{\beta'}\gamma_5 \\
&= -\det\begin{pmatrix} g_{\mu\nu} & g_{\mu}^{\kappa} & \bar{P}_{\mu} & \Delta_{\mu} \\ g_{\kappa\nu} & 4 & \bar{P}_{\kappa} & \Delta_{\kappa} \\ \bar{P}_{\nu} & \bar{P}^{\kappa} & \bar{P}^2 & \bar{P}\cdot\Delta \\ \Delta_{\nu} & \Delta^{\kappa} & \bar{P}\cdot\Delta & \Delta^2 \end{pmatrix}\gamma_5 \\
&= \Bigg[-g_{\mu\nu}\det\begin{pmatrix} 4 & \bar{P}^{\kappa} & \Delta^{\kappa} \\ \bar{P}_{\kappa} & \bar{P}^2 & \bar{P}\cdot\Delta \\ \Delta_{\kappa} & \bar{P}\cdot\Delta & \Delta^2 \end{pmatrix} + g_{\kappa\nu}\det\begin{pmatrix} g_{\mu}^{\kappa} & \bar{P}^{\kappa} & \Delta^{\kappa} \\ \bar{P}_{\mu} & \bar{P}^2 & \bar{P}\cdot\Delta \\ \Delta_{\mu} & \bar{P}\cdot\Delta & \Delta^2 \end{pmatrix} \\
&\quad - \bar{P}_{\nu}\det\begin{pmatrix} g_{\mu}^{\kappa} & 4 & \Delta^{\kappa} \\ \bar{P}_{\mu} & \bar{P}_{\kappa} & \bar{P}\cdot\Delta \\ \Delta_{\mu} & \Delta_{\kappa} & \Delta^2 \end{pmatrix} + \Delta_{\nu}\det\begin{pmatrix} g_{\mu}^{\kappa} & 4 & \bar{P}^{\kappa} \\ \bar{P}_{\mu} & \bar{P}_{\kappa} & \bar{P}\cdot\bar{P} \\ \Delta_{\mu} & \Delta_{\kappa} & \bar{P}\cdot\Delta \end{pmatrix}\Bigg]\gamma_5 \\
&= -g_{\mu\nu}\Big[4\Delta^2\bar{P}^2 + 2(\bar{P}\cdot\Delta)^2 - 4(\bar{P}\cdot\Delta)^2 - \bar{P}^2\Delta^2 - \bar{P}^2\Delta^2\Big]\gamma_5 \\
&\quad + \det\begin{pmatrix} g_{\mu\nu} & \bar{P}_{\nu} & \Delta_{\nu} \\ \bar{P}_{\mu} & \bar{P}^2 & \bar{P}\cdot\Delta \\ \Delta_{\mu} & \bar{P}\cdot\Delta & \Delta^2 \end{pmatrix}\gamma_5 \\
&\quad - \bar{P}_{\nu}\Big[\bar{P}_{\mu}\Delta^2 + 4(\bar{P}\cdot\Delta)\Delta_{\mu} + \bar{P}_{\mu}\Delta^2 - \Delta_{\mu}(\bar{P}\cdot\Delta) - 4\bar{P}_{\mu}\Delta^2 - (\bar{P}\cdot\Delta)\Delta_{\mu}\Big]\gamma_5 \\
&\quad + \Delta_{\nu}\Big[\bar{P}_{\mu}(\bar{P}\cdot\Delta) + 4\Delta_{\mu}\bar{P}^2 + (\bar{P}\cdot\Delta)\bar{P}_{\mu} - \Delta_{\mu}\bar{P}^2 - 4(\bar{P}\cdot\Delta)\bar{P}_{\mu} - \bar{P}^2\Delta_{\mu}\Big]\gamma_5 \\
&= \Big[(\bar{P}\cdot\Delta)^2 - \bar{P}^2\Delta^2\Big]g^{\mu\nu}\gamma_5 + t\,\bar{P}^{\mu}\bar{P}^{\nu}\gamma_5 + \bar{P}^2\Delta^{\mu}\Delta^{\nu}\gamma_5 - (\bar{P}\cdot\Delta)\Delta^{\mu}\bar{P}^{\nu}\gamma_5 - (\bar{P}\cdot\Delta)\bar{P}^{\mu}\Delta^{\nu}\gamma_5
\end{aligned}
$$

Sandwiched between nucleon and Δ states we can apply eq. A.1 and conclude

$$
\begin{aligned}
&\langle\Delta \mid \epsilon_{\mu\kappa\alpha\beta}\bar{P}^{\alpha}\Delta^{\beta}\epsilon_{\nu}{}^{\kappa}{}_{\alpha'\beta'}\bar{P}^{\alpha'}\Delta^{\beta'}\gamma_5 \mid N\rangle \\
=&\langle\Delta \mid \left(\Big[(\bar{P}\cdot\Delta)^2 - \bar{P}^2\Delta^2\Big]g^{\mu\nu} + \Big[\bar{P}^2 + \frac{1}{2}(\bar{P}\cdot\Delta)\Big]\Delta^{\mu}\Delta^{\nu} - \Big[(\bar{P}\cdot\Delta) + \frac{t}{2}\Big]\bar{P}^{\mu}\Delta^{\nu}\right)\gamma_5 \mid N\rangle \quad .
\end{aligned}
\tag{C.13}
$$

On the other hand side we find

$$\begin{aligned}
&\frac{3(M_\Delta+M_N)}{M_N}\Bigg(\frac{1}{2\big[(M_\Delta+M_N)^2-t\big]}\Big[-M_\Delta\kappa_1^{\mu\nu}+\kappa_2^{\mu\nu}\Big]\\
&+\frac{1}{\big[(M_\Delta-M_N)^2-t\big]\big[(M_\Delta+M_N)^2-t\big]}\Big[(M_\Delta^2-M_N^2+t)\kappa_2^{\mu\nu}-2M_\Delta^2\kappa_3^{\mu\nu}\Big]\Bigg)\\
=&-\kappa_M^{\mu\nu}+\frac{3(M_\Delta+M_N)}{M_N\big[(M_\Delta-M_N)^2-t\big]\big[(M_\Delta+M_N)^2-t\big]}\Bigg((M_\Delta^2-M_N^2+t)\bar{P}^\mu\Delta^\nu\\
&+\Big[\frac{1}{2}(M_\Delta^2-M_N^2+t)-2M_\Delta^2\Big]\Delta^\mu\Delta^\nu-\frac{\big[(M_\Delta-M_N)^2-t\big]\big[(M_\Delta+M_N)^2-t\big]}{2}g^{\mu\nu}\Bigg)\gamma_5 \quad .
\end{aligned} \tag{C.14}$$

Using the kinematical relations in eq. B.1 one ends up with

$$\kappa_E^{\mu\nu}=\frac{3(M_\Delta+M_N)}{M_N}\left(-\frac{M_\Delta}{2q^+}\kappa_1^{\mu\nu}+\Big[\frac{1}{2q^+}+\frac{\sigma}{\sigma^2-4M_\Delta^2t}\Big]\kappa_2^{\mu\nu}-\frac{2M_\Delta^2}{\sigma^2-4M_\Delta^2t}\kappa_3^{\mu\nu}\right) \quad . \tag{C.15}$$

Here we have adopted the notation from chapter 4 with

$$\begin{aligned}
\sigma=&M_\Delta^2-M_N^2+t\\
q^+=&(M_\Delta+M_N)^2-t \quad .
\end{aligned}$$

Finally we evaluate

$$\begin{aligned}
\kappa_C^{\mu\nu}=&\frac{3(M_\Delta+M_N)}{M_N\big[(M_\Delta-M_N)^2-t\big]\big[(M_\Delta+M_N)^2-t\big]}\Big[(\bar{P}\cdot\Delta)\,\Delta^\mu\Delta^\nu-t\bar{P}^\mu\Delta^\nu\Big]\gamma_5\\
=&\frac{3(M_\Delta+M_N)}{M_N(\sigma^2-4M_\Delta^2t)}\left(\frac{M_\Delta^2-M_N^2}{2}\Delta^\mu\Delta^\nu-t\bar{P}^\mu\Delta^\nu\right)\gamma_5\\
=&\frac{3(M_\Delta+M_N)}{M_N(\sigma^2-4M_\Delta^2t)}\left(\frac{\sigma}{2}\Delta^\mu\Delta^\nu-tP'^\mu\Delta^\nu\right)\gamma_5\\
=&\frac{3(M_\Delta+M_N)}{M_N(\sigma^2-4M_\Delta^2t)}\Big(-t\kappa_2^{\mu\nu}+\frac{\sigma}{2}\kappa_3^{\mu\nu}\Big) \quad .
\end{aligned} \tag{C.16}$$

We can resume the results of eqs. C.12, C.15 and C.16 and write

$$\begin{pmatrix}\kappa_M\\ \kappa_E\\ \kappa_C\end{pmatrix}=\frac{3(M_\Delta+M_N)}{M_N}\begin{pmatrix}\frac{M_\Delta}{2q^+} & -\frac{1}{2q^+} & 0\\ -\frac{M_\Delta}{2q^+} & \frac{1}{2q^+}+\frac{\sigma}{\sigma^2-4M_\Delta^2t} & -\frac{2M_\Delta^2}{\sigma^2-4M_\Delta^2t}\\ 0 & -\frac{t}{\sigma^2-4M_\Delta^2t} & \frac{\sigma}{2\sigma^2-8M_\Delta^2t}\end{pmatrix}\begin{pmatrix}\kappa_1\\ \kappa_2\\ \kappa_3\end{pmatrix} \tag{C.17}$$

Inversion and transposition of this matrix gives the result that was given in 4.12.

Bibliography

[1] R. Hofstadter and R. W. McAllister, Phys. Rev. **98** (1955) 217.

[2] M. Gell-Mann, Phys. Rev. **125** (1962) 1067.

[3] O. W. Greenberg, Phys. Rev. Lett. **13** (1964) 598.

[4] M. Y. Han and Y. Nambu, Phys. Rev. **139** (1965) B1006.

[5] G. 't Hooft, Nucl. Phys. B **33** (1971) 173.

[6] C. N. Yang and R. L. Mills, Phys. Rev. **96** (1954) 191.

[7] D. J. Gross and F. Wilczek, Phys. Rev. Lett. **30**, 1343 (1973).

[8] H. D. Politzer, Phys. Rev. Lett. **30** (1973) 1346.

[9] H. Fritzsch, M. Gell-Mann and H. Leutwyler, Phys. Lett. B **47** (1973) 365.

[10] S. Weinberg, Phys. Rev. Lett. **31** (1973) 494.

[11] S. Bethke, Nucl. Phys. Proc. Suppl. **135** (2004) 345 [arXiv:hep-ex/0407021].

[12] J. Stachel, arXiv:nucl-ex/0510077.

[13] R. A. Schumacher, arXiv:nucl-ex/0512042.

[14] G. 't Hooft, Nucl. Phys. B **138**, 1 (1978).

[15] T. Suzuki, Nucl. Phys. Proc. Suppl. **30**, 176 (1993).

[16] S. Weinberg, PhysicaA **96** (1979) 327.

[17] J. Gasser and H. Leutwyler, "Chiral Perturbation Theory To One Loop," Annals Phys. **158** (1984) 142,

[18] E. Jenkins and A. V. Manohar, Phys. Lett. B **255**, 558 (1991).

[19] P. A. M. Dirac, Rev. Mod. Phys. **21**, 392 (1949).

[20] V. B. Berestetsky and M. V. Terentev, Sov. J. Nucl. Phys. **24**, 547 (1976) [Yad. Fiz. **24**, 1044 (1976)].

[21] V. A. Karmanov, Fiz. Elem. Chast. Atom. Yadra **19**, 525 (1988).

[22] V. A. Karmanov and J. F. Mathiot, Nucl. Phys. A **602**, 388 (1996).

[23] F. M. Dittes, D. Mueller, D. Robaschik, B. Geyer and J. Horejsi, Phys. Lett. B **209**, 325 (1988).

[24] X. D. Ji, Phys. Rev. D **55**, 7114 (1997) [arXiv:hep-ph/9609381].

[25] X. D. Ji and J. Osborne, Phys. Rev. D **58**, 094018 (1998) [arXiv:hep-ph/9801260].

[26] X. D. Ji, J. Phys. G **24** (1998) 1181 [arXiv:hep-ph/9807358].

[27] X. D. Ji, Phys. Rev. Lett. **78**, 610 (1997) [arXiv:hep-ph/9603249].

[28] J. R. Ellis and R. L. Jaffe, Phys. Rev. D **9**, 1444 (1974) [Erratum-ibid. D **10**, 1669 (1974)].

[29] J. Ashman *et al.* [European Muon Collaboration], Phys. Lett. B **206** (1988) 364.

[30] A. Airapetian *et al.* [HERMES Collaboration], Phys. Rev. D **75**, 012007 (2007).

[31] A. V. Radyushkin, Phys. Lett. B **380**, 417 (1996) [arXiv:hep-ph/9604317].

[32] D. Y. Ivanov, B. Pire, L. Szymanowski and O. V. Teryaev, Phys. Lett. B **550**, 65 (2002) [arXiv:hep-ph/0209300].

[33] P. Hoodbhoy and X. D. Ji, Phys. Rev. D **58**, 054006 (1998) [arXiv:hep-ph/9801369].

[34] M. Diehl, Eur. Phys. J. C **19**, 485 (2001) [arXiv:hep-ph/0101335].

[35] B. Pasquini, M. Pincetti and S. Boffi, Phys. Rev. D **72**, 094029 (2005) [arXiv:hep-ph/0510376].

[36] M. Penttinen, M. V. Polyakov, A. G. Shuvaev and M. Strikman, Phys. Lett. B **491**, 96 (2000) [arXiv:hep-ph/0006321].

[37] M. Burkardt, Int. J. Mod. Phys. A **18**, 173 (2003) [arXiv:hep-ph/0207047].

[38] A. V. Belitsky, X. d. Ji and F. Yuan, Phys. Rev. D **69**, 074014 (2004) [arXiv:hep-ph/0307383].

[39] M. Diehl, Phys. Rept. **388**, 41 (2003) [arXiv:hep-ph/0307382].

[40] A. Airapetian *et al.* [HERMES Collaboration], Phys. Rev. Lett. **87**, 182001 (2001) [arXiv:hep-ex/0106068].

[41] S. Stepanyan *et al.* [CLAS Collaboration], Phys. Rev. Lett. **87**, 182002 (2001) [arXiv:hep-ex/0107043].

[42] N. Kivel, M. V. Polyakov and M. Vanderhaeghen, Phys. Rev. D **63**, 114014 (2001) [arXiv:hep-ph/0012136].

[43] C. Munoz Camacho *et al.* [Jefferson Lab Hall A Collaboration], Phys. Rev. Lett. **97**, 262002 (2006) [arXiv:nucl-ex/0607029].

[44] P. A. M. Guichon, M. Guidal and M. Vanderhaeghen, Nucl. Phys. A **666**, 234 (2000).

[45] L. L. Frankfurt, M. V. Polyakov, M. Strikman and M. Vanderhaeghen, Phys. Rev. Lett. **84**, 2589 (2000) [arXiv:hep-ph/9911381].

[46] K. Goeke, M. V. Polyakov and M. Vanderhaeghen, Prog. Part. Nucl. Phys. **47**, 401 (2001) [arXiv:hep-ph/0106012].

[47] V. Pascalutsa and M. Vanderhaeghen, arXiv:hep-ph/0611050.

[48] L. Tiator, D. Drechsel, O. Hanstein, S. S. Kamalov and S. N. Yang, Nucl. Phys. A **689**, 205 (2001) [arXiv:nucl-th/0012046].

[49] C. E. Carlson, Phys. Rev. D **34**, 2704 (1986).

[50] A. Idilbi, X. d. Ji and J. P. Ma, Phys. Rev. D **69** (2004) 014006 [arXiv:hep-ph/0308018].

[51] V. Pascalutsa and M. Vanderhaeghen, arXiv:hep-ph/0611317.

[52] P. A. M. Guichon, L. Mosse and M. Vanderhaeghen, Phys. Rev. D **68**, 034018 (2003) [arXiv:hep-ph/0305231].

[53] M. Guidal, S. Bouchigny, J. P. Didelez, C. Hadjidakis, E. Hourany and M. Vanderhaeghen, Nucl. Phys. A **721**, 327 (2003) [arXiv:hep-ph/0304252].

[54] J. C. Collins, L. Frankfurt and M. Strikman, Phys. Rev. D **56**, 2982 (1997) [arXiv:hep-ph/9611433].

[55] M. Vanderhaeghen, P. A. M. Guichon and M. Guidal, Phys. Rev. Lett. **80**, 5064 (1998).

[56] P. A. M. Guichon and M. Vanderhaeghen, Phys. Rev. Lett. **91**, 142303 (2003) [arXiv:hep-ph/0306007].

[57] Y. C. Chen, A. Afanasev, S. J. Brodsky, C. E. Carlson and M. Vanderhaeghen, Phys. Rev. Lett. **93**, 122301 (2004) [arXiv:hep-ph/0403058].

[58] H. Leutwyler, Phys. Lett. B **48**, 431 (1974).

[59] N. Isgur and G. Karl, Phys. Rev. D **19**, 2653 (1979) [Erratum-ibid. D **23**, 817 (1981)].

[60] B. Julia-Diaz, D. O. Riska and F. Coester, Phys. Rev. C **69**, 035212 (2004) [arXiv:hep-ph/0312169].

[61] L. Y. Glozman, W. Plessas, K. Varga and R. F. Wagenbrunn, Phys. Rev. D **58**, 094030 (1998) [arXiv:hep-ph/9706507].

[62] F. Cardarelli, I. L. Grach, I. M. Narodetsky, E. Pace, G. Salme and S. Simula, Phys. Lett. B **332**, 1 (1994) [arXiv:nucl-th/9405014].

[63] V. B. Berestetsky and M. V. Terentev, Sov. J. Nucl. Phys. **25**, 347 (1977) [Yad. Fiz. **25**, 653 (1977)].

[64] M. Diehl, T. Feldmann, R. Jakob and P. Kroll, Nucl. Phys. B **596**, 33 (2001) [Erratum-ibid. B **605**, 647 (2001)] [arXiv:hep-ph/0009255].

[65] S. Boffi, B. Pasquini and M. Traini, Nucl. Phys. B **649**, 243 (2003) [arXiv:hep-ph/0207340].

[66] N. Isgur and G. Karl, Phys. Rev. D **18**, 4187 (1978).

[67] R. G. Moorhouse, Phys. Rev. Lett. **16**, 772 (1966).

[68] F. Schlumpf, J. Phys. G **20**, 237 (1994) [arXiv:hep-ph/9301233].

[69] L. Susskind, Phys. Rev. **165**, 1535 (1968).

[70] H. J. Melosh, Phys. Rev. D **9**, 1095 (1974).

[71] F. Schlumpf, Mod. Phys. Lett. A **8**, 2135 (1993) [arXiv:hep-ph/9302268].

[72] S. Boffi, B. Pasquini and M. Traini, Nucl. Phys. B **680** (2004) 147 [arXiv:hep-ph/0311016].

[73] A. Mukherjee and M. Vanderhaeghen, Phys. Lett. B **542**, 245 (2002) [arXiv:hep-ph/0206159].

[74] A. Mukherjee and M. Vanderhaeghen, Phys. Rev. D **67**, 085020 (2003) [arXiv:hep-ph/0211386].

[75] G. P. Lepage, J. Comput. Phys. **27**, 192 (1978).

[76] F. Coester, Prog. Part. Nucl. Phys. **29**, 1 (1992).

[77] R. L. Jaffe and X. D. Ji, Phys. Rev. Lett. **67** (1991) 552.

[78] C. E. Carlson and C. R. Ji, Phys. Rev. D **67** (2003) 116002 [arXiv:hep-ph/0301213].

[79] H. F. Jones and M. D. Scadron, Annals Phys. **81** (1973) 1.

[80] R. C. E. Devenish, T. S. Eisenschitz and J. G. Korner, Phys. Rev. D **14**, 3063 (1976).

[81] C. H. Llewellyn Smith, Phys. Rept. **3** (1972) 261; S. L. Adler, Annals Phys. **50** (1968) 189.

[82] W. Bartel *et al.*, Nucl. Phys. B **58**, 429 (1973).

[83] T. Janssens, R. Hofstadter, E. B. Hughes and M. R. Yearian, Phys. Rev. **142**, 922 (1966).

[84] O. Gayou *et al.*, Phys. Rev. C **64**, 038202 (2001).

[85] V. Punjabi *et al.*, Phys. Rev. C **71**, 055202 (2005) [Erratum-ibid. C **71**, 069902 (2005)] [arXiv:nucl-ex/0501018].

[86] C. B. Crawford *et al.*, Phys. Rev. Lett. **98**, 052301 (2007) [arXiv:nucl-ex/0609007].

[87] J. D. Lachniet, "A High precision measurement of the neutron magnetic form factor using the CLAS detector," PhD thesis (2005) [UMI-31-86035]

[88] G. Kubon *et al.*, Phys. Lett. B **524**, 26 (2002) [arXiv:nucl-ex/0107016].

[89] H. Anklin *et al.*, Phys. Lett. B **428**, 248 (1998).

[90] W. Xu *et al.*, Phys. Rev. Lett. **85**, 2900 (2000) [arXiv:nucl-ex/0008003].

[91] P. Markowitz *et al.*, Phys. Rev. C **48**, 5 (1993).

[92] W. Xu *et al.* [Jefferson Lab E95-001 Collaboration], Phys. Rev. C **67**, 012201 (2003) [arXiv:nucl-ex/0208007].

[93] R. Madey *et al.* [E93-038 Collaboration], Phys. Rev. Lett. **91**, 122002 (2003) [arXiv:nucl-ex/0308007].

[94] H. Zhu *et al.* [E93026 Collaboration], Phys. Rev. Lett. **87**, 081801 (2001) [arXiv:nucl-ex/0105001].

[95] G. Warren *et al.* [Jefferson Lab E93-026 Collaboration], Phys. Rev. Lett. **92**, 042301 (2004) [arXiv:nucl-ex/0308021].

[96] D. I. Glazier *et al.*, Eur. Phys. J. A **24**, 101 (2005) [arXiv:nucl-ex/0410026].

[97] C. Herberg *et al.*, Eur. Phys. J. A **5** (1999) 131.

[98] M. Ostrick *et al.*, Phys. Rev. Lett. **83**, 276 (1999).

[99] D. Rohe *et al.*, Phys. Rev. Lett. **83**, 4257 (1999).

[100] J. Bermuth *et al.*, Phys. Lett. B **564**, 199 (2003) [arXiv:nucl-ex/0303015].

[101] J. Golak, G. Ziemer, H. Kamada, H. Witala and W. Gloeckle, Phys. Rev. C **63**, 034006 (2001) [arXiv:nucl-th/0008008].

[102] I. Passchier *et al.*, Phys. Rev. Lett. **82**, 4988 (1999) [arXiv:nucl-ex/9907012].

[103] L. Tiator and S. Kamalov, AIP Conf. Proc. **904**, 191 (2007) [arXiv:nucl-th/0610113].

[104] H. J. Weber, Annals Phys. **207**, 417 (1991).

[105] E. Pace, G. Salme, F. Cardarelli and S. Simula, Nucl. Phys. A **666**, 33 (2000) [arXiv:nucl-th/9909025].

[106] K. Joo *et al.* [CLAS Collaboration], Phys. Rev. Lett. **88**, 122001 (2002) [arXiv:hep-ex/0110007].

[107] J. J. Kelly *et al.* [Jefferson Lab Hall A Collaboration], Phys. Rev. Lett. **95**, 102001 (2005) [arXiv:nucl-ex/0505024].

[108] C. Mertz *et al.*, Phys. Rev. Lett. **86**, 2963 (2001) [arXiv:nucl-ex/9902012].

[109] R. Beck *et al.*, Phys. Rev. Lett. **78**, 606 (1997).

[110] S. Stave *et al.*, Eur. Phys. J. A **30**, 471 (2006) [arXiv:nucl-ex/0604013].

[111] N. F. Sparveris *et al.*, Phys. Lett. B **651**, 102 (2007) [arXiv:nucl-ex/0611033].

[112] A. W. Thomas, W. Weise, The structure of the nucleon Wiley-VCH

[113] S. Simula, arXiv:hep-ph/0406074.

[114] M. Gockeler, R. Horsley, D. Pleiter, P. E. L. Rakow, A. Schafer, G. Schierholz and W. Schroers [QCDSF Collaboration], Phys. Rev. Lett. **92**, 042002 (2004) [arXiv:hep-ph/0304249].

[115] B. Pasquini and S. Boffi, Phys. Rev. D **73**, 094001 (2006) [arXiv:hep-ph/0601177].

[116] M. D. Scadron and H. F. Jones, Phys. Rev. **173**, 1734 (1968).